Antigen-specific immunotherapy:

Identification of T cell epitopes in Autoimmune Hepatitis Type 2 and characterisation of bystander suppression mechanisms

Naomi Richardson

A thesis submitted to the University of Birmingham for
the degree of Doctor of Philosophy

Institute of Immunology and Immunotherapy
College of Medical and Dental Science
University of Birmingham
March 2021

Abstract

A diverse and effective T cell repertoire is critical for protection against pathogens and prevention of self-reactivity. Central and peripheral tolerance mechanisms delete and actively suppress self-reactive T cells with autoimmune potential. However, these regulatory processes are not perfect, hence, individuals can develop autoimmune, allergic and chronic inflammatory diseases potentiated by poorly regulated effector T cells.

Current treatments for autoimmune diseases are rarely curative and rely heavily on broad-range immunosuppressive drugs. Antigen-specific immunotherapies (ASI) induce protective immunity targeted towards pathogenic T cells and require identification of disease-relevant antigen(s) and a tolerogenic delivery system. In complex, multi-antigen diseases, it may be sufficient to induce tolerance to immunodominant antigen(s) only, due to the process of bystander suppression. We first studied the cellular and molecular mechanisms involved in peptide immunotherapy using transgenic mice with T cell receptor specificity to one of two myelin antigenic peptides. We then expanded upon these findings using wild-type mice to study bystander suppression in the context of a complete T cell repertoire.

Despite the tolerogenic propensity of the liver, autoreactive T cells can orchestrate chronic immune damage and eventual loss of organ function without medical intervention. We targeted Autoimmune Hepatitis Type 2 which has a clearly defined autoantigen, CYP2D6. We characterised two T cell epitopes from CYP2D6. These T cell epitope peptides have the potential to form the basis of a novel peptide-based immunotherapy to treat Autoimmune Hepatitis Type 2.

Acknowledgements

First and foremost, I would like to extend my significant gratitude to David for the introduction to antigen-specific immunotherapy which inspired me to apply for this PhD in the very beginning. Thank you for sharing your significant experience, academic guidance, mentorship and at times, emotional support throughout this project in some of the strangest possible times. Thank you for pushing me to challenge myself, whilst letting me know that it is alright if things do not go to plan, which happened more often than I would like to recall!

All members of the Wraith lab have been invaluable in providing continued support, advice, conversation and laughs throughout, so many thanks to my friends and colleagues: Lora, Joe, Dina, Sky and Maher. A special thanks to Heather for training me up in the lab and showing me the ropes, without whom I would have almost certainly been lost. Thanks to Suz for helping to organise BCH sample access. Thank you to Ye for his infectious positivity as secondary supervisor and for helping to map out continued research in autoimmune liver disease, which I hope will be an exciting and productive venture.

Thank you to my wonderful parents, Jane and Kevan for all you have done in getting me to this point. I dedicate this thesis to you; I might have thrown in the towel many times over without your encouragement, pep talks and unwavering belief in me. Thank you to Mike – we have gone through this journey together and have managed to keep each other together enough to (just about!) maintain sanity even in lockdowns. Looking forward to more fun and free times ahead.

Table of Contents

3. Characterisation of bystander suppression mechanisms *in vitro* and *in vivo*

4. Identification of human T cell epitopes from the autoantigen CYP2D6

5. Fine mapping of T cell epitopes from autoantigen CYP2D6

List of Figures

1. Introduction

3. Characterisation of bystander suppression mechanisms *in vitro* and *in vitro*

4. Identification of human T cell epitopes from the autoantigen CYP2D6

5. Fine mapping of T cell epitopes from autoantigen CYP2D6

List of Tables

List of Abbreviations

AIH	Autoimmune Hepatitis
AILD	autoimmune liver disease
AIM	Activation Induced Marker
AIT	Allergen immunotherapy
ANA	anti-nuclear antibodies
APC	antigen presenting cells
ASGPR	anti-asialoglycoprotein receptor antibodies
ASI	antigen-specific immunotherapy
AZA	azathioprine
Breg	regulatory B cells
BSA	bovine serum albumin
CDR	complementarity determining regions
CFA	Complete Freud's Adjuvant
CMV	cytomegalovirus
CNS	central nervous system
CPDA	citrate phosphate dextrose adenine
cpm	counts per minute
CTL	CD8+ T cytotoxic lymphocytes
CTV	Cell Trace Violet
CYP2D6	cytochrome P450 2D6
DC	dendritic cells
EAE	experimental autoimmune encephalomyelitis
EBV-LCL	Epstein-Barr Virus- (EBV-) Lymphoblastoid Cell Lines
ELISA	enzyme-linked immunosorbent assay
ER	endoplasmic reticulum
FACS	fluorescence-activated cell sorting

FMO	fluorescence minus one
FTCD	formiminotransferase cyclodeaminase
GdE	gadolinium-enhanced
GWAS	genome-wide association studies
HBRC	Human Biomaterials Resource Centre
HCC	hepatocellular carcinoma
HCV	Hepatitis C
HLA	human leukocyte antigen
HSC	hepatic stellate cells
IAIHG	International Autoimmune Hepatitis Group
IBD	inflammatory bowel disease
iTreg	induced T regulatory cells
KC	Kupffer cells
KLH	Keyhole Limpet Protein
LC-1	anti-liver cytosol antibodies
LKM-1	anti-liver kidney microsomal antibodies
LSEC	liver sinusoidal endothelial cells
MBP	Myelin Basic Protein
MFI	median fluorescent intensity
MHC	Major histocompatibility complex
MoA	mechanism of action
moDC	monocyte-derived dendritic cells
MOG	Myelin Oligodendrocyte Protein
MS	multiple sclerosis
MTb	*Mycobacterium tuberculosis* H37Ra
mTEC	medullary stromal cells
nTreg	natural T regulatory cells

pANCA	anti-perinuclear neutrophil cytoplasmic antibodies
PBC	primary biliary cholangitis
PBMC	peripheral blood mononuclear cells
PIT	peptide immunotherapy
PLP	Proteolipid Protein
PMA	phorbol 12-myristate 13-acetate
pMHC	Peptide loaded major histocompatibility complex
PPD	Purified Protein Derivative
PRED	prednis(ol)one
PSC	primary sclerosing cholangitis
RA	rheumatoid arthritis
RBC	red blood cells
RRMS	relapsing-remitting multiple sclerosis
SI	Stimulation Index
SLA/LP	anti-soluble liver antigen/liver-pancreas antibodies
SMA	anti-smooth muscle antibodies
ssDC	steady state dendritic cells
T1D	type 1 diabetes
TCR	T cell receptor
TMB	tetramethylbenzidine
Treg	Regulatory T cells
TSHR	thyrotropin receptor

CHAPTER 1

INTRODUCTION

1.1 T cell development and subsets

The effective functioning of the adaptive immune system is reliant on its extraordinarily sophisticated ability to distinguish and respond effectively to antigens of invading pathogens or cancer-associated neoantigens whilst maintaining a state of non-responsiveness to self-antigens of the body's own tissues.

T cell development in the thymus is fundamental to the establishment of self-tolerance, by systematic deletion of self-reactive T cells and the selection of $CD25^{high}$ $FoxP3^{+}$ regulatory T cell (Treg) (Gallegos and Bevan, 2004). T cell progenitors first undergo somatic rearrangement of the T cell receptor (TCR) α and β chain loci with insertion of non-coded nucleotides into the hyper-variable domains to produce novel TCR genes. Pairing of the resulting proteins generates a vast array of TCR with novel amino acid sequences in the complementarity determining regions (CDR) that typically dominate interactions with antigen (Marrack et al., 2008). It is estimated that each individual possesses an astounding 10^{15} different αβ TCR permutations (Arstila et al., 1999).

Inevitably, this immature thymocyte pool contains non-functional TCRs which are unable to bind antigen presenting major histocompatibility complexes (MHC) and TCRs which are reactive for self-peptides. Positive selection for immunocompetence is directed by the affinity between TCR and peptide-MHC (pMHC) complexes presented within the thymic cortex (Anderson and Takahama, 2012). Immature thymocytes carrying TCRs with no pMHC engagement die by neglect, those with high self-affinity TCRs receive apoptotic

signals, and low-affinity engagement leads to induction of survival signals (Starr et al., 2003). This drives their differentiation into single positive (SP) $CD8^+$ or $CD4^+$ thymocytes depending on whether they engage MHC Class I or MHC Class II molecules. Subsequent negative selection within the thymic medulla is mediated by dendritic cells presenting endogenous antigens and medullary stromal cells (mTEC) expressing the autoimmune regulator gene (AIRE). AIRE enables mTEC to express self-antigens which would not ordinarily be present in the thymus (Liston et al., 2003). SP thymocytes with high affinity for tissue-specific self-antigens are deleted by apoptosis. Low affinity thymocytes are allowed to enter the periphery (Palmer, 2003).

Thymic processes are also responsible for generating an essential moderator of autoreactivity, thymic resident and peripheral T regulatory cells (tTreg & pTreg). pTreg are essential to prevent systemic autoimmunity (Sakaguchi et al., 1995) through active suppression of pathogenic autoreactive T cells in the periphery (Piccirillo and Shevach, 2004). Treg have been shown to undergo stronger TCR signalling during positive selection compared to conventional $CD4^+$ T cells and compete for intermediate and high-affinity self-ligands in the thymus (Moran et al., 2011). TCR engagement in the thymus activates intracellular NF-KB signalling, directly promoting the expression of Treg master transcription factor FoxP3 (Long et al., 2009). pTreg can also be generated *de novo* within the periphery, particularly during the resolution of immune responses.

However, these selection processes are not perfect. Low affinity self-reactive T lymphocytes that have 'escaped' the checkpoints of central tolerance can potentiate autoimmune reactivity (Liu et al., 1995). Escaped self-reactive T cells are controlled in healthy individuals by peripheral tolerance mechanisms, including ignorance of tissue-

specific self-antigens by physiological segregation, the removal of T cell co-stimulation (Jenkins and Schwartz, 1987), deletion by activation-induced cell death (Alderson et al., 1995), the induction of T cell anergy (DeSilva et al., 1991), and suppression mediated by nTreg and iTreg (Sakaguchi et al., 2009).

1.2 Antigen processing, T cell activation and regulation

The MHC locus, known as human leukocyte antigen (HLA) in the human setting, is one of the most polymorphic regions of the mammalian genome (Flajnik and Kasahara, 2001). This polymorphism is intrinsic to the success of the immune system, maintaining diversity of haplotypes within the population, in addition to enabling each haplotype to bind a wide range of self and pathogen-derived peptide antigens which in turn are recognised by TCR present on T lymphocytes. HLA haplotypes may diverge considerably (>30 amino acids) or by only a few amino acids - termed micro-polymorphism (Marsh et al., 2010).

MHC Class I molecules are located on the surface of almost all nucleated cells and present peptides derived from intracellular sources via the cytosolic proteasomal degradation pathway (Fig.1.1) to $CD8^+$ T cells. The Class I repertoire therefore consists predominantly of virally-encoded peptides and self-peptides. In contrast, MHC Class II are located primarily on specialised antigen presenting cells (APC), such as dendritic cells (DC), which reside in environment-exposed sites, capturing extracellular antigenic material by phagocytosis or endocytosis prior to enzymatic antigen processing within the endosomal compartments and loading onto MHC-II. Endosomal antigen processing involves multiple enzymes which function most effectively in the acidic pH of the endosome: protein unfolding using thioreductases (Jensen, 1991; Collins et al., 1991),

generation of large fragments using endopeptidases (e.g. cysteine protease cathepsins and aspartic protease cathepsins) (Van Der Drift et al., 1990), and trimming peptide ends once loaded onto MHC-II using exopeptidases (Turk et al., 2000). The structure of the MHC Class II peptide binding groove is open-ended, meaning that the length of binding peptides is not limited by enclosing MHC-II loops. As such, MHC-II can bind significantly longer peptides (average length 15-17aa) with greater flexibility for presentation to $CD4^+$ T cells.

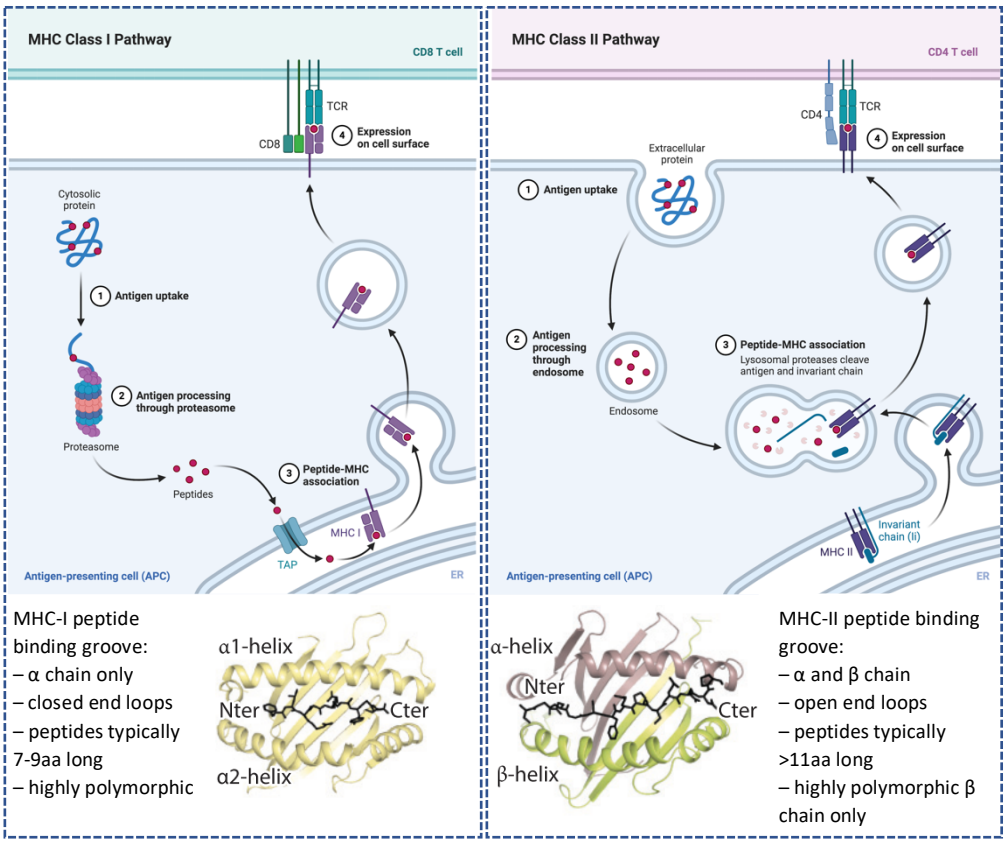

Figure 1.1: Summary of MHC Class I and Class II antigen processing and presentation pathways. Left: Cytosolic proteins typically undergo proteasomal cleavage to generate short peptides for loading onto MHC-I molecules within the endoplasmic reticulum (ER). The closed structure of the MHC-I peptide cleft is encoded by the MHC-I α chain and is biased towards shorter peptides. **Right:** Antigen presenting cells take up extracellular proteins into early endosomes where proteases (e.g. cathepsins, aminopeptidases etc.) generate peptides for loading onto MHC-II in late endosomes. The structure of the MHC-II peptide cleft is open ended and can accommodate longer peptides. Usually the core binding region is around 9aa, but the surrounding peptide flanking regions (PFR) make significant contribution to MHC-II binding affinity. Figure generated using Biorender and Pymol.

Precise regulation of T cell activation is critical to effective immune responses and homeostasis. TCR-pMHC engagement initiates intracellular signalling cascades involving transcription factor activation and cytoskeletal remodelling that ultimately leads to T cell activation, regulation of cytokine production, proliferation, cell survival and differentiation (Smith-Garvin et al., 2009; Hwang et al., 2020). On a single cell level, T cell stimulation must meet threshold requirements for full activation; determined by TCR-pMHC affinity and interaction duration, as well as supporting signals via costimulatory molecule CD28 and cytokines which support T cell survival and differentiation into effector populations (Zikherman and Au-Yeung, 2015). CD28 ligation reduces stimulation threshold required for T cell activation and promotes T cell survival by induction of anti-apoptotic protein BCL-XL (Boise et al., 1993). If TCR-pMHC-II binding occurs without

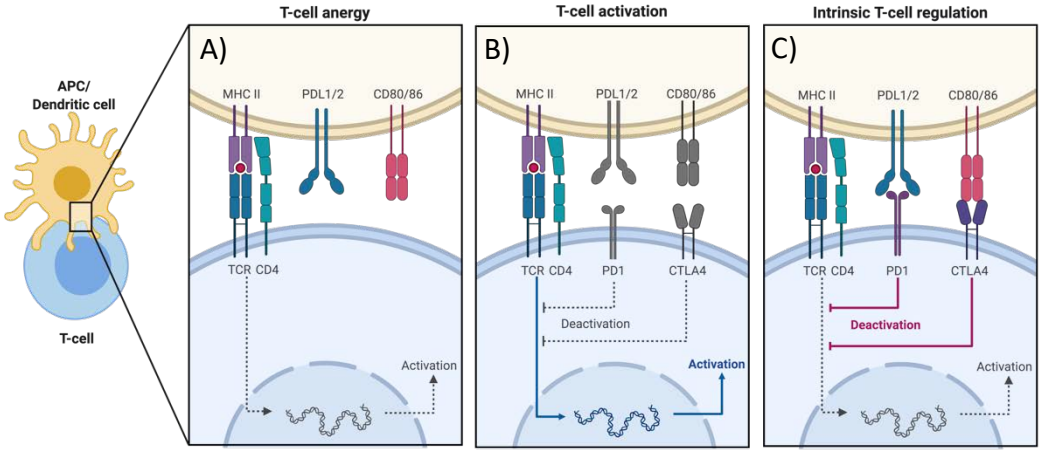

Figure 1.2: Summary of T cell signalling outcomes based on activation and regulation pathways induced by TCR engagement and supporting costimulatory and coinhibitory molecules. Engagement of pMHC-II and TCR at an immune synapse can lead to: **A)** T cell anergy if pMHC-II-TCR ligation occurs without costimulatory help from CD80/CD86 binding to T cell CD28, **B)** T cell activation if pMHC-II-TCR ligation occurs with costimulatory help from CD80/CD86 binding to T cell CD28 (amongst other activating signals), or **C)** T cell regulation if pMHC-II-TCR ligation occurs alongside interaction of co-inhibitory negative signal regulators (e.g. PD-1 and CTLA-4).

costimulation, cells are unable to be fully activated and instead enter a state of non-responsiveness, or anergy. Conversely, coinhibitory molecules (e.g. CTLA-4, PD-1) exert inhibitory signals to negatively affect T cell activation (Riley et al., 2002; Greenwald et al., 2005). T cells express these molecules after activation to intrinsically, negatively regulate their function and prevent aberrant immune responses. The balance between activating and inhibitory signals is essential to mount effective immune responses to foreign/neo-antigens while maintaining immune homeostasis (Fig.1.2).

Regulatory T cells can suppress a wide range of immune cells, but primarily inhibit activation and expansion of naïve and memory Tconv, either by direct contact or indirectly via suppression of antigen-presenting cells. Granzyme^{+} Treg can induce apoptosis in activated Tconv using the perforin pathway (Grossman et al., 2004). Treg compete with Tconv for access to growth factor IL-2; Treg express the high affinity IL-2R, CD25, thereby acting as an IL-2 'sink' to inhibit Tconv survival and proliferation (Thornton and Shevach, 1998; de la Rosa et al., 2004) .

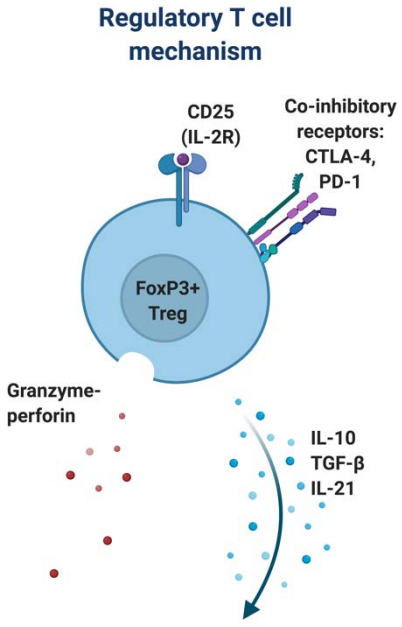

Figure 1.3: Treg suppressive mechanisms. Treg can inhibit Tconv survival and proliferation by scavenging growth factor IL-2 via their high affinity IL-2R, CD25. Treg can inhibit both Tconv and APC via secreted suppressive cytokines and via contact dependent coinhibitory receptors. Treg can also induce apoptosis in target cells via the granzyme-perforin pathway.

The role of Treg immunosuppressive cytokines is a core aspect of their function *in vivo* and in disease models (McGeachy and Anderton, 2005). TGF-β can be produced as membrane-bound and soluble forms upon Treg activation and blocking TGF-β signalling *in vitro* reduces Treg suppression of Tconv proliferation in some experimental settings (Nakamura et al., 2001, 2004) but not others (Piccirillo et al., 2002; Baecher-Allan et al., 2002). *In vivo,* the data is more clear; TGF-β knockout and deficient mice develop spontaneous T cell mediated autoimmunity (Li et al., 2006, 2007; Marie et al., 2006).

IL-10 is considered to be a master regulator of immune suppression and is produced by Treg upon activation, by non-conventional regulatory T cells most notably FoxP3$^-$ Tr1 cells, as well as activated Th2 and Th17 cells (Fiorentino et al., 1989; McGeachy et al., 2007). With the development of IL-10 GFP reporter mice, other cell types have shown the ability to produce IL-10, including regulatory B cells (Breg) (Mauri and Menon, 2017) and dendritic cells (Boonstra et al., 2006). IL-10 knockout and deficient mice do not develop systemic autoimmunity, but have a pronounced defect in controlling inflammation at localised barrier sites (Rubtsov et al., 2008) and are not able to respond positively to PIT and prevent experimental autoimmune encephalomyelitis (EAE) by peptide immunotherapy (PIT) (Burkhart et al., 1999).

Treg surface expression of co-inhibitory receptors also plays a significant role in immune suppression. For example, CTLA-4 is expressed constitutively on human and mouse Treg and is upregulated upon Treg activation (Takahashi et al., 2000; Dieckmann et al., 2001). CTLA-4 deficiency or blocking *in vivo* results in systemic autoimmunity, which can be recovered by transfer of CTLA competent Treg (Bachmann et al., 1999; Takahashi et al., 2000). CTLA-4 suppressive mechanisms include direct competition for

binding to APC costimulatory molecules CD80/CD86 to block Tconv activation (Van Der Merwe et al., 1997; Schneider et al., 2006) and inhibitory cell signal transduction to induce Tconv cell cycle arrest (Krummel and Allison, 1996). CTLA-4–CD80/CD86 interactions have been further elucidated to include an active process of CTLA-4 capture and trans-endocytosis of costimulatory molecules from CD80-GFP expressing cell lines (Qureshi et al., 2011; Hou et al., 2015). CTLA-4 signalling can render dendritic cells even more tolerogenic by upregulation of IDO expression after engagement with CD80/CD86 (Lippens et al., 2016). The specific functions of other coinhibitory receptors expressed at high levels by Treg: PD-1 LAG3, TIM3, TIGIT can also contribute to contact-dependent cell suppression by specialised mechanisms (Anderson et al., 2016).

1.3 Antigen-specific immunotherapy to treat autoimmune diseases

Autoimmune diseases display a diverse range of chronic inflammation and tissue damage disorders mediated by self-reactive immune cells. Autoimmune conditions have steadily increased in prevalence over recent decades, with current estimates suggesting 1 in 8 people worldwide have at least one autoimmune condition. Lerner et al., revealed rapidly increasing rates of rheumatic, endocrine, gastrointestinal and neurological autoimmune diseases of between 4 and 7% per annum (Lerner et al., 2015). The unmet need for curative therapies that target the immunological cause of disease has never been greater, as autoimmune diseases often require lifelong therapy involving broad-range immunosuppressive drugs which, at best, slow down disease progression.

Antigen-specific immunotherapy (ASI) offer the possibility of altering disease course by addressing their underlying cause, i.e. loss of immunological tolerance, by

suppressing alloreactive/autoreactive T cells in order to re-instate immunological balance. ASI has been practiced clinically for more than a century since Noon and Freeman's seminal findings that increasing subcutaneous dose of grass pollen could desensitize a hay-fever patient (Noon, 1911). ASI development in the contexts of both allergy and autoimmunity are discussed in detail in review (Richardson and Wraith, 2021).

Antigen-specific immunotherapy relies on the administration of disease-associated whole antigen or $CD4^+$ T cell epitope peptides. Use of whole antigen in allergies is a well-established approach designed to reduce IgE hyper-reactivity, downregulate Th2 activity and cytokine release, induce $FoxP3^+$ Treg cells and/or Tr1 cells, and generate long-lasting IgG blocking antibodies (Fig.1.4A) (Satoguina et al., 2005; Meiler et al., 2008; Möbs et al., 2012; Novak et al., 2012; Shamji et al., 2012). Whole allergen, however, can elicit unpredictable adverse reactions mediated by allergen-specific IgE (Maurer et al., 1994; Kehry and Yamashita, 1989). Genetically modified recombinant antigens with altered IgE-binding motifs to reduce the risk of IgE cross-linking, represent a powerful tool for engineering a safer product for desensitisation (Klimek et al., 2015; Campana et al., 2019). Alternatively, peptides representing $CD4^+$ T cell epitopes can be administered to induce similar mechanisms of allergen-specific tolerance and remove risk of IgE crosslinking events. Allergen-derived peptide delivery has shown efficacy in prevention of bee venom (Muller et al., 1998; Texier et al., 2000), grass pollen (Ellis et al., 2017), cat dander (Oldfield et al., 2002; Campbell et al., 2009), peanut (Jones et al., 2009; Wasserman et al., 2019) and birch pollen allergies (Möbs et al., 2010; Spertini et al., 2016).

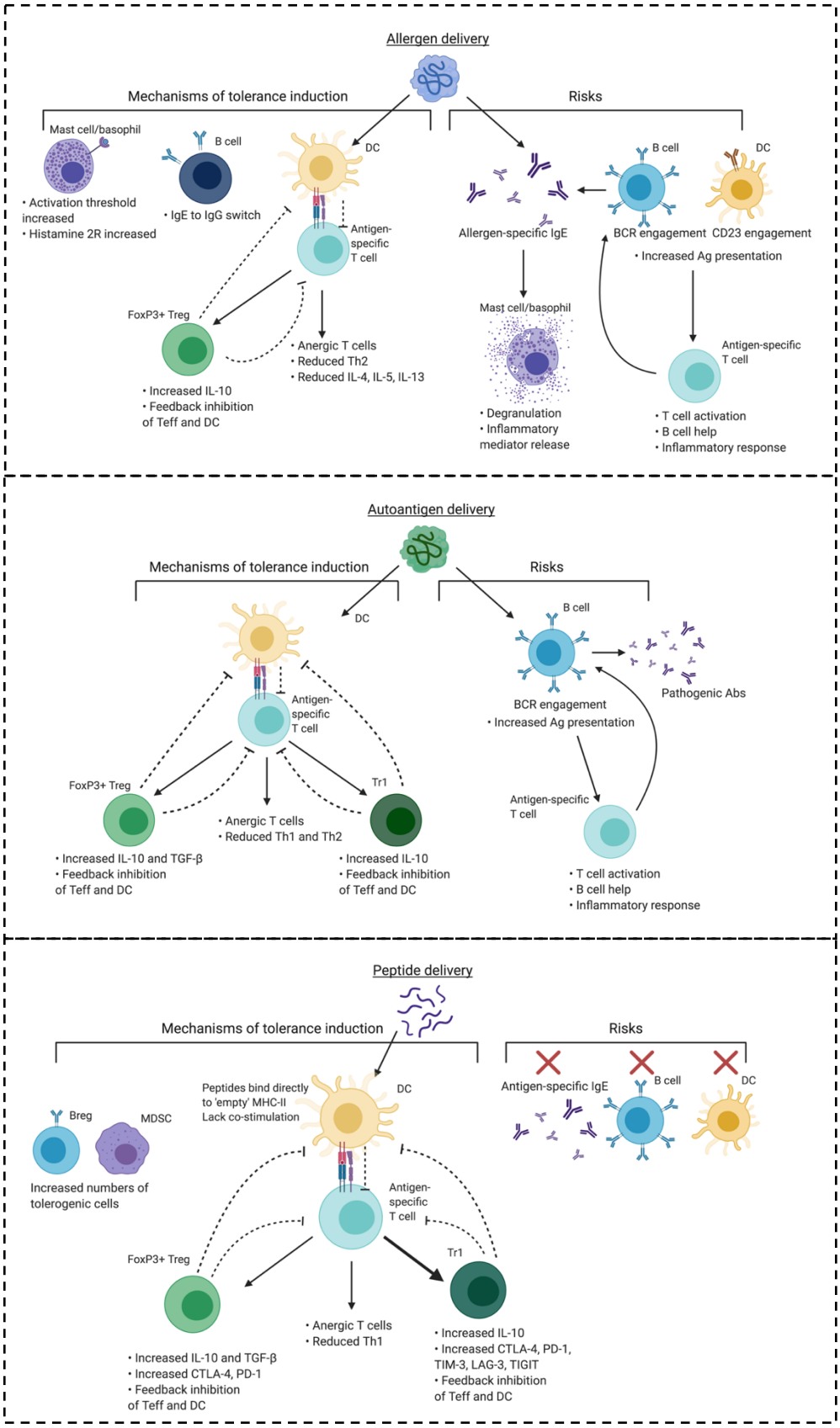

Figure 1.4: Summarised mechanism of action of ASI/AIT and associated risks. Antigen-specific immunotherapies have varying mechanisms of action and potential risks depending on whether they utilise **A)** intact allergen, **B)** intact autoantigen, or **C)** peptides representing T cell epitopes of either allergen or autoantigen. Promotion of activity denoted by black arrows, inhibition of activity denoted by black dashed lines and mitigation of risks denoted by red crosses.

In autoimmune disease settings, delivery of intact antigen is not appropriate, as it can also induce the generation of pathogenic antibodies, which could cause severe adverse reactions in patients (Fig.1.4B). The majority of early work in autoimmune disease ASI was in multiple sclerosis (MS). Myelin basic protein (MBP) accounts for $^1/_3$ of protein of the myelin sheath and is a major antigenic target for pathogenic T cells which promote neurodegeneration. MBP-specific T cells have been isolated from the central nervous system (CNS) and blood of MS patients and the blood of healthy individuals (Burns et al., 1983; Pette et al., 1990; Ota et al., 1990; Meinl et al., 1993). The first trials of antigen-specific immunotherapy to treat MS in the 1970s, injected whole antigen MBP isolated from human, porcine or bovine sources and did not promote immunological or symptomatic improvement (Campbell et al., 1973; Gonsette et al., 1977; Romine et al., 1980). The field then shifted towards mucosal tolerance, as experiments pioneered by Weiner and colleagues in a number of animal autoimmune diseases models, including EAE, showed overwhelming efficacy of fed antigen to prevent and reverse disease (Faria and Weiner, 1999). Unfortunately, in clinical trials, oral tolerance induction was deemed to be safe but ineffective (Eastwood and Reingold, 1997). This may have been due to the relative low doses of antigen used in patients compared to those tested in animals. For example, in order to desensitise patients orally with peanut allergy, 800mg of pure peanut protein was required (Syed et al., 2014). Such a high amount of protein would not only be extremely expensive if using recombinant protein, and highly inefficient due to degradation within the stomach prior to exerting tolerogenic effects in the gut. Further, self-antigens are much weaker antigens that allergens, requiring administration of yet higher doses of protein.

As such, concerted efforts to identify $CD4^+$ T cell epitope peptides from defined autoantigens has been a research focus (Fig.1.4C). T cell epitopes identified from MBP in EAE and MS patients enabled the development of one of the first peptide immunotherapy in autoimmune diseases (Anderton and Wraith, 1998; Mazza et al., 2002; Streeter et al., 2015; Prakken et al., 2004; Thrower et al., 2009). Defined T cell epitope peptides delivered in a tolerogenic manner (e.g. highly soluble, no adjuvant, dose escalation) control autoreactivity and prevent immunopathology in experimental models of EAE and other autoimmune diseases (Matta et al., 2010; Kang et al., 2005; Kuchroo et al., 1994), both by subcutaneous injection and intranasal inhalation (Metzler and Wraith, 1993; Bettelli et al., 2003).

At present, there have been 2 very promising clinical trials of peptide immunotherapy (ATX-MS-1467) in MS patients (Streeter et al., 2015; Chataway et al., 2018). Delivery of tolerogenic ATX-MS-1467 peptides over 16 weeks as part of a phase 1b trial in relapsing-remitting multiple sclerosis (RRMS) significantly reduced T1 gadolinium-enhanced (GdE) brain lesions by 78% throughout treatment, without any safety warnings (Chataway et al., 2018). New lesions remained reduced at study completion but returned to baseline on after treatment ended. This temporary nature of tolerance induction correlates with the duration of induced tolerance observed in euthymic mice (Metzler and Wraith, 1999).

Based on the success of work in MS, peptide immunotherapy is now being applied to other autoimmune diseases. The development of ATX-GD-59 to treat Graves' disease not only induced T cell tolerance towards the autoantigen thyrotropin receptor (TSHR), but also B cell tolerance by measuring a reduction in αTSHR antibodies in a HLA-DR3

restricted challenge model (Jansson et al., 2018). Recent translation to Phase 1 clinical trial resulted in improved free thyroid hormone levels in 7/10 patients treated, indicating the potential for treating Graves' hyperthyroidism using this novel immunotherapy (Pearce et al., 2019).

These clinical studies highlight the disease-modifying effects of peptide immunotherapy and provides significant support for further clinical trials in these disease settings, as well as translation of PIT to a wider range of autoimmune diseases. The complexity of autoimmune diseases poses a significant challenge, as immune responses vary considerably between patients and at different time points of disease progression (Mazza et al., 2002; Ponsford et al., 2001). At present, our knowledge of disease-initiating and propagating autoantigens in many autoimmune diseases is woefully incomplete and further complicated by epitope spreading (Vanderlugt and Miller, 1996). Autoimmune diseases with clearly defined single antigen targets are likely to be more amenable to resolution using peptide therapies, unless complex mixtures of tolerising peptides are used. To alleviate the requirement for successful targeting of every single T cell reactive region of every contributing autoantigen, novel interventions should attempt to induce bystander suppression (Introduction 1.5)

1.4 Cellular and molecular mechanisms of peptide immunotherapy

Previous research from the Wraith group has determined key mechanistic understanding of peptide immunotherapy, primarily using the Tg4 transgenic mouse model, in which >90% of $CD4^+$ T cells are specific to the MBP_{Ac1-9} peptide (Liu et al., 1995). Delivery of escalating dose of high affinity MBP_{Ac1-9} [4Y] peptide will induce antigen-specific tolerance

via expansion of regulatory FoxP3$^-$ Tr1 cells and IL-10 dependent feedback mechanisms sufficient to prevent MBP-driven EAE (Liu and Wraith, 1995; Sundstedt et al., 2003a; Gabryšová et al., 2009a).

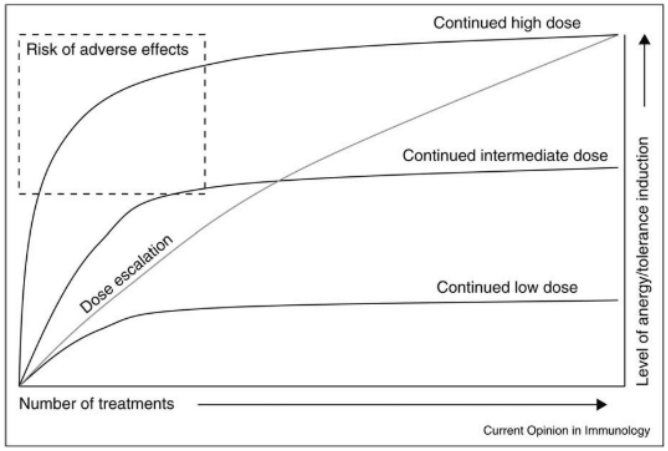

Figure 1.5: Peptide immunotherapy dose escalation rationale. Dose escalation enables high dose of antigen to be delivered, sufficient to generate significant tolerance induction, whilst avoiding adverse events.

Sabatos-Peyton CA, Verhagen J, Wraith DC. Antigen-specific immunotherapy of autoimmune and allergic diseases. *Curr Opin Immunol* (2010) **22**: 609–615.

The escalating dose protocol is integral to the safety and efficacy of peptide-based tolerance induction (Fig.1.5). Repeated administration of high-dose/affinity antigen is able to induce the highest level of tolerance but has higher risk of side effects. Low-dose antigen by contrast, reduces risk but does not induce robust tolerance (Gabryšová and Wraith, 2010; Sabatos-Peyton et al., 2010). In fact, the initial low doses re-program antigen-specific T cells gradually both at the epigenetic, transcriptome and protein level (Burton et al., 2014; Bevington et al., 2020), allowing for high doses required for robust tolerance without induction of adverse effects.

The mechanism of action of peptide immunotherapy in this context is summarised in Figure 1.6. Short, soluble peptides representing T cell epitope delivered in a tolerogenic manner (i.e. peptide alone without adjuvant) are selectively taken up by steady state dendritic cells (ssDC) in lymphoid organs for presentation to cognate T cells without the need for antigen processing and are therefore coined antigen-processing independent

epitopes or apitopes. Shepard, et al., show that MBP_{Ac1-9} [4Y] peptide can be detected on the surface of Tg4 mouse splenic ssDC, but not B cells or monocytes up to 2 hours after one dose of MBP_{Ac1-9} [4Y] subcutaneously (Shepard et al., 2021). ssDC are tolerogenic and well-suited to promote the restoration of Teff vs Treg balance. A proportion of MHC Class II on ssDCs are 'empty' or transiently loaded with low affinity peptides (Santambrogio et al., 1999); therefore, higher affinity exogenous peptides delivered in an ASI can bind directly to MHC-II for presentation to $CD4^+$ T cells. ssDC provide low levels of costimulation (CD80/CD86) to T cells and are less efficient in antigen uptake and presentation (Hawiger et al., 2001; Steinman et al., 2003). As such, both naïve and effector/memory antigen-specific T cells do not receive sufficiently activatory signal

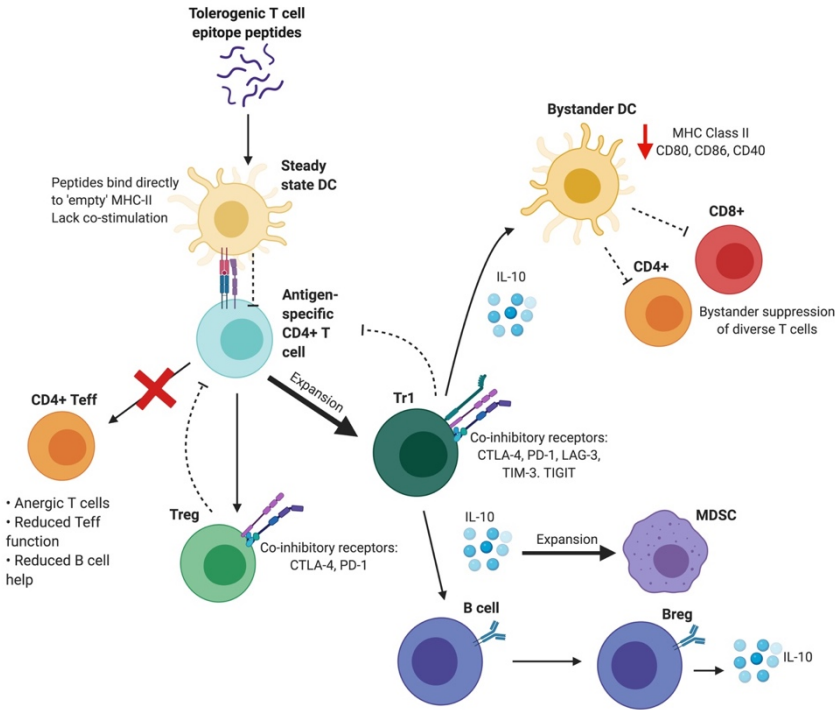

Figure 1.6: Mechanism of action of peptide immunotherapy using apitopes. Repeated doses of soluble peptides representing T cell epitopes can bind directly to transiently loaded MHC-II on ssDC. These DC are unable to properly prime and activate antigen-specific T cells, resulting in T cell anergy and conversion to IL-10^+ FoxP3^- Tr1 cells which are epigenetically primed at tolerance signature genes. Tolerised Tr1 cells are no longer able to respond to the target antigen and are able to exert bystander regulatory effects on neighbouring DC to downregulate immune responses in a non-antigen specific manner. MDSC generation and increased IL-10^+ Bregs have been reported in mouse models.

from TCR engagement alone to become activated (Mueller et al., 1989) and can instead be diverted into a state of functional anergy (Gimmi et al., 1993) by repeated antigen exposure in which they no longer respond to antigen via classical inflammatory signalling pathways but instead exert a regulatory phenotype.

Shepard, et al. also highlighted the importance of peptide solubility to the safety and efficacy of peptide immunotherapy. Whereas repeated doses of the highly soluble $MBP_{Ac1\text{-}9}$ [4Y] peptide were readily captured by ssDC and were able to generate T cell tolerance towards MBP protein and protected against EAE disease development, increasingly insoluble variants of this peptide were not able to dissipate freely to reach the ssDC and were not able to establish tolerance (Shepard et al., 2021). Instead, insoluble peptides can aggregate at the site of injection or be captured by inflammation-biased skin DC, instead switching the outcome towards localised hypersensitivity and inflammatory mediator release.

Throughout the dose escalation protocol, antigen-specific T cell engagement of TCR with tolerogenic peptide establishes epigenetic priming of both inflammatory and tolerance-related gene blocs. Analysis of chromatin structure showed that tolerised T cells are less inducible at immune response gene sites, such as Il2, Il3, Tnf, Csf2, Ccl1, Cd40lg, Nr4a3, and Nfkb1, whilst becoming more inducible for anergy/tolerance-associated genes, including inhibitory receptors Ctla4, Tigit, Lag3, Havcr2 (TIM-3), and Pdcd1 (PD-1), the transcription factors Nfil3 and Maf, and the immune-suppressive cytokines IL-10 and IL-21 (Bevington et al., 2020). This programming is reflected at the transcriptome and proteome level, with tolerised T cells progressively becoming more anergic/tolerised in phenotype over the course of treatment, with key distinguishing cell

surface markers being TIGIT, TIM-3, LAG-3, CTLA-4, intracellular transcription factors cMAF and Nfil3 and increased secretion of IL-10. Tolerised antigen-specific Tr1 cells do not express FoxP3 mRNA or protein, therefore are not classical Treg (Burton et al., 2014). Where others have highlighted the similarity of the Tr1 phenotype to exhausted T cells observed in cancer (Anderson et al., 2016), Tr1 suppressive cells in our PIT model are highly functional, as their surface marker and IL-10 expression is tightly linked to stimulation with antigen. Furthermore, stimulation of peptide-induced Tr1 with IL-2 *in vitro* restores their ability to proliferate in response to antigenic stimulation, effectively 'rescuing' them from their state of anergy (Anderson et al., 2005).

As a result of tolerance induction, $CD4^+$ T cell immunity directed towards the target antigen is quenched and Teff cell proliferation and secretion of IFN-γ/IL-2 are suppressed in an IL-10 dependent manner (Sundstedt et al., 2003a; Gabryšová et al., 2009a). Gabrysova et al., determined that activated Tr1 cells limit the expression of CD80/CD86 on the surface of naïve dendritic cells *in vitro* (Gabryšová et al., 2009a) in an IL-10 dependent manner. Inhibited dendritic cells also produce lower levels of IL-12. As such, dendritic cells in close proximity to tolerised Tr1 cells are themselves rendered tolerogenic and are less able to activate subsequent T cells (antigen-specific or non-specific) and promote their differentiation to Th1 cells. This is hypothesised to be the primary mechanism by which peptide immunotherapy can establish bystander suppression.

1.5 Bystander suppression: relevance to ASI and proposed mechanisms

'Linked suppression' occurs when antigen-specific T cell tolerance induction to an immunodominant epitope of Antigen A leads to suppression of immune responses against other epitopes within Antigen A. 'Bystander suppression' enables antigen-specific T cells directed against Antigen A to directly and/or indirectly dampen immune responses against Antigens B, C, etc., by involvement of T cell mediated suppression of antigen presenting cells as well as neighbouring T cells of different specificities. These two terms are at times used interchangeably in the literature but were first coined by Howard Weiner in his investigations of oral tolerance induction (Miller et al., 1991). As identification of disease-relevant autoantigens and T cell epitopes is challenging, and at present we have limited understanding of the autoantigenic profile of highly complex autoimmune diseases, effective bystander suppression may alleviate the requirement for comprehensive knowledge of the autoantigen(s) and circumvent the need to induce tolerance to all epitopes within an autoantigen.

The process by which tolerance can be 'spread' is still poorly understood, although its presence has been demonstrated in murine models of autoimmune diseases and in the context of allergy. Anderton et al., revealed a tolerogenicity hierarchy between three EAE-relevant encephalitogenic peptides derived from myelin: MBP_{Ac1-9}, MBP_{89-101} and proteolipid protein $PLP_{139-151}$, each showing differential abilities to induce antigen-specific tolerance and multi-antigen bystander suppression. Delivery of MBP_{Ac1-9} was able to induce tolerance in MBP_{Ac1-9}-specific T cells and to MBP_{89-101}-specific T cells, therefore exhibiting linked suppression. MBP_{89-101} was poorly tolerogenic, later shown to be due to the peptide having a dominant cryptic epitope (Anderton et al., 2002). By contrast,

tolerance induction using $PLP_{139-151}$ peptide was able to control T cell responses not only towards $PLP_{139-151}$, but also towards MBP_{Ac1-9} and MBP_{89-101} by bystander suppression. The ability for tolerance to $PLP_{139-151}$ to 'spread' to the MBP epitope peptides was reliant on $PLP_{139-151}$-treated mice being immunised with whole MBP antigen, as opposed to MBP epitopes separately. This suggests the need for MBP antigenic epitopes to be presented within the draining lymph node at the same time as the tolerogenic $PLP_{139-151}$ peptide for the bystander effect to occur. Importantly, the bystander effect was sufficiently strong when treating with $PLP_{139-151}$ that EAE induced not only by PLP protein but also either MBP protein was suppressed (Anderton and Wraith, 1998). In cat allergy, peptide-induced tolerance to Fel d1 not only suppressed patient responses to Fel d1 but also to cat dander - a mixture of multiple cat allergens (Campbell et al., 2009).

The role of IL-10 is thought to be central in establishing broader regulation following antigen-specific therapy. The pleiotropic regulatory cytokine IL-10 can be secreted by anergic Tr-1 like cells, Treg, Breg and dendritic cells (Ng et al., 2013). Its role in establishing bystander suppression is proposed to be due to its ability to downregulate costimulatory molecules and MHC-II on the surface of APCs (Sundstedt et al., 2003a; Perona-Wright et al., 2007; Corinti et al., 2001). This suppresses the antigen-presentation and T cell priming potency of APCs, thereby reducing the likelihood of subsequent immune responses not only to the initial antigen targeted but also other disease-relevant antigens within the inflamed tissue. The Delta1-Notch-1 pathway has been suggested to play a role in a model of linked suppression, as upregulation of Delta1 on tolerised T cells can engage Notch1 on neighbouring T cells to suppress their expansion (Hoyne et al., 1997, 1999). Tolerance induced Tr1 cells also express increased levels of coinhibitory receptors CTLA-4, LAG-3, PD-1 and TIGIT (White and Wraith, 2016; Burton et al., 2014).

CTLA-4 is known to be highly suppressive towards antigen-presenting cells by stripping off CD80/CD86 from the APC surface, reducing capacity for downstream T cell activation (Hou et al., 2015; Ovcinnikovs et al., 2019). Furthermore, signalling via CTLA-4 promotes T cells to secrete TGF-β (Chen et al., 1998). Treg clones induced by ingestion of MBP protein generated high levels of both TGF-β and IL-10 (Faria and Weiner, 1999). These cells were also able to prevent EAE when disease was initiated via MBP or PLP – highlighting the bystander effects (Chen et al., 1994).

Antigen-specific immunotherapies based on single antigen specificities are unlikely to be as effective in complex and dynamic multi-antigen diseases such as type 1 diabetes (T1D) and rheumatoid arthritis (RA) unless they can evoke strong 'bystander suppression' controlling pathogenic T cells of multiple antigen-specificities (Anderton and Wraith, 1998). Therefore, understanding the mechanism of action of bystander suppression and how best to incorporate it into peptide-based or carrier system-based ASI will prove crucial to resolve the dilemma of which antigen(s) to target in a specific disease.

1.6 Carrier systems in development for ASI

The Wraith lab and others have reviewed the vast range of carrier systems under development for the treatment of autoimmune and allergic conditions previously (Serra and Santamaria, 2019; Wraith, 2018, 2016; Richardson et al., 2020). Briefly, carrier systems are broadly based on the central themes: i) targeting the DC:T cell interaction and ii) targeting antigens to the liver where liver tolerance mechanisms can establish

intra- and extra-hepatic tolerance. The current approaches in development are summarised in Fig.1.7.

a) Autologous tolerogenic cells

Immature dendritic cells are tolerogenic in the steady state; express low levels of MHC Class II, CD80, CD86 and CD40 costimulatory molecules. Only after encountering danger signals (e.g. PAMPs) do dendritic cells become potent T cell activating agents. Certain populations of DC, e.g. liver DC produce IL-10 in response to stimulation in order to maintain tolerance (Goddard et al., 2004). If antigens are presented by immature dendritic cells, T cells are not stimulated sufficiently and instead are diverted into anergy, apoptosis or regulatory T cell phenotypes, as in direct peptide-based immunotherapy (Perona-Wright et al., 2007; Shepard et al., 2021). As such, a number of groups have developed methods to generate standardised monocyte-derived DC populations (moDC) which can be treated with Vitamin D3 or rapamycin to increase their tolerance induction potential (Morelli and Thomson, 2007; Domogalla et al., 2017). Normally, tolDC are 'fed' antigen prior to re-infusion to direct their function towards specific antigens. In RA, tolDC generated by two different approaches, (i) dexamethasone, vitamin D3 and monophosphoryl lipid A or ii) inhibition of the NF-KB pathway, possess distinct tolerogenic phenotypes and have progressed to testing in the clinic (Hilkens et al., 2010; Bell et al., 2017; Benham et al., 2015). Importantly, these drug treatments rendered tolDC refractory to inflammatory signals *in vitro* which would usually reverse their tolerogenic state.

b) Peptide MHC-II Nanoparticles (pMHC-NP)

Santamaria and colleagues have developed artificial APCs; nanoparticles coated with MHC Class II and antigenic peptide (Clemente-Casares et al., 2016). Antigen is delivered to T cells in the context of engineered MHC-II without costimulation, establishing immunological tolerance by inducing IL-10 expressing $CD4^+$ T cells through a negative feedback mechanism (Metzler and Wraith, 1993; Gabryšová et al., 2009b; Clemente-Casares et al., 2016; Gabryšová and Wraith, 2010; Umeshappa et al., 2019). The resulting

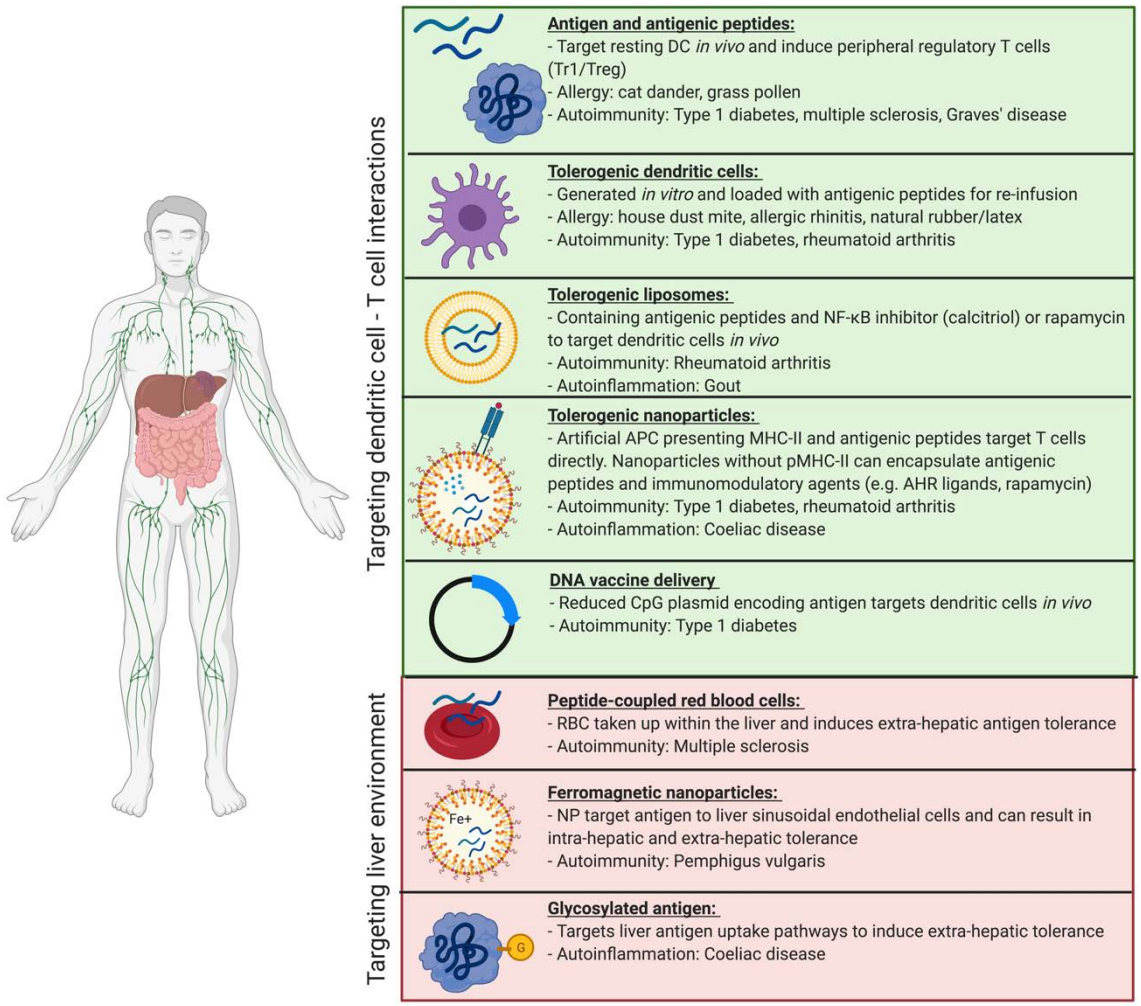

Figure 1.7: ASI approaches currently in development broadly target DC:T cell interactions or tolerogenic liver compartment to re-instate immune tolerance. Antigen-specific immunotherapies range from simple antigen/peptide only approaches to complex carrier systems for antigen delivery. Each approach in development are listed with their key features and any allergic or autoimmune diseases they have been applied to in pre-clinical/clinical assessments.

Tr1 cells express IL-10 and co-inhibitory receptors (Groux et al., 1997; Gagliani et al., 2013), but have also been reported to express low levels of inflammatory cytokines such as TNF-α, IL5 and GM-CSF (Singha et al., 2017), which may render them less appropriate in allergic contexts. Their recent murine studies show the trafficking of these nanoparticles to the liver, where they were able to induce antigen-specific tolerance to murine liver autoantigens CYP2D22 and FTCD (Umeshappa et al., 2019, 2020). They also report strong bystander suppression effects between one liver autoantigen and another, which is particularly encouraging. Further promising data has shown ferromagnetic particles loaded with antigenic peptides target the liver sinusoidal endothelial cells (LSEC) to generate antigen-specific FoxP3$^+$ Treg within the hepatic compartment, which are then able to control autoimmunity elsewhere (Carambia et al., 2015). This data supporting the use of ferromagnetic liver-targeting NP and the apparent success of erythrocyte-based antigen delivery (Kontos et al., 2013) suggests that targeting antigens to the liver may offer a route to achieve either intrahepatic or extrahepatic tolerance induction.

c) Liposomes:

Typically, tolerogenic liposomes involve the encapsulation of antigenic peptides alone or with additional immunosuppressive agents, including rapamycin (Getts et al., 2012; Maldonado et al., 2015; Saito et al., 2019). These liposomes are likely to interact with different APC populations based on their size, as large nanoparticles (>400nm) are sequestered within the liver, whereas smaller nanoparticles are able to interact directly with ssDC within draining lymph nodes (Hartwell et al., 2015). The primary effect of such liposome treatments in mouse models of autoimmune disease was the induction of FoxP3$^+$ Treg, indicating a potentially different mechanism of action (MoA) to peptide immunotherapy or artificial APCs (Getts et al., 2015).

d) Peptide conjugated erythrocytes

Red blood cells (RBC) coated with tolerogenic peptides prior have been reported to target macrophages and Kupffer cells (KC) in the spleen and liver, respectively, to promote expansion of $FoxP3^+$ Treg cells (Grimm et al., 2015; Kontos et al., 2015). RBC and larger liposomes which target the liver as a site for tolerance induction take advantage of the liver's propensity to maintain tolerance in the face of constant supply of blood-borne and gut antigens. Heymann and colleagues elucidated that KC induce tolerance by tracking OVA-loaded liposomes using intra-vital microscopy. KC were the primary cell type within the liver to internalise labelled particulates and promoted the expansion of $CD25^+FoxP3^+$ OVA-specific Treg *in vivo*. (Heymann et al., 2015).

Although each of these carrier system approaches have been tested in pre-clinical mouse models of autoimmune disease, so far only apitopes and tolerogenic DCs have been translated to completed, published clinical trials. Thus far, only the peptide-based approach has been adapted for treatment of allergic diseases. Any one of these novel carrier approaches could improve on currently available peptide-only methods; however, caution must be taken when using such carrier systems over long periods of time. It is most likely that tolerance induction via carriers will be temporary, consistent with peptide immunotherapy trials of MS patients. Therefore, patients will need regular and long-term administration of tolerogenic NP/cells. Injection of high numbers of NP/cells in repeated doses increases the risk of aggregation and/or the development of anti-drug antibodies towards these interventions. This would inhibit the treatment benefit whilst potentially causing harmful immunological effects. To our knowledge, none of these

carrier systems have been monitored in mouse or human settings to determine the duration of tolerance induced, the need for repeated administration or the immunological risks associated with long-term maintenance therapy.

We argue that there is sufficient evidence both in pre-clinical and clinical settings for the efficacy and safety of peptide immunotherapy without the need for a carrier system. If peptides are selected from autoantigens properly and carefully assessed, their tolerogenic potential is extremely powerful. We would also argue that short-term immune suppression may be required to control immune pathology in cases where autoimmune/inflammatory damage is ongoing and difficult to overcome, but that PIT could subsequently be used to establish and maintain specific tolerance over longer periods of time.

1.7 Introduction to liver immunology

The liver is a critical organ involved in immune tolerance. As the liver receives both arterial blood and blood from the gut via the portal vein, it is regularly exposed to both dietary and microbial antigens, which could establish excessive and prolonged inflammation, tissue damage and fibrosis if unregulated. Therefore, diverse populations of immune cells, stromal cells and hepatocytes work in synergy to resolve localised inflammation and avoid unnecessary immune responses to innocuous stimuli (Jenne and Kubes, 2013; Crispe, 2009). The liver microenvironment is well adapted to maintain homeostasis due to its unique populations of APC with tolerogenic characteristics, feedback mechanisms to control inflammation, high density of innate immune cells and

richness of suppressive soluble mediators, summarised in Fig 1.8 (Richardson et al., 2020).

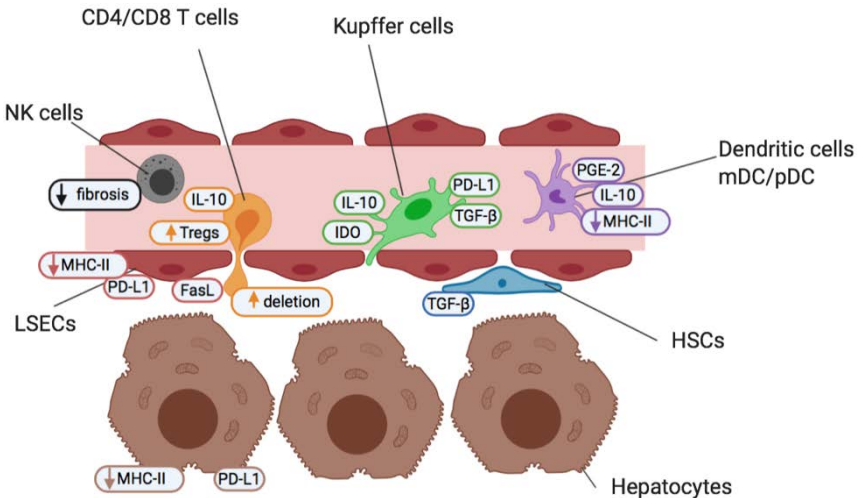

Figure 1.8: Cells of the liver sinusoid environment and their functions help maintain a state of homeostatic tolerance in the liver. Non-parenchymal resident Kupffer cells, hepatic stellate cells (HSC) , liver sinusoidal endothelial cells (LSECs) and dendritic cells (myeloid mDC and plasmacytoid pDC) form an early detection system at liver sinusoids. They contribute to the maintenance of a TGF-β and IL-10 rich cytokine milieu under steady-state conditions. High numbers of innate-like NK cells, MAIT and γδT cells are present. NK cells act as pro-inflammatory agents, and promote the recruitment of effector immune cells, but are also key regulators of fibrosis. Both APCs and hepatocytes offer reduced antigen-presentation capacity and lower levels of costimulation than other APCs elsewhere in the body. This maintain a state of "active" tolerance, whereby if required, inflammation and T cell activation is readily engaged.

1.8 Autoimmune liver diseases

Autoimmune liver disease (AILD) are divided into 3 distinct clinical diagnoses, autoimmune hepatitis (AIH), primary biliary cholangitis (PBC) and primary sclerosing cholangitis (PSC). They are distinguished by the molecular and cellular targets of immune pathology alongside the location of observed liver damage (Fig.1.9). PBC and PSC both affect cholangiocytes lining bile ducts, with PBC predominantly destroying small, interlobular bile ducts while PSC targets larger bile ducts and is characterised by

inflammatory fibrosis in the intrahepatic and extrahepatic biliary tree (Talwalkar and Lindor, 2003; Karlsen and Boberg, 2013). In AIH, the target is hepatocytes themselves, leading to interface hepatitis and significant lymphocyte infiltration primarily around the portal tracts (Geller, 2014). All 3 diseases develop to severe liver fibrosis without medical intervention.

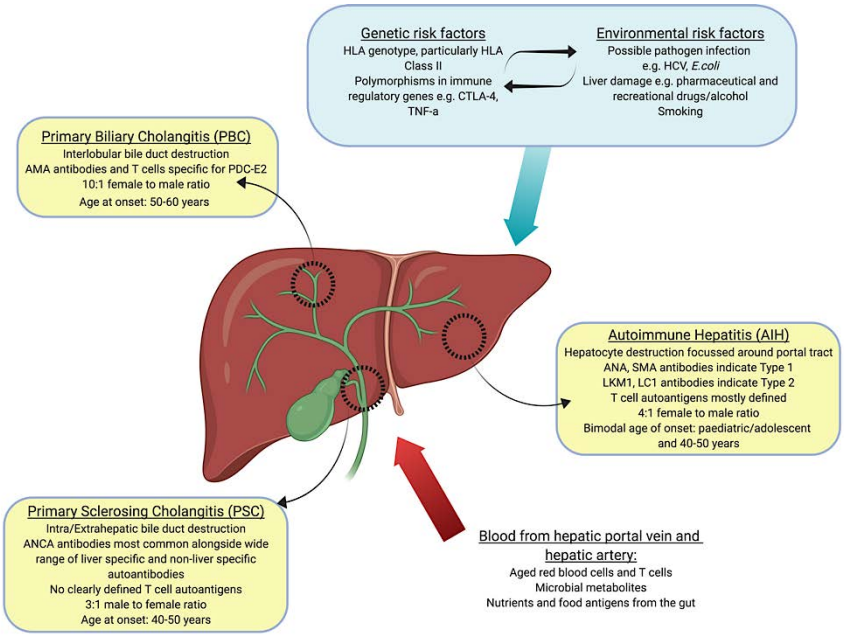

Figure 1.9: Summary of autoimmune liver diseases, liver tissues affected and key features (yellow boxes). Blood borne factors challenge the maintenance of immune tolerance are listed as inputs (red arrow). Genetic, environmental and lifestyle factors which could affect the maintenance of tolerance are listed as inputs (blue box and arrow).

AIH disease characteristics and epidemiology

Based on the current understanding of autoantigens in autoimmune liver diseases and the severe unmet clinical need in AIH, the remainder of this Introduction will focus mainly on AIH leading into the application of peptide immunotherapy to autoimmune hepatitis. Autoimmune hepatitis is a chronic progressive liver disease that is female biased (70-80% female) and can be diagnosed in adults and children of any age or ethnicity (European Association for the Study of the Liver, 2015). However, AIH does have a broadly bimodal

distribution of presentation in childhood/early juvenile years or in middle age (Manns et al., 2010; European Association for the Study of the Liver, 2015). AIH is rare, affecting between 16-20 individuals per 100,000 (Boberg et al., 1998; Ngu et al., 2010; Van Gerven et al., 2014; Werner et al., 2008) but appears to be increasing in prevalence. A long-term Danish study observed an almost two-fold increase in the annual incidence rate of AIH between 1994 and 2012 (Grønbæk et al., 2014). King's College Hospital hepatology referral centre has reported a seven-fold increase in AIH referrals over the past 30 years (Vergani et al., 2007). Patients range from asymptomatic to acute liver disease at diagnosis with no pattern identified to classify patients most at risk from rapid progression. Early diagnosis is critical to improved outcome. Cirrhosis is already present in a third of adult AIH patients and half of children at diagnosis and is the primary risk factor associated with development of hepatocellular carcinoma (HCC) (European Association for the Study of the Liver, 2015). To benefit early diagnosis, the International Autoimmune Hepatitis Group (IAIHG) developed a scoring system based on specific symptomatic, biochemical and tissue criteria (Alvarez et al., 1999; Hennes et al., 2008).

AIH diagnosis and autoantigens

Hypergammaglobulinemia and elevated aminotransferase enzyme levels (ALT & AST) are indicators of chronic liver damage and the presence of circulating liver-specific autoantibodies confirms abnormal immune regulation, according to IAIHG guidelines (Alvarez et al., 1999; Hennes et al., 2008). A biopsy indicating lymphoplasmocytic infiltrate and fibrosis, particularly around the hepatic-portal tract interface, is required to confirm AIH diagnosis (Manns, *et al*., 2010).

For clinical and research purposes, patients are grouped into AIH Type 1 or AIH Type 2 by the presence of their autoantibody profile to liver antigens. Interestingly, age-matched patients usually follow similar trajectories and treatment protocols regardless of autoantibody profile (Muratori et al., 2015), indicating that age of onset may be a more relevant determinant of disease outcome. AIH-2 is rarely seen as adult onset disease, but is reported to represent ~30% of paediatric AIH patients (Manns and Vogel, 2006). AIH-2 is considered a more aggressive form of disease; patients are more likely to present with cirrhosis and are more likely to be treatment refractory requiring higher dose long-term immunosuppression or eventual liver transplant (Mieli-Vergani and Vergani, 2013).

The vast majority (~75%) of AIH-1 patients are positive for anti-nuclear antibodies (ANA) and/or anti-smooth muscle antibodies (SMA) (Werner et al., 2008; Grønbæk et al., 2014). These autoantibodies are not specific to AIH-1 patients and the autoantigens responsible are poorly defined (von Mühlen and Tan, 1995; McMillan and Haire, 1979). ANA can react to histones, ribonucleoproteins ds-DNA and chromatin (Verstegen et al., 2009). SMA also have a range of specificities, predominantly to F-actin (Czaja et al., 1996; Lidman et al., 1976). The remainder of patients who lack ANA or SMA antibodies, but present with liver disease pathology in accordance with IAIHG diagnosis criteria, may possess less common autoantibodies including anti-perinuclear neutrophil cytoplasmic antibodies (pANCA), anti-liver cytosol (LC-1), anti-soluble liver antigen/liver-pancreas (SLA/LP) and/or anti-asialoglycoprotein receptor (ASGPR). Of note, SLA/LP is present in around 30% of AIH patients and has been identified in both adults and children (Dalekos et al., 1999; Kerkar et al., 2003; Manns et al., 1987). SLA/LP autoantibodies are specific to the autoantigen SLA/LP/tRNP(Ser)Sec (Vitozzi et al., 2002; Stechemesser et al., 1993) and is therefore the only defined autoantigen implicated in AIH-1 at present.

AIH-2 has a less diverse autoantigen profile and is diagnosed predominantly by the presence of anti-liver kidney microsomal antibodies (LKM-1) and to a lesser extent LC-1, specific for the liver proteins cytochrome P450 2D6 (CYP2D6) and formiminotransferase cyclodeaminase (FTCD) respectively (Ma et al., 2006; Longhi et al., 2010). Initial T cell and B cell epitope mapping studies of CYP2D6 have been published, providing evidence that CYP2D6-reactive lymphocytes circulate in AIH-2 patients but not in healthy individuals (Ma et al., 2006; Longhi et al., 2007). Our project aims to more specifically map T cell epitopes within CYP2D6 by a range of human cell-based assays and HLA transgenic humanized mouse models. Again, neither LKM-1 or LC-1 autoantibodies are restricted to AIH-2. LKM-1 antibodies are detected in 5-10% of chronic hepatitis C virus (HCV) patients (Dalekos et al., 1999; Cassani et al., 1997) possibly due to homologous sequence between HCV and CYP2D6 (Kerkar et al., 2003).

The success of antigen-specific immunotherapies in re-establishing tolerance is reliant on having strong knowledge of the autoantigens underpinning immune pathology. Therefore with our current understanding of AIH disease, it is likely that the most appropriate immediate targets for AIH-2 are CYP2D6 and FTCD and for AIH-1 SLA/LP/tRNP(Ser)Sec or ASPGR To be applicable to the majority of AIH-1 patients, however, detailed antigen identification of AMA and SMA targets is required but has proved to be extremely challenging thus far.

Genetic risk factors

Specific genetic features have been implicated in the pathogenesis of all 3 AILD diseases, with both major histocompatibility complex HLA genes and non-HLA genes showing disease associations (Mells et al., 2013). AIH-1 usually presents in middle age and has

been linked to HLA-DRB1*0301 and HLA-DRB1*0401 with co-expression of these risk alleles indicating a double-dose effect (Donaldson, 1991; Czaja et al., 1993; Montano-Loza et al., 2006). AIH-2 affects around 10% of all AIH patients, exhibits a more aggressive phenotype and has been related to the presence of HLA-DRB1*07 and DRB1*03 in cohorts in the UK and Brazil (Ma et al., 2006). AIH-2 is most commonly diagnosed in childhood and has even been recorded in infants, suggesting a potentially different aetiology to AIH-1 (Gregorio et al., 1997). 30-40% of all AIH patients will have one or more concurrent extra-hepatic autoimmune diseases, with thyroiditis (10-20%; HLA-DR3 linked), T1D (2-5%; HLA-DR4/3 linked), RA (2-5%; HLA-DR4 linked) and inflammatory bowel disease (IBD) (2-5%) being the most common (Bittencourt et al., 2008; Wong et al., 2016; Werner et al., 2008).

Genome-wide association studies (GWAS) have also linked specific regulatory gene polymorphisms with AIH. Notably these include CTLA-4 and TNF-α genes (Czaja and Donaldson, 2000; Chaouali et al., 2018; Walker et al., 2009) which are common 'hits' in diverse autoimmune disorders (Kristiansen et al., 2000; Zhernakova et al., 2013). TNF-α is located in the HLA-DR/DP locus; therefore, its appearance in GWAS studies of autoimmune diseases is unsurprising. At present it is unclear whether its influence is via linkage disequilibrium to an HLA class II gene, or whether its function and downstream signalling actively contributes to the strong correlation of certain HLA haplotypes to autoimmunity.

AIH treatment

AIH was the first autoimmune liver disease for which effective therapeutic intervention was identified in randomised clinical trials during the 1970s (Cook et al., 1971; Murray-

Lyon et al., 1973; Soloway et al., 1972). Over 50 years later, the mainstay treatment options of corticosteroids and azathioprine (AZA) remain unchanged (Mackay et al., 1965; Cook et al., 1971; Lamers et al., 2010). Prednis(ol)one (PRED) (20–30 mg/day) is the standard treatment for inducing remission and is combined with azathioprine to mitigate immune system driven damage in an attempt to avoid progression to end stage liver disease (European Association for the Study of the Liver, 2015). This treatment protocol is sufficient to obtain biochemical disease remission and to prevent further liver damage in around 80% of AIH-1 patients (Johnson et al., 1995). AIH-2 is more likely to be treatment refractory. Despite treatment, *de novo* cirrhosis occurs in around 14% of patients, increasing the likelihood of progression to transplant or HCC (Hoeroldt et al., 2011; Gleeson, 2019). For the vast majority of patients, immunosuppressive therapy is lifelong, bringing a range of side effects, including Cushingoid features, weight gain, gastrointestinal issues, osteoporeosis, diabetes mellitus, increased infection risk and risk of hepatocellular and extra-hepatic cancers (Werner et al., 2009). Around 25% of all autoimmune hepatitis patients suffer from drug related complications due to PRED/AZA toxicity or intolerance and are subsequently prescribed new generation immunotherapeutics, calcineurin inhibitors (e.g. tacrolimus) or mofetil mycophenylate (Czaja, 2016). A recent trial using the corticosteroid budesonide with AZA indicated improved efficacy to PRED and a much improved adverse effect profile (Manns et al., 2010). So far, this is yet to be translated to a change in clinical treatment practice for AIH.

AIH pathogenesis

Figure 1.10 summarises our current understanding of immune-driven liver damage in AIH. The liver is biased towards tolerance, leading to the hypothesis that external

influence may be required to break tolerance in genetically predisposed individuals, potentially with weakened Treg control. Whether Treg are reduced in frequency or functionality in AIH has been a focus in a number of studies, with the overall picture suggesting that abnormal Treg populations are involved (Longhi et al., 2004; Peiseler et al., 2012). Although the initiating event in AIH-2 is unknown, it has been suggested that viral infection may play significant role in loss of self-tolerance to liver proteins, due to cross-reaction between host antiviral T cells and autoimmune proteins (Bogdanos et al., 2004; Holdener et al., 2008; Gran et al., 1999). Molecular mimicry of host protein structures by invading pathogens offers a conceptual link between a physiological

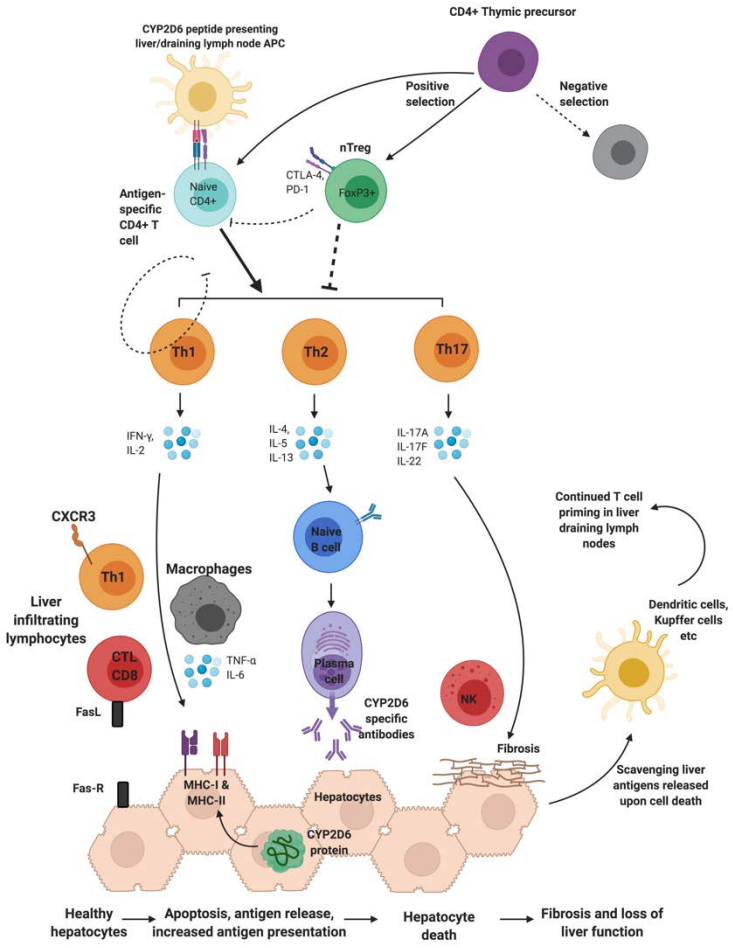

Figure 1.10: Overview of immune-mediated liver damage in AIH-2. Self-reactive T cells escape central tolerance selection and have autoimmune potential. CYP2D6 T cell epitopes presented within the HLA Class II peptide binding cleft can activate antigen-specific $CD4^+$ T cells, particularly without sufficient Treg control. The liver homing receptor CXCR3 promotes circulating T cell infiltration. Th1 secrete IL-2, IFN-γ, and TNF-α which stimulate macrophages and $CD8^+$ T cytotoxic lymphocytes (CTL). CTLs produce further IFN-γ and TNF-α. Both CD8+ CTLs and Natural Killer T cells (NKTs) can induce hepatocyte apoptosis via FasL-FasR interactions. Th17 cells secrete IL-17 and IL-22 which may cause hepatocyte death and recruit pro inflammatory innate cells. Th2 secrete IL-4. IL-10 and IL-13 and support autoantibody production and affinity maturation by B lymphocytes towards the autoantigen CYP2D6. Hepatocytes in AIH-2 are bound by anti-CYP2D6 antibodies, activating complement and engaging Fc-receptor bearing cells including Natural Killer (NK) cells. Degranulation of NK cells releases perforin and granzymes that further damage hepatocytes. Adapted from Webb et al., 2018; Oo et al., 2010.

33

$CD4^+$ T cells appear to be key drivers of pathology due to their ability to support the activation of cytotoxic $CD8^+$ T cells and B cells within the liver environment (Oo et al., 2010; Webb et al., 2018). Self-reactive $CD4^+$ T cells participate in a positive feedback loop to perpetuate autoimmune reactivity. Without effective Treg suppression, effector T cells and inflammatory mediators can escalate out of control (Oo and Adams, 2012).

1.9 Autoantigen CYP2D6 as a target in AIH-2

Cytochrome P450 2D6 (CYP2D6) is an essential liver enzyme responsible for catalysis of around 25% of pharmaceutical drugs (Gueguen et al., 1991; Wang et al., 2009). The diversity of LKM-1 antibodies in patients correlates with autoimmune hepatitis severity (Strassburg and Manns, 2002), indicating a role for epitope spreading in advancement of AIH-2, with an increasingly diverse set of pathogenic epitopes being exposed as liver damage worsens. LKM-1 Ab specific for B cell epitopes $CYP2D6_{254\text{-}288}$ and $CYP2D6_{193\text{-}212}$ cross-react with HCV proteins (Manns et al., 1991; Marceau et al., 2005) in addition to cytomegalovirus (CMV) (Kerkar et al., 2003). Molecular mimicry alone is unlikely to be sufficient for self-reactive T cells to be activated and undergo expansion, due to the mismatch of high prevalence of CMV within the population but low rate of AIH-2; however, hepatotropic adenoviral infection has been shown to be required for the breakdown of tolerance in a mouse model of autoimmune hepatitis type 2 (Holdener et al., 2008; Ehser et al., 2013).

Initial T cell epitope scanning experiments have identified a number of antigenic regions of the CYP2D6 from AIH-2 patients (Ma et al., 2006). Ma and colleagues used a CYP2D6 15mer peptide screening approach to identify polyclonal T cell responses of AIH-

2 patient peripheral blood mononuclear cells (PBMC). The breadth of the immune response (number of immunogenic peptides) and the intensity of the responses correlated with patient disease activity. Distinct peptides induced production of IFN-γ, IL-4 or IL-10, whilst IFN-γ induction overlapped with T cell proliferation. We aim to develop this approach further to identify immunodominant epitopes of the antigen. This will involve testing healthy donor and patient PBMCs for immune responses to 30mer peptides of CYP2D6. The use of long 30mer peptides and the CYP2D6 protein is vital to subject antigenic material to the natural antigen processing and presentation pathways. When using short 15mer peptides, they may function as cryptic epitope; i.e. may not undergo physiological antigen processing and bind to MHC Class II peptide binding clefts in non-native conformations, leading to neoantigen presentation and false positive responses.

1.10 Murine models of AIH

A challenge when developing new treatments for AIH is that most mouse models do not fully represent the human condition. To overcome the tolerogenic environment of the liver and induce AIH-like liver damage and immune sequelae, some models rely on use of a combination of triggering factors, often on an autoimmune susceptible genetic background. For example, administration of concanavalin A induces non-antigen specific T cell activation and severe, acute hepatitis and fulminant liver failure (Tiegs et al., 1992). It has been a useful model of acute liver damage, but does not reflect the autoantigen-driven, chronic nature of AIH. Thymectomised, PD-1 knockout mice (NTxPD-1-/-) possess severe Treg deficiency and rapidly develop spontaneous fatal autoimmune-like liver

damage, characterised by T cell infiltrate, lobular necrosis and ANA antibodies (Kido et al., 2008). This model is again likely too aggressive to be very representative of human AIH, yet has enabled the important identification that CXCL9 is required for $CXCR3^+$ Teff infiltration into the liver parenchyma (Ikeda et al., 2014).

To improve on the non-specific liver damage models available, several AIH models have been developed using disease-relevant autoantigens and triggering agents. The CYP2D6 mouse model developed by Christen et al., uses an adenoviral vector encoding for human CYP2D6 protein on C57BL/6 and FVB genetic backgrounds to establish chronic, progressive AIH-like histological and immunological features (T cell infiltrates, hepatic fibrosis, elevated AST/ALT). Delivery of hCYP2D6 protein via this viral vector is required to break liver tolerance. Importantly, this model generates αCYP2D6 antibodies with B cell epitope identity or similarity to LKM-1 antibodies in AIH-2 patients (Holdener et al., 2008; Hintermann et al., 2012). Alternatively, there is now a humanised CYP2D6/FTCD transgenic mouse available on a HLA-DR3 transgenic NOD background (Yuksel et al., 2015). These mice also exhibit strongly representative AIH-2 like liver disease, but are restricted by HLA-DR3, which does not necessarily represent all AIH-2 patients. These mouse models provide the most appropriate pre-clinical murine models available for development of autoantigen-specific immunotherapy for the treatment of AIH-2.

1.11 Peptide immunotherapy development platform

As $CD4^+$ T cells drive both T and B cell responses by direct activation and provision of activating signals, we target the identification of $CD4^+$ T cell epitopes for apitope/ASI development. For a T cell epitope to be antigenic requires: i) appropriate peptide

processing from the antigen, ii) stable peptide binding in context of MHC and iii) TCR recognition. Peptide-MHC binding is the most selective of these processes to determine T-cell epitopes (Lafuente and Reche, 2009), and as such precise identification of MHC-restricted peptides is of great significance for understanding the mechanism of immune response. Traditional epitope identification requires experimental screening of large arrays of overlapping peptides representing the whole antigen sequence which is costly and time-consuming, as well as risking the identification of cryptic epitopes. *In silico* prediction tools predict putative HLA Class II binding peptides by comparing the antigen sequence of interest to databases or algorithms of known epitope sequences (Peters et al., 2020). This approach greatly reduces the resources required for epitope mapping by selection of a shortened list of candidates.

The selected prediction tools used in this study to identify HLA-DR compatible peptide sequences were ProPRED, pan-NetMHC-II NetMHC-II and IEDB database. ProPRED and pan-NETMHC-II are designed to identify pan-HLA-DR binding regions by employing machine learning binding matrices; thus even poorly studied HLA-DR can be used in predictions (Singh and Raghava, 2002; Nielsen et al., 2008). NetMHC-II and IEDB databases use a combination of known T cell epitope databases with computational algorithms to provide a quantitative prediction of peptide binding affinity to selected HLA-DR molecules of interest (Nielsen et al., 2008; Paul et al., 2015). We select 30mer candidate peptides, incorporating predicted HLA-DR binding 'cores' of 9aa, so that these peptides would require antigen-processing and presentation, and will therefore mimic the natural antigen pathways, better representing each T cell epitope's likelihood of being presented on HLA-DR. Furthermore, some predicted binding 'cores' overlap, thus using an overlapping 15mer approach would interrupt these sequences.

Epitope prediction tools are limited by the quantity and quality of training data available, an inherent flaw in the system, hence why we utilise 30mer peptides that cover a large proportion of the target antigen in screening experiments. Consensus on predicted sequences was sought, with particular focus on AIH-2 risk alleles HLA-DR3, HLA-DR4 and HLA-DR7.

T cell repertoires are highly diverse within and between individuals, and TCRs can be both highly specific or promiscuous. As such, predicted T cell epitopes must be tested experimentally for their ability to activate T cells from different individuals. An alternative approach to identify T cell epitope peptides is to elute MHC-II bound peptides from cell lines or patient APC and perform high-throughput mass spectrometry (Peakman et al., 1999). Eluted peptides from cell lines carrying HLA-DR may not process and present antigens in the same way as primary APC *in vivo*. Peptides eluted using this approach therefore may not bind in the proper conformation when added back to APC, risking the selection of 'cryptic' epitopes.

A peptide's capacity to activate T cells (i.e. antigenicity) can be assessed by:

- IFN-γ ELISPOT: work very well for pathogenic antigens with strong 'foreign' immune responses, but less well for identification of very low frequency T cells and low potency self-antigens.
- T cell activation markers or cytokines produced: Very resource intensive to test all individuals in a cohort with all available peptides. Some peptides may stimulate rapid cytokine release but actually lead to T cell apoptosis rather than sustainable activation and proliferation. This approach later formed the basis of our activation induced marker (AIM) assays.

- Proliferation by [^{3}H]-thymidine incorporation: Radiolabelled nucleotide is incorporated into the DNA of proliferating cells, and then passed on to daughter cells. A main benefit to this approach is its scalability; 96 well plates can be very easily labelled and harvested, which is essential in stimulation experiments where each individual's PBMC/T cells are stimulated with each peptide in triplicate. This number of conditions would be incredibly intensive to run on a large scale via flow cytometry. We have also found [^{3}H]-thymidine incorporation to be a much more sensitive approach to measure cell proliferation than cell proliferation dyes detectable by flow cytometry (e.g. CFSE/CTV).
- Use of HLA-DR transgenic mice: allows for peptide binding and T cell immunogenicity to be 'isolated' in an HLA-DR restricted model system. Immunisation with candidate peptides or whole antigen enables the analysis of both T and B cell subsets response to antigen. Possibility of producing antigen-specific T cell hybridomas from activated T cells (Canaday et al., 2003).

Once antigenic peptides are identified, the T cell epitopes require precise mapping to identify the 'minimal epitope' sequence, i.e. the minimal sequence required for both HLA-DR binding and TCR reactivity. Minimal epitopes can, if required, be modified to improve peptide solubility by addition of flanking hydrophilic residues. As described previously, peptide solubility is essential for effective antigen-specific tolerance induction.

1.12 Project aims

A detailed understanding of T cell responses towards autoantigens involved in autoimmune diseases is an essential pre-requisite to the successful design of putative tolerogenic peptides which have the ability to ameliorate disease. Previous studies in the context of multiple sclerosis by the Wraith group have shown that T cell epitopes identified in patient T cell repertoire analyses can be delivered as highly soluble peptides and induce antigen-specific T cell tolerance in both mouse and human settings. This research has led to successful prevention of EAE development and more recently, very promising Phase 2 clinical trial outcomes.

The identification of autoantigens involved in autoimmune diseases can be challenging, particularly in complex inflammatory diseases where multiple antigens are at play. Autoimmune pathologies are further complicated by considerable heterogeneity between patients and the acquisition of an increasingly diverse self-reactive T cell pool due to the exposure of novel self-antigens in a process called epitope spreading (Vanderlugt and Miller, 2002). One core focus of this PhD was to develop a mouse model in which bystander suppression can be observed and manipulated to reveal key mechanistic processes involved. It may be possible to control autoreactive T cell responses to multiple antigens in a complex system by sufficient tolerance induction to a single/small number of known autoantigens. This would help to streamline the peptide immunotherapy pipeline and make the approach more attractive in the context of a wider range of autoimmune diseases. Chapter 3 tests the hypothesis that peptide immunotherapy *in vivo* induces tolerogenic phenotypes in induced Tr1 cells, Treg and antigen-presenting cells, which in combination can exert bystander suppression. The

experiments described herein begin to reveal specific cellular and molecular mechanisms involved during bystander suppression and serves as a platform to further define this process.

Chapter 4 applies our knowledge of peptide immunotherapy development to autoimmune hepatitis type 2, where the primary autoantigen is defined as liver protein CYP2D6. Chapter 4 defines the immunogenicity of CYP2D6 30mer peptides, identifying a number of highly immunogenic regions in both healthy donors and AIH-2 patients. Interestingly, AIH-1 patients, who do not possess α-CYP2D6 antibodies (LKM-1), mounted strong immune responses against a specific CYP2D6 peptide. These antigenic peptides were then taken forward to testing in HLA-DR transgenic mouse models (HLA-DR4 and HLA-DR3) to assess HLA-DR restricted responses.

Chapter 5 describes a number of human and humanised mice experimental approaches designed to isolate antigen-specific T cells for more detailed investigation of CYP2D6-specific T cells and T cell epitope mapping. The most successful of these approaches was the generation of T cell hybridomas which allowed the identification of minimal T cell epitopes of CYP2D6. These minimal epitope peptides have the potential for CYP2D6-specific tolerance induction and require testing for AIH-2 disease prevention and treatment in a suitable AIH-2 mouse model.

CHAPTER 2

MATERIALS AND METHODS

2.1 Mouse studies

2.1.1 Cell culture media

Complete RPMI for primary mouse cell culture: 500ml RPMI-1640 (Sigma-Merck; R0883), 5mM L-glutamine (Sigma-Merck; G7513), 20mM HEPES (Sigma-Merck; H0887), 100U/ml penicillin and 0.2μg/ml streptomycin (Sigma-Merck; P4333), 0.05mM β-mercaptoethanol (Sigma-Merck; M6250).

X-VIVO-15 for mouse primary cell culture: 1L X-VIVO-15 (Lonza, BE02-054Q), 100U/ml penicillin and 0.2μg/ml streptomycin (Sigma-Merck; P4333).

DMEM for hybridoma cell culture: 500ml high-glucose DMEM (Sigma-Merck; D5671) was supplemented with 5mM L-glutamine (Sigma-Merck ;G7513), 10mM HEPES (Sigma-Merck; H0887), 100U/ml penicillin and 0.2μg/ml streptomycin (Sigma-Merck; P4333), 0.05mM β-mercaptoethanol (Sigma-Merck; M6250), 1% nonessential amino acids (ThermoFisher; 11140035) and 10μg/ml ciprofloxacin (Sigma-Merck; 17850). For complete DMEM, heat-inactivated sterile-filtered FBS (ThermoFisher; 10270106) was added to 10%.

2.1.2 Cell isolation and staining buffers

FACS staining buffer: Dulbecco's PBS (Sigma-Merck; D8537), 2% sterile-filtered heat-inactivated FBS (ThermoFisher; 10270106), 2mM EDTA (Sigma-Merck; 324506).

MACS isolation buffer: Dulbecco's PBS (Sigma-Merck; D8537), 0.5% BSA (Sigma-Merck; A9418), 2mM EDTA (Sigma-Merck; 324506).

EasySep isolation buffer: Dulbecco's PBS (Sigma-Merck; D8537), 2% FBS (ThermoFisher; 10270106), 1mM EDTA (Sigma-Merck; 324506).

Magnisort isolation buffer: Dulbecco's PBS (Sigma-Merck; D8537), 3% FBS, 10mM EDTA (Sigma-Merck; 324506).

2.1.3 Synthetic peptides

All peptides were synthesised as N-terminal acetylated peptides by fluorenylmethoxycarbonyl chemistry and were >95% pure by HPLC and mass spectrometry (GL Biochem, Shanghai, China). Bystander suppression peptides were solubilised in PBS at 4mg/ml. CYP2D6 30mer peptides were solubilised in DMSO at 50mg/ml. CYP2D6 15mer peptides and 15mer variants were solubilised in DMSO at 20mg/ml. Peptides were assessed for solubility at working concentrations in working solution (e.g. cell culture media) by measuring protein concentration at OD = 280nm before and after ultra-centrifugation at 30,000 rpm for 10mins to pellet insoluble material. All peptides were stored at -80 °C, with minimal freeze-thaw cycles.

BYSTANDER SUPPRESSION PEPTIDES	
Peptide name	**Peptide sequence**
MBP_{Ac1-9} [4K]	Ac - ASQKRPSQR
MBP_{Ac1-9} [4Y]	Ac - ASQYRPSQR
MOG_{35-55}	MEVGWYRSPFSRVVHLYRNGK
Scrambled MBP_{Ac1-9} [4K]	Ac - QPAKRSRSQ
Linked hybrid MBP_{Ac1-9}-HFFK-MOG_{35-55}	Ac - ASQKRPSQRHFFKMEVGWYRSPFSRVVHLYRNGK

CYP2D6 30MER PEPTIDES	
Peptide name	**Peptide sequence**
$CYP1_{62-91}$	RRRFGDVFSLQLAWTPVVVLNGLAAVREAL
$CYP2_{96-125}$	EDTADRPPVPITQILGFGPRSQGVFLARYG
$CYP3_{125-154}$	GPAWREQRRFSVSTLRNLGLGKKSLEQWVT
$CYP4_{176-205}$	GLLDKAVSNVIASLTCGRRFEYDDPRFLRL
$CYP5_{215-244}$	EESGFLREVLNAVPVLLHIPALAGKVLRFQ
$CYP6_{235-264}$	ALAGKVLRFQKAFLTQLDELLTEHRMTWDP
$CYP7_{285-314}$	EKAKGNPESSFNDENLRIVVADLFSAGMV
$CYP8_{315-337}$*	AWGLLLMILHPDVQRRVQQEIDD
$CYP9_{329-358}$	RRVQQEIDDVIGQVRRPEMGDQAHMPYTTA
$CYP10_{366-395}$	FGDIVPLGVTHMTSRDIEVQGFRIPKGTTL
$CYP11_{405-434}$	DEAVWEKPFRFHPEHFLDAQGHFVKPEAFL
$CYP12_{445-474}$	GEPLARMELFLFFTSLLQHFSFSVPTGQPR
$CYP13_{467-496}$	SVPTGQPRPSHHGVFAFLVSPSPYELCAVP

*$CYP8_{315-337}$ proved challenging to synthesise; therefore, the peptide was shortened to 23 amino acids containing the predicted binding core at the recommendation of GL Biochem.

CYP2D6 CYP1$_{62-91}$ 15MER PEPTIDES	
Peptide name	**Peptide sequence**
CYP1.1$_{62-76}$	RRRFGDVFSLQLAWT
CYP1.2$_{65-79}$	FGDVFSLQLAWTPVV
CYP1.3$_{68-82}$	VFSLQLAWTPVVVLN
CYP1.4$_{71-85}$	LQLAWTPVVVLNGLA
CYP1.5$_{74-88}$	AWTPVVVLNGLAAVR
CYP1.6$_{77-91}$	PVVVLNGLAAVREAL
CYP2D6 CYP1.4$_{71-85}$ TRUNCATED PEPTIDES	
CYP1.4 N-1	QLAWTPVVVLNGLA
CYP1.4 N-2	LAWTPVVVLNGLA
CYP1.4 N-3	AWTPVVVLNGLA
CYP1.4 N-4	WTPVVVLNGLA
CYP1.4 N-5	TPVVVLNGLA
CYP1.4 N-6	PVVVLNGLA
CYP1.4 C-1	LQLAWTPVVVLNGL
CYP1.4 C-2	LQLAWTPVVVLNG
CYP1.4 C-3	LQLAWTPVVVLN
CYP1.4 C-4	LQLAWTPVVVL
CYP1.4 C-5	LQLAWTPVVV
CYP1.4 C-6	LQLAWTPVV

CYP2D6 CYP12 15MER PEPTIDES	
Peptide name	**Peptide sequence**
CYP12.1$_{445\text{-}459}$	GEPLARMELFLFFTS
CYP12.2$_{450\text{-}464}$	RMELFLFFTSLLQHF
CYP12.3$_{455\text{-}469}$	LFFTSLLQHFSFSVP
CYP12.4$_{460\text{-}474}$	LLQHFSFSVPTGQPR
CYP12.2$_{450\text{-}464}$ PEPTIDE VARIANTS	
Peptide name	**Peptide sequence**
KKK CYP12.2 KKK	KKKRMELFLFFTSLLQHFKKK
CYP12.2 -F	RMELFLFFTSLLQH
KKK CYP12.2 -F KKK	KKKRMELFLFFTSLLQHKKK
CYP12.2 (2K)	RKELFLFFTSLLQH
CYP12.2 (4K)	RMEKFLFFTSLLQH
CYP12.2 (5K)	RMELKLFFTSLLQH
CYP12.2 (6K)	RMELFKFFTSLLQH
CYP12.2 (7K)	RMELFLKFTSLLQH
CYP12.2 (8K)	RMELFLFKTSLLQH
CYP12.2 (11K)	RMELFLFFTSKLQH
CYP12.2 (12K)	RMELFLFFTSLKQH

2.1.4 CYP2D6 protein

Recombinant human CYP2D6 using the consensus sequence (UniProt: P10635) was manufactured to order in a mammalian protein expression cell line (CHO; Chinese Hamster Ovary) and purification with endotoxin removal <1EU/ml (Biologics International Corp. US). Due to expense associated with this protein product, usage was limited to essential experiments.

2.1.5 Mouse strains

All experimental mice were maintained under specific pathogen–free conditions in the University of Birmingham Biomedical Services Unit and experiments were performed in accordance with the UK Home Office Project Licence held by Professor David Wraith (current licence = P17E7ABFB, previous licence 30/3195). Male and female mice were used, aged 6–12 weeks. No formal randomization was undertaken; but wherever possible, mice were equally distributed between groups, based on age and sex.

The Tg4 and Tg4 CD45.1 TCR transgenic mice express Vβ8.2 TCR on 95% of CD4+ T cells, specific for MBP_{Ac1-9} in the context of MHC-II I-Au (Liu et al., 1995). Mice were phenotyped in house by flow cytometry analysis of tail vein bleeds taken after weaning.

Tg4 phenotyping antibodies				
Target	**Fluorophore**	**Clone**	**Dilution**	**Manufacturer**
Vβ8.1/8.2	FITC	KJ16-133.18	1:200	Biolegend
CD4	PerCP-Cy5.5	RM4-5	1:200	Biolegend
CD19	APC	eBio1D3	1:200	ThermoFisher
MHC-II	PE	OX-6	1:500	Biolegend

Tg4 CD45.1 phenotyping antibodies				
Target	**Fluorophore**	**Clone**	**Dilution**	**Manufacturer**
Vβ8.1/8.2	FITC	KJ16-133.18	1:200	Biolegend
CD4	PE-Cy7	GK1.5	1:200	Biolegend
CD45.1	APC	A20	1:200	Biolegend
CD45.2	PerCP-Cy5.5	104	1:200	Biolegend

B10.PL (H-2 A^u) mice were originally obtained from The Jackson Laboratory. C57BL/6 (H-2 A^b) mice were acquired from centralised stocks in BMSU, obtained from Charles River.

(B10.PL x C57BL/6) F1 mice carry both H-2 A^u and H-2 A^b MHC-II haplotypes for presentation of both MBP_{Ac1-9} and MOG_{35-55} peptides to cognate CD4 T cells, respectively.

HLA-DR4 transgenic mice (HLA-DRB1*0401, -DRA*0101) were originally generated by Lars Fugger (Fugger et al., 1994). HLA-DRA*0101/ HLA-DRB1*0401 gene constructs were inserted into (DBA/1xA/CA)F1 embryos. Offspring were bred onto IA-β knockout C57BL/6 (Ab^0) background over multiple generations to ensure no expression of the endogenous mouse MHC Class II (IA-β).

HLA-DR3 transgenic mice (Ab^0/DR3/NOD, DR3+ g7-) were imported from the Jackson Laboratory (030434). To generate these mice, NOD-congenic animals with endogenous mouse MHC class II expression eliminated (via homozygosity of the Ab0 knock-out allele [H2-Ab1tm1Doi])) were targeted for insertion of the human HLA class II molecule expression (via the DR3(DRw17) transgene).

HLA-DR7 transgenic mice (HLA-DRB1*0701, -DRA*0102) were imported from AstraZeneca R&D (Transgenic Centre, Mölndal, Sweden). The transgenic mouse line was developed to express the human MHC class II α and β cDNAs, each under the control of a separate mouse H2-Eα promoter.

All HLA-DR transgenic mice were phenotyped in house by flow cytometry analysis of tail vein bleeds taken after weaning.

HLA-DR transgenic phenotyping				
Target	**Fluorophore**	**Clone**	**Dilution**	**Manufacturer**
CD4	PerCP-Cy5.5	RM4-5	1:200	Biolegend
CD19	APC	eBio1D3	1:200	ThermoFisher
MHC-II IA/IE	PE	M5/114.15.2	1:200	Biolegend
hHLA-DR/DP/DQ	FITC	G46-6	1:50	BD Biosciences

2.1.6 Mouse immunisations

Peptide-containing adjuvant was prepared using a 1:1 mixture of Complete Freud's Adjuvant (CFA; Difco; 263810) supplemented with 8mg/ml *Mycobacterium tuberculosis* H37Ra (MTb; Difco; 231141) and PBS (Sigma-Merck; D8537) containing 1mg/ml peptide. Adjuvant mixture was sonicated for 20 mins and physically agitated by repeat pipetting in a 1ml syringe until emulsified. Adjuvant consistency can be checked by releasing a small droplet onto water, the droplet should retain its shape on the surface and show minimal dispersion. 100μg of peptide was delivered to each mouse under anaesthetic by two subcutaneous injections of 50μl adjuvant bilaterally at the base of the tail. Ten days following immunisation, mice were sacrificed by cervical dislocation and spleen and draining lymph nodes (inguinal and cervical) collected.

2.1.7 T cell proliferation assays by antigen recall in vitro

Lymphoid organs from immunised mice were dissociated through a 40μm filter (Greiner Bio-One; 542040) and cells washed twice in serum-free complete RPMI before resuspending in complete RPMI + 5% FCS for cell counting. For bystander suppression assays of (B10PL x C57BL6) F1 mice, spleen and lymph node cells were plated in complete RPMI + 5% FCS at $10x10^6$ cells/ml and $5x10^6$ cells/ml respectively, in 96 well flat-bottomed plates. For *in vitro* stimulation of HLA-DR4 and -DR3 transgenic cells, serum free X-VIVO-15 media (Lonza), supplemented with Pen/Strep was used as we determined this reduced background proliferation. In some HLA-DR4 and -DR3 experiments, lymph node cells from duplicate mice were combined.

Peptides for stimulation *in vitro* were titrated from 0.1–100μg/ml in triplicate. Purified protein derivative (PPD) at 20μg/mL was used as a positive control to assess recall to *MTb* H37Ra. Cells were incubated in a humidified atmosphere at 37°C, 5% CO_2.

Three days post-stimulation, 100μl of culture supernatant per well was transferred to a new plate and frozen for conventional ELISA. 100μl of fresh media was added to all wells before the addition of [^{3}H]-thymidine at a final concentration of 0.18MBq/ml (final concentration 0.175Ci/mmol) for the final 18 hours of culture. Cells were subjected to freeze-thaw prior to harvesting onto glass fibre filters and the incorporated radioactivity (corrected cpm) was measured on a liquid scintillation β-counter (1450 Microbeta; Wallac).

2.1.8 IFN-γ and IL-2 production by ELISA

Nunc MaxiSorb 96-well plates (ThermoFisher; 44-2404-21) were coated overnight with 0.5μg/ml anti-mouse IFN-γ capture antibody (Clone XMG1.2; Biolegend; 505802) or 0.5μg/ml IL-2 capture antibody (Clone JES6-5H4; Biolegend; 503802) in 1 x ELISA Coating Buffer (Biolegend; 421701). All washing steps between incubations were performed three times using 200μl/well PBS + 0.05% Tween-20 and all incubations took place at room temperature on a plate shaker.

Capture antibody was washed off and plates blocked with 1% BSA (Sigma-Merck; A9418) in PBS for 1 hour. Plates were washed and diluted cell culture supernatant added in 1% BSA in PBS along with cytokine standards according to manufacturer's instructions. Cell culture supernatant was incubated on ELISA plates for 2 hours. Plates were washed and 0.25μg/ml biotinylated anti-mouse IFN-γ antibody (clone XMG1.2; Biolegend;

505804) or 0.25μg/ml biotinylated anti-mouse IL-2 antibody (clone JES6-5H4; Biolegend; 503803) in 1% BSA in PBS was incubated for 1 hour. Plates were washed and HRP-Avidin (Biolegend; 405103) diluted to 1:1000 in 1% BSA in PBS and incubated for 30 mins. Plates were washed and 100μl/well of tetramethylbenzidine (TMB) substrate was used to develop the assay. The reaction was stopped with 100μl/well 1M sulfuric acid and absorption values at 450nm were measured on a SpectraMax ABS Plus plate reader (Molecular Devices). Data was analysed by interpolation to standard curve using sigmoidal 4PL function in Prism v8 (GraphPad).

2.1.9 IL-10 and IL-12/IL-23 (p40) production by ELISA

Cell culture supernatants from *in vitro* stimulation assays were analysed for IL-10 using Mouse IL-10 ELISA MAX Deluxe kit (Biolegend; 431414) and IL-12/IL-23 (p40) using Mouse IL-12/IL-23 (p40) ELISA MAX Deluxe kit (Biolegend; 431604) according to the manufacturer's instructions.

2.1.10 Mouse cell isolation from splenocytes

a) $CD4^+$ T cell isolation

Purified $CD4^+$ T cells (~90% $CD4^+$ as determined by FACS analysis) were obtained by negative selection from homogenised spleen in Magnisort buffer using mAb-coated magnetic beads (Invitrogen, ThermoFisher, 8804-6821-74) according to the manufacturer's instructions.

b) $CD4^+$ $CD25^+$ Treg cell isolation

Purified $CD4^+$ $CD25^+$ T cells (~92% $CD4^+$ $CD25^+$, ~85% $CD4^+$ $CD25^+$ $FoxP3^+$ determined by FACS analysis) were obtained by negative selection for $CD4^+$ followed by $CD25^+$ positive selection from homogenised spleen in EasySep buffer using mAb-coated magnetic beads (Stem Cell Technologies; 18783) according to the manufacturer's instructions.

c) $CD19^+$ B cell isolation

Purified $CD19^+$ cells (~90% $CD19^+$ as determined by FACS analysis) were obtained from homogenised splenocytes by positive selection in EasySep buffer using anti-CD19 mAb-coated magnetic beads (StemCell Technologies, 18954) according to the manufacturer's instructions.

d) $CD11c^+$ DC cell isolation

Tissue was homogenised through a 100μm filter (Greiner Bio-One; 542000) prior to cell incubation with TruStain FcX block (Biolegend; 101320) at 1:100 dilution for 10mins at 4°C. Enriched $CD11c^+$ cells (~70% $CD11c^+$ as determined by FACS analysis) were obtained by positive selection using anti-CD11c mAb-coated magnetic beads (Miltenyi Biotec, 130-125-835) according to the manufacturer's instructions.

2.1.11 Tolerance induction *in vivo*

To induce tolerance to MBP_{Ac1-9} Tg4 or (B10PL x C57BL/6) F1 mice were treated subcutaneously every 3–4 days with 200μl of high affinity peptide MBP_{Ac1-9} [4Y] in phosphate- buffered saline (PBS) following an escalating dose protocol. Mice were injected with 0.08μg, 0.8μg, 8μg, 40μg, 80μg, 80μg. Control mice were injected with

200μl PBS following the same injection schedule. Mice were either culled 3 days after final peptide dose, or injected 2 hours prior to tissue collection with a final dose of PBS or 80μg 4Y peptide.

Mice used fall into 1 of 4 categories: PBS-treated with final PBS dose (PBS/PBS = naïve resting), PBS-treated with final 4Y dose (PBS/4Y = naïve activated), 4Y-treated with final PBS dose (4Y/PBS = tolerised resting), or 4Y-treated with final 4Y dose (4Y/4Y = tolerised activated). In the results for each experiment, mouse groups are stated.

2.1.12 Adoptive cell transfer and immunisation

Splenic $CD4^+$ cells from PBS or MBP_{Ac1-9} [4Y] treated CD45.1 Tg4 mice were purified by magnetic bead isolation to at least 90% purity. $5x10^6$ freshly isolated $CD4^+$ cells were injected via the intra-peritoneal cavity into recipient (B10PL x C57BL/6) F1 mice.

24 hours post-cell transfer, recipient mice were immunised with 100μg MBP_{Ac1-9}-HFFK-MOG_{35-55} linked peptide suspended in CFA with 8mg/ml *MTb*, as described above. After 10 days, spleens and lymph nodes were harvested for *in vitro* re-stimulation in triplicate with MBP_{Ac1-9}-HFFK-MOG_{35-55} linked peptide, MBP_{Ac1-9} [4K] and MOG_{35-55} at a range of peptide concentrations (0.1μg/ml-100μg/ml).

2.1.13 T cell:APC cocultures

To assess how PBS or MBP_{Ac1-9} [4Y] treated Tg4 cells could affect the phenotype of naïve CD11c or CD19 cells; firstly, Tg4 mice were subjected to repeated doses of PBS or MBP_{Ac1-9} [4Y] as described previously. Splenic $CD4^+$ T cells or $CD4^+$ $CD25^+$ Treg cells were isolated

3 days after Tg4 mice received their last dose. Naïve CD11c and CD19 cells were isolated from untreated (B10PL x C57BL/6) F1 splenocytes. Co-culture assays were established in which $1x10^5$ $CD11c^+$ or $CD19^+$ cells were cultured with $1x10^6$ PBS/4Y treated $CD4^+$ or Treg in complete RPMI + 5% FCS for 24hours in a humidified atmosphere at 37°C, 5% CO_2 prior to flow cytometric staining and analysis.

2.1.14 *In vitro* bystander suppression assays

Tg4 mice were subjected to repeated doses of PBS or MBP_{Ac1-9} [4Y] as described previously. Splenic $CD4^+$ T cells were isolated three days following their last dose. Splenic $CD4^+$ T cells were also isolated from 2D2 mice and stained using Cell Trace Violet according to the manufacturer's instructions. Briefly, 2D2 $CD4^+$ cells were resuspended at $5x10^6$ cells/ml in PBS and stained with 5μM CTV for 20 mins, at room temperature in the dark. CTV uptake was quenched using complete RPMI + 5% FCS and cells washed three times in PBS to remove unbound CTV.

To assess how MBP_{Ac1-9} specific Tg4 cells could interact with MOG_{35-55} specific 2D2 cells *in vitro*, $1x10^6$ MBP_{Ac1-9} specific Tg4 $CD4^+$ T cells were co-cultured with $1x10^6$ MOG_{35-55} specific 2D2 $CD4^+$ CTV^+ T cells and $3x10^6$ irradiated (B10PL x C57BL/6) F1 splenocytes in complete RPMI + 10% FCS. Cells were stimulated in triplicate with 10μg/ml MBP_{Ac1-9}-HFFK-MOG_{35-55} linked peptide, 10μg/ml MBP_{Ac1-9} [4K] and/or 10μg/ml MOG_{35-55} for 3 days in a humidified atmosphere at 37°C, 5% CO_2 prior to flow cytometric staining and analysis.

2.1.15 Flow cytometry

a) Surface marker flow cytometry staining

Cell surface markers and intracellular proteins of Tconv, Tr1, Tregs, dendritic cells, monocytes and B cells from MBP_{Ac1-9} treated or PBS treated spleens were assessed directly *ex vivo*, after 24hours or 3 days of antigen-stimulation *in vitro*.

Cells directly from homogenised tissue or harvested from culture plates were firstly transferred to 96 U bottomed plates and spun down by centrifugation at 800g for 2min. All washing steps between antibody incubations involved re-suspension of cell pellet in 200µl FACS buffer prior to centrifugation at 800g for 2 min at least twice. All antibody incubations were conducted at 4°C in the dark unless stated otherwise.

Before incubation with antibody cocktails, anti-CD16/32 antibody (Fc-γ receptor block; TruStain FcX block (Biolegend; 101320) was added to cell suspension at a maximum concentration of $3x10^6$ cells/100µl in FACS buffer at 1:100 dilution for 10mins. Samples were washed before staining for 25mins with surface marker antibody cocktail and Fixable Viability dye ef780 (1:1000; ThermoFisher) in FACS buffer. Samples were washed and either analysed immediately on a flow cytometer (BD LSR-Fortessa; BD Biosciences with BD FACSDiva v.9), or fixed. Cells undergoing fixation were treated with 100µl Cytofix buffer (BD Biosciences, 554655) for 40mins before thorough washing. Fixed cells were analysed as soon as possible (<48hours) on BD LSR-Fortessa. Results were exported and analysed by FlowJo v.9 or 10 (FlowJo LLC, TreeStar). Gates for key markers were determined using FMO controls. Percentages positive and mean fluorescent intensity (MFI) of gated populations were analysed in Prism v8 (GraphPad).

b) Intracellular flow cytometry staining

To assess intracellular expression of cytokines and transcription factors, cells were firstly activated in complete RPMI + 5% FCS supplemented with 5ng/ml phorbol 12-myristate 13-acetate (PMA) and 500ng/ml ionomycin with GolgiStop (BD Biosciences, 554724) and incubated at 37°C for 4 hours prior to antibody staining.

Cells were treated with Fc-block and surface stained as described above. Cells were fixed with Cytofix buffer (BD Biosciences, 554655) for 30mins and treated with permeabilization buffer (ThermoFisher; 00-8333-56) for 30mins prior to intracellular antibody staining in permeabilization buffer. After intracellular staining, cells required 2 x wash using permeabilization buffer, followed by 2 x wash using FACS buffer prior to data acquisition as previously described.

c) Specialist antibody staining procedures:

Combined staining of FoxP3 and IL-10 in Tconv, Tr1 and Tregs required staining surface markers and performing fixation/permeabilization using FoxP3 staining kit (Invitrogen; 00-5523-00) according to the manufacturer's instructions. Intracellular staining with FoxP3 and IL-10 antibodies in permeabilization buffer was performed overnight at 4°C.

Complete CTLA-4 staining of Tconv, Tr1 and Tregs required three parallel staining protocols, as CTLA-4 continually cycles from the cell-surface. Surface CTLA-4 was stained along with other surface markers. Cycling CTLA-4 was stained by incubating cells for 2 hours at 37°C with CTLA-4 antibody in FACS buffer, followed by 2 x washes using permeabilization buffer. Intracellular CTLA-4 was stained alongside other intracellular markers.

d) Fluorophore-conjugated antibodies used for mouse studies:

Target	Clone	Fluorophore	Dilution	Manufacturer
Biotin	FITC	Streptavidin	1:500	BD Biosciences
CD11b	M1/70	PerCP Cy5.5	1:300	Biolegend
CD11c	N418	BV786	1:200	Biolegend
CD19	HIB19	BUV737	1:800	BD Biosciences
CD25	PC61.5	APC/FITC/ PE	1:200	ThermoFisher
CD3	17A2	AF700/ BUV737	1:100	Biolegend/ BD Biosciences
CD4	GK1.5	AF700/FITC	1:200	eBioscience/ Biolegend
CD40	3/23	PE-Cy7	1:200	Biolegend
CD40L	M91	Biotin	1:200	BD Biosciences
CD45.1	A20	PE-Cy7	1:200	Biolegend
CD45.2	104	PerCP Cy5.5	1:200	Biolegend
CD64	X54-5/7.1	PerCP Cy5.5	1:200	Biolegend
CD69	H1.2F3	FITC	1:200	Biolegend
CD8a	53-6.7	APC	1:400	ThermoFisher
CD80	16-01A1	BV421	1:200	Biolegend
CD86	GL-1	BV605	1:200	Biolegend
cMAF	sym0F1	APC	1:100	ThermoFisher
CTLA-4	UC10-4B9	PE-Cy7	1:200	Biolegend
Fc block		Purified	1:100	Biolegend
FoxP3	FJK-16S	FITC/PE-Texas Red	1:100	ThermoFisher
IL-10	JES5-2A5	FITC/APC	1:100	Biolegend
LAG-3	C9B7W	PerCP Cy5.5	1:200	Biolegend
MHC-II	M5.114.15.2	PE	1:400	Biolegend
Nfil3	S2M-E19	PE	1:100	ThermoFisher
PD-1	29F.1A12	BV711/BV421	1:300	Biolegend
PD-L1	10F.9G2	APC	1:200	Biolegend
Tbet	4B10	BV421	1:100	Biolegend
TIGIT	1G9	APC/PE	1:200	Biolegend
TIM-3	8B.2C12	PE/APC	1:200	ThermoFisher

Target	Clone	Fluorophore	Dilution	Manufacturer
Vβ8	KJ16-133.18	PE/FITC	1:200	Biolegend
Vβ11	KT11	FITC	1:200	Biolegend
XCR1	ZET	APC	1:200	Biolegend

2.1.16 $CD4^+$ T cell hybridomas

a) Generation

T cell hybridomas were produced according to methods described (Canaday, 2013). In summary, HLA-DR transgenic mice were immunised as previously described with 100μg CYP2D6 30mer peptide in CFA. Spleens were processed as previously described and cultured in complete RPMI + 10% FCS in 6 well plates at a density of 5-8x10^6 cells/ml with 10μg/ml CYP2D6 peptide. On day 3, 20U/ml of IL-2 (R&D Systems; 202-IL-010) was added to support cell proliferation. On day 5, activated splenocytes and T cell thymoma cell line BW5147 were fused at a ratio of 1:1 in PEG 1500 (Roche; 10 783 641 001). Cells were made up to 30 ml volume in warmed complete DMEM and rested for 1 hour in a 37°C water bath. Cells were diluted 5-fold in serial dilutions to generate 30ml suspensions of NEAT, 1:5, 1:25 and 1:125 before plating 100μl of cell suspension per well of 96 well U-bottomed plates. Plates were incubated in a humidified atmosphere at 37°C, 5% CO_2. After 24 hours, 100μl of 2x HAT solution (ThermoFisher; 21060017) in complete DMEM was added to each well.

From day 7-10 post-fusion, plates were inspected for the cell pellets 2-3mm in diameter which were moved to 24 well plates. 1ml of complete DMEM supplemented with 1x HT (ThermoFisher; 11067030) was added to each growing well and cells maintained until screening.

b) T cell hybridoma screening

When cells in 24 well plates were 50-80% confluent, and media starting to change colour, primary screening was performed to test for antigen-specificity. HLA-DR transgenic splenocytes were irradiated at 3000 Rads and plated at $2x10^5$ cells/well in 96 well U-bottomed plates in complete DMEM to act as APC. 100μl of well-mixed hybridoma cell suspension was added to splenocytes in duplicate, with or without 20μg/ml CYP2D6 peptide. After 24 hours, cell supernatant from screening plates was analysed for IL-2 production by conventional ELISA.

Hybridomas which produced more IL-2 when Ag-stimulated in primary screen were maintained in 6 well plates in complete DMEM + 1x HT and progressed to secondary screening for antigen-selectivity. Briefly, $2x10^5$ irradiated HLA-transgenic splenocytes/well or human HLA-DR4+ EBV-LCL (Preiss cells, ECACC; 86052111) were plated with $1x10^5$ hybridoma/well and antigen at a range of concentrations. IL-2 production was measured by ELISA after 24 hours in culture. Sub-cloning by limiting dilution is recommended for the most specific hybridomas if they were generated from fusion plates containing more than 10% positive wells. Specific details of experimental set-up can be found in text and figure legends.

c) Fixed APC T cell hybridoma screen

Antigen-specific T cell hybridoma activation was tested using live vs fixed Preiss cells as APC. 0.5% PFA solution was used to fix APC, PFA was dissolved in distilled water and 1M NaOH, before neutralising to pH 7.0 using 0.1M HCl and adding PBS to final concentration. Preiss cells were fixed at $5x10^6$ cells/ml for 5mins at room temperature. Fixation was quenched using equal volume 0.4M glycine and cells were washed 3x in PBS

before resuspension in media. $2x10^5$ live or fixed Preiss cells, were plated with $1x10^5$ hybridoma/well and antigen at a range of concentrations. IL-2 production was measured by ELISA after 24 hours in culture.

d) Freezing and thawing T cell hybridomas

$1\text{-}10x10^6$ T cell hybridoma cells were frozen in cryovials in 90% FCS + 10% DMSO. Cells were transferred to a Mr Frosty™ container (ThermoFisher; 5100-0050) for 24 hours of storage at -80°C before transferring to liquid nitrogen storage. T cell hybridomas were thawed quickly in 37°C water bath prior to through washing in serum free media prior to cell counting.

2.2.18 Statistical analyses

Data presented was performed using statistical packages in Prism v8 (GraphPad) as described in figure legends and text. Grouped data was first assessed for normality prior to application of an appropriate parametric or non-parametric test. Asterisks denote p value significance; * $p < 0.05$, ** $p < 0.01$, *** $p < 0.001$, **** $p < 0.0001$. Further detail on analyses can be found in Appendices.

2.2 Human studies

2.2.1 Cell culture media

Complete RPMI for primary human PBMC culture: 500ml RPMI-1640 (Sigma-Merck; R0883), 5mM L-glutamine (Sigma-Merck;G7513), 20mM HEPES (Sigma-Merck; H0887), 100U/ml penicillin and 0.1μg/ml streptomycin (Sigma-Merck; P4333).

X-VIVO-15 for human primary cell culture: 1L X-VIVO-15 (Lonza, BE02-054Q), 100U/ml penicillin and 0.2μg/ml streptomycin (Sigma-Merck; P4333).

2.2.2 PBMC isolation and storage

a) PBMC isolation from leukocyte cones

Leukocyte cones were acquired from NHS Blood and Transplant Service, Birmingham. Cone exterior and tubing was sterilised using 70% ethanol before draining blood product into a 50ml Falcon tube containing 5ml PBS + 2mM EDTA wash buffer. Cone interior was rinsed using 20ml wash buffer. Cell suspension was further diluted to a total of 140ml with wash buffer. 35ml cell suspension was gently layered over 15ml room temperature Ficoll Paque PLUS (GE Healthcare; GE17-1440-02). Cells were centrifuged at 1800rpm at 21°C for 30mins, without brake applied, before pipetting off the lymphocyte layer and washing cells twice in RPMI + 5% FCS.

b) PBMC isolation from whole venous blood

Healthy donor and patient bloods were collected in accordance with University of Birmingham Human Biomaterials Resource Centre (HBRC) procedures and ethics

agreement (HBRC-150-Oo) in CPDA vacutainer tubes (citrate phosphate dextrose adenine solution; Greiner Bio-One; 456056). Blood samples were anonymised and were usually processed within 4 hours of collection, and no longer than 24 hours post-collection. Whole blood was first centrifuged for 10mins at 1800rpm, at room temperature, with no brake, to separate plasma from cellular material. Plasma was heat-inactivated for 35mins at 56°C, then centrifuged for 15mins at 3000rpm to remove complement proteins. Heat-inactivated plasma was sterile filtered before use and frozen for long term storage at -20°C. The cellular blood fraction was resuspended up to its original volume using sterile PBS + 2mM EDTA and isolated using density gradient centrifugation on Ficoll Paque Plus at a ratio of 1 part blood : 2 parts Ficoll, as previously described.

c) Freezing and thawing PBMCs

Cells were pelleted by centrifugation and resuspended in freezing medium (40% complete RPMI, 50% hAB serum (Sigma-Merck; H4522), 10% DMSO (Sigma-Merck, D2650)). Vials were first frozen at -80°C in a Mr Frosty™ container for 24 hours before transferring to liquid nitrogen storage. The cell vial was thawed in a water bath at 37°C before pipetting cells into 14ml of complete RPMI. Cells were washed twice by centrifugation at 1800rpm for 5mins followed by resuspension in 10ml with RPMI + 5% FCS.

2.2.3 HLA-DR typing healthy donor PBMCs

Genomic DNA was extracted from ~5x10^6 cells using Qiagen miniprep extraction kit (Qiagen; 51306) and eluted into PCR grade water. DNA concentration was measured using a Qubit dsDNA assay kit (ThermoFisher; Q32850) and adjusted to ~30ng/ml. HLA-

DR typing was performed using a PCR based array system according to manufacturer's instructions (Olerup-SSP; 101.101-48u). PCR products were run on a 2% agarose-ethidium bromide gel at 100V for 1 hour before analysing DNA band patterns.

2.2.4 *In vitro* PBMC stimulation assays

a) Determining optimal CYP2D6 peptide concentration

PBMCs from 7 healthy donors were thawed and plated in complete RPMI + 10% hAB serum at $1x10^6$ cells/ml in 24 well plates. PBMCs were stimulated with 50μg/ml, 20μg/ml or 10μg/ml of individual CYP2D6 30mer peptides in triplicate. As CYP2D6 30mer peptides ranged in MW from 3177.67-3625.09g/mol, the 3 peptide concentrations represent ≈15μmol/L, 6μmol/L and 3μmol/L. Similar peptide stimulation assays reported previously stimulated with 10μmol/L peptide (Ma et al., 2006). Plates were incubated in a humidified atmosphere at 37°C, 5% CO_2.

At day 4, 6 and 8 post-stimulation, duplicate 100μl of cell suspension were transferred to 96 well U-bottom plates and labelled with [^{3}H]-thymidine at 0.018MBq/well (final concentration 0.175Ci/mmol) for the last 18 hours of culture. Plates were harvested as described above. Mean average [^{3}H]-thymidine incorporation as counts per minute (cpm) were plotted over the time-course. Conversion to Stimulation Index (SI) enables proliferation comparison between different donors with different baseline proliferation. SI represents the ratio of the mean cpm of stimulated condition over the mean cpm of unstimulated condition. Proliferative responses were considered positive when an SI $\geq$ 3 and cpm $\geq$ 1000.

b) Determining optimal PBMC isolation method with small blood volumes

30ml of whole venous blood was collected from 2 healthy individuals into CPDA Vacuette tubes. Blood samples were split into 3 x 5ml and 3 x 2ml fractions to test three PBMC isolation methods: Ficoll Paque Plus, MACSprep PBMC isolation kit (Miltenyi Biotec; 130-115-169) and EasySep PBMC isolation kit (StemCell Technologies; 19654). Blood to Ficoll ratio were 5ml blood:3ml Ficoll and 2ml blood:1.5ml Ficoll in 15ml Falcon tubes. Tubes were centrifuged at 1800rpm, 21°C for 20mins, without brake. The lymphocyte layer was collected and washed in complete RPMI. Remaining 5ml and 2ml blood samples were used in MACSprep and EasySep isolations according to the manufacturer's instructions. Cell yield/ml of whole blood and cell viability was recorded. Isolated PBMC were utilised in a peptide stimulation assay to assess whether the preparation method altered the cells ability to respond to antigen. $1x10^6$ cells/ml of each donors' 5ml blood preparation were stimulated in duplicate with 20 μg/ml CYP2D6 peptides or PPD. On day 8, duplicate 100μl of cell suspension was transferred to 96 well U-bottom plates and labelled with [^{3}H]-thymidine at 0.018MBq/well for the last 18 hours of culture. Plates were harvested as described above.

c) Optimising PBMC culture medium for immunosuppressed patient PBMCs

11 adult AIH patient PBMCs were stimulated with CYP2D6 peptides cultured in: complete RPMI + 10% autologous plasma or X-VIVO-15 media supplemented with Pen/Strep. Proliferative response as log(10) Stimulation Index between media conditions was analysed in Prism v8 (GraphPad) by Brown-Forsythe & Welch ANOVA; accounting for variance in SD with Games-Howell adjustment for multiple comparisons.

2.2.5 Healthy donor PBMC stimulation assays

Healthy donor PBMCs were thawed and plated at a density of $1x10^6$ cells/ml in complete RPMI + 10% hAB serum. Duplicate wells were stimulated with 20μg/ml of each CYP2D6 peptide or PPD. Plates were incubated in a humidified atmosphere at 37°C, 5% CO_2.

On day 4, 6 and 8 post-stimulation, duplicate 100μl of cell suspension were transferred to 96 well U-bottom plates and labelled with [^{3}H]-thymidine at 0.018MBq/well (final concentration 0.175 Ci/mmol) for the last 18 hours of culture. Plates were harvested as previously described.

[^{3}H]-thymidine incorporation was measured as counts per minute (cpm) and plotted over the time-course. Data was converted to Stimulation Index as the ratio of the mean cpm of stimulated condition over the mean cpm of unstimulated condition. Proliferative responses were considered positive when an SI $\geq$ 3 and cpm $\geq$ 1000.

Statistical analysis was performed in Prism v8 (GraphPad) between groups of healthy donors of different HLA-DR allelic variants. Where indicated in the text/figure legend, grouped data was analysed for Gaussian distribution by D'Agostino & Pearson normality test. If data followed Gaussian distribution, parametric Brown-Forsythe & Welch ANOVA was applied, to account for varying Standard Deviations between groups. If data was non-Gaussian, non-parametric Kruskal-Wallis ANOVA was applied. To correct for multiple comparisons using statistical hypothesis testing, a further test was applied: if groups have n > 50 => Games-Howell adjustment; if groups have n < 50 => Dunnett's T adjustment.

2.2.6 AIH2 paediatric, AIH2 adult and AIH1 adult PBMC stimulation assays

AIH patient PBMCs were fresh used on the day of isolation. PBMCs were plated in complete X-VIVO-15 medium at a density of $1x10^6$ cells/ml in 96 well plates in triplicate and stimulated with 20μg/ml of each CYP2D6 peptide or PPD. At day 8 post-stimulation, cells were labelled with [^{3}H]-thymidine for 16-20 hours as previously described. Plates were harvested as previously described.

Statistical analysis between groups: paediatric AIH2 vs adult AIH2 vs adult AIH1 vs healthy donor was performed in Prism v8 (GraphPad) and are described in the text/figure legend in each case.

2.2.7 T cell cytokine multiplex assay

Culture supernatants from PBMC stimulation assays (AIH2 (n=8), AIH1 patients (n=11), healthy donors (n=5)) were analysed for the presence of 13 cytokines using the LEGENDplex Th Cytokine Panel (Biolegend; 740721). Cytokines analysed were: IL-5, IL-13, IL-2, IL-6, IL-9, IL-10, IFN-γ, TNF-α, IL-17A, IL-17F, IL-4, IL-21, IL-22, allowing for distinction between the cytokine secretion status of Th1, Th2, Th9, Th17, Th22 and T follicular cells. Cell culture supernatants were pooled from original triplicate stimulation wells and analysed in duplicate for all CYP2D6 peptides, PPD and unstimulated conditions. Data analysis was performed using the LEGENDPLEX Vigene V8.0 software to interpolate data with the cytokine standard curves before plotting and statistical analysis in Prism v8 (GraphPad).

2.2.8 T cell epitope screening in human PBMCs

a) Antigen-specific T cell line generation by repeated antigen re-stimulation

Ag-responsive healthy donors were first identified using the time-course proliferation assay. Briefly, healthy donor PBMCs were cultured in complete RPMI + 10% hAB serum at $1x10^6$ cell/ml in 6 well plates, and stimulated with: PPD at 20μg/ml, model antigen Keyhole Limpet Haemocyanin (KLH) at 20μg/ml, MBP protein at 50μg/ml or CYP2D6 30mer peptide at 20μg/ml. After 7 days, cells were fed with fresh media supplemented with 20IU/ml IL-2, and duplicate aliquots of 100μl of cell suspension was pulsed for 16-20 hours with [^{3}H]-thymidine to measure active proliferation. On day 12, cells were re-stimulated with a second dose of antigen, 20IU/ml IL-2 and irradiated autologous PBMCs (3000 Rads) to act as antigen-presenting cells at a ratio of 1 T cell:5 APC. On the day of each re-stimulation, antigen-specificity was tested by specific proliferation to Ag. Triplicate wells of $2x10^4$ T cells in the presence of $1x10^5$ irradiated autologous PBMCs were either left unstimulated or stimulated with Ag. After 2 days in culture, 100μl of cell suspension was pulsed for 16-20 hours with [^{3}H]-thymidine to measure active proliferation and harvested as described previously. An Ag-specific TCL was determined to have a δcpm > 1000 and an SI > 3. Every 3-4 days post-restimulation, cells were supplemented with an additional 20IU/ml IL-2. Two further rounds of re-stimulation could be undertaken every 12-14 days until a T cell line is generated. TCL could then be cloned by stimulation with 10μg/ml PHA (Sigma-Merck; 11082132001) at 0.1/0.3/1 cell/well in the presence of irradiated autologous PBMCs as APC. This method is based on previously published work from the Wraith laboratory (Mazza et al., 2002).

b) Activation Induced Marker (AIM) flow cytometry-based assay

We adapted methodology reported (Reiss et al., 2017) utilising viral and model antigens to identify antigen-specific T cells, we developed a protocol to identify cell surface marker expression correlating with antigen-stimulated, actively proliferating $CD4^+$ T cells. These cell surface markers were later used for fluorescence activated cell sorting (FACS) and cell cloning experiments.

PBMC from healthy donor leukocyte cones were thawed from frozen stocks and plated as whole PBMC at $3x10^6$ cells/well of a 96 well flat-bottomed plate in triplicate. As a comparator, $CD4^+$ isolated cells (Miltenyi Biotec; 130-096-533) were plated at $1x10^6$ cells/well with CD4 -ve irradiated cells at $2x10^6$ cells/well of a 96 well flat-bottomed plate in triplicate. $CD4^+$ cells undergoing Cell Trace Violet staining before stimulation were resuspended at $5x10^6$ cells/ml in PBS then stained with 5μM CTV for 20mins, at room temperature in the dark. To quench CTV stain, 5x volume of complete RPMI + 5% FCS was incubated with cell suspension for 5mins.

Cells were cultured in complete X-VIVO-15. Cells were stimulated with CYP2D6 30mer peptide and PPD at 20μg/ml, or SEB (Sigma-Merck; S4881) at a concentration of 1μg/ml. Cells were stimulated for 9 hours, 18 hours, 24 hours, 4 days and 8 days before harvesting and antibody staining. To perform CD69/CD40L assay: PBMC and isolated $CD4^+$ cells were incubated for 30 minutes prior to stimulation and again prior to staining with an anti-CD40 antibody (Biolegend, 102802) at a concentration of 0.5μg/ml.

Cell surface antibody staining was performed as previously described, firstly, cells were treated with human Fc block (Biolegend, 422302) at 1:100 dilution prior to surface antibody staining with a cocktail of surface marker antibodies and Fixable Viability dye

ef780 (1:1000; ThermoFisher) in FACS buffer as previously described. Stained, unfixed cells were analysed immediately on (BD LSR-Fortessa; BD Biosciences with BD FACSDiva v.9). Results were exported and analysed by FlowJo v.9 or 10 (FlowJo LLC, TreeStar). Gates for key markers were determined using FMO controls on SEB stimulated cells. Percentages positive and mean fluorescent intensity (MFI) of gated populations were analysed in Prism v8 (GraphPad). AIM^+ cells were sorted using a BD Aria (BD Biosciences with BD FACSDiva v.9).

c) AIM FACS sorting and cloning

Live $CD4^+$ T cells were FACS isolated on day 8 post-stimulation based on their expression of CD25/OX40 and CD25/CD71. 50 AIM^+ cells were sorted directly into individual wells of 96 U bottomed plates containing 50µl XVIVO media supplemented with 100U/ml rhIL-2 (R&D Systems; 202-IL-010) and rested overnight in a humidified atmosphere at 37°C, 5% CO_2. 24h post-cell sorting, cells were stimulated with 10µg/ml PHA (Sigma-Merck; 11082132001) every 14 days to establish polyclonal T cell populations. Cells were maintained in 50U/ml rhIL-2 throughout the growth phase. Cells were tested every 14 days for specificity to antigen.

d) Anti-human antibodies used:

Target	Clone	Fluorophore	Dilution	Manufacturer
CD14	63D3	APC-Cy7	1:200	Biolegend
CD16	eBioCB16	APC-Cy7	1:200	ThermoFisher
CD19	BC96	APC-Cy7	1:200	Biolegend
CD25	BC19/PC61.5	FITC/PE-Cy7	1:200	Biolegend
CD3	UCHT1	AF700	1:200	Biolegend
CD4	OKT4	BV650	1:300	Biolegend

Target	Clone	Fluorophore	Dilution	Manufacturer
CD40L	24-31	PerCP Cy5.5	1:100	Biolegend
CD69	FN50	APC	1:200	BD Biosciences
CD71	CY1G4	PE-Cy7	1:200	Biolegend
CXCR5	J252D4	PE-Cy7	1:200	Biolegend
Fc block		Purified	1:100	Biolegend
HLA-DR	L243	BV711	1:200	Biolegend
HLA-DR	L243	unconjugated	1:200	Biolegend
OX40	BerACT35	PE	1:100	Biolegend

2.2.9 Statistical analyses

Data presented was performed using statistical packages in Prism v8 (GraphPad) as described in figure legends and text. Grouped data was first assessed for normality prior to application of an appropriate parametric or non-parametric test. Asterisks denote p value significance; * $p < 0.05$, ** $p < 0.01$, *** $p < 0.001$, **** $p < 0.0001$. Further detail on analyses performed can be found in Appendices.

CHAPTER 3

IDENTIFICATION OF BYSTANDER SUPPRESSION MECHANISMS *IN VIVO* AND *IN VITRO*

3.1 Introduction

Bystander suppression occurs between T cells of differing specificities whereby T cells specific to Antigen A are able to suppress responses of T cells specific to Antigen B either by direct (cell-contact mediated) or indirect (cytokine mediated) action. Multi-antigen suppression has been observed in various animal models and has also been inferred in clinical applications of antigen-specific immunotherapy, in which tolerance induction to a single epitope/antigen can offer broader protection. Despite this, little is known about the cellular or molecular mechanisms underpinning the bystander effect.

Due to the technical challenges involved with antigen identification and subsequent T cell epitope mapping required for the many potential antigens associated with complex autoimmune diseases, understanding of bystander suppression may mean that only T cells specific for a single or a small number of dominant antigens require immunotherapeutic modulation. Provided the bystander suppression between the tolerised antigen and other disease-relevant antigens is sufficient, it may not be necessary to induce antigen-specific tolerance to each and every antigen involved in the initiation and progression of complex autoimmune diseases.

Transgenic Tg4 mice are commonly used as the gold-standard model for monitoring the effects of peptide immunotherapy *in vivo* (Liu et al., 1995; Anderton and Wraith, 1998; Gabryšová et al., 2009a; Gabryšová and Wraith, 2010; Burton et al., 2014; Bevington et al., 2020). 95% of CD4+ cells from the Tg4 mouse are specific to MBP_{Ac1-9} and can be rendered tolerant both to the epitope MBP_{Ac1-9} and MBP as a whole protein by repeated antigen stimulation using the high affinity highly soluble peptide variant MBP_{Ac1-9} [4Y]. We also brought 2D2 transgenic mice into the University of Birmingham animal facility, allowing for the assessment of T cell responses towards the immunodominant MOG_{35-55} peptide.

The mice used to investigate bystander suppression *in vivo* and *in vitro* were the F1 generation of wild type B10.PL and C57BL/6 mice, (hereafter called (B10.PLxB6)F1 mice). These (B10.PLxB6)F1 offspring carry both MHC Class II molecules H-2 A^u and H-2 A^b. H-2 A^u is the MHC restriction element for the immunodominant epitope of myelin basic protein MBP_{Ac1-9}, while H-2 A^b enables T cell responses against the immunodominant myelin oligodendrocyte glycoprotein epitope MOG_{35-55}. Firstly, to confirm the presence of T cells responsive to both MBP_{Ac1-9} and MOG_{35-55} peptides, tail vein bleeds from (B10.PLxB6)F1 mice were antibody stained for TCR Vβ8 and Vβ11 chains indicative of cells that carry compatible TCRβ chains for MBP_{Ac1-9} and MOG_{35-55} reactive T cells, respectively. MBP_{Ac1-9} specific cells are restricted to $V\beta8^+$ T cells, but not all $V\beta8^+$ T cells are specific for MBP_{Ac1-9}. The same relationship exists between Vβ11 and MOG_{35-55} specific T cells. Consistently, peripheral blood $CD4^+$ cells were 10% $V\beta8^+$ and 12% $V\beta11^+$ (data not shown).

A linked hybrid peptide composed of the two MBP and MOG epitopes joined with a HFFK linker region, hereafter called MBP_{Ac1-9}-MOG_{35-55}, was synthesised as a means to

restrict delivery of both peptides to the same antigen-presenting cell. The hybrid peptide should be captured by dendritic cells and cleaved within endocytic compartments by cathepsin enzymes at the HFFK linker region before presentation on their respective MHC-II molecules. This can be used to compare T cell responses to MBP_{Ac1-9} and MOG_{35-55} with presentation of epitopes on the same APC vs MBP_{Ac1-9} and MOG_{35-55} peptides delivered separately, where epitopes are not limited to presentation by the same APC (NB: separate peptides may be presented on the same APC by chance).

Figure 3.1A summarises our current understanding of the cellular mechanisms underpinning peptide-based immunotherapy, the primary outcomes of which are the effective modulation of pathogenic $CD4^+$ T cells which are progressively suppressed by negative feedback regulation, and the expansion of anergic IL-10^+ regulatory Tr1 cells during repeated antigen-stimulation of the dose escalation protocol. The resulting Tr1 cells are derived from antigen-specific $CD4^+$ T cells and are $FoxP3^-$, IL-10^+ and express high levels of co-inhibitory molecules including CTLA-4, PD-1. Previously published work by the Wraith group has shown that antigen-presenting cells downregulate CD80/CD86/CD40 when cultured with tolerant $CD4^+$ T cells in vitro (Gabryšová et al., 2009a). Therefore, we hypothesise Tr1 cells are able to suppress nearby APC by T cell secreted cytokines (i.e. IL-10 or TGF-β) and/or cell-contact mediated signalling both *in vitro* and *in vivo*. As a result, suppressed APCs are less capable of inducing robust T cell activation in a non-antigen-specific manner.

Previous work from our laboratory has not focused heavily on the phenotype of $FoxP3^+$ Treg, following tolerance induction, as the generation of $FoxP3^-$ Tr1 cells was by far a more striking effect of PIT in the Tg4 model. This thesis chapter sheds light on both

Tr1 and Treg to highlight how these regulatory T cell subsets share phenotypic and functional markers of tolerance induction and are both able to exert suppressive effects on APC and other T cells (Fig.3.1B). This chapter also studies in detail how dendritic cells and B cells are altered as a result of interaction with tolerant T cells, building on previous work showing the link between IL-10 expression by Tol T cells on dendritic cell suppression (Fig.3.1C) (Sundstedt et al., 2003b; Gabryšová et al., 2009a).

Chapter aims and key questions to address:

- Phenotypic assessment of Tconv, Tr1 and Treg after tolerance: identification of features which could contribute to APC suppression or suppression of other T cells *in vivo;* Tg4 mice.
- Phenotypic assessment of APCs after PIT tolerance induction ($CD11c^+$ dendritic cells and $CD19^+$ B cells) *in vivo;* Tg4 mice.
- Establish an *in vitro* system in which bystander suppression can be observed; co-culture of Tg4 $CD4^+$ T cells with 2D2 $CD4^+$ T cells and (B10.PLxB6)F1 APC.
- Establish an *in vivo* system in which bystander suppression can be observed; wild-type (B10.PLxB6)F1 mice.
    - *Does bystander suppression rely on target antigens being presented in close physical proximity?*
    - *Are tolerant T cells alone sufficient to exert bystander suppression or do APC need t be exposed to the tolerance induction protocol?*
    - *Do T cell and APC observations made in TCR transgenic Tg4 mice translate to those in tolerised wild-type (B10.PLxB6)F1 mice?*

Figure 3.1: Bystander suppression working model

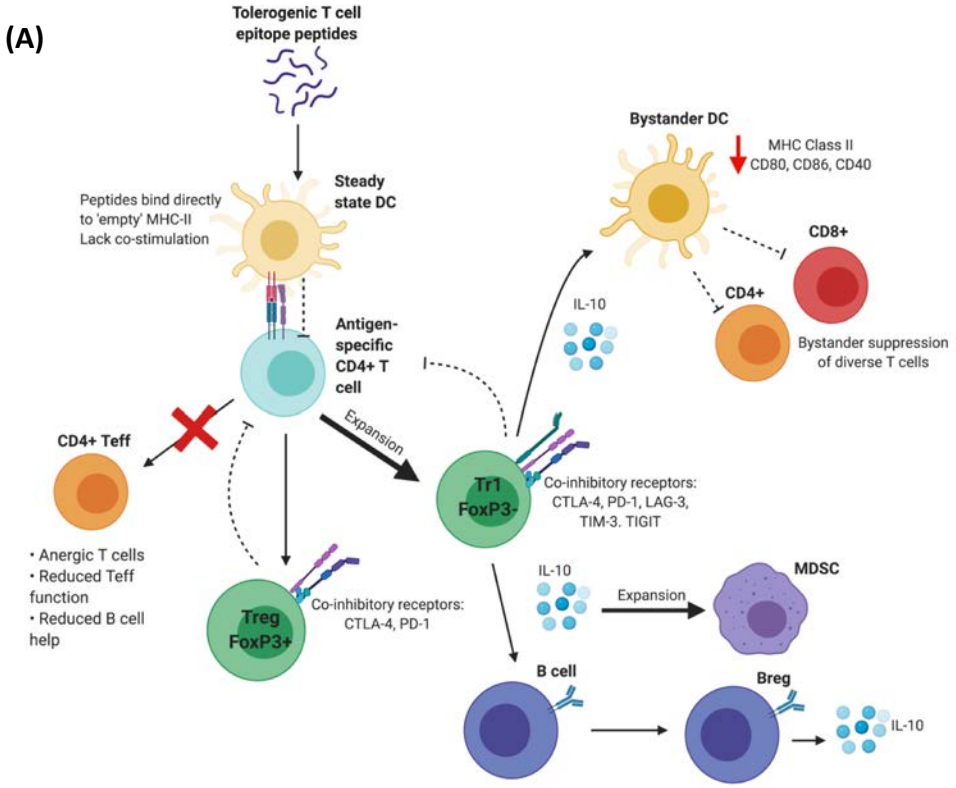

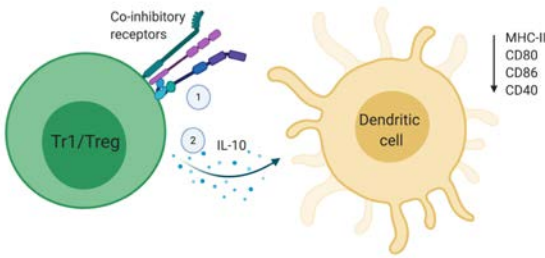

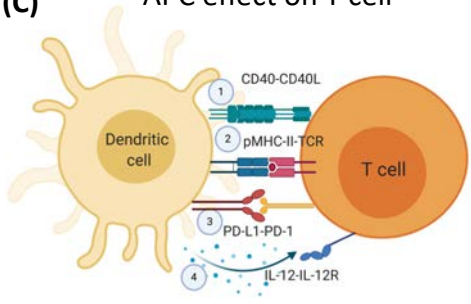

Fig.3.3 T cell IL-10 production
Fig.3.4 T cell TIGIT/PD-1/TIM-3 LAG-3 expression
Fig.3.5 T cell CTLA-4 expression
Fig.3.7 T cell CD40L expression

Fig.3.8 DC provision of CD80/ CD86/CD40
Fig.3.9 B cell provision of CD80/ CD86/CD40
Fig.3.10 DC and B cell PD-L1 expression

3.2 Assessing the phenotype and functionality of tolerised Tg4 $CD4^+$ cells

As in previous mechanistic studies of peptide immunotherapy, the first set of experiments were conducted in the Tg4 mouse, in which $CD4^+$ T cells recognise the MBP_{Ac1-9} peptide and are rendered tolerant by repeated antigen stimulation (Liu et al., 1995; Anderton and Wraith, 1998; Gabryšová et al., 2009a; Gabryšová and Wraith, 2010; Burton et al., 2014; Bevington et al., 2020). Tg4 mice were treated with PBS or MBP_{Ac1-9} [4Y] by s.c. dose escalation protocol (Methods 2.1.10). Briefly, Tg4 mice were injected subcutaneously every 3-4 days with PBS or high affinity MBP_{Ac1-9} [4Y] peptide following a dose escalation of 0.08µg, 0.8µg, 8µg, 80µg, 80µg, 80µg. Some experiments utilised mice 3 days following their last dose, representing naïve and tolerised resting conditions (PBS/PBS & 4Y/PBS), whilst others were treated with one final dose of either PBS or MBP_{Ac1-9} [4Y], resulting in PBS/PBS, PBS/4Y, 4Y/PBS and 4Y/4Y treatment groups representing naïve resting, naïve activated, tolerant resting and tolerant activated conditions, respectively.

Figure 3.2 shows response of $CD4^+$ cells isolated from spleen using magnetic isolation, 3 days after Tg4 mice received their last dose of MBP_{Ac1-9} [4Y] or PBS. Splenic $CD4^+$ cells were isolated to a typical purity of >90% $CD4^+$ cells. These PBS or Tol $CD4^+$ cells were tested for response to MBP_{Ac1-9} [4K] *in vitro* by co-culture with irradiated $CD4^-$ Tg4 splenocytes from PBS-treated mice (acting as APC fraction). Fig.3.2A confirms that MBP_{Ac1-9} [4Y] treated Tg4 $CD4^+$ cells were not able to respond to MBP_{Ac1-9} [4K] restimulation by proliferation, IFN-ɣ or IL-2 production. MBP_{Ac1-9} [4Y] treated Tg4 $CD4^+$ cells when restimulated *in vitro* expressed high levels of IL-10. Purified $CD4^+$ cells of this

Figure 3.2: Tg4 CD4$^+$ cells are anergic and produce high titres of IL-10

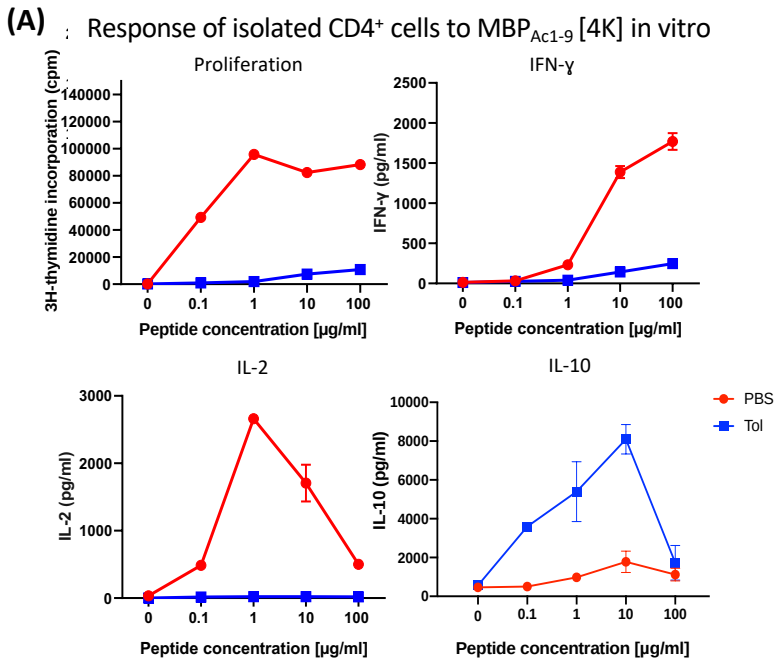

Figure 3.2: Magnetic isolation of splenic CD4$^+$ T cells by negative selection produces high quality purity and functionality. Tg4 mice (n=4) were treated with PBS or MBP_{Ac1-9} [4Y] by s.c. dose escalation protocol (Methods 2.1.10). Spleens were harvested, homogenised and cells subject to magnetic isolation for CD4$^+$ T cells. **(A)** Isolated CD4 cells from PBS treated mice respond to MBP_{Ac1-9} (red), whereas MBP_{Ac1-9} [4Y] treated CD4 are tolerised (blue). Briefly, CD4$^+$ T cells were plated at 1x10^6/ml with 3x10^6/ml irradiated Tg4 CD4$^-$ splenocytes in the presence of MBP_{Ac1-9} peptide in triplicate. After 3 days, 100µl of culture supernatant was removed for IFN-ɣ, IL-2 and IL-10 ELISA, whilst the remaining 100µl cell suspension was incubated for 16-20 hours with 0.18MBq/ml [^{3}H]-thymidine. [^{3}H]-thymidine incorporation was measured on a scintillation reader as corrected counts per minute (cpm). Graphs display mean values for each peptide over the tested concentration range.

nature were used in subsequent *in vitro* assays and adoptive transfer experiments.

3.2.1 Expansion of IL-10$^+$ FoxP3$^-$ Tr1 and FoxP3$^+$ Treg

Spleen cells were harvested from PBS treated or tolerised Tg4 mice 2 hours after their final doses of PBS or 4Y peptide (Fig.3.3A). Figure 3.3B shows representative flow cytometry plots of IL-10 expression and FoxP3 expression gated on all live CD4$^+$ cells isolated from spleen of Tg4 mice in PBS/PBS, PBS/4Y, 4Y/PBS and 4Y/4Y treatment groups. The expansion of IL-10$^+$ CD4 was substantial after tolerance induction, from <1% IL-10$^+$ in PBS/PBS mice up to 35-40% in 4Y/4Y mice (Fig.3.3B & 3.3E), in line with previous data. FoxP3$^+$ CD4$^+$ were also expanded by tolerance induction, with FoxP3$^+$ cells representing 3-4% of CD4$^+$ in PBS/PBS (PBS) mice and 6-9% of CD4$^+$ in 4Y/4Y (Tol) mice (Fig.3.3B & 3.3D). In these experiments, cells required PMA/Ionomycin stimulation and protein transport inhibitors for 4 hours in order to see IL-10 staining, yet this step increased CD25 on Tconv cells; therefore, Treg in this work are defined only by CD4$^+$FoxP3$^+$. Naïve (PBS/PBS) Treg are predisposed to express IL-10 compared to naïve Tconv CD4$^+$ cells (5.9% IL-10$^+$ vs 0.97% IL-10$^+$). The numbers of Treg expressing IL-10 is also significantly increased after tolerance induction from 5.9% in PBS/PBS mice up to 56.0% in tolerised activated 4Y/4Y mice (Fig.3.3C & 3.3E).

However, it is important to appreciate that the numbers of FoxP3$^-$ cells expressing IL-10 hugely outweighs the numbers of FoxP3$^+$ cells expressing IL-10 (Fig.3.3F & 3.3G). For direct comparison, 150,000 live CD4$^+$ cells were collected from all spleens: a mean average of 2048 cells were IL-10$^+$ in PBS/PBS mice, which were predominantly FoxP3$^+$ Treg (78% IL-10$^+$ cells are FoxP3$^+$), whereas in 4Y/4Y mice a mean average of 41,348 cells

Figure 3.3: CD4⁺ Tr1 and Treg T cells express IL-10 after tolerance induction

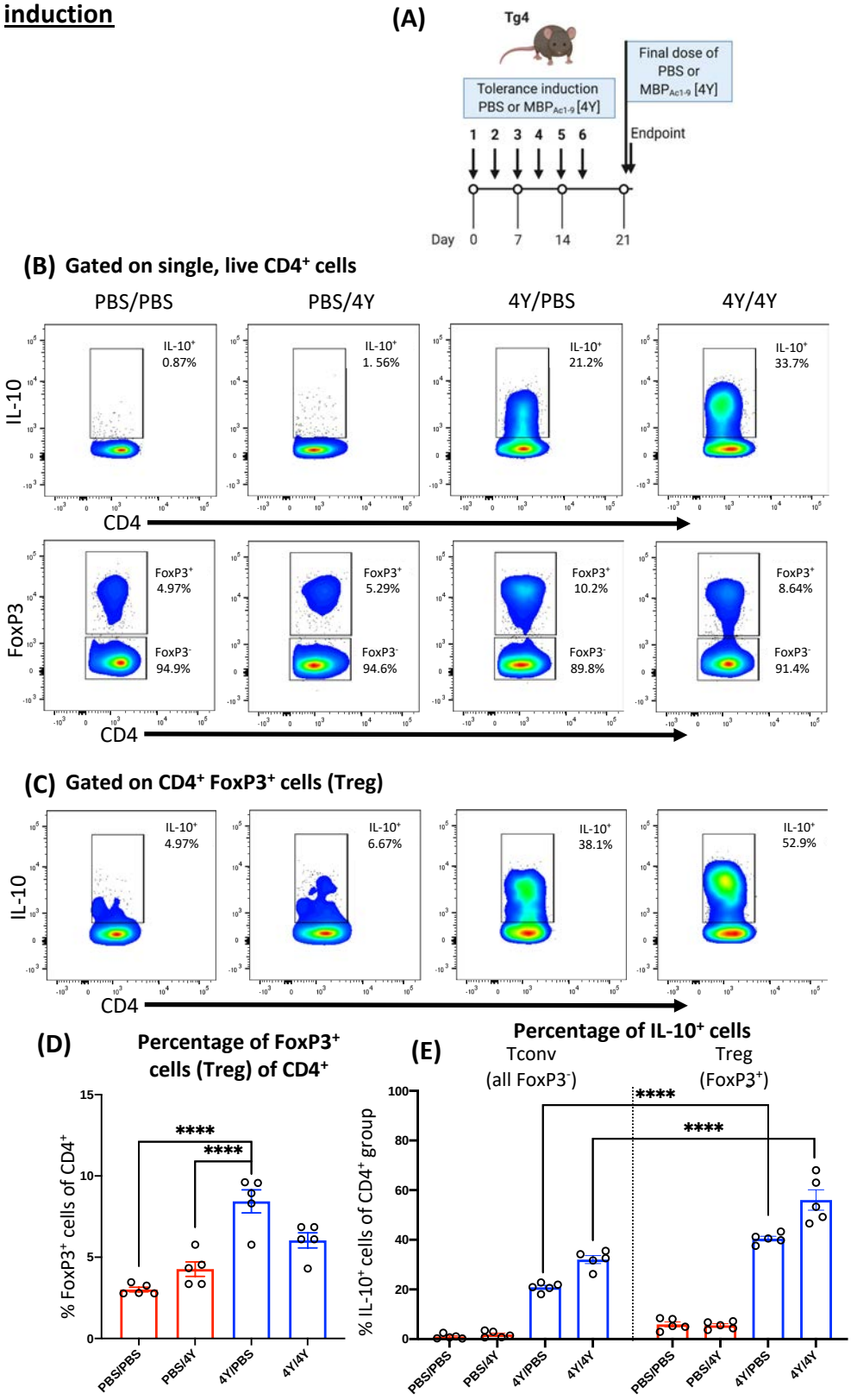

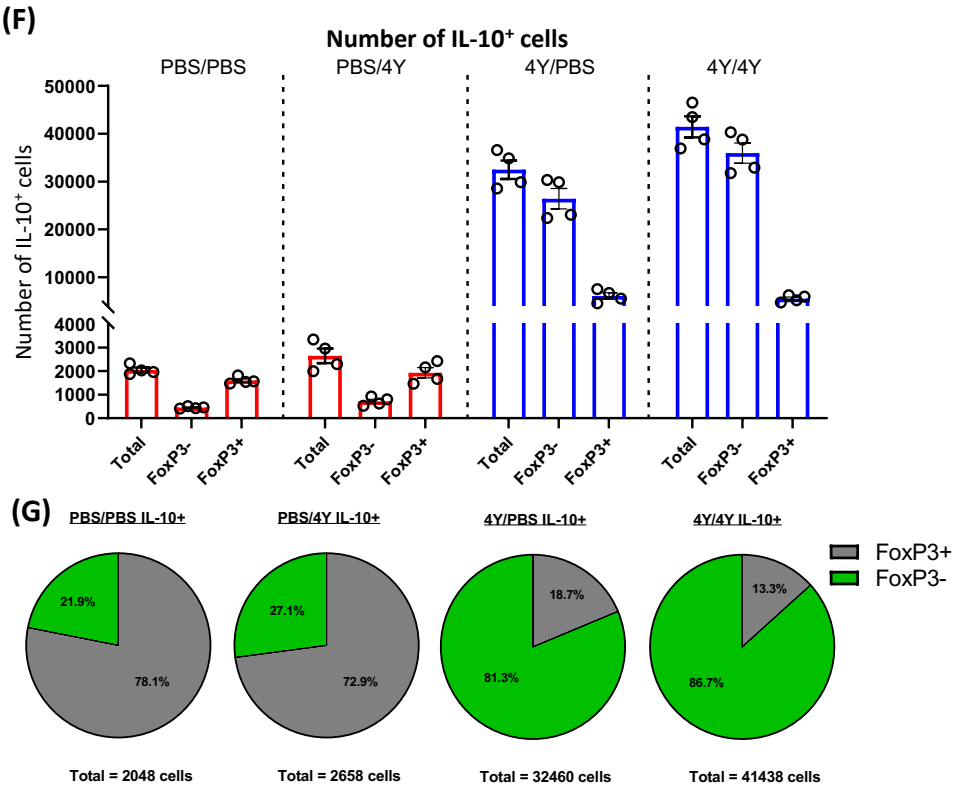

Figure 3.3: Tg4 mice after tolerance induction with MBP_{Ac1-9} [4Y] peptide undergo IL-10⁺ cell expansion of FoxP3⁻ CD4 cells (Tr1) and FoxP3⁺ CD4 cells (Treg). (A) Tg4 mice were treated with PBS or MBP_{Ac1-9} 4Y by s.c. dose escalation protocol. Mice were treated with one final dose of either PBS or MBP_{Ac1-9} [4Y], resulting in PBS/PBS, PBS/4Y, 4Y/PBS and 4Y/4Y conditions. Isolated splenocytes were stimulated *in vitro* for 3 hours with PMA/I prior to surface marker and intracellular cytokine staining. **(B)** Representative flow cytometry plots gated on single, live CD4+ cells show expansion of IL-10⁺ CD4⁺ cells but not FoxP3⁺ CD4⁺ after tolerance induction. **(C)** Representative flow cytometry plots gated on Treg show expansion of IL-10⁺ cells after tolerance induction. Statistical significance within Tconv and Treg groups and between Tconv and Treg groups calculated by ANOVA (Appendix 1). **(D & E)** IL-10⁺ cells after tolerance induction are predominantly FoxP3⁻ Tr1 not FoxP3⁺ Treg. Bar graphs display individual and mean average values of 5 mice per group (±SEM), collated from 3 repeat experiments.

were IL-10$^+$ and these were overwhelmingly FoxP3$^-$ (86.7% IL-10$^+$ cells were FoxP3$^-$). Median fluorescence intensity of IL-10 was not significantly different between FoxP3$^-$ IL-10$^+$ Tr1 and FoxP3$^+$ IL-10$^+$ Treg in different treatment groups (data not shown), suggesting that the amount of IL-10 expressed on an individual cell basis is similar.

In summary, tolerance induction expands populations of both Tr1 IL10$^+$ and Treg IL-10$^+$ cells. That Treg cells also increase their capacity to produce IL-10 as a result of antigen-specific tolerance induction in the Tg4 mouse has not previously been revealed. However, in tolerised mice, IL-10 expression remains very heavily biased towards FoxP3$^-$ Tr1 cells.

3.2.2 Tolerant T cells express increased co-inhibitory receptors

Tr1 cells previously reported in Tg4 tolerant mice were shown to express higher levels of co-inhibitory receptor (CIR) molecules by mRNA and/or protein expression (Burton et al., 2014), and that CIR expression correlated with IL-10. To confirm this at the protein level and to assess CIR cell surface expression of Treg alongside Tr1, splenocytes from Tg4 mice treated as previously described were fluorochrome-conjugated antibody stained for IL-10, FoxP3 and CIRs TIGIT, PD-1, TIM-3, LAG-3 and CTLA-4.

Figure 3.4 displays representative flow cytometry plots of coinhibitory receptor expression by PBS/PBS or 4Y/4Y treated populations of: bulk CD4$^+$ cells, Tr1 cells (FoxP3$^-$ IL-10$^+$) and Treg (FoxP3$^+$). All coinhibitory receptors tested (TIGIT, TIM-3, PD-1, LAG-3; Fig.3.4, and CTLA-4; Fig.3.5) were significantly increased in bulk CD4$^+$ T cells after tolerance induction.

When dissecting this response further by splitting $CD4^+$ cells into $FoxP3^+$ Treg and $FoxP3^-$ IL-10^+ Tr1 cells, the generation of IL-10^+ Tr1 cells was positively correlated with increased co-inhibitory receptor expression of these cells. Mean percentage of IL-10^+ $FoxP3^-$ Tr1 cells in PBS/PBS mice were 7.16% $TIGIT^+$, 19.4% PD-1^+, 20.9% TIM-3^+ and 3.24% LAG-3^+, increasing in tolerised 4Y/4Y mice to mean percentage 22.7% $TIGIT^+$, 70.5% PD-1^+, 43.4% TIM-3^+ and 12.2% LAG-3^+ (Fig.3.4A-D).

Naïve $FoxP3^+$ Treg prior to tolerance induction express high levels of co-inhibitory receptors compared to both bulk $CD4^+$ or IL-10^+ $FoxP3^-$ Tr1: PBS/PBS Treg were 14.7% $TIGIT^+$, 35.9% PD-1^+, 20.6% TIM-3^+ and 8.0% LAG-3^+. Interestingly, Treg are also conditioned during the tolerance induction protocol to significantly increase expression of CIRs. Treg cells from tolerised 4Y/4Y mice were 57.0% $TIGIT^+$, 77.6% PD-1^+, 65.0% TIM-3^+ and 19.0% LAG-3^+ (Fig.3.4A-D). Hence, Treg in tolerised mice are not only increased in their ability to secrete the suppressive cytokine IL-10, they are also enhanced in their expression of CIRs which may contribute to direct cell-cell suppression and intrinsic cellular suppression. Treg may not undergo as dramatic a quantitative expansion as $FoxP3^-$ IL-10^+ cells, but their suppressive quality is certainly increased.

Due to the rapidly cycling biology of CTLA-4 between the cell surface and intracellular compartments, we stained for CTLA-4 by cell surface staining (4°C for 25mins), cycling (37°C for 2 hours) and total intracellular protein (surface staining + fix/perm intracellular staining) (Methods 2.1.17). Surface expression of CTLA-4 is significantly increased by tolerance induction in bulk $CD4^+$ cells, as well as Tr1 (IL-10^+ $FoxP3^-$) and Treg ($FoxP3^+$) subsets (Fig.3.5A). Increase in mean percentage of cells expressing surface CTLA-4 in bulk

Figure 3.4: Tolerance induction increases coinhibitory molecule expression by IL-10$^+$ Tr1 and FoxP3$^+$ Treg cells

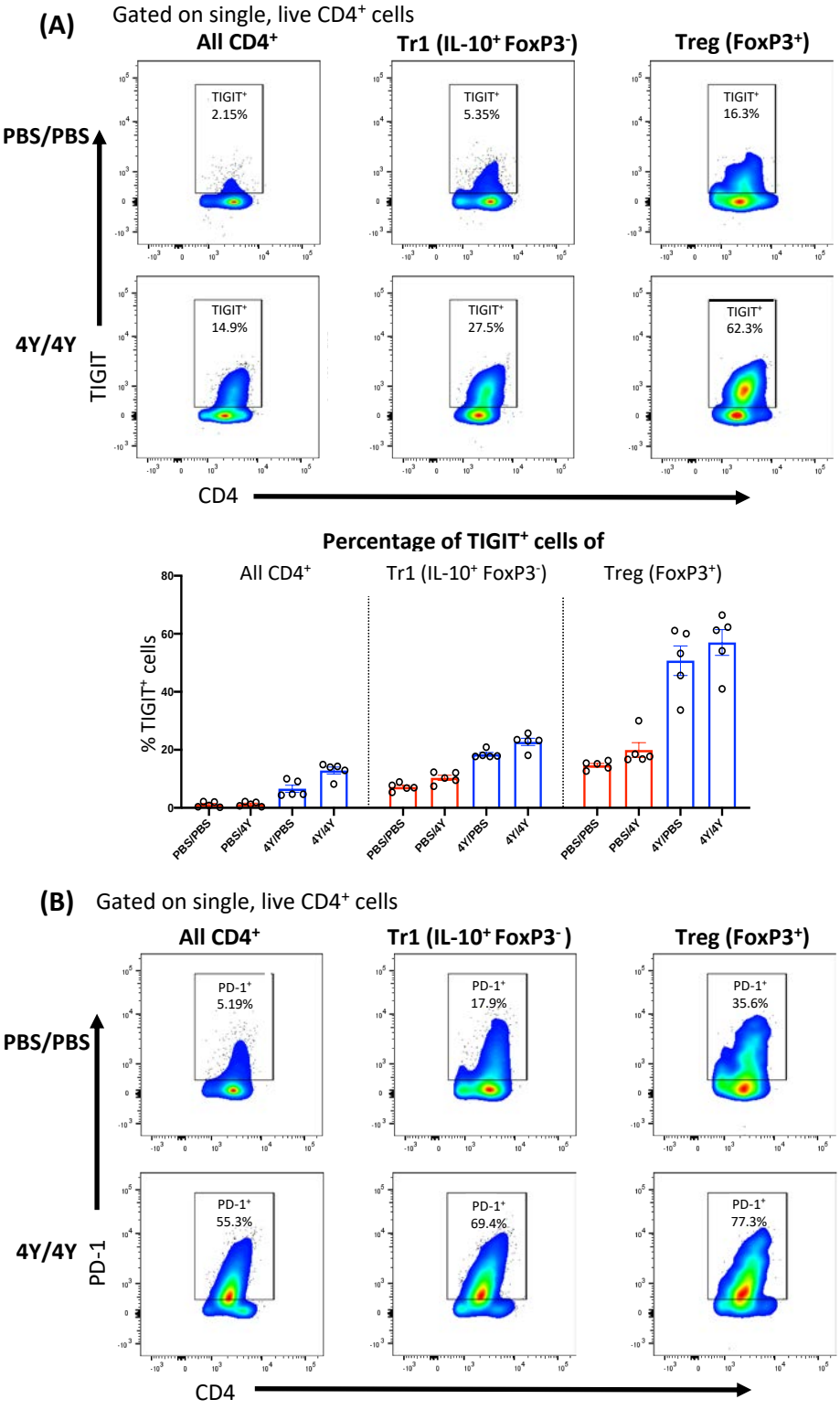

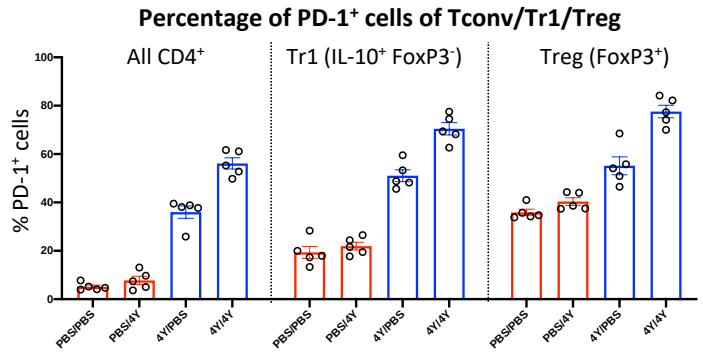

(C) Gated on single, live CD4+ cells

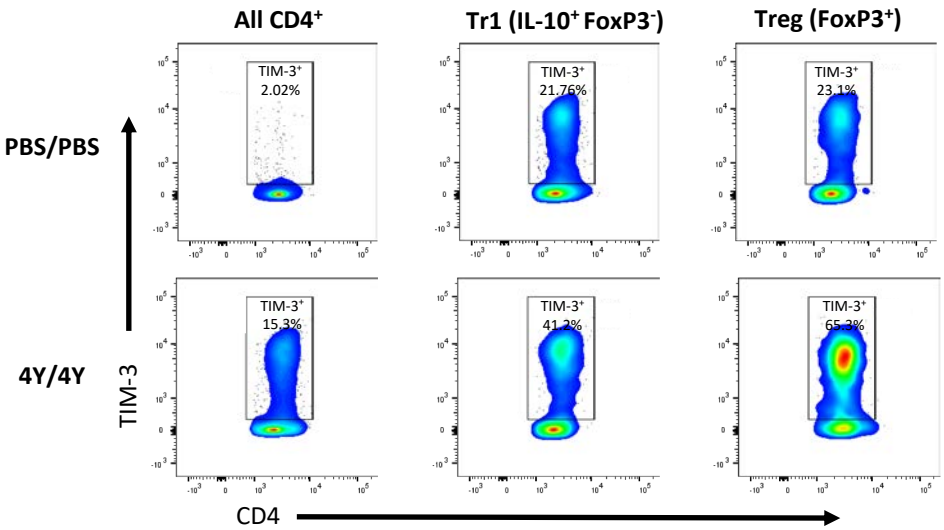

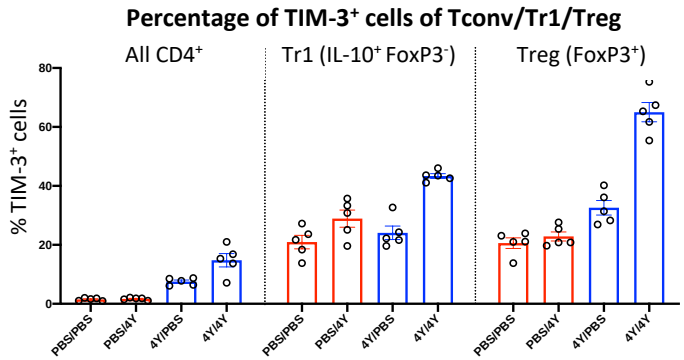

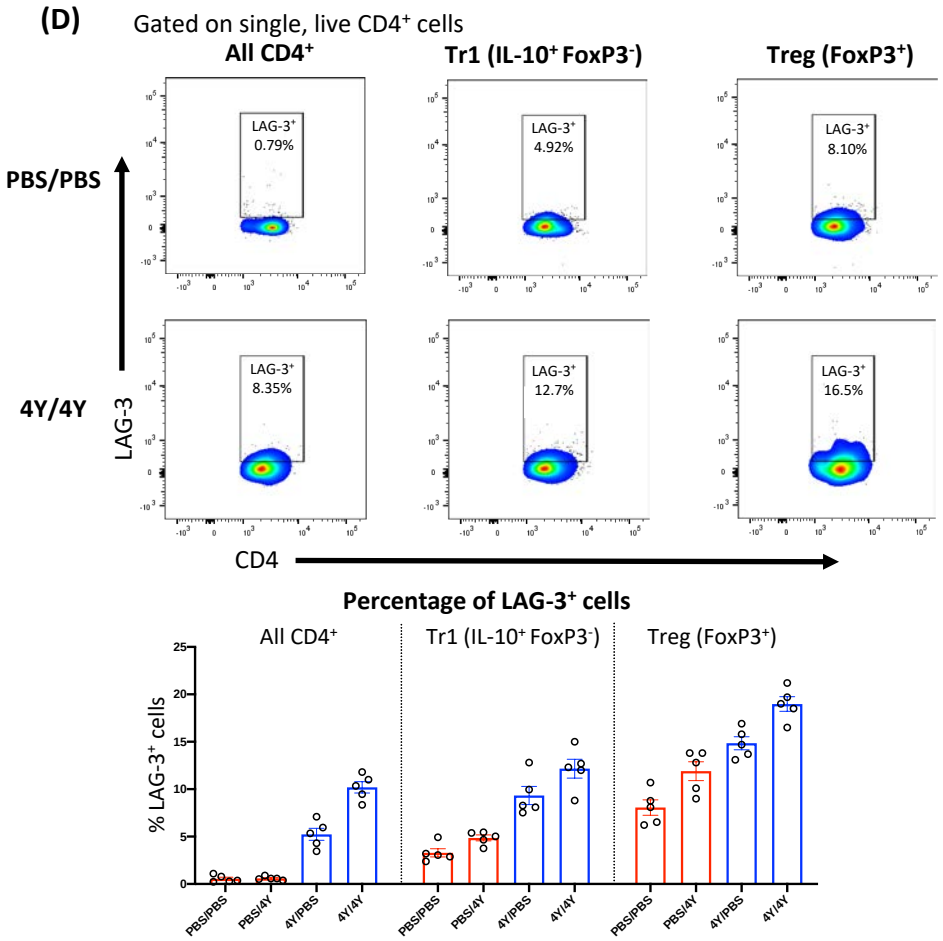

Figure 3.4: Tg4 mice after tolerance induction with MBP_{Ac1-9} [4Y] peptide undergo expansion of TIGIT$^+$/PD-1$^+$/TIM-3$^+$/LAG-3$^+$ cells. Tg4 mice were treated as previously, resulting in PBS/PBS, PBS/4Y, 4Y/PBS and 4Y/4Y conditions. Isolated splenocytes were stained for cell surface expression of coinhibitory receptors. Representative flow cytometry plots gated on single, live CD4$^+$ cells for: All CD4$^+$ cells (unstimulated), Tr1 cells (IL-10$^+$ FoxP3$^-$ CD4$^+$) (stimulated for optimal IL-10 expression) and FoxP3$^+$ Tregs (unstimulated for optimal FoxP3 expression). Expression of **A)** TIGIT$^+$ cells, **(B)** PD-1$^+$ cells, **(C)** TIM-3$^+$ cells and **(D)** LAG-3$^+$ cells with corresponding summary bar charts. Bar graphs display individual and mean average values of 5 mice per group (±SEM), collated from 3 repeat experiments. Statistical significance within Tconv, Tr1 and Treg groups and between Tconv, Tr1 and Treg groups calculated by ANOVA (Appendix 2).

$CD4^+$ was observed from 1.0% in PBS/PBS mice to 4.05% in 4Y/4Y mice. Tr1 cells are rare in number prior to tolerance induction, but express higher levels of surface CTLA-4 than Tconv. Tr1 cells are markedly increased in their surface CTLA-4 expression after tolerance. Mean percentage of Tr1 cells expressing surface CTLA-4 was 10.8% in PBS/PBS mice increasing to 25.5% in 4Y/4Y mice. Treg, however, undergo the most dramatic expansion of CTLA-4^+ cells as a result of tolerance: mean percentage of Tr1 cells expressing surface CTLA-4 was 3.72% in PBS/PBS mice rising to 45.8% in 4Y/4Y mice. Interestingly, the amount of CTLA-4 expressed by each cell subset by MFI is highest in tolerised Tr1 cells, suggesting at the single cell level, tolerised Tr1 have an increased presence of CTLA-4 at the cell surface compared to both Treg and Tconv (Fig.3.5A).

When assessing the functionally relevant cycling pool of CTLA-4, we find that Tr1 cells have highest levels of cycling CTLA-4 after antigen exposure, in the naïve activated and tolerised activated conditions (Fig.3.5B; mean percentage Tr1 cells CTLA-4^+: PBS/PBS 10.5%, PBS/4Y 45.5%, 4Y/PBS 52.7%, 4Y/4Y 56.6%). Treg are predisposed to cycle CTLA-4, as they have the highest % of CTLA-4^+ cells in the naïve resting condition (PBS/PBS: bulk $CD4^+$ 1.90%, Tr1 10.5%, Treg 25.5% CTLA-4^+). Treg CTLA-4 cycling capacity is also significantly increased after tolerance induction (Treg: PBS/PBS 25.5%, PBS/4Y 31.9%, 4Y/PBS 41.2%, 4Y/4Y 63.4% CTLA-4^+). Here, the amount of CTLA-4 expressed by MFI is similar across all cell types, suggesting that the prior MFI difference between tolerised Tr1 and Treg at the surface is not due to a difference in available cycling CTLA-4 within each cell, but could instead be due to increased residency time of CTLA-4 on the surface of Tr1.

Figure 3.5: Staining for surface vs circulating vs total CTLA-4 reveals the effect of tolerance induction on CD4⁺ cell CTLA-4 expression

(A) Surface staining at 4°C
Gated on single cells

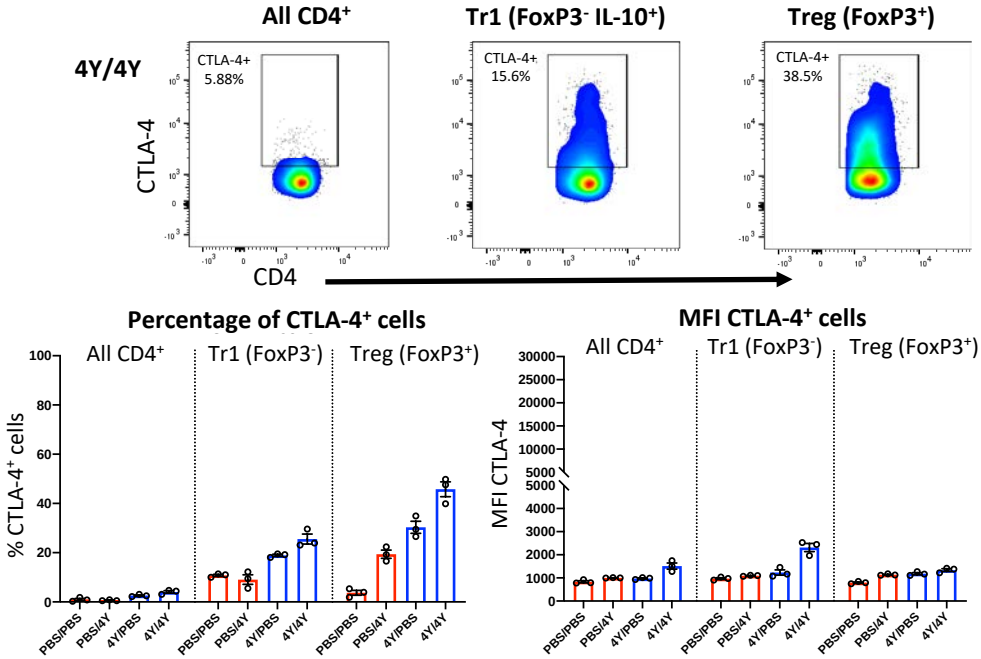

(B) Staining at 37°C for 2 hours
Gated on single cells

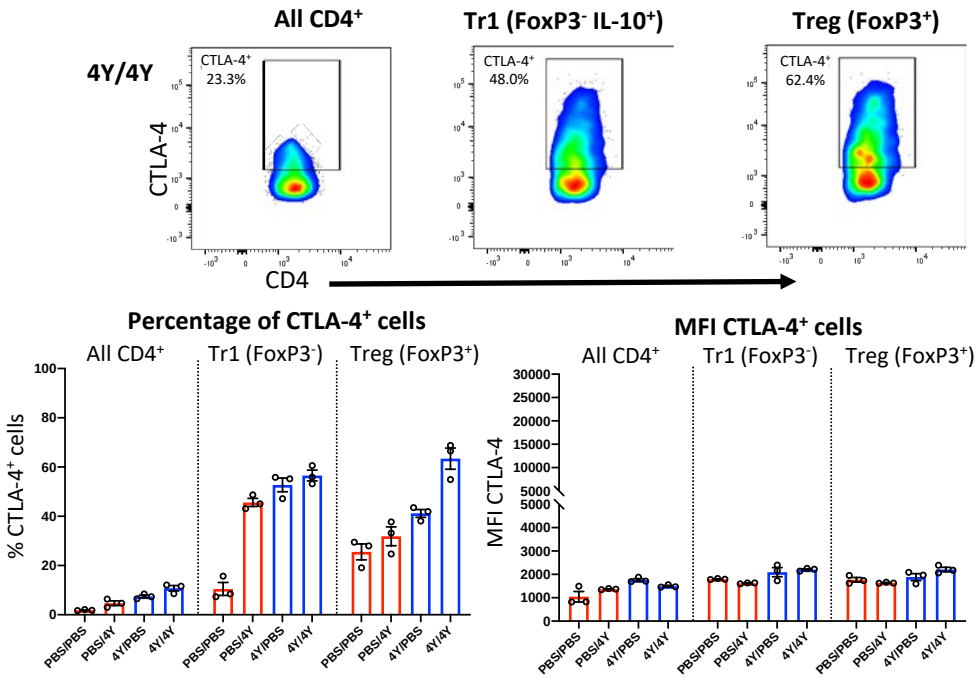

(C) Total CTLA-4 expression: surface staining at 4°C & intracellular staining with fix/perm procotol
Gated on single cells

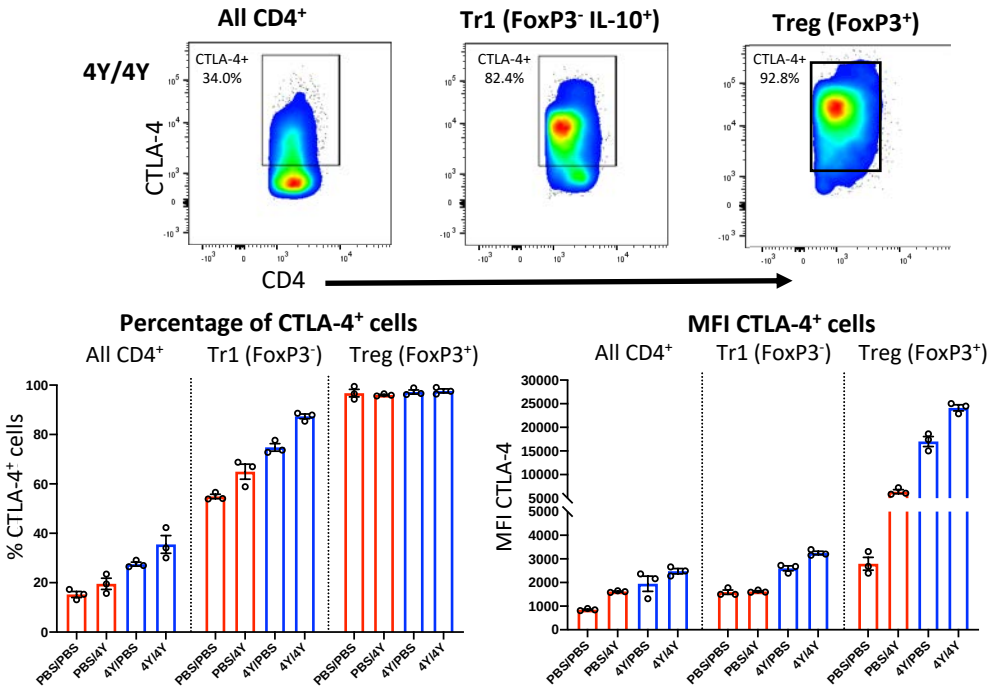

Figure 3.5: Tg4 mice after tolerance induction with MBP_{Ac1-9} [4Y] peptide undergo expansion of CTLA-4$^+$ cells. Tg4 mice were treated as previously described, resulting in PBS/PBS, PBS/4Y, 4Y/PBS and 4Y/4Y conditions. Isolated splenocytes were stained for CTLA-4. Representative flow cytometry plots gated on single, live CD4$^+$ cells for: All CD4$^+$ cells, IL-10$^+$ FoxP3$^-$ Tr1 and FoxP3$^+$ Tregs. Expression of **(A)** cell surface CTLA-4 stained at 4°C, **(B)** circulating CTLA-4 stained at 37°C for 2 hours and **(C)** total intracellular CTLA-4 assessed by combination of surface and intracellular staining each with corresponding summary bar chart. Bar graphs display individual and mean average values of 3 mice per group (±SEM), collated from 2 repeat experiments. Statistical significance calculated by ANOVA (Appendix 3).

Finally, to complete the picture of CTLA-4 expression in our CD4 T cell populations, we assessed total cellular CTLA-4 by staining at both surface level and intracellularly after cell fixation/permeabilization (Fig.3.5C). The proportion of bulk $CD4^+$ and Tr1 expressing CTLA-4 were increased after tolerance. Notably, Tr1 cells were increased for CTLA-4 from 54.9% in PBS/PBS mice to 87.3% in 4Y/4Y mice. Intracellular CTLA-4 expression by MFI reveals that bulk $CD4^+$ and Tr1 cells do not constitutively retain a very large pool of CTLA-4, but that tolerance induction increases their CTLA-4 pool and by extension their CTLA-4-based suppressive potential. Treg by contrast constitutively express CTLA-4 intracellularly even as naïve Treg (>96% CTLA-4^+) (Fig.3.5C) as previously described (Ovcinnikovs et al., 2019). However, Treg that had been subjected to tolerance induction expressed significantly higher amounts of CTLA-4 by MFI, providing further evidence for Treg modulation throughout tolerance induction. This data shows Treg possess constitutive expression of CTLA-4 which can be retained in intracellular compartments until Treg receive the required signals to increase CTLA-4 transport to the cell surface where it can exert its contact dependent cell-extrinsic suppression.

3.2.3 IL-10^+ Tr1 cells are associated with transcription factors c-MAF and NFIL-3

The transcription factors c-MAF and NFIL-3 both contribute to the regulation of IL-10 production by $CD4^+$ T cells and Tbet represents the master transcription factor for cells of the Th1 lineage. The proportion of $CD4^+$ T cells with c-MAF, NFIL-3 and Tbet protein expression was strikingly increased after tolerance induction (Fig.3.6A&B; average mean expression in PBS/PBS mice compared to 4Y/4Y mice: 9.24% to 48.2% c-MAF^+, 3.04% to 50.0% $Nfil3^+$, 2.93% to 18.52% $Tbet^+$). On a single cell basis, the amount of Tbet protein per cell on average by MFI was not affected by tolerance induction, whilst NFIL-3 protein

Figure 3.6: CD4⁺ T cells after tolerance induction show differential transcription factor expression correlating with IL-10⁺

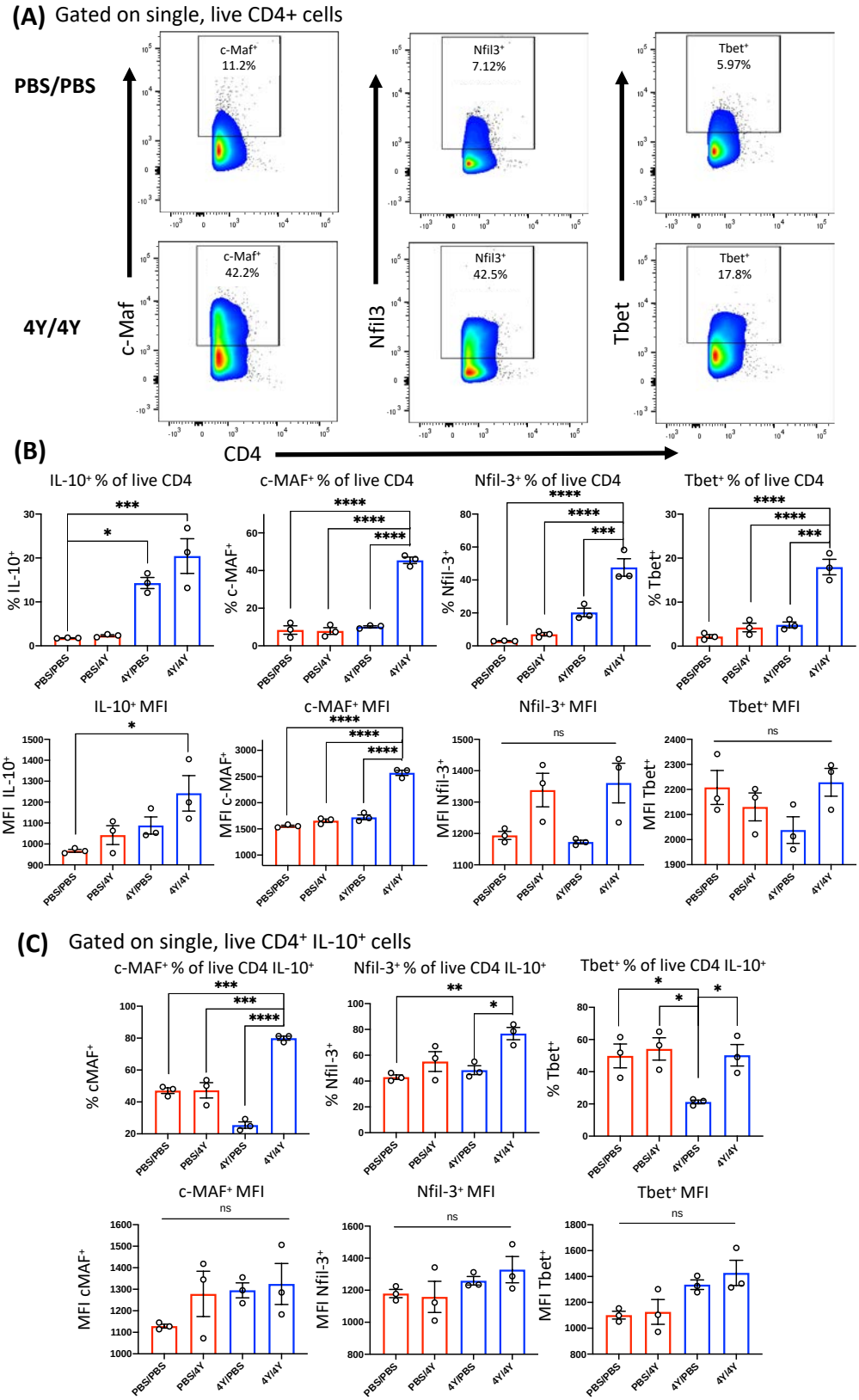

Figure 3.6: Tg4 mice after tolerance induction with MBP_{Ac1-9} [4Y] peptide undergo expansion of c-MAF, NFIL-3 and $Tbet^+$ cells which correlate with IL-10. Tg4 mice were treated as previously, resulting in PBS/PBS, PBS/4Y, 4Y/PBS and 4Y/4Y conditions. Isolated splenocytes were stained for cell surface expression of coinhibitory receptors. **(A)** Representative flow cytometry plots showing c-MAF, NFIL-3 and Tbet expression in PBS/PBS and 4Y/4Y mice gated on single, live CD4+ cells and **(B)** summary bar graphs of IL-10 and transcription factor expression. **(C)** Summary bar charts of transcription factor expression of $CD4^+$ $IL\text{-}10^+$ cells showing correlation between IL-10 and c-MAF, NFIL-3 and Tbet. Bar graphs display individual and mean average values of 3 mice per group (±SEM), collated from 2 repeat experiments. Statistical significance calculated by ANOVA.

expression level was most responsive to recent antigen exposure (greatest in PBS/4Y and 4Y/4Y conditions) and c-MAF expression was increased following tolerance induction (Fig.3.6B).

Expression of c-MAF and NFIL-3 was highly associated with IL-10 production (Fig.3.6C: average mean expression of IL-10$^+$ CD4 in 4Y/4Y mice: 79.8% c-MAF $^+$, 78.3% NFIL-3$^+$). IL-10$^+$ Tr1 cells retain high levels of the Th1 master transcription factor Tbet after tolerance induction (~50% Tbet$^+$) despite bulk CD4+ cells from 4Y/4Y treated mice losing the ability to secrete IFN-ɣ in response to peptide stimulation (Fig.3.2B), suggesting that Th1 cells readily convert to Tr1 and retain Tbet during the process.

3.2.4 Tolerised T cells are prevented from CD40L upregulation

CD40L is transiently expressed on activated T cells upon TCR stimulation. CD40L binding to CD40 on APCs then drives clustering of CD40 required for downstream signalling to 'license' APCs in order to drive the maturation and survival of DC and B cell mediated immune responses (Elgueta et al., 2009). Figure 3.7 displays clear upregulation of CD40L expression by naïve activated CD4$^+$ T cells (PBS/4Y mice; 29.05% of CD4$^+$ cells are CD40L$^+$), which is absent from naïve resting cells (PBS/PBS mice; 0.37% of CD4+ cells are CD40L$^+$) and both tolerised resting (4Y/PBS mice; 0.39% of CD4$^+$ cells are CD40L$^+$)) and tolerised activated cells (4Y/4Y mice; 0.53% of CD4$^+$ cells are CD40L$^+$).

T cells that are prevented from CD40L expression upon TCR engagement are subsequently unable to support DC maturation and IL-12 production to drive antigen-specific Th1 responses towards the target antigen.

Figure 3.7: Tolerised Tg4 CD4⁺ T cells are prevented from CD40L upregulation

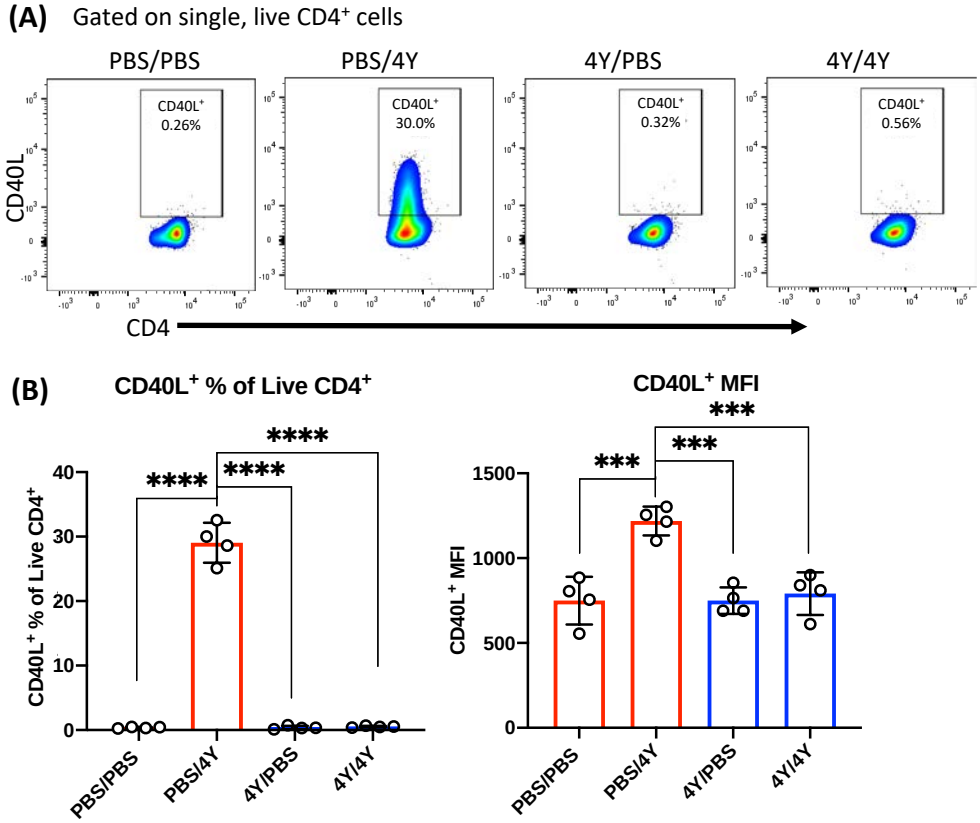

Figure 3.7: Naïve CD4⁺ Tg4 cells robustly upregulate the expression of CD40L upon antigen stimulation, whilst tolerised CD4⁺ Tg4 cells do not. Tg4 mice were treated as previously, resulting in PBS/PBS, PBS/4Y, 4Y/PBS and 4Y/4Y conditions. Isolated splenocytes were stained for cell surface expression of CD40L. **(A)** Representative flow cytometry plots gated on single, live CD4⁺ CD40L⁺ cells for each treatment group and **(B)** summary bar charts showing CD40L expression as percentage of CD4⁺ cells and MFI. Bar graphs display individual and mean average values of 4 mice per group (±SEM), collated from 2 repeat experiments. Statistical significance calculated by ANOVA.

3.3 Dendritic cells and B cells are modulated by tolerance induction *in vivo*

The Wraith group has previously studied aspects of antigen-presenting cells and their interactions with tolerised T cells. Gabryšová et al. identified that tolerogenic T cells are able to suppress naïve DC expression of costimulatory molecules and IL-12 when cultured *in vitro* (Gabryšová et al., 2009a). As our working model for bystander suppression revolves around the interaction between tolerised T cell → APC → non-tolerised T cell, we wanted to investigate the effect of tolerance induction on APC *in vivo*, in particular dendritic cells and B cells.

3.3.1 MHC-II and costimulatory molecule expression by APC is suppressed by tolerance induction

Firstly, splenic dendritic cells ($CD11c^+$ $MHC\text{-}II^+$) and B cells ($CD19^+$) were stained directly from Tg4 mice treated as previously described to result in 4 treatment groups (PBS/PBS, PBS/4Y, 4Y/PBS, 4Y/4Y) (Fig.3.8A). Figure 3.8B shows representative flow cytometry plots of DC gating, Live→Single cells→$CD3^-CD19^-$→$CD11c^+MHC\text{-}II^+$, and costimulatory molecule expression. Figure 3.8C summarises the expression of MHC-II, CD80, CD86 and CD40 of DC (n=4 mice per group) as percentage +ve for each marker and MFI.

Comparison of dendritic cells from naïve activated PBS/4Y mice vs tolerised activated 4Y/4Y mice showed a 55.6% reduction in MHC-II expression by MFI (Fig.3.8C). The overall proportion of $CD11c^+MHC\text{-}II^+$ DCs in each treatment group was not significantly altered (not shown).

The proportion of $CD80^+$ DC was significantly reduced between PBS/4Y treated and 4Y/4Y treated mice (83.4% to 53.0% $CD80^+$), as was CD80 expression as MFI

Figure 3.8: Effect of tolerance induction on antigen-presenting cells: dendritic cells

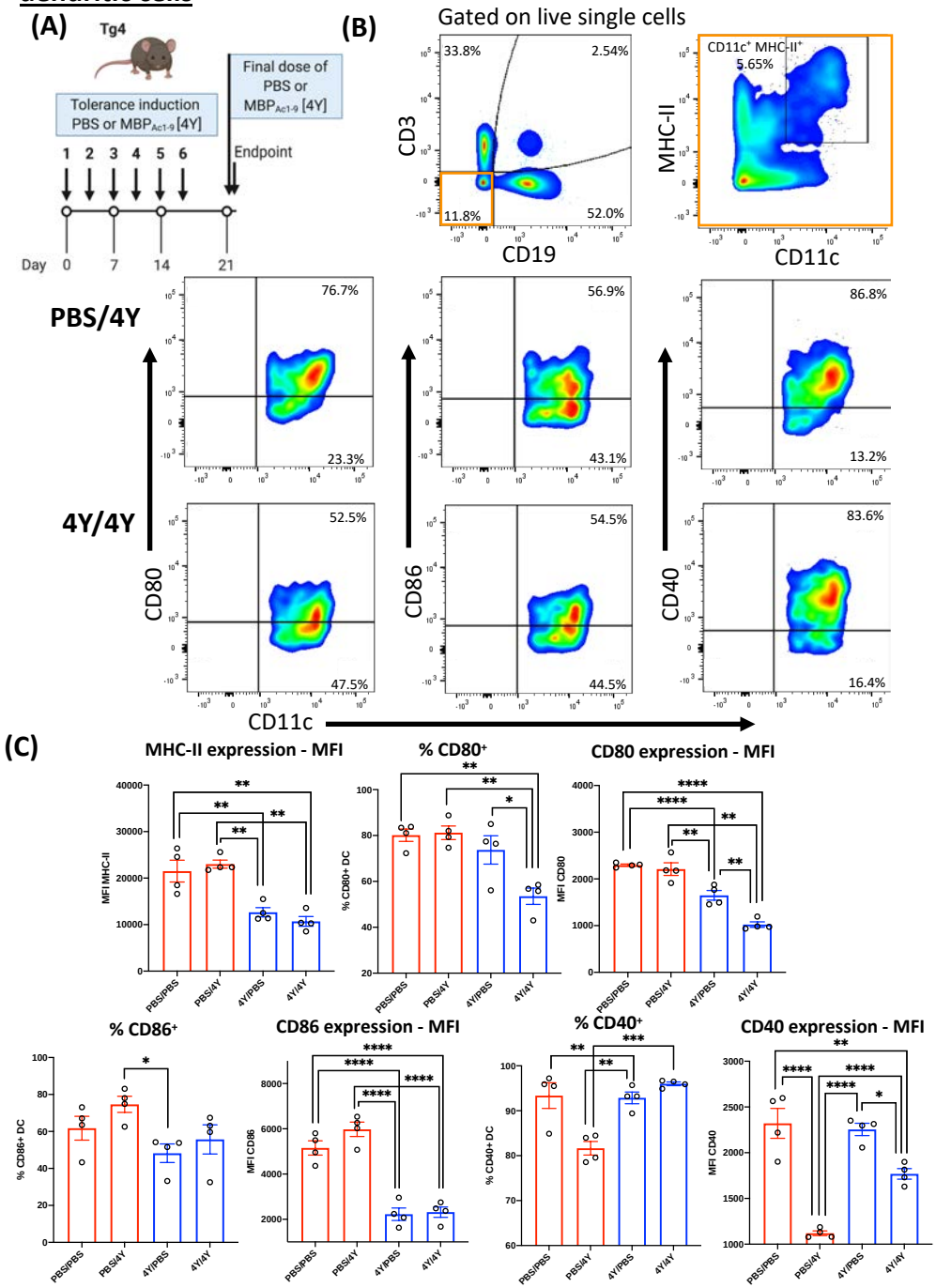

Figure 3.8: Phenotype of CD11c$^+$ MHC-II$^+$ cells from Tg4 mice treated with PBS or MBP$_{Ac1-9}$ [4Y] peptide. (A) Tolerance induction strategy, **(B)** Representative flow cytometry plots of CD11c$^+$ MHC-II$^+$ DC and **(C)** corresponding bar charts showing MHC-II and costimulatory molecule expression as % and MFI, with statistical difference tested by ANOVA.

(reduction in expression level by 54.3%). Expression of CD80 was further suppressed between tolerised resting (PBS/4Y) and tolerised active (4Y/4Y), indicating that CD80 was very rapidly downregulated after TCR stimulation (within 2 hours) and could partially recover between antigen doses (within 3 days) (Fig.3.8C).

The percentage of $CD86^+$ DC was also reduced between PBS/4Y treated and 4Y/4Y treated mice (77.1% to 59.4% $CD86^+$). Assessment of CD86 expression as MFI shows that CD86 reduced by 60% in DC exposed to tolerance induction. CD86 expression by MFI remains at similarly low levels between tolerised resting (4Y/PBS) and tolerised active (4Y/4Y), suggesting that CD86 expression takes longer than 3 days to recover towards pre-tolerised levels and is not affected further by very recent antigen exposure (Fig.3.8C).

By contrast, the number of $CD40^+$ DC remains >95% even after tolerance induction. In fact, DC from naïve activated (PBS/4Y) mice express significantly less CD40 both as a % +ve and MFI, suggesting that *in vivo*, expression of CD40 by dendritic cells is reduced after potent T cell activation, allowing for negative regulation of the immune response. CD40 expression by MFI shows a reduction of 23.2% between PBS/PBS and 4Y/4Y DC and a reduction of 19.8% between 4Y/PBS and 4Y/4Y DC (Fig.3.8C). This data shows tolerised resting cells are not altered in their DC CD40 expression; however, when tolerised cells encounter antigen (4Y/4Y), the normal downregulation of CD40 is less strong compared to naïve activated cells. This may be due to a level of compensation between T cell CD40L and DC CD40 expression levels, as when CD40L is high (PBS/4Y) DC production of CD40 is reduced, and when Tol T cells are prevented from upregulation of CD40L DC production of CD40 remains high. Both CD80 and CD86 are suppressed far below the expression levels of dendritic cells from PBS/PBS highlighting that the potency

of the effect of T cell tolerance on DC. Considering our CTLA-4 expression data in tolerant T cells (Tr1 and Treg) alongside the robust control of CD80 and CD86 expression on DC, we hypothesised that tolerant T cells were more potent mediators of CTLA-4-CD80/86 trans-endocytosis.

Splenic B cells were gated as Live→Single cells→$CD3^{-}CD19^{+}$ and stained for costimulatory molecule expression (Fig.3.9B). Figure 3.9C summarises the expression of MHC-II, CD80, CD86 and CD40 of B cells as percentage +ve for each marker and as MFI.

B cells upregulate MHC-II, CD80 and CD86 upon T cell activation with peptide *in vivo* (PBS/4Y), which is largely prevented in tolerised mice (4Y/PBS and 4Y/4Y) (Fig.3.9C). It is important to note that expression of CD80 and CD86 by B cells is extremely low in comparison to DC (PBS/PBS: CD80 ↓14x, CD86 ↓32x). MFI of CD86 is suppressed in tolerised resting cells, yet is recovered by recent antigen exposure. Expression of CD40 as a percentage of B cells is unaffected by either recent antigen exposure or tolerance induction. However by MFI, CD40 expression is reduced upon recent antigen exposure and T cell activation, even in tolerised mice, closely resembling the CD40 expression pattern in DC.

Analysis of DC/B cell MHC-II and costimulatory molecule expression directly out of the mouse revealed the extent to which DC are better adapted for T cell activation compared to B cells. DC express very high levels of CD80 and CD86, dwarfing expression by B cells. DC in particular are highly receptive to the effects of T cell tolerance, highlighted by the significant downregulation of MHC-II, CD80 and CD86. What is particularly interesting is

Figure 3.9: Effect of tolerance induction on antigen-presenting cells: B cells

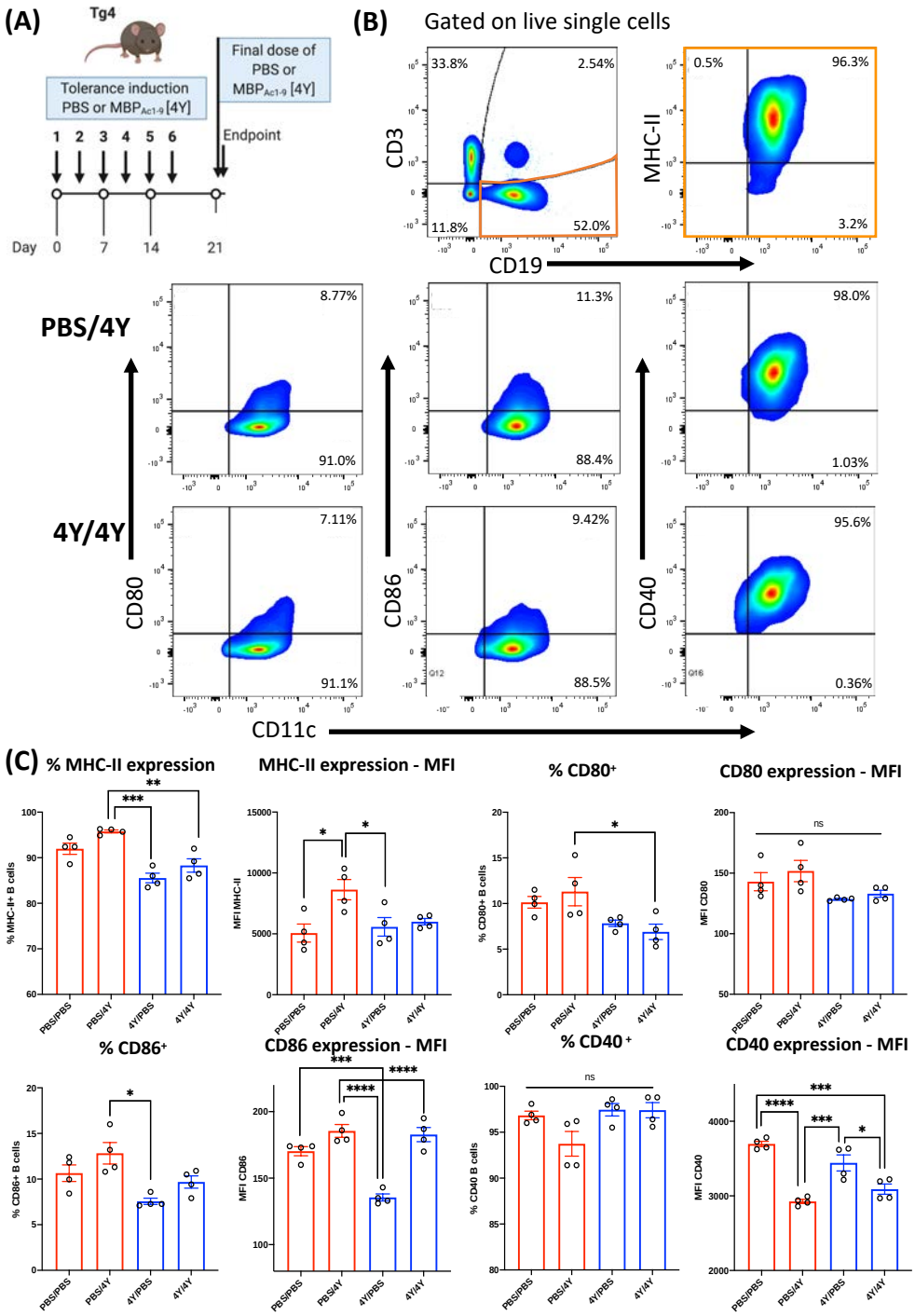

Figure 3.9: Phenotype of CD19+ cells from Tg4 mice treated with PBS or MBP_{Ac1-9} [4Y peptide. (A) Tolerance induction strategy **(B)** Representative flow cytometry plots of $CD19^+$ B cells and **(C)** corresponding bar charts showing MHC-II and costimulatory molecule expression as % and MFI, with statistical difference tested by ANOVA.

that CD80 and CD86 suppression appears to have different kinetics, with CD86 being suppressed on a longer timescale, whereas maximal suppression of CD80 requires more frequent antigen exposure.

3.3.2 PD-L1 expression by APC is not boosted by tolerance induction

Tg4 mice were treated with PBS and MBP_{Ac1-9} [4Y] as previously described prior to antibody staining directly *ex vivo* with a dendritic cell and B cell panel including PD-L1. PD-L1 is a negative regulator of T cell activation and clonal expansion along with its co-inhibitory receptor PD-1; however, this interaction is not essential to establish antigen-specific T cell tolerance (Konkel et al., 2010). We have already determined that PD-1 is highly upregulated on the surface of both IL-10^+ Tr1 cells and Treg after peptide immunotherapy. We hypothesised that PD-L1-PD-1 interactions could play a role in bystander suppression particularly if PD-L1 is upregulated on the surface of APC populations after tolerance induction.

PD-L1 was upregulated on the surface of DC and B cells after recent antigen exposure in both naïve activated and tolerised activated conditions (Fig.3.10). However, in tolerised 4Y/4Y mice, PD-L1 was less strongly expressed by DC and B cells both as a proportion of PD-$L1^+$ cells and by MFI compared to PBS/4Y mice. This demonstrates that PD-$L1^+$ APC are not increased in number or by level of PD-L1 expression as a result of peptide treatment, and that PDL-1 is therefore not likely to play a role in bystander suppression of non-antigen specific T cells.

Figure 3.10: Effect of tolerance induction on antigen-presenting cells: expression of PD-L1

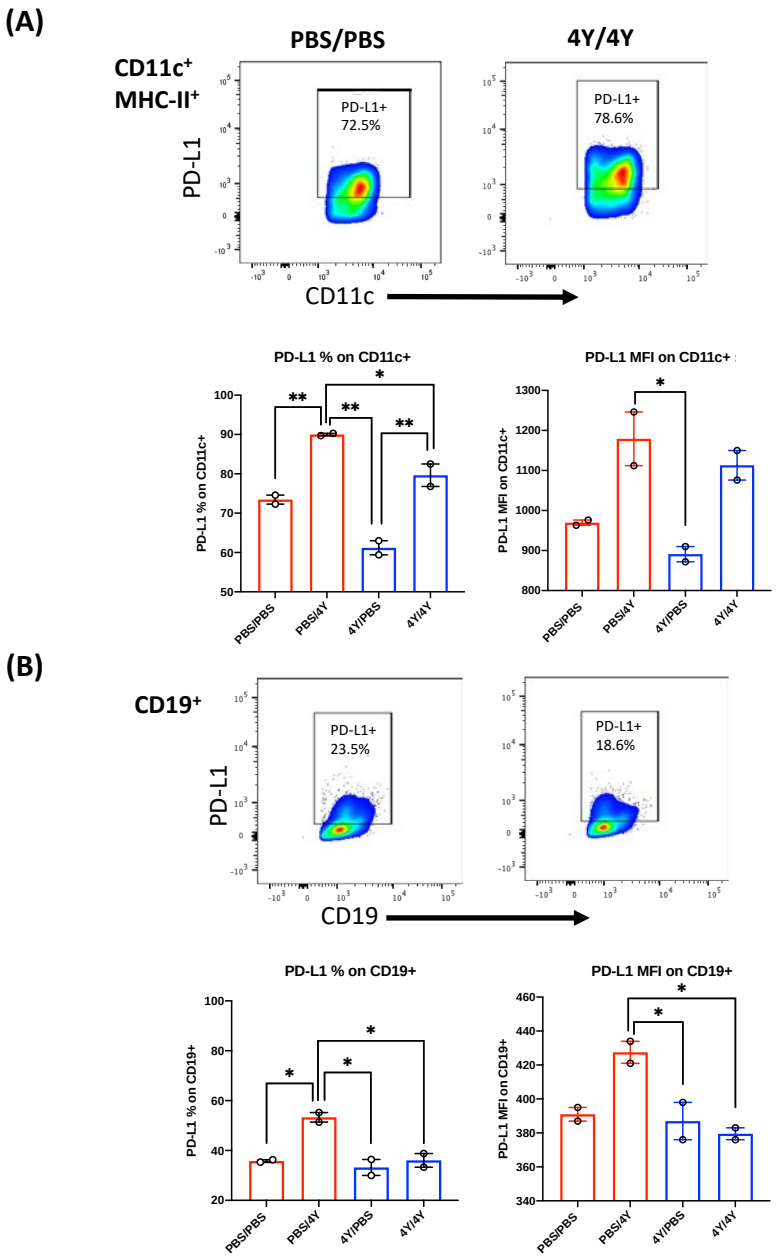

Figure 3.10: PD-L1 expression of CD11c$^+$ MHC-II$^+$ and CD19$^+$ cells from Tg4 mice treated with PBS or MBP$_{Ac1-9}$ [4Y] peptide. Tg4 mice were treated as previously, resulting in PBS/PBS, PBS/4Y, 4Y/PBS and 4Y/4Y conditions. Isolated splenocytes were stained for cell surface expression of inhibitory marker PD-L1 **(A)** Representative flow cytometry plots of CD11c$^+$ MHC-II$^+$ cells with corresponding bar charts and **(B)** Representative flow cytometry plots of CD19$^+$ cells with corresponding bar charts . Statistical difference tested by ANOVA.

3.4. Naïve antigen-presenting cells are modulated by co-culture with tolerant CD4$^+$ T cells *in vitro*

3.4.1 Dendritic cell modulation by co-culture with tolerant CD4+ T cells in vitro

To better assess how T cells are able to exert suppressive effects on DC and B cells and to establish a system in which different suppressive pathways could be manipulated, we set up a series of co-culture experiments where PBS or Tol CD4$^+$ T cells from Tg4 mice were cultured with naïve (B10.PLxB6)F1 CD11c$^+$ cells or CD19$^+$ cells (APC) (Fig.3.11A). These co-cultures initially had very simple conditions: APC + PBS or Tol CD4$^+$ T cells either with or without additional MBP_{Ac1-9} peptide stimulation *in vitro* (Fig.3.11B), which later progressed to include blocking IL-10 and CTLA-4 pathways (Fig.3.14). Figure 11C depicts the MHC-II and co-stimulatory molecule expression profile of (B10.PLxB6)F1 CD11c$^+$ (DC) cells after 24h in co-culture with either PBS CD4$^+$ or Tol CD4$^+$ from Tg4 mice.

Figure 3.12 summarises all expression data of naïve (B10.PLxB6)F1 CD11c$^+$ cell co-culture with 8 PBS and 8 Tol CD4$^+$ Tg4 collated from 2 independent experiments. MHC-II expression of CD11c$^+$ cells was not significantly impacted by 24h in culture with either PBS or Tol Tg4 cells (Fig.3.12A). DC expression of both CD80 and CD86 were very potently suppressed when exposed to activated Tol CD4$^+$ cells *in vitro* (Fig.3.12B&C). The number of CD80$^+$ DC was reduced from 89.2% to 79.2% by culture with PBS vs Tol CD4$^+$ cells in the absence of peptide stimulation, dropping further to just 31.2% CD80$^+$ when in the presence of Tol CD4$^+$ cells stimulated with MBP_{Ac1-9} [4K] peptide. At a population level, looking at MFI, DC co-cultured in the naïve activated PBS CD4 + MBP_{Ac1-9} [4K] condition strongly upregulated CD80 expression, indicative of DC maturation, which was abrogated when DC were exposed to Tol CD4 + MBP_{Ac1-9} [4K]. Expression of CD86 follows an almost

Figure 3.11: In vitro effect of Tg4 Tol CD4⁺ T cells on naïve DC costimulatory molecule expression

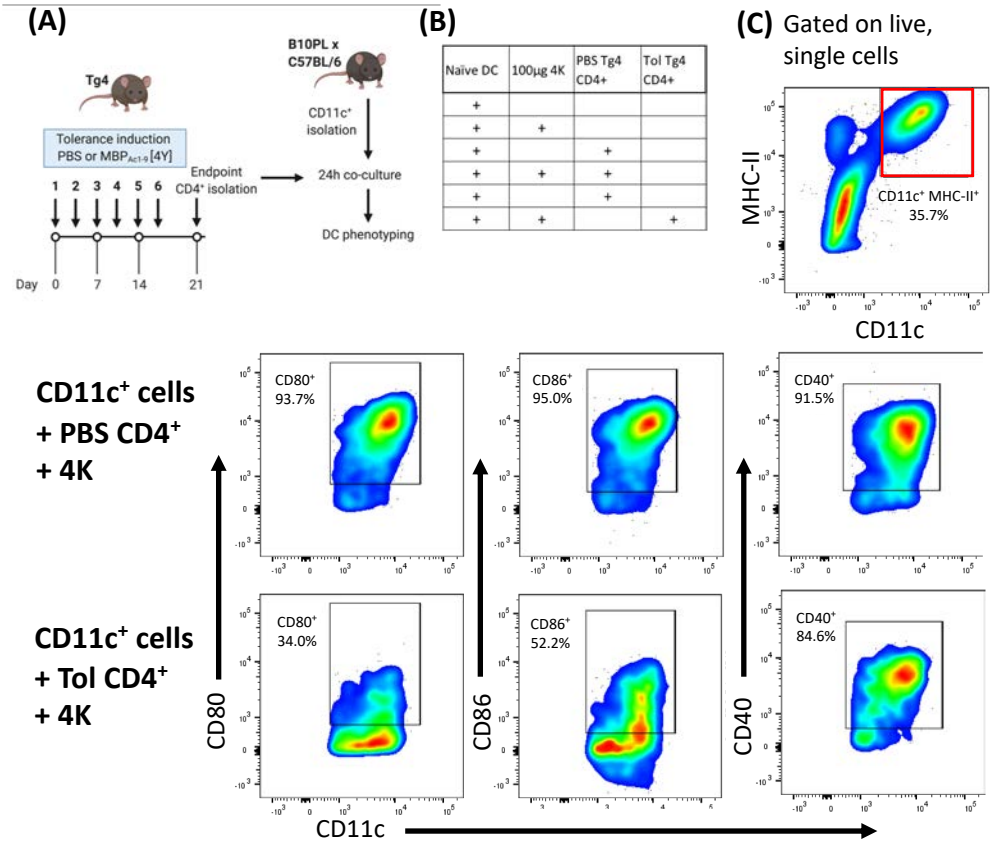

Figure 3.11: Phenotype of naïve (B10.PLxC57BL/6) F1 CD11c⁺ cells after stimulation with co-culture with PBS or Tol Tg4 CD4⁺ cells and MBP_{Ac1-9} 4K peptide. (A) Tg4 mice were treated with PBS (n=8) or MBP_{Ac1-9} 4Y (n=8) by s.c. dose escalation protocol. 3 days after the last dose, spleens were harvested and CD4⁺ T cells isolated. CD11c⁺ cells were isolated from B10.PL x C57BL/6 mice. **(B)** Culture conditions in 96 U bottomed plates: 50,000 APC: 100,000 CD4⁺ cells. Cells were cultured for 24h before antibody staining **(C)** Representative flow cytometry plots of CD11c⁺ MHC-II⁺ cell gating and costimulatory molecule expression with PBS CD4 vs Tol CD4 Tg4 cells in the presence of 4K peptide.

Figure 3.12: In vitro effect of Tg4 Tol CD4+ T cells on naïve DC costimulatory molecule expression

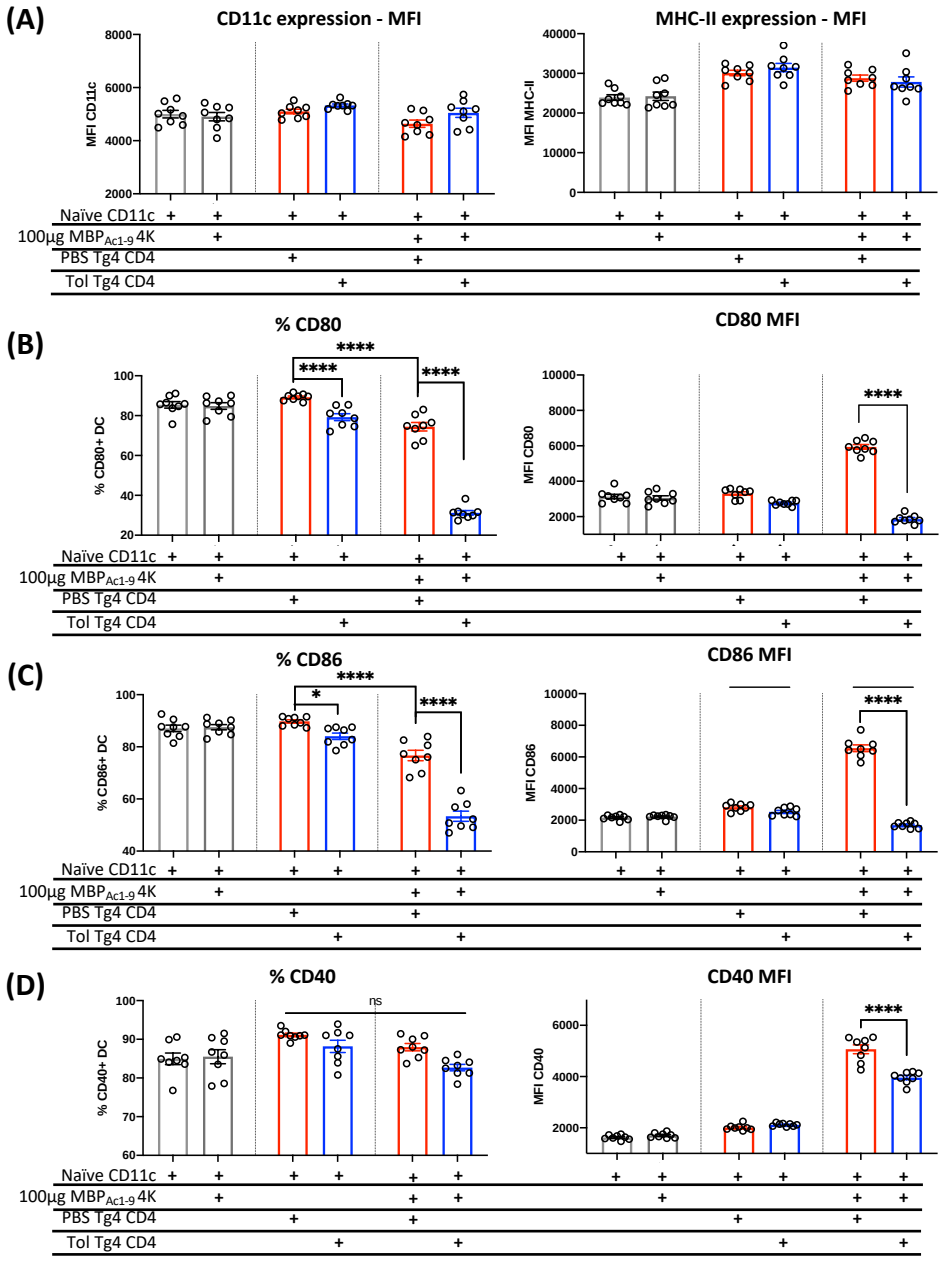

Figure 3.12: Phenotype of naïve (B10.PLxC57BL/6) F1 CD11c$^+$ cells after stimulation with MBP$_{Ac1-9}$ peptide and co-culture with PBS or Tol Tg4 CD4$^+$ cells. CD11c$^+$ cells from naïve B10.PL x C57BL/6 mice were co-cultured with PBS (red bars) or MBP$_{Ac1-9}$ treated Tol (blue bars) Tg4 CD4+ cells as described previously. After 24h CD11c$^+$ cells were stained for MHC-II and costimulatory molecules CD80/CD86/CD40. Surface marker expression is summarized as a percentage of CD11c$^+$ cells and Median Fluorescence Intensity. Statistical difference between key conditions assessed by ANOVA.

identical pattern: DC co-cultured in the naïve activated PBS CD4 + MBP_{Ac1-9} [4K] condition strongly upregulated CD86 expression, yet when those DC were exposed to Tol CD4 + 4K, this upregulation was completely prevented. Similar to our observations directly *ex vivo* from tolerised Tg4 mice, DC in these co-culture with activated Tol $CD4^+$ cells were suppressed in their expression of CD80 and CD86 below the background level of untouched DC, providing further evidence of the strength of suppressive effect of Tol T cells on DC. Percentage of $CD40^+$ (B10.PLxB6)F1 $CD11c^+$ cells and their expression by MFI was significantly reduced after co-culture with Tol $CD4^+$ in the presence of MBP_{Ac1-9} [4K]. When cultures were stimulated with peptide, DC in both settings upregulated CD40 by MFI, but Tol $CD4^+$ cultures to a much lesser extent (Fig.3.12D; DC CD40 MFI of PBS $CD4^+$ culture increased by 2.5x with peptide stimulation, DC CD40 MFI of Tol $CD4^+$ culture increased by 1.87x with peptide stimulation).

This data repeats key experiments published previously describing the *in vitro* effect of Tol $CD4^+$ on DC phenotype and very closely resembles the suppression observed (Gabryšová et al., 2009a). It is interesting that when stimulated *in vitro*, DC in contact with Tol T cells are prevented from upregulation of CD40, whilst DC isolated from Tol Tg4 mice *ex vivo* subject to the entire tolerance induction protocol are not significantly prevented from CD40 expression, highlighting a divergence of *in vivo* vs *in vitro* assessments.

We then progressed to a more complex variation of this experiment to include the addition of blocking Ab against IL-10R and CTLA-4 as well as comparing the effect of bulk CD4 vs Treg $CD4^+CD25^+$ isolated from Tg4 mice. $CD4^+CD25^+$ Treg isolated by magnetic

Figure 3.13: Effect of blocking IL-10-R and CTLA-4 pathways on bulk T or isolated Treg co-culture with naïve CD11c$^+$ cells

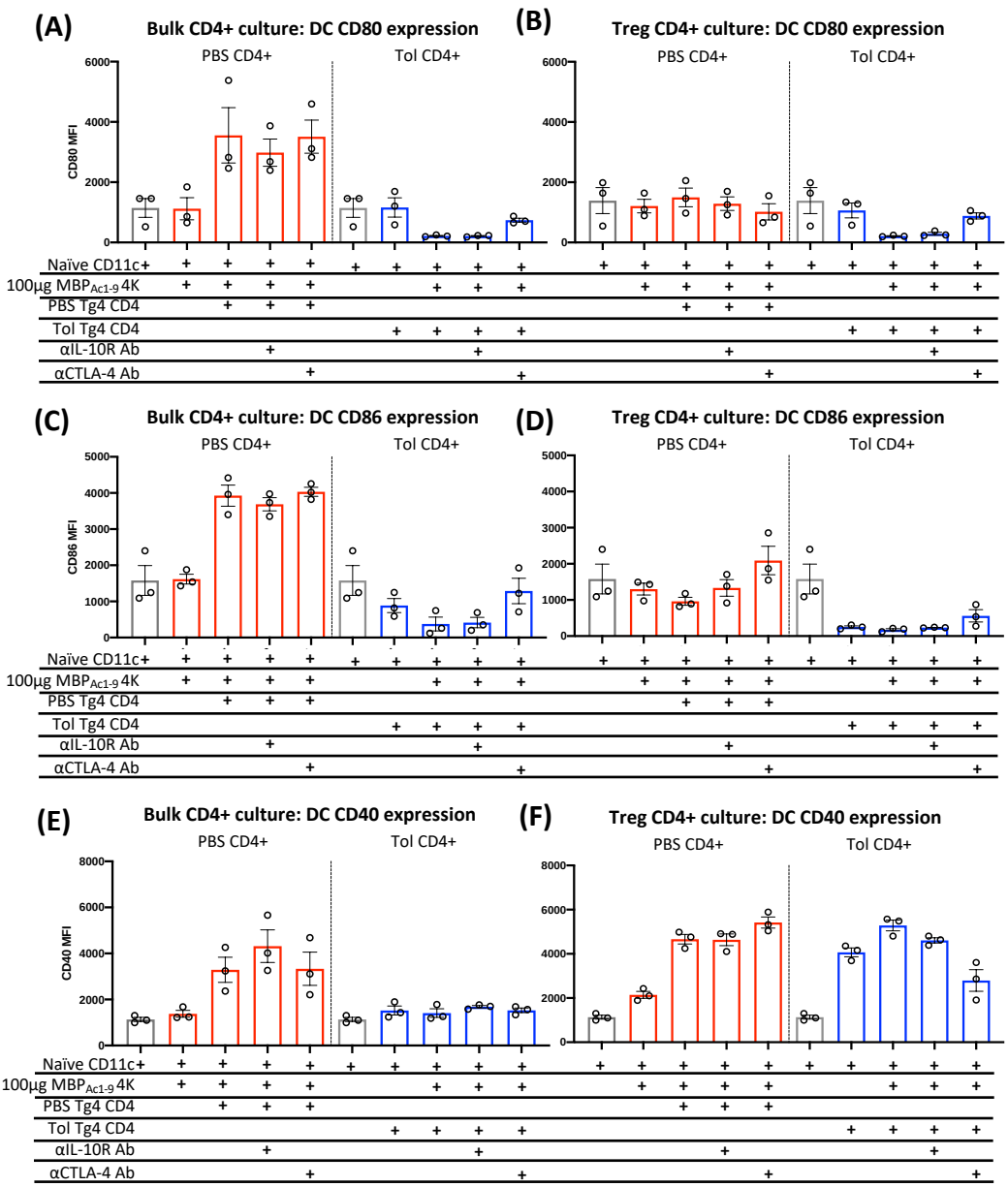

Figure 3.13: Phenotype of naïve (B10.PLxC57BL/6) F1 CD11c$^+$ cells following co-culture with CD4$^+$ cells or Treg Tg4 cells with stimulation with MBP$_{Ac1-9}$ [4K] peptide and blocking αIL-10R/αCTLA-4 Ab. CD11c$^+$ cells from naïve (B10.PLxC57BL/6) F1 mice were co-cultured with either PBS (red bars) or MBP$_{Ac1-9}$ [4Y] treated (blue bars) bulk CD4$^+$ or CD4$^+$CD25$^+$ Treg Tg4 cells. 1µg/ml αIL-10R/αCTLA-4 was incubated with cell cultures for 2h cultures before stimulation. After 24h CD11c$^+$ cells were stained for MHC-II and costimulatory molecules CD80/ CD86/CD40. Surface marker expression is summarized as a percentage of CD11c$^+$ cells and Median Fluorescence Intensity.

separation were on average 90% $CD4^+$, 80% $CD25^+$ and 80% $FoxP3^+$ (not shown). Figure 3.13 summarises DC expression data under each condition. As this experiment could only be completed once in its entirety due to COVID disruption, there are no statistical tests applied to the data. However, it does show specific trends which are worth detailing as part of this thesis.

As previously in Fig.3.12B&C, DC expression of CD80 and CD86 is robustly upregulated when cultured with MBP_{Ac1-9} [4K] stimulated PBS treated $CD4^+$ cells. This upregulation is prevented and suppressed even below background DC levels by co-culture with MBP_{Ac1-9} [4K] stimulated Tol $CD4^+$ cells (Fig.3.13A&C). The addition of blocking IL-10R Ab to co-culture wells with MBP_{Ac1-9} stimulated Tol $CD4^+$ cells did not alter CD80/CD86 expression, whereas blocking CTLA-4 in these conditions partially restored CD80/CD86 expression. When DC were cultured with naïve, PBS treated $CD4^+CD25^+$ Treg, upregulation of CD80/CD86 upon T cell stimulation with MBP_{Ac1-9} [4K] was abrogated, showing that Treg constitutively regulate DC CD80/86 expression *in vitro* (Fig.3.13B&D). Expression of CD80 was further suppressed when DC were exposed to peptide-activated Tol Treg, whilst CD86 was suppressed equally strongly by both unstimulated and stimulated Tol Treg, indicating a potential bias for naïve Treg cells to suppress CD86 > CD80. The addition of αIL-10R Ab did not affect DC expression of CD80/CD86 when cultured with either PBS or Tol Treg, whereas once again αCTLA-4 Ab partially reversed CD80/CD86 suppression. In this co-culture system, we can therefore hypothesise that CTLA-4 mediated CD80/CD86 suppression is dominant over IL-10 mediated suppression of CD80/CD86.

Furthermore, ligation of CD40 has been shown to trigger upregulation of CD80/86 (Elgueta et al., 2009; Caux et al., 1994; Pinchuk et al., 1996), thus without effective CD40L provision by Tol CD4+ cells (Fig.3.6), DC are both unable to increase expression of CD80/86 in response to CD40L-CD40 signalling and more susceptible to increased CTLA-4 mediated trans-endocytosis.

As previously shown in Fig.3.12E, DC CD40 is upregulated upon co-culture with MBP_{Ac1-9} [4K] stimulated PBS $CD4^+$ cells and prevented from upregulation upon exposure to MBP_{Ac1-9} [4K] stimulated Tol $CD4^+$ cells (Fig.3.13E). Addition of αIL-10R Ab in this system further boosted CD40 expression, suggesting a role for IL-10 in negative feedback to control CD40 expression after initial response has been raised. However, neither αIL-10R Ab or αCTLA-4 reversed CD40 suppression by Tol $CD4^+$, suggesting alternative mechanisms involved. It has been shown in human DC that ligation of CD40L-CD40 upregulates DC production of CD40 (Caux et al., 1994; Pinchuk et al., 1996). As Tol T cells are unable to upregulate CD40L in response to antigen exposure (Fig.3.6), CD40L availability may be the primary limiting factor required for high CD40 expression. By contrast, co-culture with both PBS and Tol Treg in the presence of MBP_{Ac1-9} [4K] peptide permitted DC CD40 upregulation (Fig.3.13F), posing the question as to why Treg may be less able to modulate CD40 compared to Tol CD4 of which cells the vast majority of cells would be either anergic Tconv, or IL-10^+FoxP3^- Tr1. A caveat with this experiment is that after tolerance induction, a greater proportion of $CD4^+$ cells express CD25 despite being anergic, therefore in the isolated Treg pool from Tol Tg4, there is likely to be contamination of cells that are not natural Treg. To improve purity of this Treg pool, we could have cell sorted our Treg on the basis of $CD4^+CD25^+$ and secondary lymphoid homing markers CCR7 and CD62L, or by expression of cycling CTLA-4. To give more

confidence in this data and to have enabled robust statistical analysis, I would have needed to do at least one more full independent repeat of this experiment but was constrained by COVID disruptions.

3.4.2 B cell modulation by co-culture with tolerant CD4$^+$ T cells in vitro

Figure 3.14 summarises the experimental protocol required for in vitro co-culture of naïve (B10.PLxB6)F1 CD19$^+$ cells with PBS or MBP$_{Ac1-9}$ [4Y] treated Tg4 CD4$^+$ T cells and the flow cytometry gating strategy of B cell costimulatory markers. Purity of isolated CD19$^+$ cells was >90% (data not shown).

B cell MHC-II expression is increased upon exposure to MBP$_{Ac1-9}$ [4K] peptide-activated PBS CD4$^+$ cells and is increased to a lesser extent with peptide-activated Tol CD4$^+$ cells (Fig.3.15A). Both CD80 and CD86 expression is prevented from upregulation by co-culture with MBP$_{Ac1-9}$ [4K] stimulated Tol CD4$^+$ cells (Fig.3.15B&C). Unlike the dendritic cell cultures, expression levels of CD80/CD86 on B cells are not reduced below that of background, suggesting that suppression of B cells *in vitro* is less robust than DC. This reflects recent work published from Prof. Walker's group at UCL showing that CTLA-4 targets CD80/CD86 specifically from migratory DC (Ovcinnikovs et al., 2019), we would have liked to have repeated these experiments to distinguish between migratory and resident DC in the spleen. B cell expression of CD40 is similarly upregulated upon co-culture with both MBP$_{Ac1-9}$ [4K] stimulated PBS and Tol CD4$^+$ cells, exposing a further difference between *in vitro* suppression of DC and B cells (Fig.3.15D).

Figure 3.14: In vitro effect of Tg4 Tol CD4+ T cells on naïve B cell costimulatory molecule expression

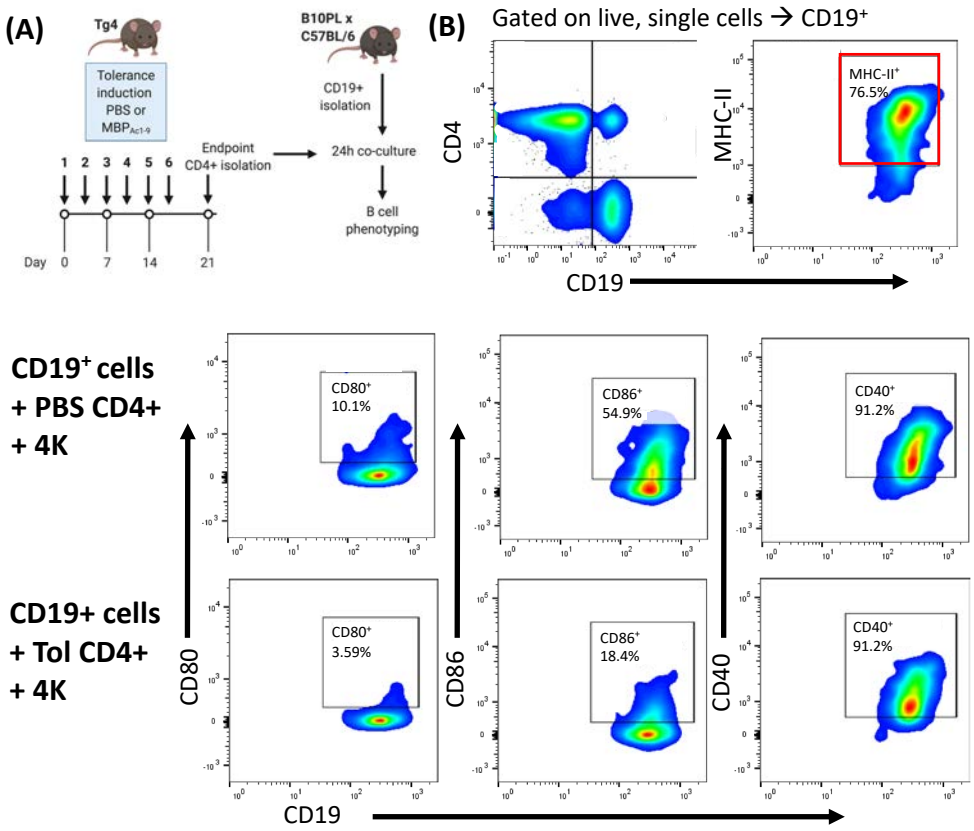

Figure 3.14: Phenotype of naïve (B10.PLxC57BL/6) F1 CD19⁺ cells after stimulation with co-culture with PBS or Tol Tg4 CD4⁺ cells and MBP_{Ac1-9} 4K peptide. (A) Tg4 mice were treated with PBS (n=8) or MBP_{Ac1-9} 4Y (n=8) by s.c. dose escalation protocol. 3 days after the last dose, spleens were harvested and CD4⁺ T cells isolated. CD19⁺ cells were isolated from B10.PL x C57BL/6 mice. **(B)** Culture conditions in 96 U bottomed plates: 50,000 APC: 100,000 CD4⁺ cells. Cells were cultured for 24h before antibody staining **(C)** Representative flow cytometry plots of CD11c+ MHC-II+ cell gating and costimulatory molecule expression with PBS CD4 vs Tol CD4 Tg4 cells in the presence of 4K peptide.

Figure 3.15: In vitro effect of Tg4 Tol CD4$^+$ T cells on naïve B cells costimulatory molecule expression

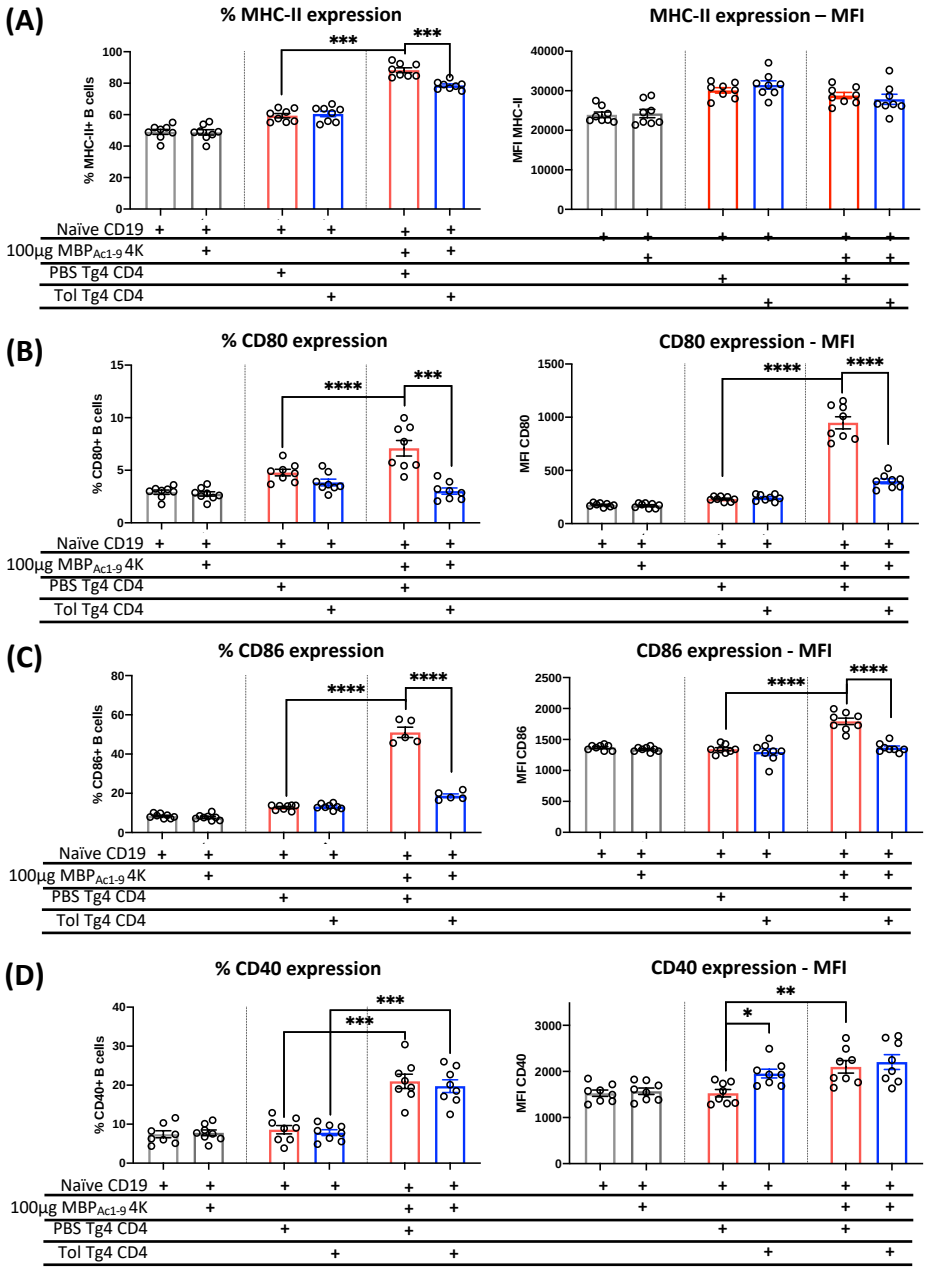

Figure 3.15: Phenotype of naïve (B10.PLxC57BL/6) F1 CD19$^+$ cells after stimulation with co-culture with PBS or Tol Tg4 CD4$^+$ cells and MBP$_{Ac1-9}$ [4K] peptide. CD19$^+$ cells from naïve (B10.PLxC57BL/6) F1 mice were co-cultured with PBS (red bars) or MBP$_{Ac1-9}$ [4Y] treated Tol (blue bars) Tg4 CD4$^+$ cells as described previously. After 24h CD19$^+$ cells were stained for MHC-II and costimulatory molecules CD80/CD86/CD40. Surface marker expression is summarized as a percentage of CD19$^+$ cells and Median Fluorescence Intensity. Statistical difference between conditions assessed by ANOVA.

3.4.3 Production of IL-10 and IL-12 by DC co-culture with tolerant CD4$^+$ T cells *in vitro*

Despite attempting various means of staining for IL-10 and IL-12 within DC and B cell populations, both with and without exogenous stimulation with peptide antigen, LPS and/or αCD40 mAb, I was unable to identify IL-10$^+$ B cells (Breg) or DC (data not shown).

As direct antibody staining using the Tg4 model was not able to identify clear populations of DC or B cells expressing IL-10 or expression of IL-12p70 by DC, sandwich ELISA was used to monitor IL-10 and IL-12p70 production from APC:T cell co-culture experiments. By ELISA, it is not possible to identify the cellular source of measured cytokines, therefore we cannot determine whether our APC populations express IL-10 as expression would be drowned out by that of T cells. DC:PBS T cell co-cultures do not generate IL-10, whilst DC:Tol T cell co-cultures are induced to produce high levels of IL-10 upon $MBP_{Ac1\text{-}9}$ [4K] stimulation, which is further increased by blocking IL-10R (Fig.3.16A).

IL-12 production is DC restricted and is reliant on CD40L-CD40 signalling (Snijders et al., 1998; Ma et al., 2015). DC:PBS T cell co-cultures secrete very high concentrations of IL-12 promoting the expansion of the Th1 response to $MBP_{Ac1\text{-}9}$ [4K], which is then further boosted by the addition of IL-10R blocking Ab (Fig.3.16B). In this system, effective IL-10 signalling can help control the extent of the immune response by dampening IL-12 production.

Figure 3.16: Expression of IL-10 and IL-12 in Tg4 T cell:naïve DC co-cultures

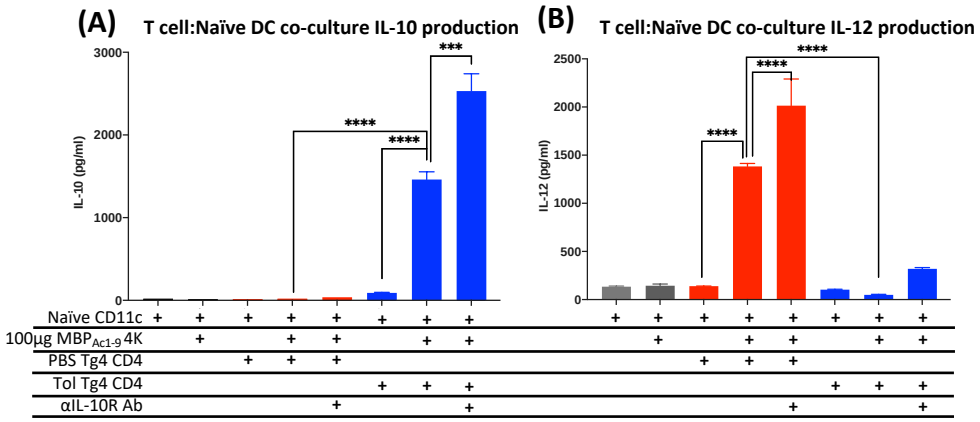

Figure 3.16: Expression of IL-10 and IL-12 from co-cultures of (B10.PLxC57BL/6) F1 CD11c$^+$ with PBS or Tol Tg4 CD4$^+$ cells and MBP$_{Ac1-9}$ [4K] peptide. CD11c$^+$ cells from naïve (B10.PLxC57BL/6) F1 mice were co-cultured with PBS (red bars) or MBP$_{Ac1-9}$ [4Y] treated Tol (blue bars) Tg4 CD4$^+$ cells as described previously. After 24h cell culture supernatant was analysed for IL-10 and IL-12 concentration by ELISA.

3.5 Introduction to the bystander model: (B10.PLxB6)F1 mice and MBP_{Ac1-9}/ MOG_{35-55} peptides

As described previously, a linked hybrid peptide comprised of the two MBP and MOG epitopes joined with a HFFK linker region, hereafter called MBP_{Ac1-9}-HFFK-MOG_{35-55}, was synthesised as a means to deliver both peptides to the same antigen-presenting cell. To establish that the MBP_{Ac1-9}-HFFK-MOG_{35-55} hybrid peptide functioned as intended and was able to stimulate both MBP_{Ac1-9} and MOG_{35-55} specific T cells *in vivo*, (B10.PLxB6)F1 mice were immunised with 100µg MBP_{Ac1-9}-HFFK-MOG_{35-55} in CFA adjuvant. 10 days post-immunisation, spleen and lymph node were isolated and stimulated *in vitro* with a serial dilution of hybrid MBP_{Ac1-9}-HFFK-MOG_{35-55}, MBP_{Ac1-9} peptide, MOG_{35-55}, and a scrambled sequence variant of MBP_{Ac1-9} in triplicate. After 3 days of *in vitro* stimulation, cell culture supernatants were assessed for IFN-ɣ concentration and cells were pulsed with [^{3}H]-thymidine for 16-20hours. Figure 3.17 shows proliferative responses and IFN-ɣ production of draining lymph node cells (Fig.3.17A) and spleen (Fig.3.17B) in response to *in vitro* stimulation with MBP/MOG peptides.

Mice immunised with MBP_{Ac1-9}-HFFK-MOG_{35-55} hybrid peptide were able to generate strong immune responses to the hybrid peptide as well as to MBP_{Ac1-9} and MOG_{35-55} peptides individually, showing that during the processes of immunisation and recall, the hybrid peptide was effectively split into its constitutive epitopes for priming of separate T cells populations towards both MBP_{Ac1-9} and MOG_{35-55}. Mice did not generate responses towards the scrambled MBP peptide, towards which they were not primed *in vivo*.

Figure 3.17: (B10.PL x C57BL/6) F1 immunisation with linked peptide MBP_{Ac1-9}-HFFK-MOG_{35-55}

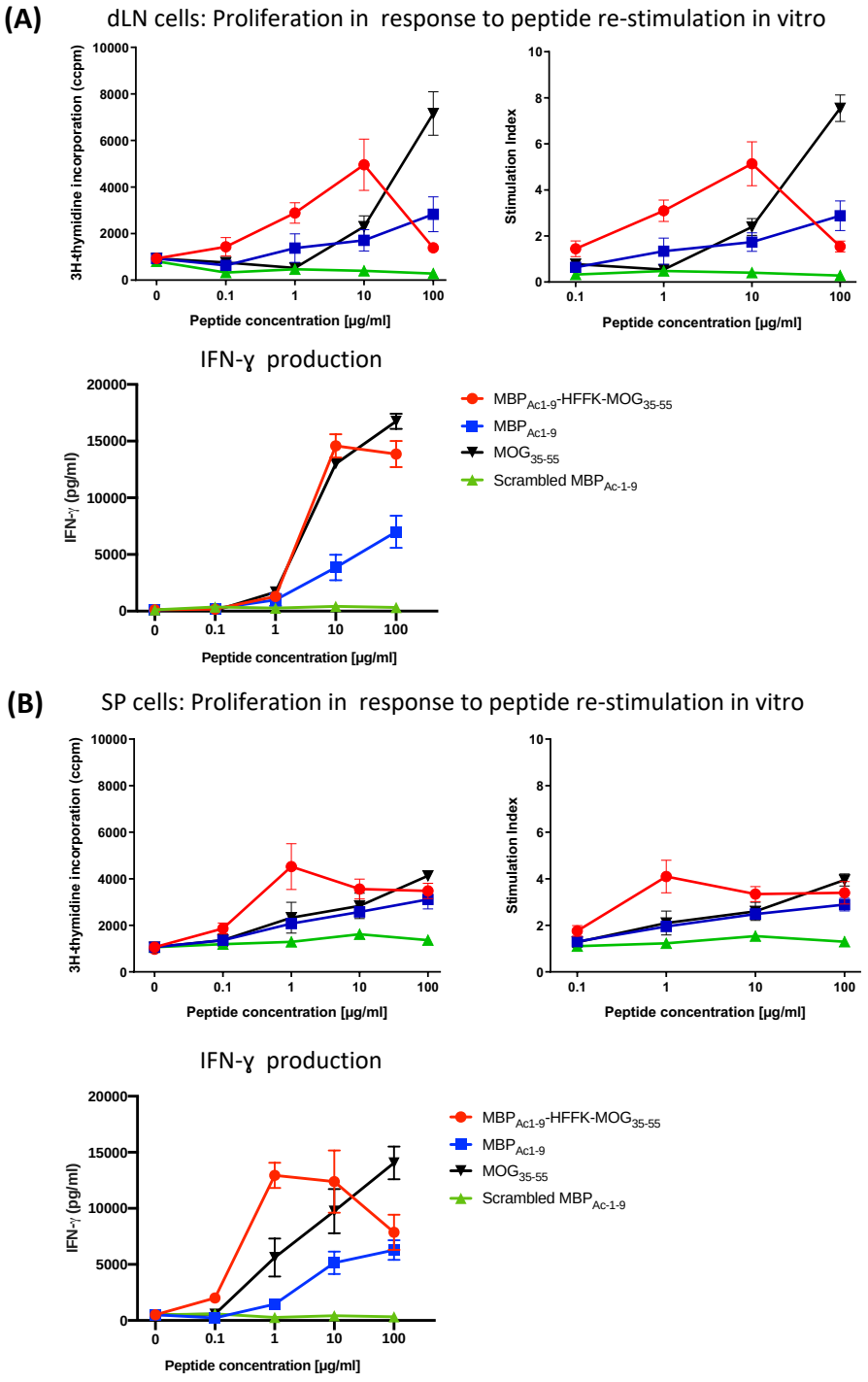

Figure 3.17: Proliferation and IFN-γ recall responses of (B10.PL x C57BL/6) F1 mice after immunisation with MBP_{Ac1-9}-HFFK-MOG_{35-55}. (B10.PL x C57BL/6) F1 mice (n=4) were immunised with 100µg of MBP_{Ac1-9}-HFFK-MOG_{35-55} linked peptide in 100µl CFA supplemented with 8mg/ml

MTb. 10 days post-immunisation, **(A)** draining lymph node and **(B)** spleen cells were isolated and plated at 5 x 10^6 cells/ml or 10 x 10^6 cells/ml, respectively, in complete RPMI supplemented with 10% FCS. Cells were then stimulated with a serial dilution of MBP_{Ac1-9}-HFFK-MOG_{35-55} (red lines), MBP_{Ac1-9} (blue lines), $MBP_{scrambled}$ (green lines) or MOG_{35-55} (black lines) in triplicate. 3 days after in vitro stimulation, 100µl of culture supernatant was removed for IFN-ɣ ELISA, whilst the remaining 100µl cell suspension was incubated for 16-20 hours with 0.18MBq/ml [^{3}H]-thymidine. [^{3}H]-thymidine incorporation was measured on a scintillation reader as corrected counts per minute (cpm) then converted to Stimulation Index (SI). SI = cpm of stimulated condition/cpm of unstimulated condition. Graphs display mean values for each peptide over the tested concentration range.

3.6 Evidence of bystander suppression *in vitro:* co-culture of Tg4 and 2D2 $CD4^+$ T cells

To assess whether we could observe bystander suppressive effects between T cells of different antigen specificities *in vitro*, we set up a series of co-culture experiments in which transgenic Tg4 $CD4^+$ T cells (MBP_{Ac1-9} specific) and transgenic 2D2 $CD4^+$ T cells (MOG_{35-55} specific) can be monitored. Figure 3.18A summarises the protocol schematic, briefly: Tg4 mice tolerised using repeated s.c. injection of MBP_{Ac1-9} [4Y] peptide prior to splenic $CD4^+$ cell isolation, naïve splenic $CD4^+$ cells were isolated from 2D2 mice and stained using proliferation dye Cell Trace Violet and bulk splenocytes from (B10.PLxB6)F1 mice were irradiated to act as antigen-presenting cells. Tg4 and 2D2 cells can be differentiated by the presence of TCR genes Vβ8 and Vβ11, respectively (Fig.3.18B). Proliferation of 2D2 $CD4^+$ cells can be monitored alongside additional activation markers (CD25/CD69) in response to peptide stimulation. 2D2 + PBS Tg4 + SP cell cultures stimulated with hybrid MBP_{Ac1-9}-HFFK-MOG_{35-55} peptide and separate MBP_{Ac1-9}+ MOG_{35-55} reveal clear 2D2 $CD4^+$ proliferation in response to the MOG_{35-55} components (Fig.3.18C&D). Stimulation with separate peptides generates higher 2D2 proliferation, which is to be expected due to increased molarity of MOG_{35-55} in 10µg MOG_{35-55} ($3.87x10^{-3}$ moles) vs 10µg hybrid MBP_{Ac1-9}-HFFK-MOG_{35-55} peptide ($2.39x10^{-3}$ moles). In subsequent *in vivo* antigen challenge experiments, equimolar amounts of MBP_{Ac1-9}-HFFK-MOG_{35-55} and separate peptides were used, i.e. for 100µg of linked hybrid peptide, 33µg of MBP_{Ac1-9} [4K] and 66µg MOG_{35-55} was used.

To assess whether the proliferation of naïve 2D2 $CD4^+$ cells is affected by co-culture with PBS or Tol Tg4 $CD4^+$ when stimulated using hybrid or separate peptides, the

Figure 3.18: Evidence of bystander suppression *in vitro:* experimental set-up

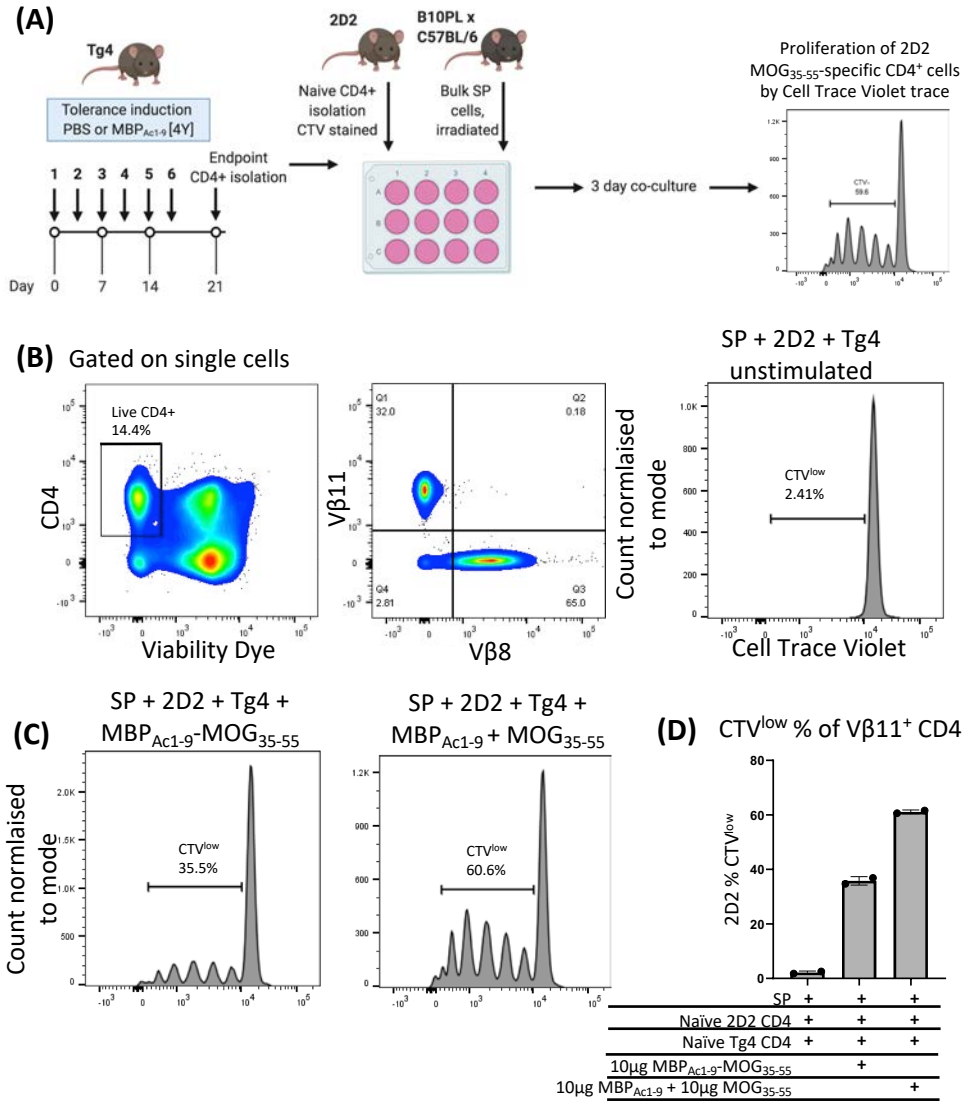

Figure 3.18: Proliferation of MOG_{35-55} specific $CD4^+$ T cells from 2D2 mice can be monitored by Cell Trace Violet *in vitro*. (A) $CD4^+$ T cells from PBS or MBP_{Ac1-9} (4Y) treated Tg4 mice (Vβ8 TCRβ chain) were cultured with naïve Cell Trace Violet stained $CD4^+$ T cells from 2D2 mice (Vβ11 TCRβ chain) and irradiated (B10.PL x C57BL/6) F1 splenocytes to act as antigen-presenting cells. Cells were stimulated with either 10μg MBP_{Ac1-9}-MOG_{35-55} linked peptide or 10μg MBP_{Ac1-9} + 10μg MOG_{35-55} peptides separately for 3 days prior to antibody staining and flow cytometry. **(B)** Gating strategy for Vβ11+ CD4+ cells from 2D2 mice which had been stained with CTV on day 0 (unstimulated control). **(C)** CTV traces of 2D2 CD4+ cells in cultures stimulated with 10μg MBP_{Ac1-9}-MOG_{35-55} linked peptide and 10μg MBP_{Ac1-9} + 10μg MOG_{35-55}. **(D)** Proliferation of 2D2 CD4+ cells as percentage CTV^{low}.

Figure 3.19: Evidence of bystander suppression *in vitro*

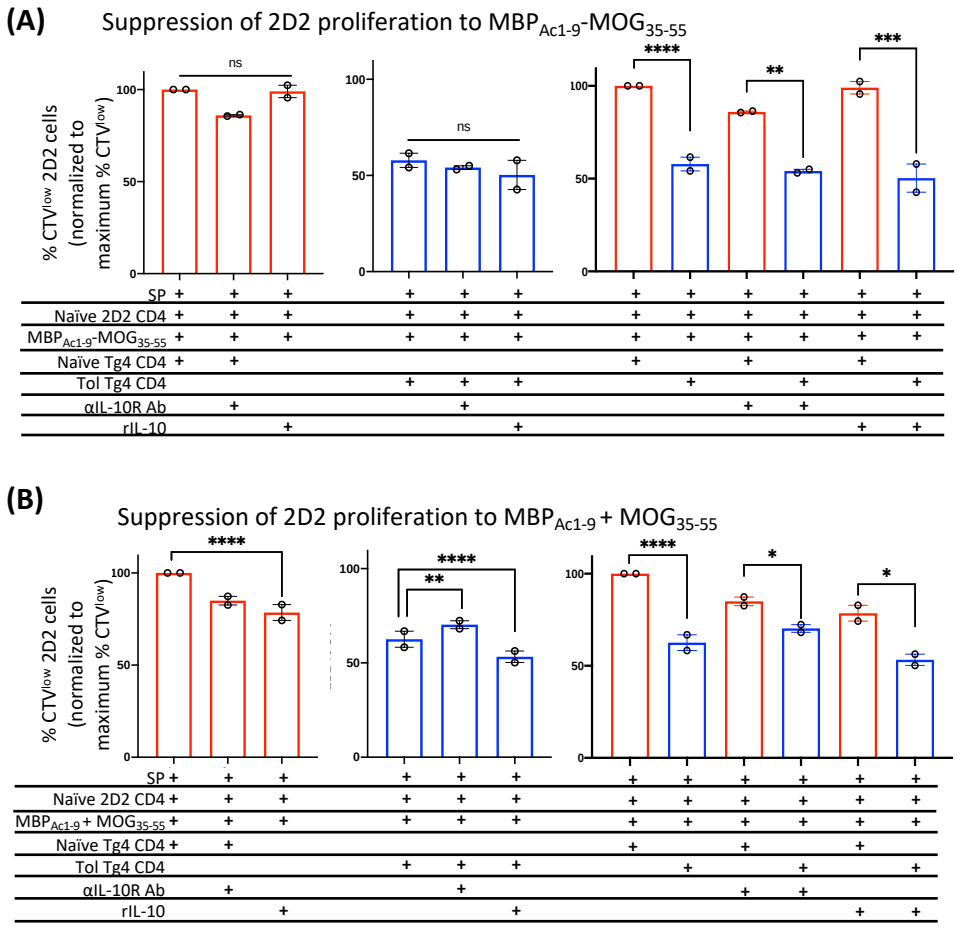

Figure 3.19: Proliferation of MOG_{35-55} specific $CD4^+$ T cells from 2D2 mice can be suppressed by interactions with Tol Tg4 $CD4^+$ cells *in vitro*. Cells were treated and cultured as described in Fig.23. **(A)** 2D2 CD4+ proliferation as % CTV^{low} when stimulated with 10µg MBP_{Ac1-9}-MOG_{35-55} linked peptide in the presence of naïve PBS Tg4 CD4+ cells (red bars) or Tol Tg4 CD4+ cells (blue bars) with addition of αIL-10R Ab or exogenous rmIL-10. **(B)** 2D2 $CD4^+$ proliferation as % CTV^{low} when stimulated with 10µg MBP_{Ac1-9}-MOG_{35-55} linked peptide in the presence of naïve PBS Tg4 CD4+ cells (red bars) or Tol Tg4 CD4+ cells (blue bars) with addition of αIL-10R Ab or exogenous rmIL-10. 2D2 proliferation was normalised to maximum proliferation possible i.e. 2D2 % CTV^{low} + naïve Tg4 $CD4^+$ + peptide stimulation = 100%.

percentage of CTV^{low} 2D2 $CD4^+$ cells was normalised to the maximum (i.e. in maximally stimulated culture: 2D2 $CD4^+$ + naïve Tg4 $CD4^+$ + peptide stimulation = 100% proliferation). Fig.3.19A displays 2D2 proliferation when stimulated with hybrid MBP_{Ac1-9}-MOG_{35-55} peptide with PBS Tg4 cells (red bars) vs Tol Tg4 cells (blue bars). Co-culture with Tol Tg4 cells significantly reduces the proportion of 2D2 cells which proliferate in response to peptide (Fig.3.19A). In this system, both disruption of IL-10 signalling using αIL-10R Ab and promotion of IL-10 signalling by addition of exogenous recombinant mouse IL-10 (rmIL-10) did not affect 2D2 proliferation, indicating that when each APC presents both MBP_{Ac1-9} and MOG_{35-55} peptides, Tol Tg4 and naïve 2D2 $CD4^+$ T cells are likely to be clustered around the central APC and the bystander suppressive effect is not heavily reliant on IL-10. This correlates with previous data published, in which IL-10 was not required for *in vitro* bystander suppression, but was essential for *in vivo* bystander suppression (O'Neill et al., 2004).

Fig.3.19B shows 2D2 proliferation when stimulated with separate MBP_{Ac1-9} and MOG_{35-55} peptide with PBS Tg4 cells (red bars) vs Tol Tg4 cells (blue bars). Co-culture with Tol Tg4 cells again significantly reduces the proportion of 2D2 cells that proliferate in response to peptide. However, in this system, where peptides are able to act independently and not limited to a single APC, the action of IL-10 comes into effect. In conditions with stimulated Tol Tg4 $CD4^+$ T cells, Tol Tg4 cells would generate significant amounts of IL-10 (Fig.3.2). Prevention of IL-10 signalling using αIL-10R Ab partially restores 2D2 proliferation and additional rmIL-10 further inhibits 2D2 proliferation, suggesting that when peptides are presented distant from one another on separate APC, IL-10 is a more powerful mediator of bystander suppression than when peptides are

presented by the same APC and cognate T cells are brought within extremely close proximity, sufficient for cell-cell contact.

3.7 Evidence of bystander suppression *in vivo*: (B10.PLxB6)F1 mice

To determine whether bystander suppression can be observed between MBP and MOG epitopes, and whether this bystander effect is APC-centric (i.e. enhanced when peptides are presented by the same APC); *in vivo* tolerance experiments were conducted in (B10.PLxB6)F1 mice (summarised in Figure 3.20A). Briefly, (B10.PLxB6)F1 mice were injected subcutaneously every 3-4 days with PBS or high affinity MBP_{Ac1-9} [4Y] peptide as previously described. Mice were then immunised with MBP_{Ac1-9}-HFFK-MOG_{35-55} hybrid peptide or separate peptides MBP_{Ac1-9} and MOG_{35-55}. Splenocytes and draining lymph node cells were harvested and stimulated in triplicate with a serial dilution of MBP_{Ac1-9}-HFFK-MOG_{35-55}, MBP_{Ac1-9} and MOG_{35-55} peptides as previously described (Fig.3.17A&B).

Figure 3.20B shows T cell proliferative responses to MBP_{Ac1-9}. As expected, MBP_{Ac1-9} tolerised mice are prevented from T cell proliferation in response to MBP_{Ac1-9} compared to PBS treated mice. This holds true whether mice were primed *in vivo* with the hybrid peptide or separate peptides and it is interesting to note that MBP_{Ac1-9} tolerised mice immunised with separate MBP_{Ac1-9} and MOG_{35-55} peptides were fully anergic towards MBP_{Ac1-9} in the spleen but not draining lymph node. By contrast, tolerised mice immunised with hybrid peptide were anergic to MBP_{Ac1-9} stimulation both in SP and LN. This may suggest that in situations where there are ongoing immune responses to non-tolerised antigen (MOG_{35-55}), that tolerance towards the tolerised antigen (MBP_{Ac1-9}) can be rendered less effective. This could be due to IL-2 secretion by

Figure 3.20: Evidence of bystander suppression *in vivo*: cell proliferation

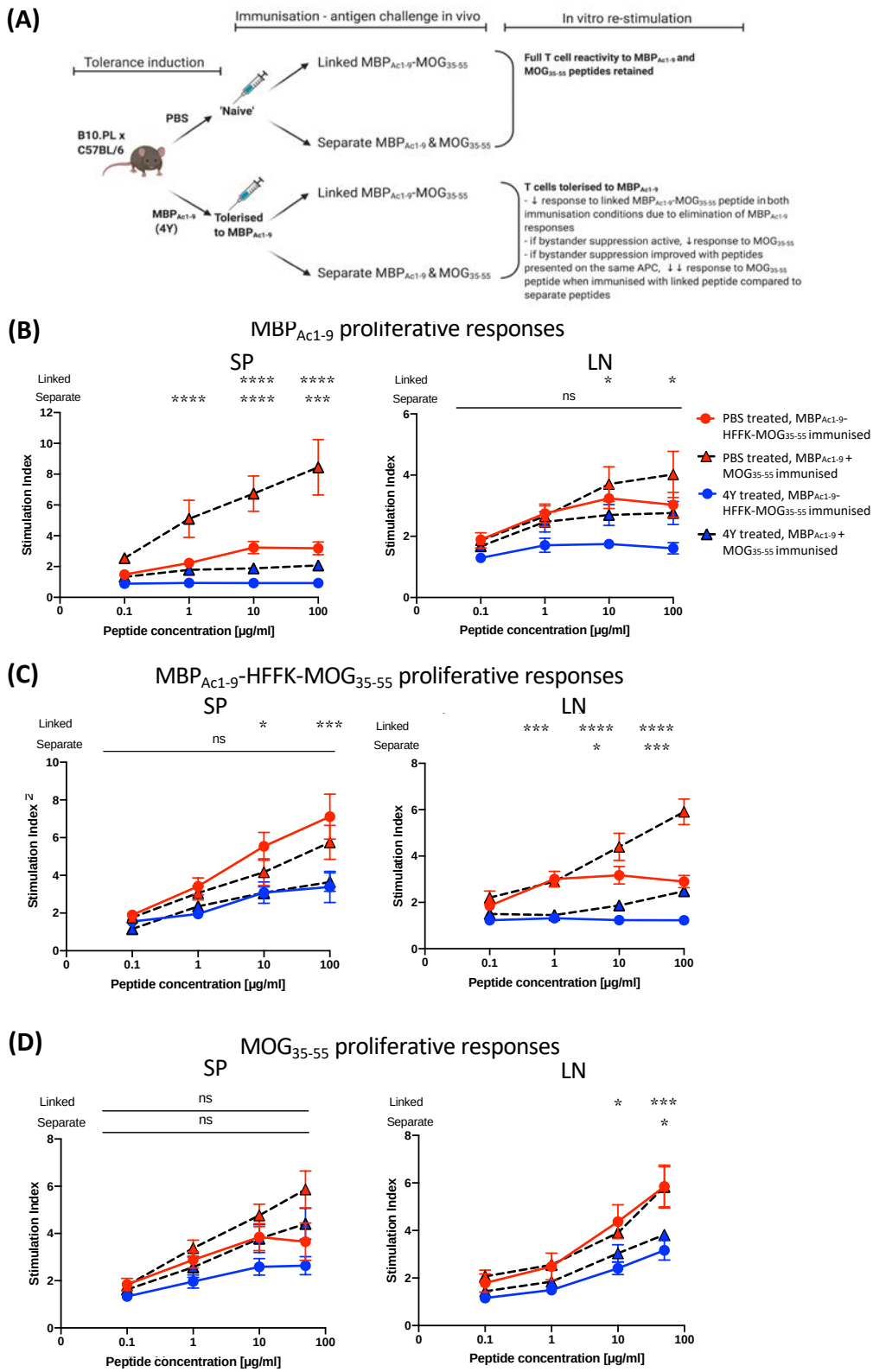

Figure 3.20: Antigen recall responses of (B10.PL x C57BL/6) F1 mice by cell proliferation after MBP_{Ac1-9} [4Y] tolerance induction and subsequent immunisation. (A) Protocol schematic. (B10.PL x C57BL/6) F1 mice (n=12) were subject to repeated doses of PBS (red icons) or escalating doses of MBP_{Ac1-9} [4Y] (blue icons). Mice were immunised 3 days after the last dose with either 100µg of MBP_{Ac1-9}-HFFK-MOG_{35-55} linked peptide (solid coloured lines), or 33µg MBP_{Ac1-9} and 66µg MOG_{35-55} separate peptides (black dashed lines). After 10 days, spleen (left) and draining lymph node (right) cells were isolated and plated at $10x10^6$ cells/ml or $5x10^6$ cells/ml, respectively, in complete RPMI supplemented with 10% FCS. Cells were stimulated with a serial dilution of **(B)** MBP_{Ac1-9} [4K], **(C)** MBP_{Ac1-9}-HFFK-MOG_{35-55} or **(D)** MOG_{35-55} in triplicate. 3 days after in vitro stimulation, 100µl of culture supernatant was removed for ELISA, whilst the remaining 100µl cell suspension was incubated for 16-20 hours with 0.18MBq/ml [^{3}H]-thymidine. [^{3}H]-thymidine incorporation was measured on a scintillation reader as corrected counts per minute (cpm) then converted to Stimulation Index (SI). SI = cpm of stimulated condition/cpm of unstimulated condition. Graphs display proliferation as mean SI for each peptide over the tested concentration range with statistical difference between PBS and Tol cells stimulated with each peptide assessed by ANOVA.

activated MOG_{35-55}-specific T cells acting on tolerant MBP_{Ac1-9} specific T cells to reverse anergy (Anderson et al., 2005).

MBP_{Ac1-9} [4Y] tolerised mice are suppressed in their response to MBP_{Ac1-9}-HFFK-MOG_{35-55} compared to PBS treated mice in both SP and LN, which is enhanced when mice were immunised with the hybrid peptide compared to separate peptides (Fig.3.20C). In the draining lymph nodes, MBP_{Ac1-9} specific T cells are fully anergic and MOG_{35-55} specific T cells are significantly suppressed when mice were immunised with the hybrid peptide. At higher concentrations of peptide *in vitro*, a low level of response to MBP_{Ac1-9}-HFFK-MOG_{35-55} remained when mice had been immunised with the separate peptides.

Most importantly, mice tolerised to MBP_{Ac1-9} consistently showed reduced T cell responses to MOG_{35-55} peptide, indicating that bystander suppression feedback loops were taking place (Fig.3.20D). In the spleen, suppression of MOG_{35-55} responses after immunisation with the hybrid peptides was statistically significant. Although suppression using separate peptides did not reach statistical significance, suppression was consistently observed. However, in dLN cells, the proliferative response to MOG_{35-55} was more drastically suppressed and showed clear statistical significance when comparing PBS and Tol hybrid immunised mice as well as when comparing PBS and Tol separate immunised mice. The extent to which T cell proliferation was suppressed was higher when mice had been immunised with MBP_{Ac1-9}-HFFK-MOG_{35-55} compared to separate MBP_{Ac1-9} and MOG_{35-55} peptides, confirming our hypothesis that bystander suppression is more effective when T cells of different specificities are brought together to respond to peptides on the surface of a single APC. An alternative rationale is that interaction with

tolerant cells blocks antigen processing by APC, which would affect the hybrid peptide more than the separate peptides.

Figure 3.21 displays the IFN-ɣ response in these settings and confirms the suppression of IFN-ɣ producing Th1 effector responses to MBP_{Ac1-9} and MOG_{35-55} peptides after tolerance induction to MBP_{Ac1-9}. As in the proliferation assays, T cell responses by IFN ɣ production to MBP_{Ac1-9} were quenched in both SP and dLN regardless of whether mice had been immunised with hybrid or separate peptides (Fig.3.21A). IFN-ɣ production in response to *in vitro* stimulation with hybrid MBP_{Ac1-9}-HFFK-MOG_{35-55} peptide was significantly reduced when mice were previously tolerised to MBP_{Ac1-9} (Fig.3.21B). Suppression of IFN-ɣ production was stronger when mice had been immunised with hybrid compared to separate peptides, reflecting the proliferation data from these assays. Most importantly, IFN-ɣ production in response to MOG_{35-55} after prior tolerance induction to MBP_{Ac1-9} was significantly suppressed (Fig.3.21C). As before, this suppression of T cell reactivity towards MOG_{35-55} was significantly more pronounced in dLN compared to SP. In dLN cultures, MOG_{35-55} specific IFN-ɣ production was almost completely suppressed when mice has been immunised with hybrid MBP_{Ac1-9}-HFFK-MOG_{35-55} peptide, whereas immunisation with the separate peptides permitted IFN-ɣ, albeit still significantly less than in non-tolerised mice.

Therefore, by both T cell proliferation and IFN-ɣ production, we can be confident that both bystander and linked suppression can be observed between MBP_{Ac1-9} and MOG_{35-55} in (B10.PLxB6)F1 mice undergoing tolerance induction to $MBP_{Ac1-9.}$ Suppression is more pronounced in the linked setting using the hybrid peptide to restrict peptides to

Figure 3.21: Evidence of bystander suppression in vivo: IFN-γ production

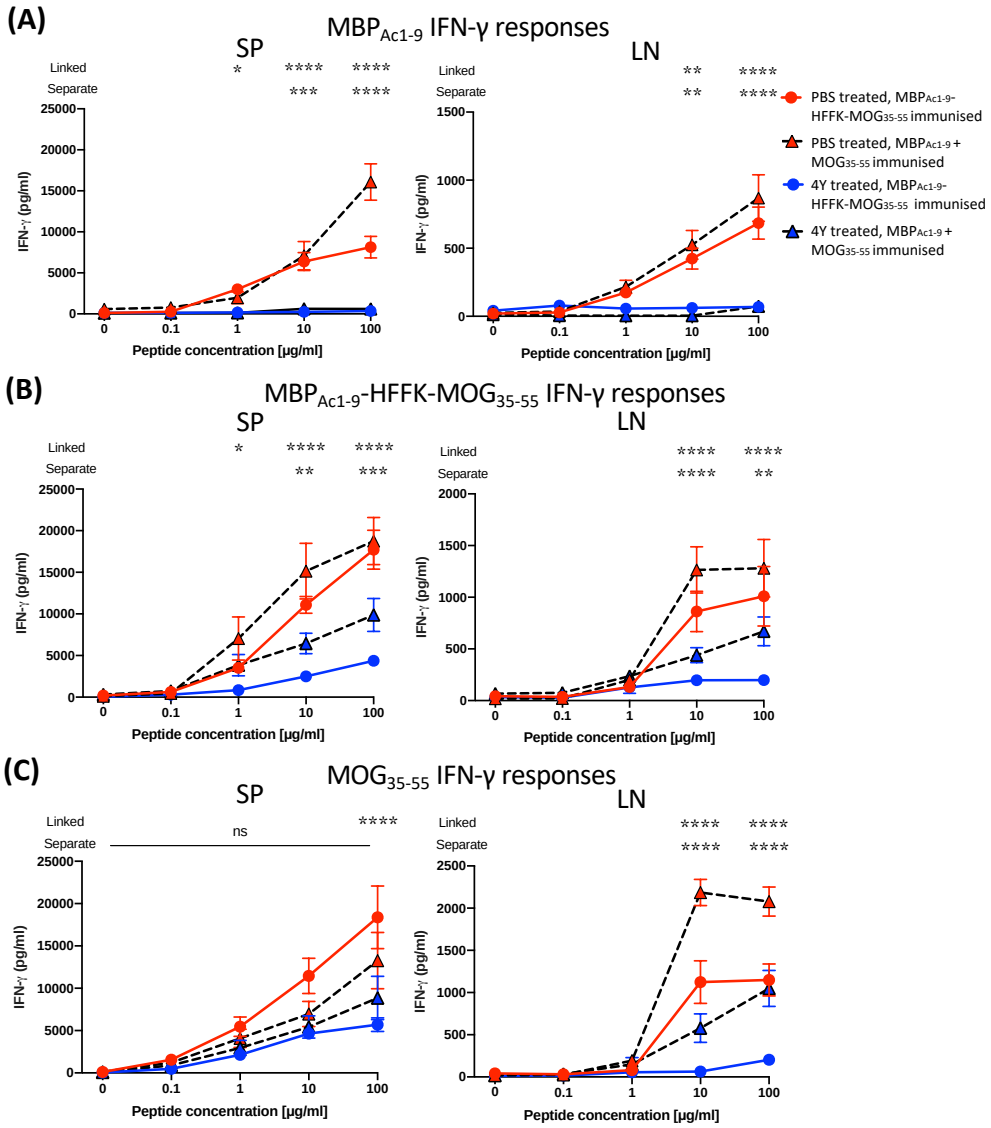

Figure 3.21: Antigen recall responses of B10.PL x C57BL/6 mice by IFN-γ production after MBP_{Ac1-9} tolerance induction and subsequent immunisation. B10.PL x C57BL/6 mice (n=12) were treated as described previously. Briefly, PBS treated mice (red icons) or MBP_{Ac1-9} (blue icons) were immunised with either 100µg of MBP_{Ac1-9}-HFFK-MOG_{35-55} hybrid peptide (solid coloured lines), or 33µg MBP_{Ac1-9} and 66µg MOG_{35-55} separate peptides (black dashed lines). Cell culture supernatant was analysed for IFN-γ concentration after *in vitro* peptide re-stimulation with **(A)** MBP_{Ac1-9}, **(B)** MBP_{Ac1-9}-HFFK-MOG_{35-55} or **(C)** MOG_{35-55}. Graphs display mean IFN-γ production for each peptide over the tested concentration range with statistical difference between PBS and Tol cells assessed by ANOVA.

the same APC, yet bystander suppression is still consistent even between peptides presented on separate APC using the separate peptides.

3.8 Assessing the phenotype of T cells and APC in (B10.PLxB6)F1 mice after tolerance induction

(B10.PLxB6)F1 mice were treated as previously described to induce antigen-specific tolerance to MBP_{Ac1-9} peptide. Mice were culled 2h after their last dose of PBS or MBP_{Ac1-9} [4Y] *in vivo* prior to splenocyte isolation and antibody staining. In this set-up there were only PBS/PBS or 4Y/4Y conditions. To assess IL-10 production, splenocytes were stimulated *in vitro* for 3 hours with PMA/I then stained for cell surface co-inhibitory markers and intracellular IL-10 (Fig.3.22). $CD4^+$ cells from (B10.PLxB6)F1 mice after tolerance induction were increased for IL-10 expression, this includes Th2 cells which are able to express IL-10 (and were not gated out of this analysis) as well as both Tr1 and Treg populations, as at this time I had not yet optimised the co-staining protocol for both FoxP3 and IL-10 (Fig.3.22B). The $V\beta8^+$ TCR beta chain is required for $CD4^+$ T cells that are MBP_{Ac1-9} reactive, but is not restricted only to MBP_{Ac1-9} reactivity. Considering that $V\beta8^+$ T cells in naïve (B10.PLxB6)F1 mice are only ~10% of the $CD4^+$ pool and that not all $V\beta8^+$ T cells are specific for MBP_{Ac1-9}, and we know from the Tg4 mouse that around 40% of MBP_{Ac1-9} reactive $CD4^+$ T cells will become $IL\text{-}10^+$ after tolerance induction, it is striking that in tolerised F1 mice, 6% of all $CD4^+$ T cells were $IL\text{-}10^+$ suggesting a potential expansion of tolerised MBP_{Ac1-9} reactive T cells.

Unfortunately, this experiment was only conducted once in full (n=4 per group), therefore this experiment would need to be repeated at least once more to provide more

Figure 3.22: Tolerised B10.PL x C57BL/6 mice increase IL-10⁺ expression and coinhibitory markers

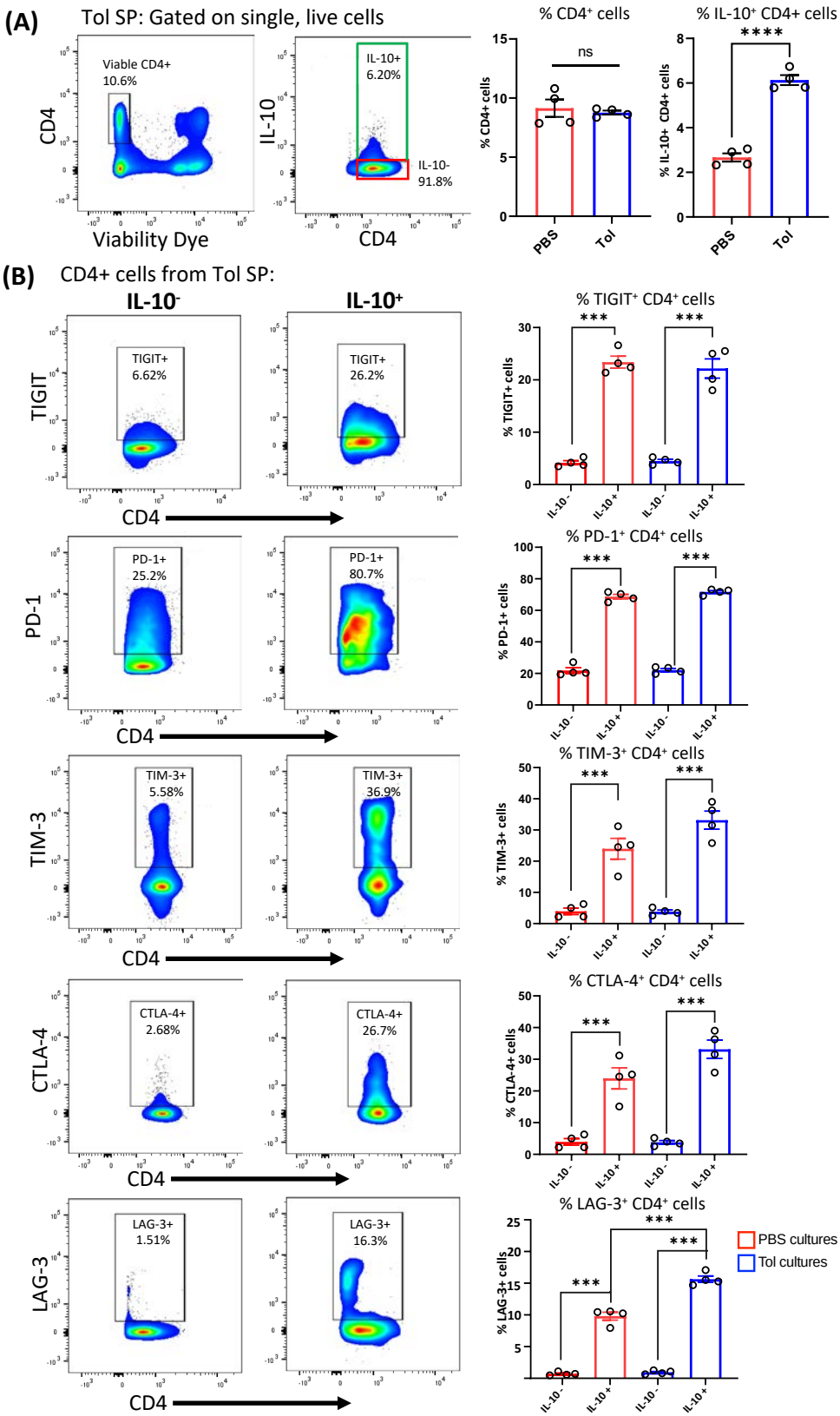

Figure 3.22: Tolerised B10.PL x C57BL/6 mice increase IL-10+ expression and coinhibitory markers. B10.PL x C57BL/6 mice were subject to MBP_{Ac1-9} [4Y] dose escalation to induce tolerance or PBS as control. Spleens were harvested 2h after the last dose of MBP_{Ac1-9} [4Y] or PBS. Splenocytes were stimulated for 3 hours with PMA/I before staining for intracellular IL-10 expression and surface co-inhibitory receptor expression. **(A)** Gating strategy for live $CD4^+$ $IL\text{-}10^+$ cells and numerical summary of % CD4 cells expressing IL-10. **(B)** Expanded $IL\text{-}10^+$ CD4+ cells express high levels of coinhibitory markers: TIGIT, PD-1, CTLA-4, TIM-3 and LAG-3. Graphs display mean MFI for each marker with statistical difference assessed by ANOVA.

confidence in these outputs. In subsequent repeats I would have: a) split the F1 mice into PBS/PBS, PBS/4Y, 4Y/PBS and 4Y/4Y conditions, b) used co-staining of FoxP3 and IL-10 to identify the contribution of Tr1 and Treg, c) stained for the TCR chain Vβ8^{+} in tolerised F1 mice to observe whether the CD4^{+} cells carrying Vβ8 are expanded in vivo, d) stained using MBP_{Ac1-9} specific I-Au tetramer to define the numbers of CD4^{+} cells that are MBP_{Ac1-9} restricted before and after tolerance induction (Radu et al., 2000).

The numbers of TIGIT/PD-1/TIM-3/LAG-3/CTLA-4 expressing CD4^{+} cells increased after tolerance induction, but this increase was restricted to IL-10^{+} CD4 cells and Tconv were not able to upregulate these markers, supporting the hypothesis that these are regulatory Tr1 or Treg as opposed to Th2 (Fig.3.22B).

To assess whether antigen-presenting cells from (B10.PLxB6)F1 mice were affected by tolerance induction, PBS or MBP_{Ac1-9}[4Y] treated mice were culled 3 days after their last *in vivo* dose and spleens collected. Splenocytes were stained for dendritic cell (CD11c^{+} MHC-II^{+}) and B cell (CD19^{+}) markers in addition to costimulatory molecules CD80, CD86 and CD40. Dendritic cell MHC-II expression by MFI was not significantly different between PBS and MBP_{Ac1-9} [4Y] treated (B10.PLxB6)F1 mice (Fig.3.23A). DC expression of CD80 and CD86 by MFI, however, was significantly suppressed in tolerised mice, whilst CD40 was unchanged (Fig.3.23C). DC in tolerised mice may, therefore, provide costimulatory molecules at a level below what is required to fully activate subsequent T cells, but this hypothesis is yet to be investigated. Future experiments should include immunisation with MOG_{35-55} or PPD alone after MBP_{Ac1-9} [4Y] tolerisation, to assess whether this suppression of DC CD80/CD86 translates to non-specific suppression and whether

Figure 3.23: Effect of MBP_{Ac1-9} tolerance induction on (B10.PL x C57BL/6) F1 $CD11c^+$ $MHC\text{-}II^+$ DCs

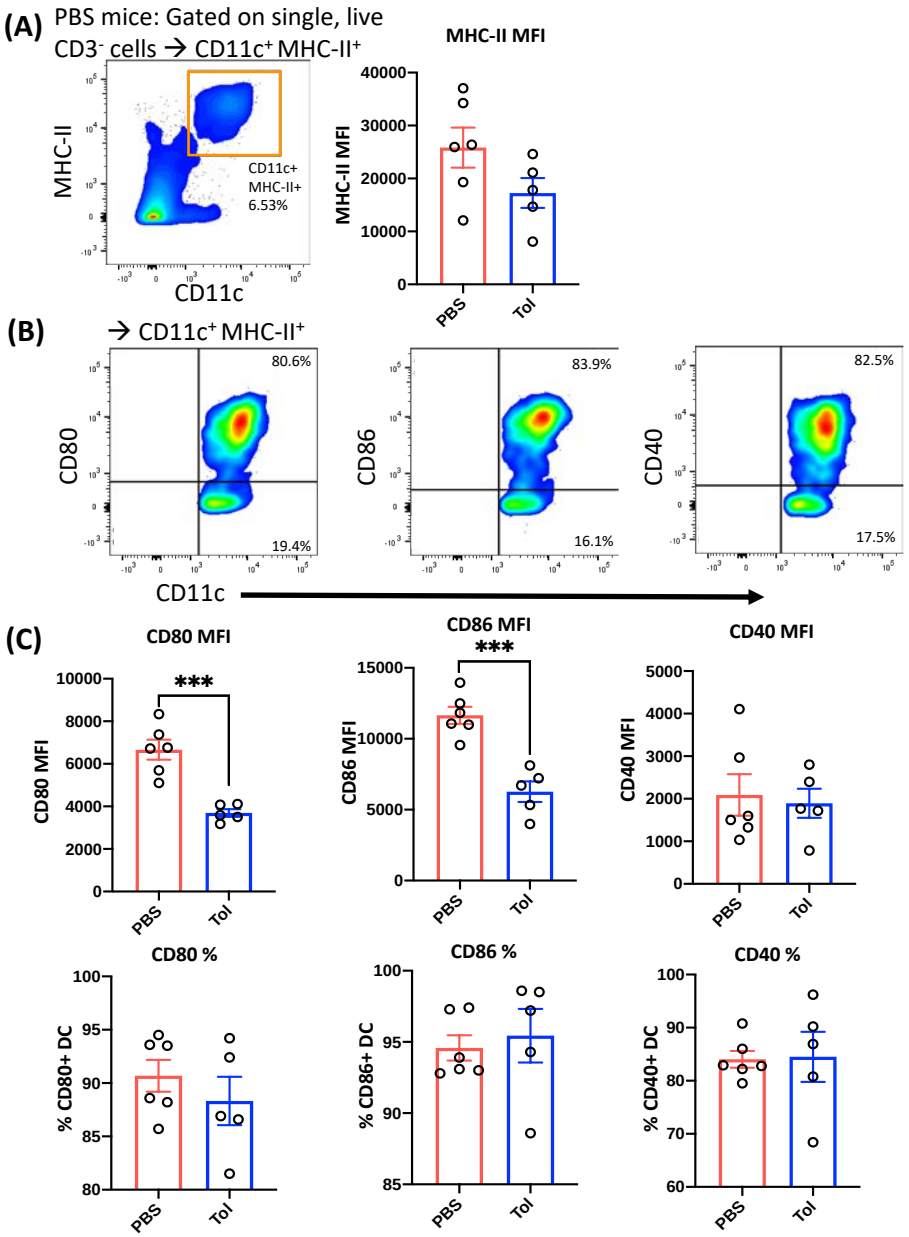

Figure 3.23: Dendritic cells from tolerised B10.PL x C57BL/6 mice have decreased expression of costimulatory molecules. B10.PL x C57BL/6 mice were subject to MBP_{Ac1-9} [4Y] dose escalation to induce tolerance (n = 5) or PBS (n = 6) as control, as described previously. Spleens were harvested 3 days after the last dose of MBP_{Ac1-9} [4Y] or PBS. **(A)** Gating strategy for dendritic cells (single cells → live → $CD3^-$ → $CD11c^+$ $MHC\text{-}II^+$) and DC MHC-II expression by MFI. **(B)** Representative flow cytometry plots of DC costimulatory molecule expression in PBS treated mice and **(C)** corresponding bar charts with statistical difference tested by ANOVA.

Figure 3.24: Effect of MBP_{Ac1-9} tolerance induction on (B10.PL x C57BL/6) F1 on $CD19^+$ B cells

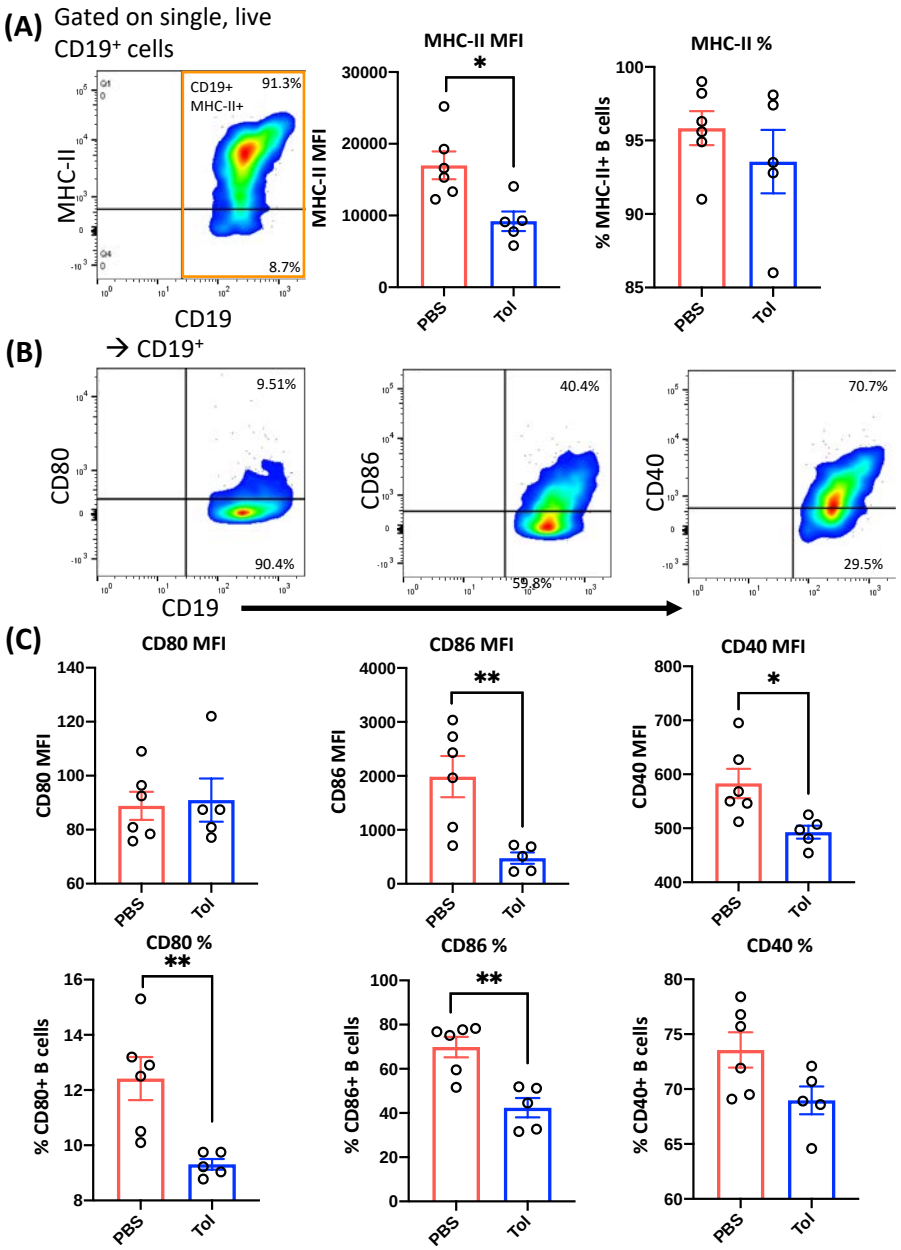

Figure 3.24: B cells from tolerised (B10.PL x C57BL/6) F1 mice have decreased expression of costimulatory molecules. B10.PL x C57BL/6 mice were subject to MBP_{Ac1-9} [4Y] dose escalation to induce tolerance or PBS as control, as described previously. Spleens were harvested 2h after the last dose of MBP_{Ac1-9} [4Y] or PBS. **(A)** Gating strategy for B cells (single cells → live → $CD19^+$ and B cell MHC-II expression **(B)** Representative flow cytometry plots of B cell costimulatory molecule expression in PBS treated mice and **(C)** corresponding bar charts with statistical difference tested by ANOVA.

CD80/CD86 suppression is reversed upon encounter with a strongly inflammatory antigen. The effect was not as pronounced as similar experiments in the Tg4 model, as the proportion of dendritic cells positive for CD80/CD86/CD40 was not significantly altered, however that we observed a significant change at all was more than we had anticipated.

B cells from tolerised mice expressed a reduced amount of MHC-II at the cell surface (Fig.3.24A). Expression of costimulatory molecules by MFI was much lower on B cells than dendritic cells: CD80 70x lower, CD86 5.75x lower, CD40 3.4x lower (comparison between mean values of PBS mice; Fig.3.23C & 3.24C). B cell expression of CD80 was very low and not significantly affected, whereas B cells expressed lower levels of both CD86 and CD40 after tolerance (Fig.3.24C). Furthermore, the number of B cells positive for both CD80 and CD86 were significantly reduced after tolerance induction, leaving fewer B cells with co-stimulatory molecule expression required to provide additional activatory signals to T cells.

As such, we can conclude that repeated antigen stimulation sufficient to induce antigen-specific T cell tolerance in wildtype mice with full TCR repertoires is able to affect the T cell priming capacities of antigen-presenting cells, in particular dendritic cells. This may be an effective route of carrying out bystander suppression of subsequent T cells of different antigen specificities.

3.9 Adoptively transferred CD4$^+$ cells from MBP$_{Ac1-9}$ [4Y] treated Tg4 mice into (B10.PLxB6)F1 mice are sufficient to establish bystander suppression

To assess whether the bystander effect is primarily T cell driven, CD4$^+$ T cells from PBS treated or MBP$_{Ac1-9}$ [4Y] treated (Tol) Tg4 CD45.1 mice were adoptively transferred into naïve recipient (B10.PLxB6)F1 mice prior to immunisation of recipients with hybrid MBP$_{Ac1-9}$-HFFK-MOG$_{35-55}$ peptide followed by restimulation *in vitro* with MBP$_{Ac1-9}$ and MOG$_{35-55}$ peptides (Fig.3.25A). Transferred Tg4 CD45.1$^+$ CD4$^+$ cells could be readily identified in spleens and lymph nodes of recipient mice at the end of the experiment – 11 days after adoptive transfer. Transferred Tg4 Tol CD4$^+$ cells retained their IL-10 expressing phenotype throughout the experiment, whereas recipient CD45.2 CD4$^+$ cells expressed very little to no IL-10 as would be expected for non-tolerised mice (Fig.3.25B).

Experiments were optimised by transfer of different numbers of Tg4 CD45.1$^+$ CD4$^+$ cells: 0.5x10^6, 1x10^6 and 5x10^6. Live CD45.1$^+$ CD4$^+$ cells could be identified in draining LN and SP even at the lowest number of transferred cells. Regardless of the number of cells transferred, Tol Tg4 CD45.1$^+$ CD4$^+$ were identified as a greater proportion of total CD4$^+$ cells than PBS Tg4 CD45.1$^+$ CD4$^+$ cells, indicative of Tol CD4 improved survival or an increased expansion in response to immunisation (Fig.3.25C). Figure 3.25D shows that even with transfer of small numbers of Tol Tg4 CD45.1$^+$ CD4$^+$, these cells retained their IL-10 expression profile.

We found that transfer of 5x10^6 Tg4 CD45.1$^+$ CD4$^+$ cells was the minimum number of cells required to observe a significant effect on MBP$_{Ac1-9}$ [4K] peptide responses after immunisation. Figure 3.26 summarises cell transfer experiments in which either 5x10^6 PBS Tg4 CD45.1$^+$ CD4$^+$ (Fig.3.26, red symbols) or 5x10^6 Tol Tg4 CD45.1$^+$ CD4$^+$ (Fig.3.26,

Figure 3.25: Immunisation of (B10.PL x C57BL/6) F1 mice after adoptive transfer of tolerised cells

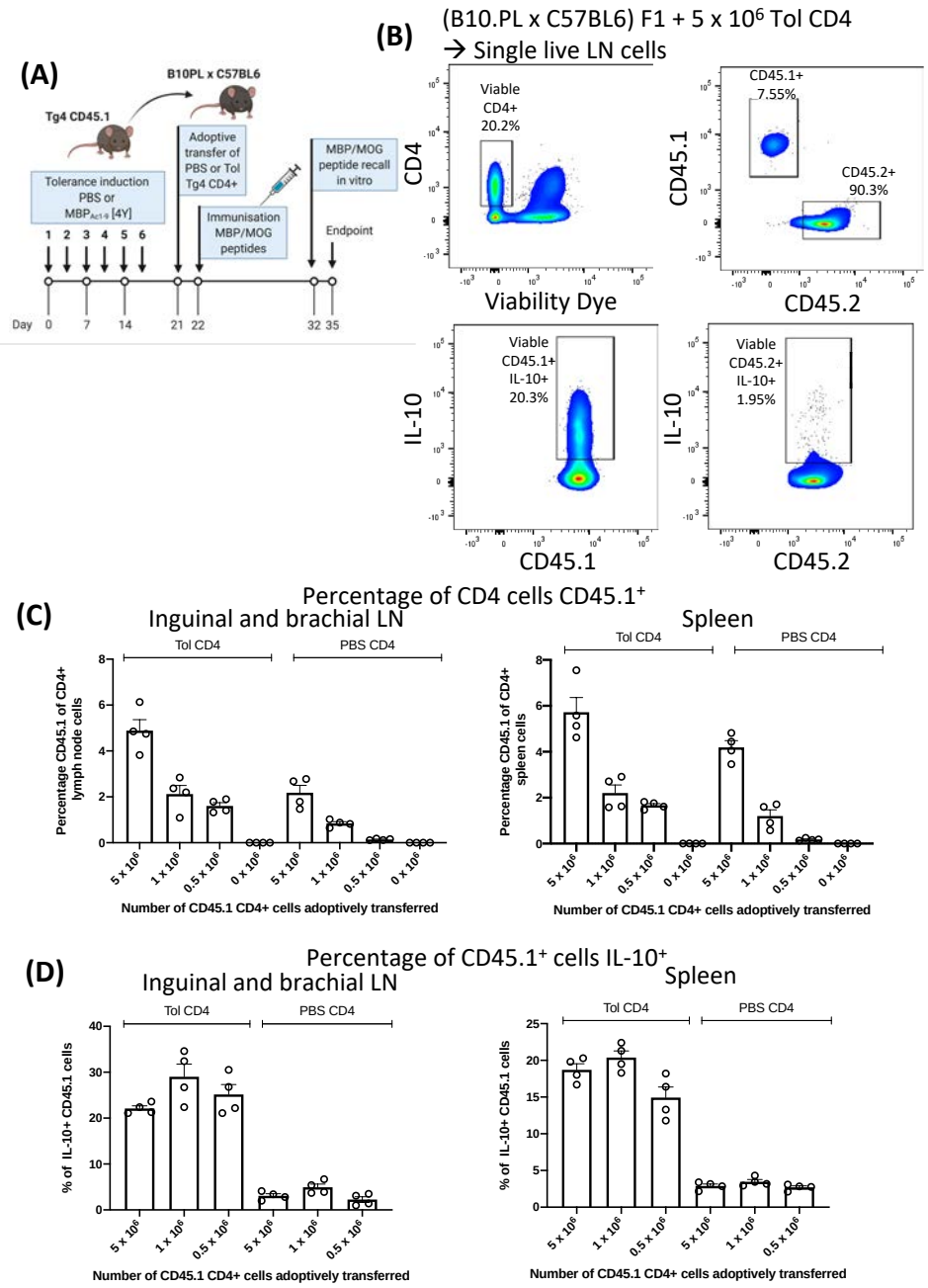

Figure 3.25: Transfer of PBS or Tol CD4 Tg4 cells into (B10.PL x C57BL/6) F1 mice can be identified after immunisation and retain IL-10 phenotype.
(A) Protocol summary:Tg4 CD45.1 mice (n = 4) were treated with PBS or MBP_{Ac1-9} [4Y] by s.c. dose escalation protocol. $0.5x10^6$, $1x10^6$ and $5x10^6$ cells PBS or Tol splenic $CD4^+$ T cells were transferred via i.p. into recipient (B10.PL x C57BL/6) F1 mice (n=4). Recipients were immunised 24 hours

later with 100µg of MBP_{Ac1-9}-HFFK-MOG_{35-55} linked peptide in CFA. **(B)** Transferred CD45.1 cells can be identified in lymphoid organs 11 days post-transfer after immunisation and Tol $CD4^+$ retain IL-10 expression. **(C)** Summary of transferred $CD45.1^+$ $CD4^+$ identified in lymphoid organs post-transfer and immunisation (mean values ± SEM). **D)** Summary of IL-10 expression by transferred $CD45.1^+$ $CD4^+$ identified in lymphoid organs post-transfer and immunisation (mean values ± SEM).

blue symbols) were adoptively transferred i.p. into (B10.PLxB6)F1 recipient mice 24h prior to immunisation with hybrid MBP_{Ac1-9}-HFFK-MOG_{35-55} peptide or separate MBP_{Ac1-9} and MOG_{35-55} peptides. After transfer of PBS Tg4 CD45.1$^+$ CD4$^+$ cells, the proliferative response to MBP_{Ac1-9} [4K] upon *in vitro* restimulation was greatly increased when compared to direct tolerance induction of (B10.PLxB6)F1 (Fig.3.20B), due to the influx of naïve MBP_{Ac1-9}-specific T cells which are then activated and expanded in the immunisation phase. T cell proliferative response to MBP_{Ac1-9} after transfer of Tol Tg4 CD45.1$^+$ CD4$^+$ was significantly reduced.

SP and dLN cell proliferative response to hybrid MBP_{Ac1-9}-HFFK-MOG_{35-55} peptide stimulation was significantly controlled with Tol Tg4 CD45.1$^+$ CD4$^+$ transfer compared to PBS Tg4 CD45.1$^+$ CD4$^+$ transfer (Fig.3.26B). In the adoptive transfer model, response to MBP_{Ac1-9}-HFFK-MOG_{35-55} peptide was suppressed more strongly when mice had been immunised with MBP_{Ac1-9} and MOG_{35-55} peptides separately.

MOG_{35-55} specific T cell proliferation in vitro was suppressed in both SP and dLN following transfer of MBP_{Ac1-9}-specific Tol Tg4 CD45.1$^+$ CD4$^+$ compared to PBS Tg4 CD45.1$^+$ CD4$^+$ cells, although to a much greater extent in dLN cells (Fig.3.26C). T cell proliferation to MOG_{35-55} was suppressed whether mice were immunised with hybrid or separate peptides; however, suppression was greatest when mice were immunised with hybrid peptide. This provides evidence that bystander suppression is exhibited between MBP_{Ac1-9} and MOG_{35-55} and is more effective when peptide antigens are presented on the same APC. The adoptive transfer experiments show that the bystander suppressive effect is primarily driven by tolerant CD4$^+$ T cells, as transferred CD4$^+$ T cells are sufficient to exert this effect in otherwise naïve mice.

Figure 3.26: Adoptive transfer of PBS treated or MBP_{Ac1-9} [4Y] treated Tg4 CD4 cells into (B10.PL x C57BL/6) F1 mice with MBP/MOG peptides

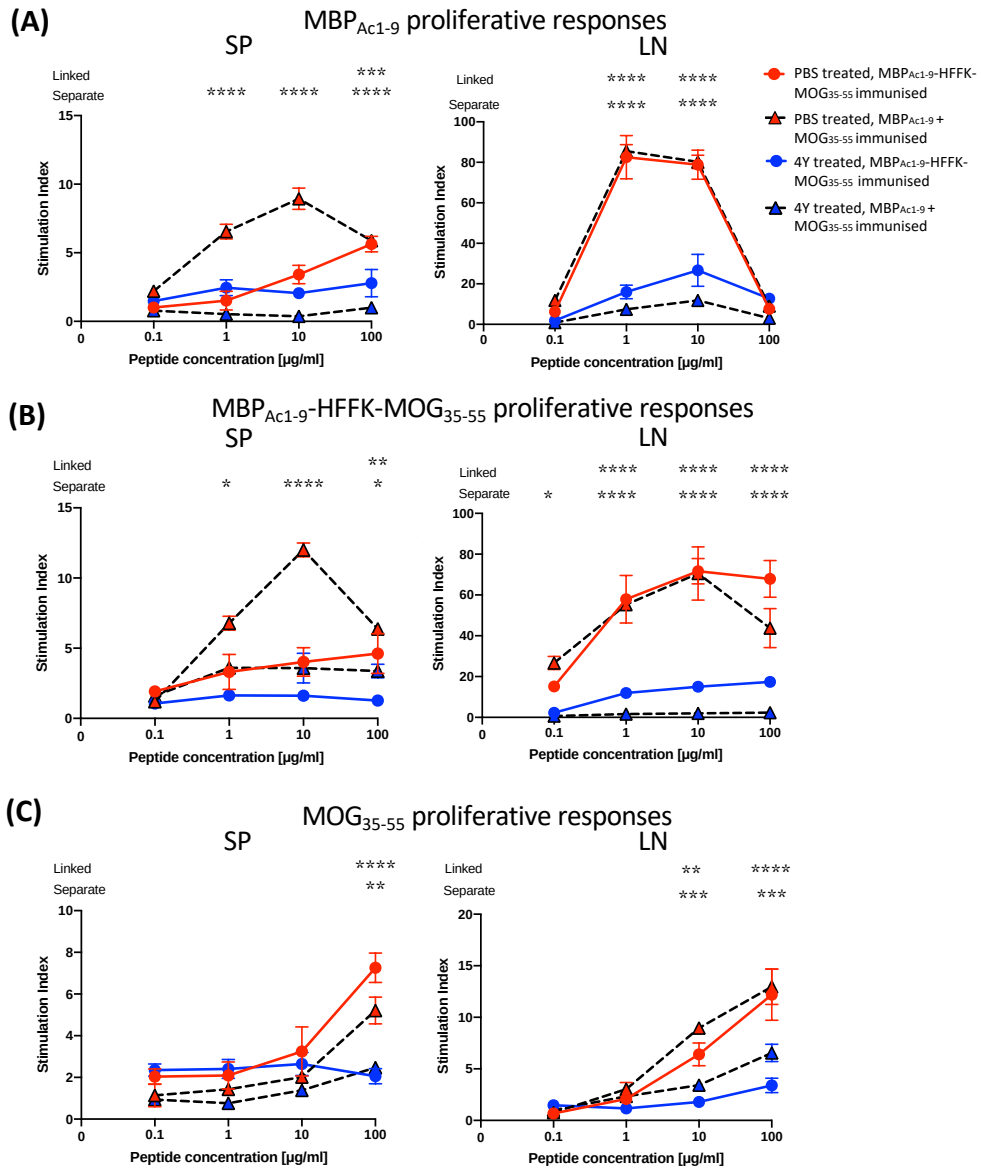

Figure 3.26: Proliferative response of (B10.PL x C57BL/6) F1 mice splenocyte or lymph node cells after adoptive transfer of PBS or MBP_{Ac1-9} [4Y] treated Tg4 CD4 cells and peptide immunization. Tg4 CD45.1 mice (n=12) were treated with PBS or MBP_{Ac1-9} [4Y] by s.c. dose escalation protocol. $5x10^6$ PBS (red icons) or MBP_{Ac1-9} [4Y] (blue icons) isolated Tg4 $CD4^+$ cells were transferred i.p. into recipient B10.PLxC57BL/6 mice (n=12). Recipients were immunised 24 hours later with either 100µg of MBP_{Ac1-9}-HFFK-MOG_{35-55} linked peptide (solid coloured lines), or 33µg MBP_{Ac1-9} and 66µg MOG_{35-55} separate peptides (black dashed lines). After 10 days,

spleen (left) and draining lymph node (right) cells were isolated and plated at $10x10^6$ cells/ml or $5x10^6$ cells/ml, respectively, in complete RPMI supplemented with 10% FCS. Cells were stimulated with a serial dilution of **(A)** MBP_{Ac1-9}, **(B)** MBP_{Ac1-9}-HFFK-MOG_{35-55} or **(C)** MOG_{35-55} in triplicate. 3 days after in vitro stimulation, 100µl of culture supernatant was removed for ELISA, whilst the remaining 100µl cell suspension was incubated for 16-20 hours with 0.18MBq/ml [^{3}H]-thymidine. [^{3}H]-thymidine incorporation was measured on a scintillation reader as corrected counts per minute (cpm) then converted to Stimulation Index (SI). SI = cpm of stimulated condition/cpm of unstimulated condition. Graphs display proliferation as mean SI for each peptide over the tested concentration range.

3.10 Discussion

In depth analysis of induced regulatory Tr1 cells and FoxP3$^+$ Treg phenotypes in Tg4 mice after tolerance induction using $MBP_{Ac1\text{-}9}$ [4Y] highlighted that induced Tr1 and Treg cells share many of the same features, most notably increased IL-10 production and increased coinhibitory receptor expression. Where previous studies of PIT in the Tg4 model have focussed on the striking expansion of Tr1 cells this work emphasises the fact that although the numbers of Treg are not significantly expanded, their suppressive quality is increased as a result of repeated tolerogenic Ag stimulation. Most impressive was the significant increase in tolerised Treg CTLA-4 available both at the cell surface and circulating intracellularly.

We find that tolerised Tg4 CD4$^+$ cells are able to exert strong suppressive effects on APC *in vivo* and *in vitro* – particularly on DC. Splenic DC after tolerisation are prevented from upregulation of CD80/CD86 upon antigen stimulation and are in fact suppressed below the level of naïve DC, suggesting highly potent suppression. Prior data using the Tg4 IL-10$^{-/-}$ revealed that suppression of CD80 and CD86 *in vivo* was reliant on the presence of IL-10 and that without IL-10, mice are not able to control EAE development when treated with tolerogenic peptide (Gabryšová et al., 2009a; Burkhart et al., 1999; O'Neill et al., 2004). We found that our *in vitro* data using IL-10 receptor blocking antibody did not reveal an essential role for IL-10, instead suggesting the importance of a CTLA-4 mediated suppression mechanism. This was highlighted by the constitutive suppression of DC CD80/CD86 when cultured with naïve Treg (constitutive CTLA-4$^+$), which was then further suppressed by culture with Tol Treg (CTLA-4^{high}).

I also assessed the expression of PD-L1 on DC after tolerance induction, with the hypothesis that this inhibitory ligand for receptor PD-1 might be increased after tolerance. This was not the case, therefore DC are not moderated in their ability to express increased PD-L1 by repeated Ag dose. Instead, we observed DC from tolerised mice reducing their PD-L1 expression. This may be due to compensation between PD-L1 and the strongly upregulated expression of PD-1 receptor on tolerised T cell populations. As PD-L1 is not increased on tolerised DC, it cannot be implicated in the next step of bystander suppression – suppressive action on subsequent T cells.

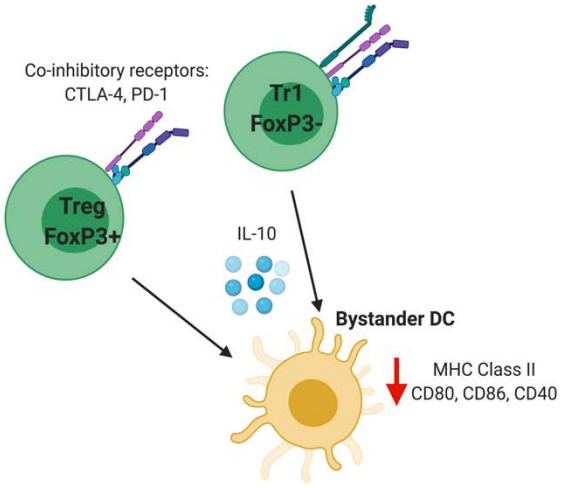

Key outcomes:

- Tolerised Tr1 and Treg express high IL-10, but Tr1 are the more dominant source.
- Tolerised Tr1 and Treg display increased co-inhibitory receptor expression (TIGIT, TIM-3, LAG-3, PD-1 and CTLA-4).
- Tolerised bulk $CD4^+$ cells suppress the expression of CD80/CD86 by DC and B cells.
- Treg are able to constitutively exert this suppression but are markedly more potent after tolerance induction.

The pathway between CD40L, CD40 and IL-12 expression was assessed in a stepwise approach. Firstly, we showed that naïve T cells transiently and rapidly upregulate CD40L in response to antigen stimulation, whereas tolerised T cells are not able to upregulate CD40L at the cell surface. It would be interesting to assess CD40L mRNA levels in PBS

treated vs 4Y treated tolerised cells to determine whether the inability to express CD40L is due to a defect in mRNA production or an increase in CD40L internalisation and lysosomal degradation.

Functional CD40L-CD40 ligation and subsequent signalling within APC is required for proper 'licensing' of DC to render them maximally effective at priming T cells (high IL-12 production, high costimulatory molecule expression) (Snijders et al., 1998; Ma et al., 2015). We found that *in vivo*, CD40 is downregulated on naïve activated DC 2h after antigen stimulation, suggesting that CD40 on DC is rapidly downregulated after T cells have received initial stimulatory signals as a negative regulation mechanism. This also occurs in tolerised activated DC, but CD40 is downregulated to a lesser extent. This differed to prior *in vitro* data (Gabryšová et al., 2009b), and my own *in vitro* data, in which CD40 was lowest after DC were co-cultured with Tol $CD4^+$ cells. Potentially, the low availability of CD40L provided by tolerised T cells reduces the CD40L-CD40 signalling after antigen encounter which itself results in less potent CD40 downregulation. Reduced CD40L-CD40 signalling also inhibits DC ability to secrete high levels of IL-12, which is required for generation of fully functionalised effector Th1 cells from naïve T cells (Snijders et al., 1998; Heufler et al., 1996). I struggled to optimise the intracellular staining of IL-12 within DC so was unable to directly assess the impact of reduced CD40L-CD40 signalling on IL-12 production. However, using ELISA, I was able to show that *in vitro*, DC cultured with naïve $CD4^+$ cells generated robust IL-12 production upon antigen encounter, whilst DC with Tol $CD4^+$ cells were not able to produce IL-12. In these experiments we noticed a distinct effect of blocking IL-10R boosting the production of IL-12.

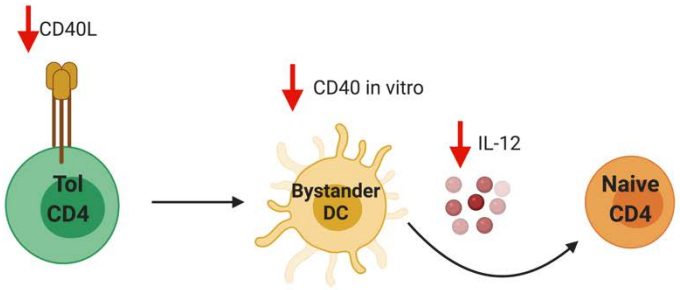

Key outcomes:

- Tolerised CD4 T cells do not upregulate CD40L after Ag stimulation.
- DC in vitro downregulate CD40 in contact with activated Tol CD4
- DC in vivo do not downregulate CD40 to as great an extent when in contact with Tol CD4.
- Bystander DC are prevented from IL-12 production, reducing naïve→Th1 cell maturation

In my hands, I could not reliably observe populations of either DC or B cells producing IL-10 directly from tolerised Tg4 mice, even with different staining protocols and with stimulation using LPS and/or CD40L. Whether this means Breg and IL-10^+ DC are not generated as a result of PIT, we cannot be sure unless we performed more in depth staining panels. Murine Breg are defined by different combinations of markers, most commonly including the plasma cell marker CD138 (Wąsik et al., 2018). IL-10^+ DC cells have previously been identified in both mouse and human settings and have been suggested to play a role in suppression of Th1, Th2 and Th17 cells depending on the disease model (Akbari et al., 2001; Liu et al., 2011), and the generation of Tr1 cells (Gregori et al., 2010).

The analysis of $CD4^+$ Treg and Tr1 cell and APC populations (dendritic cell and B cells) from the Tg4 mouse represents a view of how diverse subsets of lymphocytes are altered as a result of PIT tolerance induction using MBP_{Ac1-9} [4Y] and suggests multiple avenues for the sequence of T cell → APC →T cell interaction central to bystander suppression. This work would benefit greatly from further experiments to fine tune the role of IL-10

and co-inhibitory receptors, in particular CTLA-4 on exerting suppression of APC populations.

Potentially the most interesting work in this Chapter is in the wild type (B10.PLxB6)F1 mice which respond to both MBP_{Ac1-9} and MOG_{35-55} peptides. We were keen to assess whether PIT in these outbred mice with diverse TCR repertoire could generate bystander suppression between MBP_{Ac1-9} and MOG_{35-55} peptides, and whether we could observe similar features of tolerant T cells and APC previously identified in the Tg4 model. Our other primary aim was also to assess the extent to which bystander suppression is reliant on peptides being presented in close physiological context on the same APC (linked suppression; linked hybrid MBP_{Ac1-9}-HFFK-MOG_{35-55} peptide) vs peptides presented on different APC (*bona fide* bystander suppression; MBP_{Ac1-9} and MOG_{35-55} peptides delivered together).

Initially, we showed the linked hybrid peptide is cleaved during antigen-processing for presentation of both epitopes, sufficient to generate strong T cell responses towards both epitopes. We then established co-culture experiments to assess bystander suppression in vitro using naïve or Tol Tg4 $CD4^+$ cells, naïve 2D2 $CD4^+$ cells and irradiated splenocytes from (B10.PLxB6)F1 mice to act as APC. We found that naïve MOG_{35-55}-specific 2D2 $CD4^+$ cells were suppressed in their proliferative response to MOG_{35-55} stimulation when exposed to Tol Tg4. Suppression of 2D2 cell MOG_{35-55} proliferation was more potent when the MBP_{Ac1-9} and MOG_{35-55} epitopes were delivered as the linked hybrid MBP_{Ac1-9}-HFFK-MOG_{35-55} peptide compared to separate peptides, indicating that linked suppression where epitopes are presented on the same APC is

more potent than *bona fide* bystander suppression. IL-10 pathway blocking or promotion did not affect 2D2 cell MOG_{35-55} suppression when stimulated with linked peptides, whereas cultures stimulated with separate peptides were at least partially reliant on IL-10 mediated suppression. Hence, in vitro, the linked suppression effect (central APC) is not IL-10 dependent and is presumably exerted by cell-contact mediated effects, whereas the bystander suppression effect (distinct APC) is at least partially reliant on IL-10. It would be useful to repeat this experiment using Tg4 IL-$10^{-/-}$ cells, to ensure complete deficiency in IL-10 provision and signalling which may have been incomplete when using IL-10R Ab. This co-culture set-up could be utilised for more complex mechanistic experiments by preventing each coinhibitory receptor, TGF-β and Notch signalling to identify the specific cell-cell mechanisms behind linked and bystander suppression.

(B10.PLxB6)F1 mice could be successfully rendered tolerant to MBP_{Ac1-9} by repeated antigen dose and were subsequently suppressed in their proliferative and IFN-γ responses to MOG_{35-55}. In line with the *in vitro* data, *in vivo* linked suppression via (linked hybrid MBP_{Ac1-9}-HFFK-MOG_{35-55}) was more potent than bystander suppression (separate MBP_{Ac1-9} + MOG_{35-55}) in dampening the response to MOG_{35-55}. We were impressed that the number of IL-10^+ cells in the $CD4^+$ population increased to around 6% after tolerance induction. Considering ≅10% of $CD4^+$ cells are $V\beta8^+$ prior to tolerance and not all are responsive to MBP_{Ac1-9}, that IL-10^+ reached 6% was surprising. In the Tg4 mouse, only 35-40% of $CD4^+$ cells are IL-10^+ after tolerance, so we might have expected 3.5-4% to be IL-10^+ in the F1 mice. This suggests an expansion of MBP_{Ac1-9} specific IL-10 producing $CD4^+$ T cells in the outbred model. IL-10^+ $CD4^+$ T cells from tolerised (B10.PLxB6)F1 mice expressed increased levels of co-inhibitory receptor molecules (TIGIT, TIM-3, PD-1, CTLA-4 and LAG-3), in line with Tr1 data from the Tg4 mouse. I would have needed to repeat

this experiment with FoxP3 staining to assess whether these cells were predominantly Tr1 or Treg.

Again, we were impressed to see moderate suppression of both dendritic cells and B cells isolated from tolerised F1 mouse spleens. Both CD80 and CD86 were suppressed, while CD40 expression was not affected. That we could observe suppression of APC populations even in these outbred mice where only 6% of $CD4^+$ cells were IL-10^+ indicates the potent effect these induced regulatory cells can have.

Finally, we wanted to assess whether the APC populations had to be exposed to the tolerance induction protocol themselves to exert bystander suppression or whether introduction of Tol $CD4^+$ cells was sufficient using adoptive transfer of Tol Tg4 $CD4^+$ cells into naïve F1 mice. Upon immunisation, the F1 mice were suppressed in their response to $MBP_{Ac1\text{-}9}$ and to the bystander epitope $MOG_{35\text{-}55}$. Again, as we had observed previously, suppression was greatest when immunising with the linked hybrid $MBP_{Ac1\text{-}9}$-HFFK-$MOG_{35\text{-}55}$ peptide. These experiments demonstrated that the APC do not require exposure to the PIT protocol to become suppressed, but that just $5x10^6$ Tol $CD4^+$ cells are sufficient to result in bystander suppression.

Concluding statement

The data of this Chapter provides a strong grounding into the effects of peptide-based antigen-specific immunotherapy on diverse subsets of cells. Tr1 cells were observed to undergo similar expansion and possess similar phenotype as in previous studies (Burton et al., 2014), but for the first time we analysed distinctive phenotypic changes in Treg. Although the number of Treg did not change, their suppressive qualities were enhanced

and therefore Treg may play more of a role in mediating antigen-specific tolerance and disease prevention/resolution than previously appreciated. APC in contact with Tol T cells and those isolated directly from tolerised mice were significantly suppressed in CD80/CD86 expression, indicating the potency of T cell mediated APC suppression as a result of PIT. We also identified that lack of CD40L appears to be the driving factor for dendritic cell inability to generate IL-12 as opposed to lack of CD40 itself, which in vivo is not significantly suppressed as a result of PIT.

We have determined that bystander suppressive effects, extending tolerance from the target antigenic peptide to moderate non-target T cell responses can be mediated by both direct cell-contact mediated suppression (via CTLA-4, potentially other surface ligand-receptor pairs) as well as secreted suppressive cytokines (via IL-10, potentially TGF-β) of both subsequent T cells and APC. We also identified that bystander suppression is sensitive to antigen proximity using linked and separate MBP/MOG peptide epitopes. It is likely that the strength and mechanisms of bystander suppression are highly context-dependent and the tools developed in this Chapter should serve as a useful platform to determine these pathways more closely.

Future work

- CTLA-4 mediated transendocytosis by tolerised Tr1 and Treg

  We hypothesised that tolerant T cells mediated CTLA-4-CD80/86 trans-endocytosis. Trans-endocytosis of CD80 and CD86 has been shown to take place as a constitutive function of Treg (Qureshi et al., 2011; Hou et al., 2015; Ovcinnikovs et al., 2019). We planned experiments to test trans-endocytosis of

naïve Tconv, Tol Tr1, naïve Treg and Tol Treg on CD80-GFP expressing cell lines by confocal imaging. I established efficient stable transfection of the CD80-GFP plasmid into HEK293 cells but was still working towards transfection in our PL8 cell line. PL8 are a murine B cell derived line carrying MHC-II H-2 A^u and are able to engage Tg4 T cells in an antigen-specific manner, enabling us to assess the reliance on antigen specific exposure vs non-specific CD3/CD28 stimulation for CTLA-4 mediated CD80 trans-endocytosis to occur in the naïve vs tolerant settings.

- Further assessment of tolerance in Tg4 mice
    - Role of IL-10 and CTLA-4 mediated suppression between *in vivo* and *in vitro* settings using Tg4 IL-$10^{-/-}$ and/or mice treated with αIL-10R/αCTLA-4 Ab.
    - TGF-β expression by tolerised Tr1 and Treg. We anticipate that TGF-β secretion will be primarily Treg mediated and may be dependent on the route of administration, as TGF-β has shown to be essential for oral tolerance and liver-targeted tolerance induction, but not systemic delivery of peptide via s.c. or i.n. routes (Groux et al., 1997; Weiner, 1997; Nicolson et al., 2006; Carambia et al., 2014).
    - Blocking experiments either *in vivo* or *in vitro* for TIGIT/TIM-3/PD-1/LAG-3. Each of these coinhibitory molecules could play a role in mediating cell contact-dependent bystander suppression (Anderson et al., 2016).
    - Effect of tolerance on DC subsets by staining using conventional cDC1 (XCR1) and cDC2 (CD172a CD11b) as well as plasmacytoid pDC markers (mPDCA-1/Ly6C) (Ovcinnikovs et al., 2019). We could also include gating for MHC-$II^{high}CD11c^{intermediate}$ migratory and MHC-$II^{intermediate}CD11c^{high}$ resident DC

(Guilliams et al., 2016; Ovcinnikovs et al., 2019). Migratory DC have been shown to be important in generating peripheral induced Treg (Vitali et al., 2012).

- Confocal imaging of peptide loaded (B10.PLxB6)F1 APC with Tg4 and 2D2 T cells

  We hypothesised that stimulation with linked hybrid MBP_{Ac1-9}-HFFK-MOG_{35-55} peptide compared to the two separate peptides would lead to increased T cell clustering around a central APC and may promote cell-contact mediated T:T bystander suppression.

- *In vivo* bystander suppression

  We observed moderate suppression of DC CD80/CD86 in tolerised (B10.PLxB6)F1 mice, which could cause non-specific immune suppression. To test this possibility, we could immunise both naïve and tolerised F1 mice with MOG_{35-55} or PPD. This would help determine if immune responses to autoantigens is maintained in the absence of MBP_{Ac1-9} stimulation and whether strongly inflammatory antigens override and reverse any bystander effect.

- *In vitro* bystander suppression assays

  Assessment of suppressive cytokines (IL-10 and TGF-β) in comparison to cell-contact mediated suppression (CTLA-4, PD-1, Notch, TIGIT/TIM-3/LAG-3) to exert suppression from Tol MBP_{Ac1-9} specific T cells to MOG_{35-55} specific 2D2 T cells. It would be interesting to analyse whether Tol Tg4 cells can also suppress antigen-experienced 2D2 T cells, or whether bystander suppression is only able to control naïve responses.

CHAPTER 4

IDENTIFICATION OF HUMAN T CELL EPITOPES OF THE AUTOANTIGEN CYP2D6

4.1 Introduction:

The success of antigen-specific immunotherapy approaches relies on the accurate identification of disease-relevant antigens and subsequent T cell epitope mapping prior to the design of tolerogenic peptides. This stage is a considerable bottleneck in PIT development, as autoantigen involvement in disease can be heterogenous between different patients and can further vary based on disease course. Autoimmune hepatitis type 2 possesses a less diverse autoantigen profile, as it is predominantly diagnosed by the presence of LKM-1 and to a lesser extent LC-1 autoantibodies, specific to the liver proteins cytochrome P450 2D6 (CYP2D6) and formiminotransferase cyclodeaminase (FTCD), respectively.

The peptide immunotherapy discovery platform utilises long 30mer peptides identified using a combination of *in silico* MHC Class II binding prediction tools. The biological complexity of a highly polymorphic MHC-II combined with immense diversity of potential peptides means that computational prediction tools based on known T cell epitope databases are extremely useful tools to narrow down the scope of investigation into T cell epitopes.

A benefit of using 30aa peptides is that they require antigen processing to render them an appropriate length for loading into the MHC-II peptide binding cleft. Shorter

peptides of 15aa may bind directly to surface MHC-II without processing, if they are of sufficiently high binding affinity, meaning that the short peptide approach may result in false positive hits. Initial T cell epitope mapping of CYP2D6 has been published (Ma et al., 2006), but used overlapping 15mers which could inadvertently identify cryptic epitopes. We were interested to first assess whether peptides we identified supported those identified previously in the literature.

To assess the immunogenicity of candidate 30mer peptides from CYP2D6 in healthy donors, AIH-2 patients (paediatric and adult) and AIH-1 patients (adult), we used a series of proliferation assays. 30mer peptides which are both compatible with antigen processing and presentation and are able to generate robust antigen-specific proliferation in PBMC are therefore most likely to contain CYP2D6 T cell epitopes. For logistical reasons, AIH-2 patients were analysed as 2 separate cohorts. All assays were conducted blind of any clinical patient data (sex, age, disease duration, medication, transplant status or disease severity). As such, analysis was performed purely grouping the patients by whether they were under the care of Birmingham Children's Hospital or the Queen Elizabeth Hospital Birmingham. Appendices 5 and 6 detail the clinical data of patients involved in this study as provided by BCH and Human Bioresources Centre Birmingham, respectively. Unfortunately, this data was retrieved after long delays and I was therefore not able to analyse AIH patients in light of this clinical data. Future work would perform involve analyses using disease severity, duration of disease , disease status (remission or flare) or medication as stratifying variables.

Chapter aims:

- Prediction of HLA-DR compatible peptides using computational algorithms.
- Optimisation of T cell proliferation assays to assess CYP2D6 peptide-specific proliferation indicative of peptide immunogenicity.
- Assessment of CYP2D6 peptide-specific proliferation of PBMC from a large cohort of healthy donors, cohorts of AIH-2 patients (paediatric and adult) and AIH-1 patients (adult).
- Assessment of cytokine responses by CYP2D6 peptide-stimulated PBMC in healthy donors, AIH-2 patients (adult) and AIH-1 patients (adult).

4.2 Epitope prediction *in silico*

Peptide binding algorithms allow the identification of T cell epitopes from the full-length protein sequence, greatly streamlining experimental validation. As MHC-II algorithms are less accurate predictors of T cell epitopes than their MHC-I counterparts, we chose to use a combination of prediction tools to ensure that no putative HLA Class II binding regions were omitted. We used ProPRED, NetMHC-II and panNetMHC-II to predict CYP2D6 T cell epitopes using the consensus sequence (UniProt: P10635, which are reported to generate the highest accuracy data for MHC-II molecules (Wang et al., 2008; Jensen et al., 2018).

The ProPRED prediction output (Fig.4.1) indicates a considerable number of pan-HLA-DR binding epitopes, with core binding region of 9 amino acids per epitope coloured blue and key anchor residues in red (Singh and Raghava, 2002). For our purposes, an intermediate threshold of 3% was set; the output threshold of 'percentage of best scoring natural peptides' determines the cut-off rate for predicted binders. Reducing the

Figure 4.1: Identification of putative HLA-DR compatible peptides from liver autoantigen CYP2D6 amino acid sequence

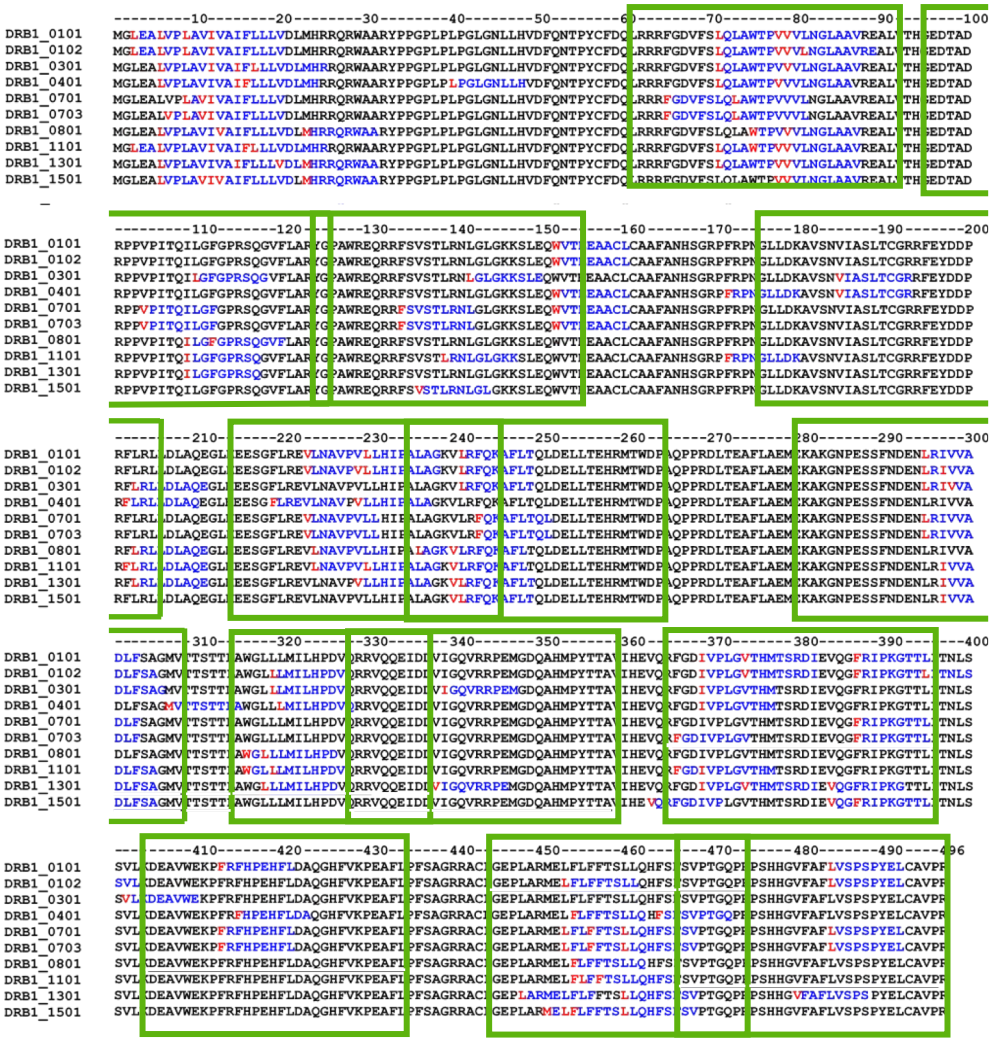

Figure 4.1: Annotated ProPRED MHC-II peptide prediction output for CYP2D6 protein sequence. The consensus sequence for human CYP2D6 was analysed for putative MHC Class II binding regions against a list of common HLA-DR molecules as determinants using ProPred. Putative binding cores of 9 amino acids (blue) with key anchor residues (red) are highlighted. 13 long peptides (23-30aa) encapsulating predicted pan-HLA-DR binding regions were selected (within green boxes), representing 355/496 aa (71.6%) of CYP2D6. Amino acids 1-32 contain bimodal signal sequence motifs targeting protein to the endoplasmic reticulum and mitochondria and were not included in predictions.

threshold to 1% will return only the top 1% of scored binding peptides providing increased stringency but potentially omitting weaker binding peptides (Sturniolo et al., 1999). When considering which regions of CYP2D6 to take forwards to antigenicity experiments, N terminal amino acids 1-32 were omitted, as this region is known to contain bimodal signal sequence motifs required for targeting to the endoplasmic reticulum and mitochondrial membranes (Avadhani et al., 2011). ProPRED analysis highlights that CYP2D6 is potentially a very rich source of antigenic peptides, due to its high number of predicted epitopes spanning the entire protein sequence. Of note, aa.71-79 LQLAWTPVV is a predicted binder for HLA-DRB1*01:01, *03:01, *04:01, *011:01 and *013:01. However, not every HLA-DR allele run in the algorithm is predicted to be compatible with this peptide, for instance the predicted peptide binding to HLA-DRB1*07:01 is 2 amino acids shifted towards the C terminus, due to its differential preference for anchoring residues. Interestingly, some regions contain predictions of multiple overlapping potential epitopes, aa. 446-474 contains 9 different epitopes with predicted compatibility with all tested HLA-DR other than -DR1 and -DR3. Selected 30mer candidates of CYP2D6 protein with MHC-II compatible epitopes are annotated within green boxes.

Outputs from NetMHC-II 3.2 (summarised in Table 4.1) are more quantitative and use a continually updated training dataset of known MHC-II binding peptides from the Immune Epitope Database. The prediction tool also estimates predicted binding affinity of a peptide to a specific MHC-Class II molecule with binders usually within a 1-1000nM affinity range. This gives an additional level of information when considering peptide response strength, kinetics and cellular behaviour. panNetMHC-II provides a similarly

Table 4.1: Summary of putative HLA-DR compatible peptides from liver autoantigen CYP2D6

Peptide number	Amino acid position	Highest predicted affinity (nM) for HLA-DR allelic variant by NetMHCII	Predicted core binding motif	30mer Sequence	Grand Average of Hydropathy value
1	62-91	15.1 (*07:01) 6.2 (*01:01) 11.3 (*01:01) 26.0 (*01:01) 12.0 (*07:01) 26.0(*01:01)	FGDVFSLQL LQLAWTPVV FSLQLAWTP LNGLAAVRE LAWTPVVVL LNGLAAVRE	RRRFGDVFSLQLAWTPVVVLNGLAAVREAL	0.53
2	96-125	49.3 (*08:01) 48.4 (*15:01)	VFLARYGPA ILGFGPRSQ	EDTADRPPVPITQILGFGPRSQGVFLARYG	-0.28
3	125-154	12.2 (*01:01) 171.5 (*04:01) 15.8 (*07:01) 16.3 (*13:01)	VSTLRNLGL RFSVSTLRN FSVSTLRNL LRNLGLGKK	GPAWREQRRFSVSTLRNLGLGKKSLEQWVT	-0.78
4	176-205	12.5 (*07:01) 18.2 (*03:01) 127.1 (*03:01) 53.9 (*07:01) 14.0 (*13:01) 22.8 (*13:01)	LDKAVSNVI FEYDDPRFL VIASLTCGR ASLTCGRRF IASLTCGRR LTCGRRFEY	GLLDKAVSNVIASLTCGRRFEYDDPRFLRL	-0.06
5	215-244	12.0 (*01:01) 16.4 (*01:01) 19.1 (*01:01) 20.6 (*01:01) 30.5 (*07:01) 67.5 (*07:01)	LLHIPALAG FLREVLNAV VLNAVPVLL HIPALAGKV LREVLNAVP REVLNAVPV	EESGFLREVLNAVPVLLHIPALAGKVLRFQ	0.56
6	235-264	49.2 (*07:01) 23.8 (*01:01) 254.3 (*03:01) 10.0 (*13:01) 10.8 (*15:01) 52.8(*15:01)	FQKAFLTQL FLTQLDELL LNAVPVLLH LAGKVLRFQ LRFQKAFLT VLRFQKAFL	ALAGKVLRFQKAFLTQLDELLTEHRMTWDP	-0.20
7	285-314	46.0 (*07:01) 49.7 (*11:01	GMVTTSTTL LAEMEKAKG	EKAKGNPESSFNDENLRIVVADLFSAGMV	-0.26
8	315-337	55.1 (*03:01) 219.8 (*03:01) 150.1 (*08:01) 9.2 (*13:01) 18.6 (*13:01)	LHPDVQRRV ILHPDVQRR LLLMILHPD LHPDVQRRV VQRRVQQEI	AWGLLLMILHPDVQRRVQQEIDD	-0.14
9	329-358			RRVQQEIDDVIGQVRRPEMGDQAHMPYTTA	-1.01
10	366-395	26.8 (*01:01) 42.9 (*07:01)	FGDIVPLGV VTHMTSRDI	FGDIVPLGVTHMTSRDIEVQGFRIPKGTTL	0.09
11	405-434	12.0 (*01:01) 48.9 (*07:01)	FLDAQGHFV FRFHPEHFL	DEAVWEKPFRFHPEHFLDAQGHFVKPEAFL	-0.57
12	445-474	19.4 (*01:01) 19.5 (*01:01)	LLQHFSFSV FTSLLQHFS	GEPLARMELFLFFTSLLQHFSFSVPTGQPR	0.17
13	467-496	4.3 (*01:01) 16.4 (*04:01)	FAFLVSPSP FLVSPSPYE	SVPTGQPRPSHHGVFAFLVSPSPYELCAVP	0.087

Table 4.1: Summary of putative HLA-DR compatible peptides from liver autoantigen CYP2D6. 13 candidate 30mer peptides selected for investigation are listed with amino acid positions, predicted 9mer core binding sequences and binding affinity (nM) for a range of common HLA-DR allelic variants (in brackets), 30mer sequence selected and the 30mer grand average of hydropathy (GRAVY) value. GRAVY score < 1 = hydrophilic and GRAVY score > 1 = hydrophobic.

Figure 4.2: Schematic of liver autoantigen CYP2D6 sequence and structural representation of selected 30mer peptides

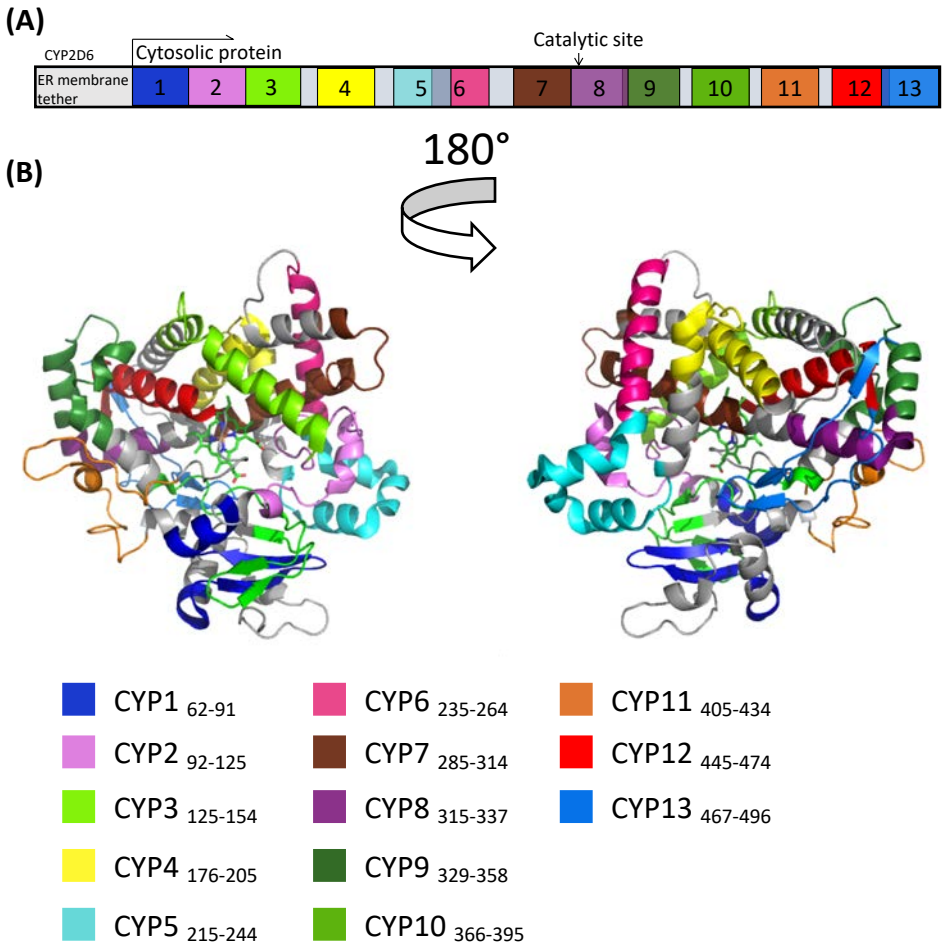

Figure 4.2: Schematic representation and 3D structure of CYP2D6 protein and selected 30mer peptides. (A) CYP2D6 protein sequence schematic annotated with the 13 candidate 30mer peptides selected for investigation. **(B)** 3D structure of CYP2D6 protein (PDB: 3TBG) aa 31-496 displayed as ribbon diagram. Centrally bound haem group is shown as sticks (green). 13 candidate 30mer peptides are coloured as above.

detailed analysis, using the same training dataset, instead focussing on predicted T cell epitopes that are predicted to bind to multiple allelic variants of HLA-DR molecules.

When compiling the data for these analyses, we determined that it would be most appropriate to investigate as many putative T cell epitopes as possible, to avoid omission of an important region. Many groups choose to assess the T cell response to 15mers, as this is the most common reported length of peptide for MHC-II. However, to ensure each core binding sequence is flanked by amino acids which allow for loading into the cleft, it is necessary to test a whole protein as overlapping 15mer peptides. Otherwise adjacent, non-overlapping 15mers may cut T cell epitopes in half, or trim off required amino acids required for proper binding.

With this in mind, we decided that we would select peptides of 30 amino acids in length that contained at least 1 predicted T cell epitope verified in both ProPRED and NetMHC-II databases (Figure 4.1 - green boxes; Table 4.1 – summary). Therefore, 13 candidate 30mers were selected covering 72% of the full length of CYP2D6 (Fig.4.2). Some peptides overlap where predicted epitopes spanned >30 amino acids consecutively, e.g. aa 215-264 (Fig.4.1). CYP2D6 is a highly globular protein and the majority of 30mer peptides represent surface exposed sequences (Fig.4.2). These represent a combination of exposed α helices, random coil and ß sheet some of which could represent B cell epitopes. CYP2D6 could be released from the intracellular compartment as a result of inflammatory processes and hepatocyte apoptosis.

This approach allows for peptides of predicted affinity for HLA-DR molecules to be selected for experimental validation without the need to produce overlapping 15mers for the entire protein sequence. It significantly reduces the cost of peptide synthesis by

approximately 45%. It also means that fewer peptides need to be tested in human and mouse experiments, meaning that all peptides can be tested in at least duplicate from one human blood draw and that fewer mice need to be used in experiments.

4.3 Optimisation of PBMC stimulation assays:

4.3.1 CYP2D6 peptide concentration

Firstly, to determine the overall optimal peptide concentration required to generate T cell proliferative responses, a screen of 5 healthy donor PBMCs was performed, stimulating with 10, 20 and 50μg/ml of each of the 13 candidate 30mer peptides derived from CYP2D6 (Table 4.1). Briefly, PBMCs were isolated from leukocyte cones collected from the NHS Blood and Transplant Service. Duplicate wells of unstimulated cells and peptide stimulated cells were plated at $1x10^6$ cells/ml in complete RPMI supplemented with 10% human AB serum in a 24 well plate. Cells were cultured for 8 days in a 5% CO_2 humidified atmosphere at 37°C. On day 8, duplicate aliquots of 100μl of cell suspension from each culture well were pulsed with 0.18MBq/ml [^{3}H]-thymidine for 16-20 hours. [^{3}H]-thymidine incorporation was measured on a scintillation reader as corrected counts per minute (cpm) and converted to stimulation index to account for individual variation in proliferation. Stimulation index (SI) is the ratio between a peptide stimulated condition cpm and the unstimulated condition cpm. Figure 4.3A depicts the mean SI value of each peptide at a range of concentrations from the 5 donors tested. From this initial screen, it is clear that different individuals respond to each peptide quite differently, some requiring a high peptide concentration of 50μg/ml to achieve a positive SI > 3, and others stimulated with the same peptide having an optimal response at 20μg/ml. The key

Figure 4.3: Optimisation of CYP2D6 peptide concentration required in PBMC stimulation assays

(A)

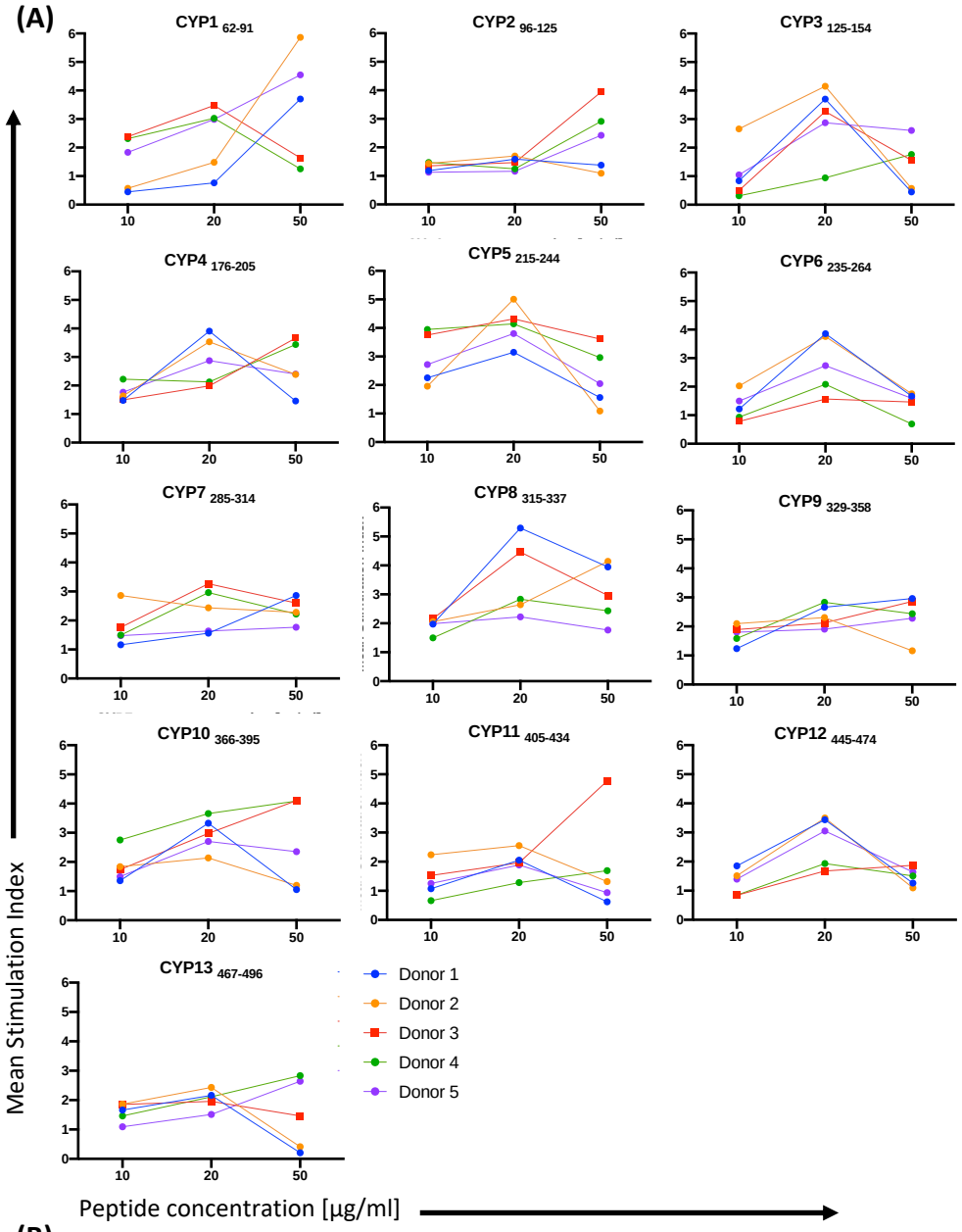

(B)

# of donors with peak Stimulation Index at peptide concentration (µg/ml):	CYP2D6 30mer peptide (aa 62-496)													Total # of peak responses
	1	2	3	4	5	6	7	8	9	10	11	12	13	
10	0	0	0	0	0	0	1	0	0	0	0	0	1	**2**
20	2	2	4	3	5	4	2	4	2	3	3	4	2	**40**
50	3	3	1	2	0	1	1	1	3	2	2	1	2	**22**

Figure 4.3: Optimisation of CYP2D6 peptide stimulation concentration. PBMCs isolated from 5 healthy donors were plated at 1 x 10^6 cells/ml in complete RPMI supplemented with 10% human AB serum and stimulated with CYP2D6 30mer peptides at 10, 20 and 50µg/ml. On day 8, duplicate aliquots of 100µl of cell suspension were incubated for 16-20hours with 0.18MBq/ml [^{3}H]-thymidine. [^{3}H]-thymidine incorporation was measured on a scintillation reader as corrected counts per minute (cpm) then converted to Stimulation Index (SI). SI = cpm of stimulated condition/cpm of unstimulated condition. **(A)** Graphs display mean SI for each peptide over the tested concentration range. (**B)** Results are summarised in table format by noting the optimal peptide concentration for each donor/peptide combination.

outcome for this experiment was to determine which concentration would be most suitable to gather representative data from the largest number of donors. The corresponding summary table (Fig.4.3B) counts the peak response (highest SI) for each donor stimulated with each peptide. Overall, the peak response was most likely to be at 20μg/ml. Therefore, subsequent stimulation assays used CYP2D6 peptides at 20μg/ml.

4.3.2 PBMC isolation method for small volumes of blood

Due to the small amount of blood permitted to be drawn from the paediatric AIH2 patients, and that we were only able to take one blood sample from each patient in the group, it was imperative that maximum numbers of PBMCs could be isolated from each patient blood sample. Our group would typically use Ficoll density gradient centrifugation, however, this can be challenging with blood volumes of < 10ml. We wanted to compare this method of PBMC isolation with pre-made isolation kits available. Blood was collected from two healthy donors and split into 5ml or 2ml volumes, before PBMCs were isolated using the three comparative methods: Ficoll, StemCell technologies EasySep PBMC isolation kit or Miltenyi MACSprep PBMC isolation kit. Figure 4.4A show the cell yield (x10^6 cells per ml blood collected) and viability (mean$\pm$ SEM). Cell yield was comparatively high when isolating by Ficoll or MACSprep. EasySep yields significantly fewer cells than MACSprep. All three methods achieved high cell viability of over 94%; however, MACSprep achieves significantly higher viability than both other methods (Fig.4.4A).

To test whether isolating PBMCs using different methods affected their functionality, donor cells were plated in triplicate 96 well plates at 1x10^6 cells/ml in

Figure 4.4: Optimisation of PBMC isolation method when using small blood volumes

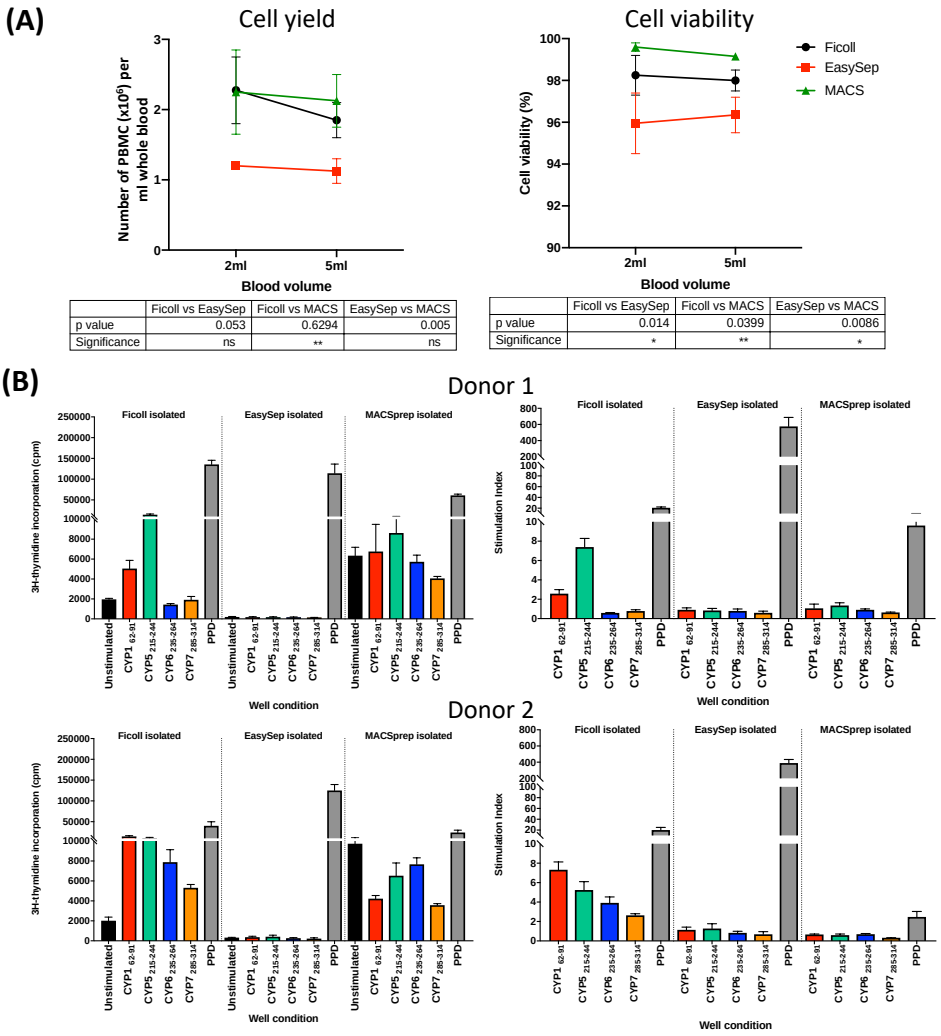

	Ficoll vs EasySep	Ficoll vs MACS	EasySep vs MACS
p value	0.053	0.6294	0.005
Significance	ns	**	ns

	Ficoll vs EasySep	Ficoll vs MACS	EasySep vs MACS
p value	0.014	0.0399	0.0086
Significance	*	**	*

Figure 4.4: Testing three different means of PBMC isolation from small volumes of whole blood to optimize yield, cell viability and functionality. Heathy donor blood (n=2) was subject to 1) Ficoll Paque PLUS density gradient centrifugation, 2) EasySep PBMC Kit or 3) MACSprep PBMC Kit. **(A)** Cell viability and yield per ml of blood shown as mean (±SEM). Statistical significance between cell isolation methods was analysed by unpaired t test. **(B)** Cells from 5ml samples were plated at 1 x 10^6 cells/ml in 96 well flat-bottomed plates and stimulated in triplicate with 20µg/ml of CYP2D6 peptides or PPD as a positive control. On day 8, wells were incubated for 16-20hours with [^{3}H]-thymidine to a final concentration of 0.18MBq/ml. Proliferation is shown as mean counts per minute (left;±SEM) and mean SI (right;±SEM).

complete RPMI + 10% human AB serum. Cells were left unstimulated, or stimulated with 20μg/ml CYP2D6 peptides $CYP1_{62\text{-}91}$, $CYP5_{215\text{-}244}$, $CYP6_{235\text{-}264}$ and $CYP7_{285\text{-}314}$ and 20μg/ml *Mycobacterium tuberculosis* Purified Protein Derivative (PPD) as a positive control. Cells were incubated with [^{3}H]-thymidine on day 8 post-stimulation for the final 16-20 hours of culture. Figure 4.4B shows raw cpm of [^{3}H]-thymidine incorporation (left panels) and Stimulation index (right panels). For both donors, only cells isolated by Ficoll were able to mount significant proliferative responses to CYP2D6 peptides (cpm>1000; SI>3). Cells isolated by EasySep showed very poor/little functionality towards CYP2D6 peptides unless they were stimulated with PPD, a strongly stimulating antigenic mixture. MACSprep isolated cells were able to proliferate in response to CYP2D6 peptides, but had much higher background cpm for unstimulated cells, indicating that the isolation process had initialised cell proliferation prior to antigen stimulation, making it unsuitable prior to assessing proliferation in response to peptide. Both EasySep and MACSprep kits utilise an antibody mixture to bind to PBMC cell subsets, prior to magnetic isolation. The process of binding antibodies to PBMC has rendered the isolated cells less responsive to CYP2D6 peptides, and with a higher background proliferation respectively. Ficoll isolated cells are effectively unmanipulated, as they are not labelled with any isolation antibodies, but are simply separated from red blood cells and platelets by density. The resulting cells were high yield, >97% viable and most importantly, responded strongly to stimulating antigens. The process takes longer than either isolation kit, and requires more care to perform, but was far superior for our requirements. Therefore, when performing all future PBMC isolation on small volume AIH2 patient blood samples and all 'normal' volume blood samples, Ficoll isolation was used.

4.4 Healthy donor PBMC stimulation assays

To assess the antigenicity of each candidate CYP2D6 30mer, a cohort of healthy donor PBMCs was collected from leukocyte cones. Figure 4.5 shows an example of a representative healthy donor (B17) proliferation timecourse assay. Healthy donor PBMCs were cultured at $1x10^6$ cells/ml in complete RPMI + 10% human AB serum, in a 24 well plate. Duplicate wells were stimulated with CYP2D6 peptides or PPD 20μg/ml, or left unstimulated. From days 4-8, duplicate aliquots of 100μl cell suspension were pulsed with [^{3}H]-thymidine for 16-20 hours, later to be harvested and [^{3}H]-thymidine incorporation measured on a scintillation reader. Raw counts (cpm) are shown over the timecourse in Fig. 4.5A. The timecourse assay allows for the assessment of both primary and secondary immune responses. In general, first exposure to antigen will have a peak response on day 6-8, whereas antigens with a secondary response will peak on day 4-6. For example, we would expect most adults who have been vaccinated with the BCG vaccine to have a strong early response to protein component PPD, whereas younger adults who may not have received the BCG vaccine are more likely to have a strong late response to this antigenic mix. CYP2D6 peptides that show cpm>1000 (Fig.4.5A) and SI>3 (Fig.4.5B) are classed as having a significant proliferative response, indicating both antigenicity and compatibility with the individual's MHC-II alleles.

Figure 4.6 summarises the proliferative responses of 43 healthy donors set-up in the same experiment, measuring proliferation on day 4, 6 and 8. These healthy donors were HLA-DR typed in our laboratory. They represent a diverse group of HLA-DR serotypes, allowing us to compare the antigenicity of CYP2D6 peptides between healthy donors

Figure 4.5: PBMC proliferation assay of healthy donor PBMCs to CYP2D6 30mer peptides over an 8 day timecourse

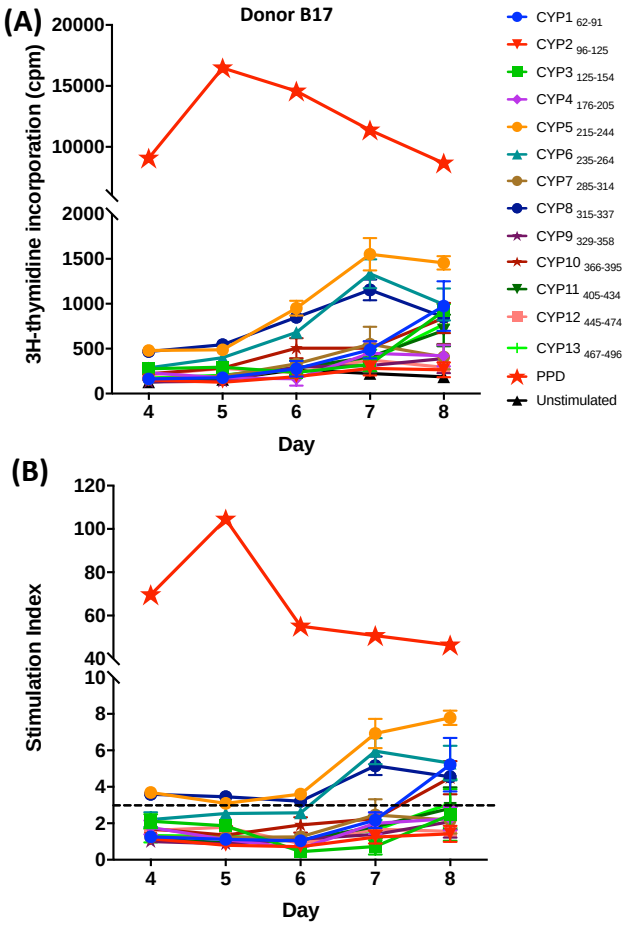

Figure 4.5: Proliferative response of donor B17 to CYP2D6 30mer peptide stimulation as measured by [^{3}H]-thymidine incorporation at day 4-8 post-stimulation. PBMCs were plated at 1 x 10^6 cells/ml in complete RPMI + 10% human AB serum and stimulated with 20µg/ml CYP2D6 30mer peptide in duplicate. Unstimulated control wells and positive controls stimulated with PPD were also set up in duplicate. On day 4-8, duplicate aliquots of 100µl of cell suspension was incubated for 16-20hours with 0.18MBq/ml [^{3}H]-thymidine. [^{3}H]-thymidine incorporation was measured on a scintillation reader as corrected counts per minute (cpm). **A)** Proliferation over time for each stimulation condition as measured by cpm (mean±SEM). **B)** Proliferation converted to Stimulation Index, (SI; mean±SEM). SI = stimulated cpm/ mean unstimulated cpm. SI ≥ 3 (dotted line) is classed as a positive proliferative response.

carrying different HLA-DR variants. The heatmap displays proliferation represented by stimulation index by colour scale starting at SI≥3 in response to each CYP2D6 peptide and positive control antigen PPD on day 4, 6 and 8.

There are 14 donors that share HLA-DR alleles (HLA-DR genotype and alternative alleles of DR51/52/53; Appendix 4) with at least one other, but these donors show distinct patterns of reactivity to CYP2D6 peptides, which is a good indicator that there are no individuals tested twice in the cohort. We are not able to trace any information from NHSBT to confirm whether they indeed were all different individuals. It also indicates that the likelihood of mounting a strong response to a specific peptide is not shared between donors with the same HLA-DR profile, suggesting that HLA-DR alone is not a strong predictor of peptide response in this cohort.

It is clear from the heatmap in Figure 4.6A and associated numerical summary (Fig.4.6B), that there are antigenic regions within a large proportion of the CYP2D6 protein. Only 1 peptide had a response rate of less than 5%. The remaining 12 peptides generated responses in at least 10% of donors tested, and 8/12 had a response rate of over 20%, which is relatively high in a healthy cohort. $CYP5_{215\text{-}244}$ and $CYP1_{62\text{-}91}$ were the most antigenic peptides overall, generating SI>3 in 44% and 42% of healthy donors, respectively.

If these healthy donors are categorised by HLA-DR serotype (Fig.4.7), groups of the most common serotypes are: HLA-DR7$^+$ n=16, HLA-DR3$^+$ n=13, HLA-DR4$^+$ n=11, HLA-DR1$^+$ n=12, HLA-DR2$^+$ n=11, HLA-DR11$^+$ n=10, HLA-DR13+ n=8. Most healthy donors are heterozygous and are therefore represented in two groups. The summary table displays the number of proliferative responses to each peptide within each HLA-DR group, and the

Figure 4.6: Summary of healthy donor PBMC proliferation in response to CYP2D6 30mer peptides over an 8 day time-course

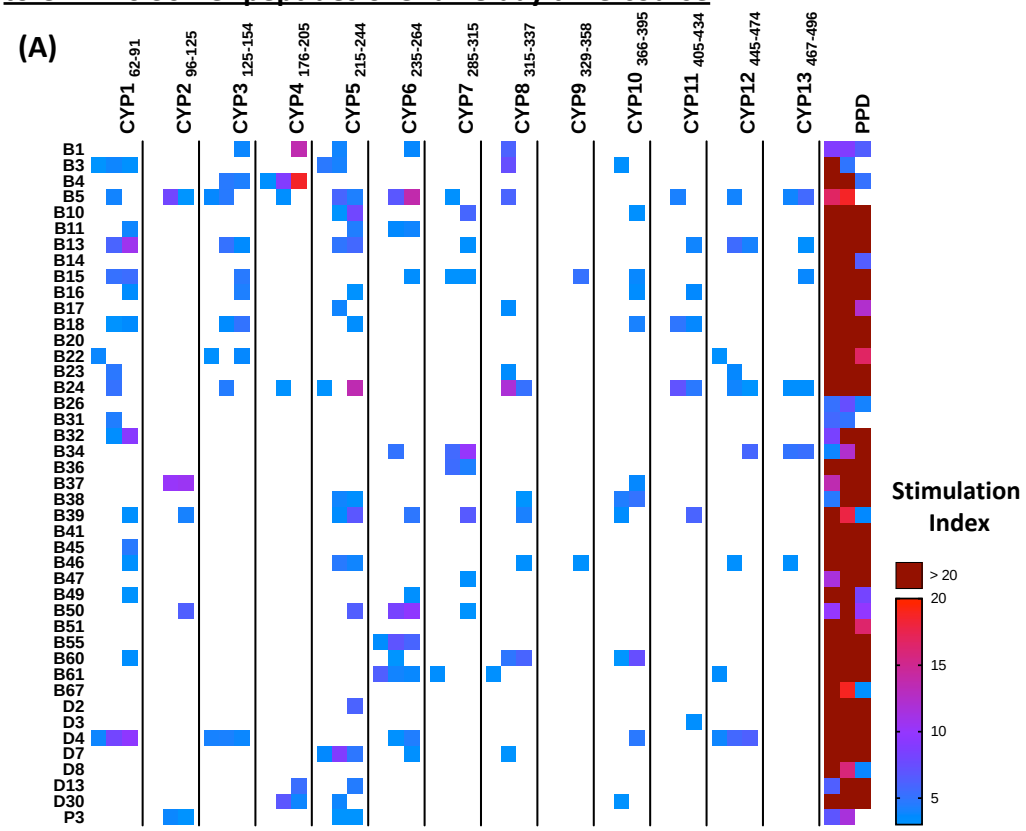

(B)

	CYP1 62-91	CYP2 96-125	CYP3 125-154	CYP4 176-205	CYP5 215-244	CYP6 235-264	CYP7 285-314	CYP8 315-337	CYP9 329-358	CYP10 366-395	CYP11 405-434	CYP12 445-474	CYP13 467-496
# responders	18	5	10	6	19	13	10	12	2	11	7	9	6
% responders	42	12	23	14	44	30	23	28	4.7	26	16	21	14

Figure 4.6: Proliferative responses of healthy donor PBMCs to CYP2D6 peptide stimulation as measured by [^{3}H]-thymidine incorporation at day 4-8 post-stimulation. PBMCs (n=43) isolated from leukocyte cones, plated at 1 x 10^6 cells/ml in complete RPMI + 10% human AB serum were stimulated with 20µg/ml CYP2D6 peptide in duplicate. Unstimulated control wells and positive controls stimulated with PPD were also set up in duplicate. On day 4, 6 and 8, duplicate aliquots of 100µl of cell suspension were incubated for 16-20 hours with 0.18MBq/ml [^{3}H]-thymidine. [^{3}H]-thymidine incorporation was measured on a scintillation reader as corrected counts per minute (cpm). **A)** Heatmap displays proliferation on day 4, 6, 8 (adjacent grid squares) for each donor, as mean Stimulation Index represented on a colour scale. **B)** Numerical summary of the number of donors with a positive response (SI ≥ 3) to each peptide and the corresponding percentage (2 s.f.) of positive responders from the cohort.

Figure 4.7: Healthy donor PBMC proliferation, subdivided by HLA Class II of individuals

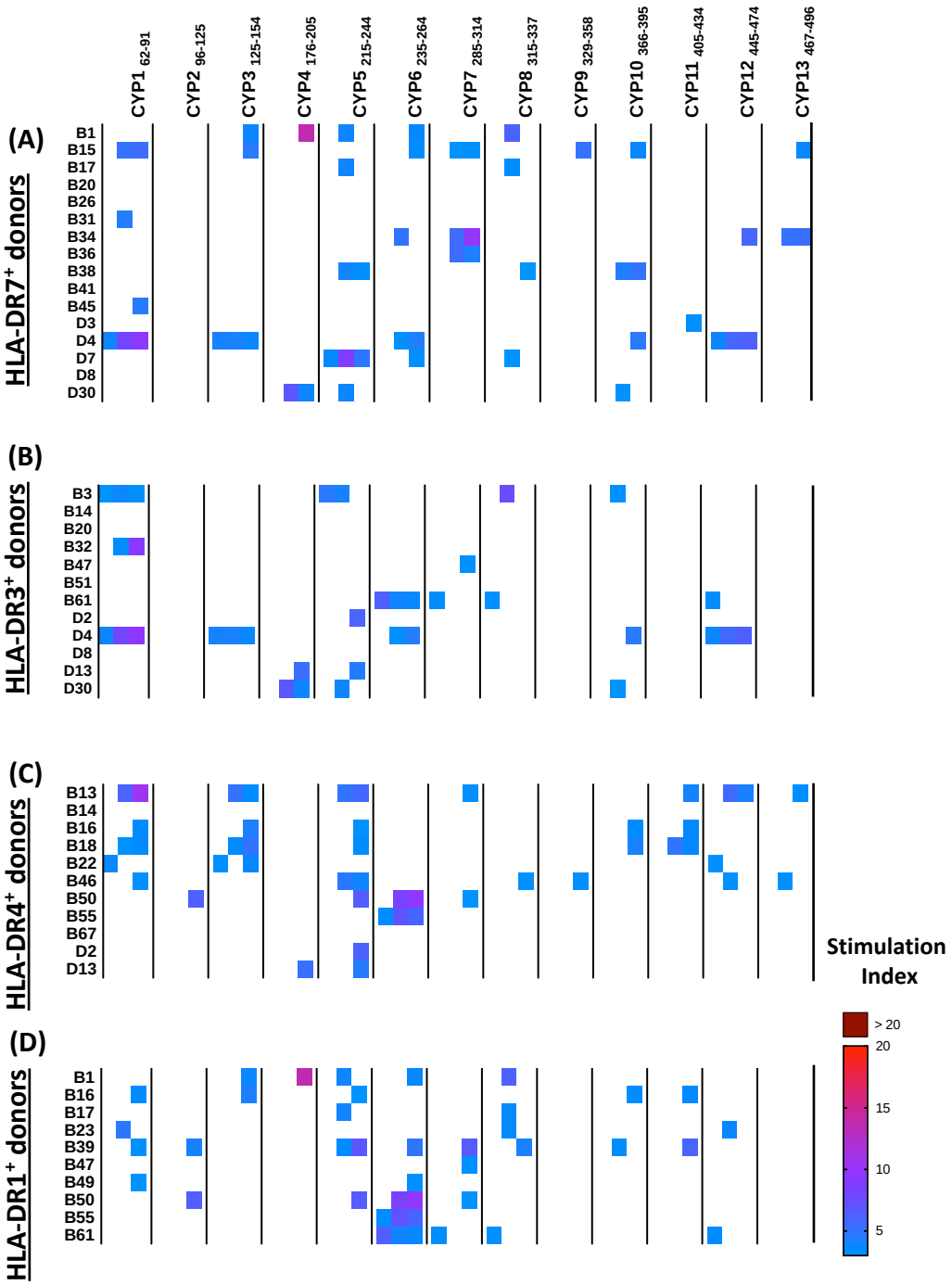

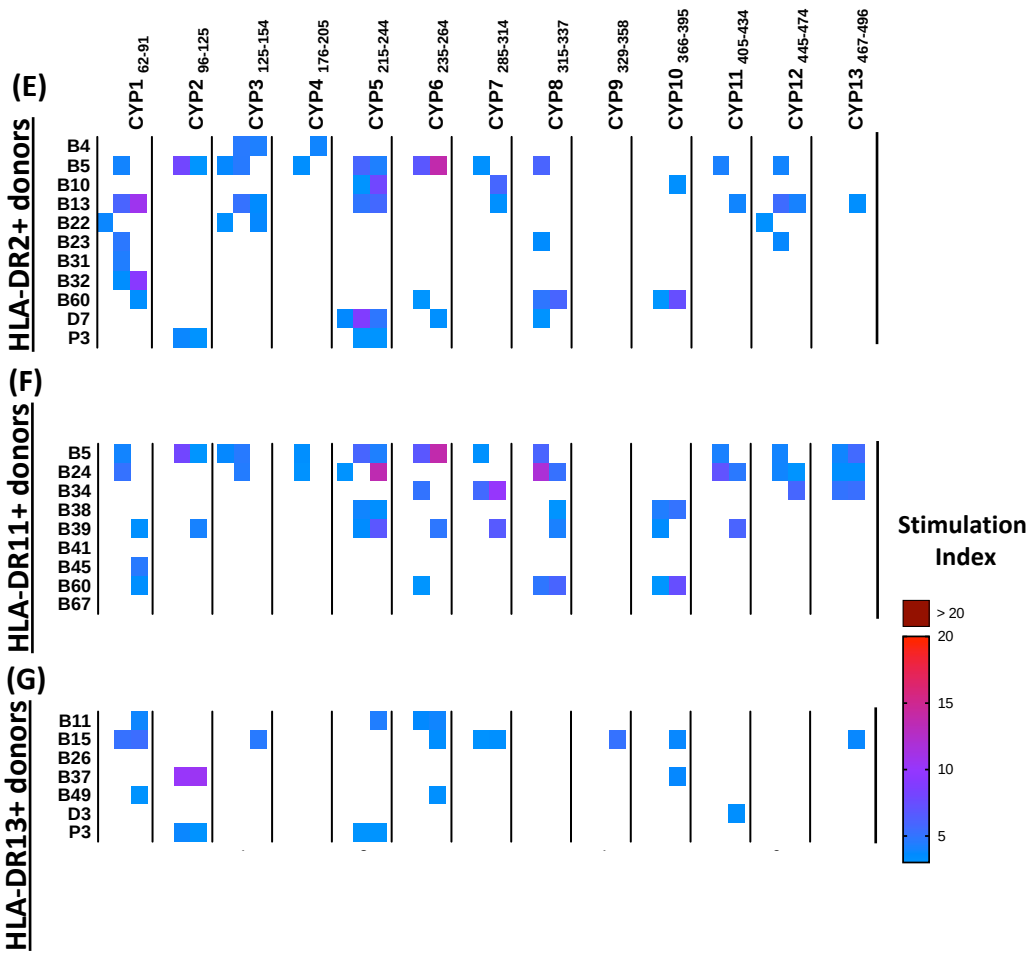

Figure 4.7: Heatmap summaries of healthy donor proliferative grouped by HLA-DR allele. Healthy donor PBMCs (n=43) were assayed for immune responses to CYP2D6 peptides as described in Fig.4.5. All healthy donors were HLA-DR typed by PCR (Olerup SSP; 101.101-48u) and grouped according to common serotypes: **(A)** HLA-DR7 (n=16), **(B)** HLA-DR3 (n=13), **(C)** HLA-DR4 (n=11), **(D)** HLA-DR1 (n=12), **(E)** HLA-DR2 (n=11), **(F)** HLA-DR11 (n=10), **(G)** HLA-DR13 (n=8).

Table 4.2: Summary of proliferative responses by healthy donor PBMCs grouped by HLA-DR allele

		CYP1 62-91	CYP2 96-125	CYP3 125-154	CYP4 176-205	CYP5 215-244	CYP6 235-264	CYP7 285-314	CYP8 315-337	CYP9 329-358	CYP10 366-395	CYP11 405-434	CYP12 445-474	CYP13 467-496
HLA-DR7 (n=16)	# responders	4	0	2	2	4	2	2	1	1	2	0	2	1
	% responders	25	0	13	13	25	13	13	6.3	6.3	13	0	13	6.3
HLA-DR3 (n=12)	# responders	3	0	1	2	4	2	2	2	0	4	0	3	0
	% responders	25	0	8.3	17	33	17	17	17	0	33	0	25	0
HLA-DR4 (n=11)	# responders	5	1	4	1	7	2	2	1	1	2	3	3	2
	% responders	46	9.1	36	9.1	64	18	18	9.1	9.1	18	27	27	18
HLA-DR1 (n=10)	# responders	2	2	2	1	5	6	4	5	0	2	2	2	0
	% responders	20	20	20	10	50	60	40	50	0	20	20	20	0
HLA-DR2 (n=11)	# responders	7	2	4	2	5	3	3	4	0	2	2	4	1
	% responders	64	18	36	18	46	27	27	36	0	18	18	36	9.1
HLA-DR11 (n=9)	# responders	5	2	2	2	4	4	3	5	0	3	3	3	3
	% responders	56	22	22	22	44	44	33	56	0	33	33	33	33
HLA-DR13 (n=7)	# responders	3	2	1	0	2	3	1	0	1	2	1	0	1
	% responders	43	29	14	0	29	43	14	0	14	29	14	0	14

Table 4.2: Summary of proliferative responses of healthy donor PBMCs grouped by HLA-DR allele to CYP2D6 peptide stimulation. PBMCs (n=43) from healthy donors were analysed for immune responses to CYP2D6 peptides as described in Fig.4.4. Proliferation on day 4, 6, 8 was converted to Stimulation Index (mean SI). A donor with a peak SI ≥ 3 for a specific peptide is classed as a "responder'.

rate of positive responses (Table 2). From this summary, it appears that there are certain peptides that associate more frequently with proliferation of PBMCs carrying specific HLA-DR molecules. For example, $CYP8_{315-337}$ had a response rate of 28% when looking at the entire healthy donor cohort, but when considering HLA-DR11$^+$ donors specifically, this response rate doubles to 56%. As a crude approach, the HLA-DR$^+$ groups with above average response rate for the greatest number of peptides in order are: HLA-DR11$^+$ 10/13 peptides, HLA-DR2$^+$ 9/13 peptides, HLA-DR4$^+$ 7/13 peptides, HLA-DR1$^+$ 6/13 peptides, HLA-DR13$^+$ 5/13 peptides, HLA-DR3$^+$ 3/13 peptides, HLA-DR7$^+$ 1/13 peptides. This data is somewhat surprising considering that AIH2 has been reported to highly associated with HLA-DR7 and HLA-DR3 in patient cohorts and GWAS studies (Ma et al., 2006). There may be some sampling errors in this dataset, as not all HLA-DR groups had the same number of donors, and some groups were quite small < 10 donors. However, the trend does show, particularly in the case of HLA-DR7, that simply possessing this AIH2 risk allele does not increase PBMC responses to CYP2D6 peptides.

To confirm this trend with statistical comparisons, the proliferation data from each donor was transformed to $\log_{(10)}$ SI (Fig.4.8). This transformation is required in order to convert the unidirectional, not-normally distributed SI data (Fig.4.8A) to a logarithmic scale (Fig.4.8B), effectively re-setting the baseline to SI = 1 (no change between unstimulated and stimulated condition). It is easier to visualise ratio data on a logarithmic scale for this reason. The transformation also allows for statistical comparison between the HLA-DR groups, as $\log_{(10)}$ SI data follows Gaussian distribution.

Figure 4.8: Proliferation data can be transformation to log(10) when performing statistical comparisons between groups

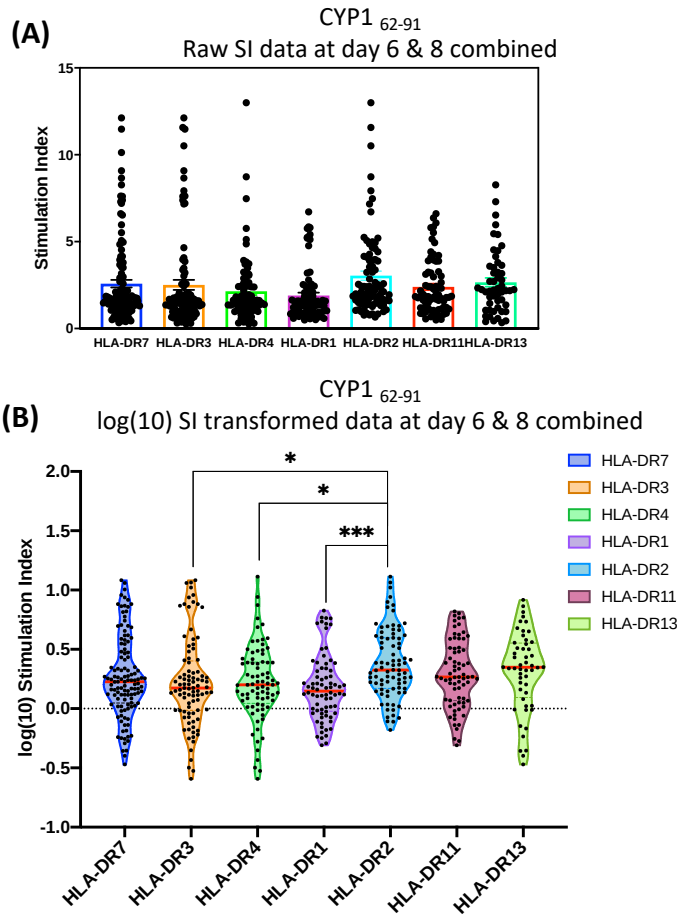

Figure 4.8: Healthy donors proliferation data grouped by HLA-DR allele shown as raw data and log(10) transformed data. A) Stimulation Index was transformed to log(10) values to better visualise the data. **B)** Log(10) SI values for each donor on day 6 and 8, where peak responses are observed are displayed as violin plots. log(10) SI values follow Gaussian distribution by D'Agostino & Pearson normality test for grouped data. Statistical difference between log(10) SI values in each group was analysed Brown-Forsythe & Welch ANOVA; accounting for variance in SD with Games-Howell adjustment for multiple comparisons.

Figure 4.9: Is there a statistically significant difference between proliferation responses of HLA-DR+ serotypes?

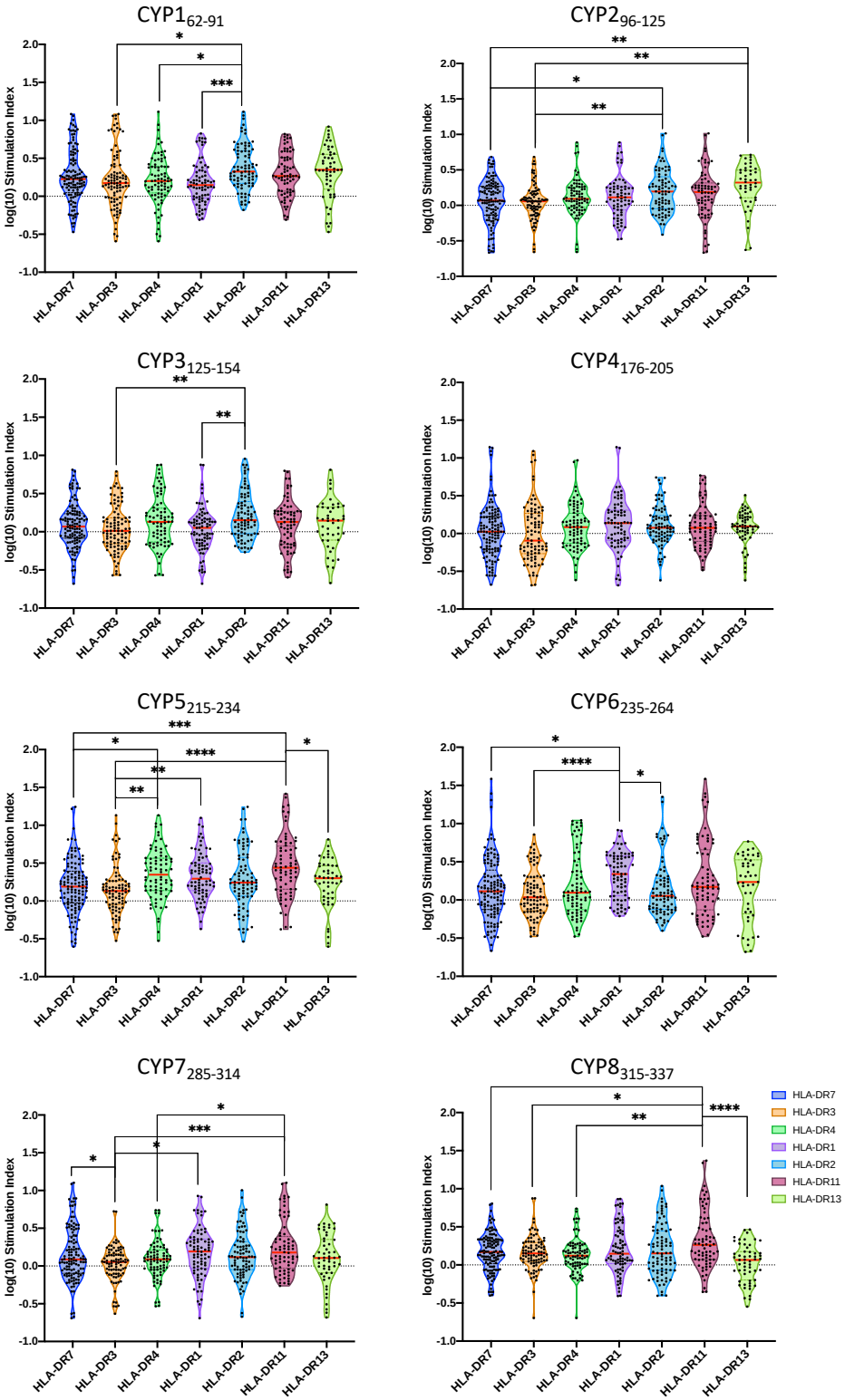

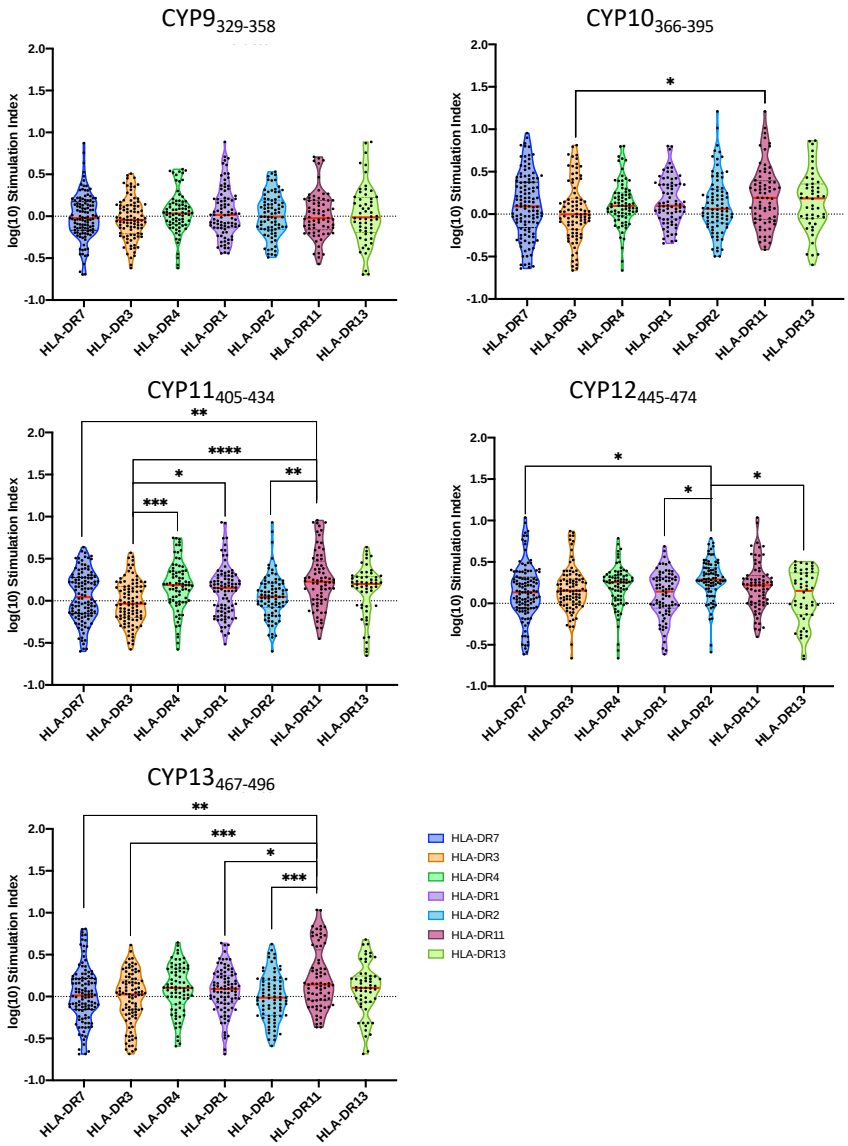

Figure 4.9: Healthy donors log(10) Stimulation Index grouped by HLA-DR serotype. Stimulation Index were transformed to log(10) values. Log(10) SI values for each donor on day 6 and 8, are displayed as violin plots. log(10) SI values followed Gaussian distribution by D'Agostino & Pearson normality test for grouped data. Statistical difference between log(10) SI values in each group was analysed Brown-Forsythe & Welch ANOVA; accounting for variance in SD with Games-Howell adjustment for multiple comparisons.

Figure 4.9 displays the $\log_{(10)}$ SI transformed data on day 6 and 8 (time of peak proliferative response occurs) for healthy donor stimulation assays, each donor SI value at each timepoint is one point, with mean SI value for the group indicated by a red horizontal line. The majority of peptides indicate a statistically significant difference in proliferative responses between two or more groups. Interestingly, the statistical analysis confirms the initial trend of HLA-DR7 and HLA-DR3 positive healthy donors being at a lower likelihood of generating strong immune responses to CYP2D6 peptides. For example, $CYP1_{62\text{-}91}$, which was across the whole healthy donor cohort a highly antigenic peptide (42% responders), shows a distinct preference for HLA-DR2 over HLA-DR3, HLA -DR4 and HLA -DR1.

4.5 AIH patient PBMC stimulation assays

4.5.1 Proliferation of Autoimmune Hepatitis patients is inhibited if PBMCs are cultured in autologous plasma

Figure 4.10 shows matched proliferation assays at day 8 post-stimulation for AIH2 patient P13, cultured in either: complete RPMI + 10% autologous heat-inactivated plasma (Fig.4.10A), complete RPMI + 10% human AB serum (Fig.4.10B) or X-VIVO-15 serum free media (Fig.4.10C). PBMCs were cultured at $1x10^6$ cells/ml in triplicate in a 96 well plate. After 8 days, cells were pulsed with 0.18MBq/ml [^{3}H]-thymidine for 16-20 hours. [^{3}H]-thymidine incorporation was measured as previously described. It is convention to use autologous plasma to culture PBMCs, if available, as it will tend to reduce immune responses between the PBMCs and exogenous proteins within serum from other sources. However, in our hands, when AIH2 patient PBMCs were cultured in the presence of

autologous plasma, proliferation in response to antigen was suppressed. As Figure 4.10A shows, [^{3}H]-thymidine incorporation cpm was extremely low for all CYP2D6 conditions and PPD, resulting in cpm far below 1000, and SI values of 1 for all stimulated conditions. In contrast, when autologous plasma was replaced with human AB serum or cells were cultured in a serum free media, proliferation was greatly increased with cells showing a strong response to $CYP1_{62\text{-}91}$ in particular. Unstimulated cell proliferation remained low, which meant that SI values surpassed the cut-off of SI>3 of 'positive response' for $CYP1_{62\text{-}91}$. Mean [^{3}H]-thymidine incorporation cpm was closely comparable between the human AB and X-VIVO-15 conditions, at 3233.75 and 3556.5 respectively. Both conditions met the SI threshold of >3 to be classed as a 'positive response'. PPD response varied between the human AB serum and X-VIVO-15 media conditions, although this is most likely due to the peak PPD response occurring earlier than day 8, and X-VIVO-15 being reported as an improved medium for maintenance of haematopoietic cells.

Subsequently, when sufficient numbers of cells were obtained from autoimmune hepatitis patients, we screened their responses to CYP2D6 peptides and PPD when cultured in RPMI supplemented with 10% autologous plasma vs serum-free X-VIVO-15. Figure 4.11 summarises the $\log_{(10)}$ SI data for 11 adult AIH patients where matched proliferation assays could be set-up. Where patients responded to peptides in serum-free X-VIVO-15, similar responses when cultured in autologous plasma were very rare. All CYP2D6 peptides generated a mean average (red line) higher response in X-VIVO-15 in comparison to autologous plasma. $CYP1_{62\text{-}91}$, $CYP4_{176\text{-}205}$, $CYP8_{315\text{-}337}$, $CYP9_{329\text{-}358}$, $CYP10_{366\text{-}395}$ and $CYP13_{467\text{-}496}$ all generated significantly higher proliferative responses when cells were grown in X-VIVO-15. PPD, as a strongly activating, positive control antigen showed even more pronounced differences, demonstrating that autologous plasma from patients

Figure 4.10: PBMCs from patients on immunosuppressant drugs require culturing in media without autologous plasma

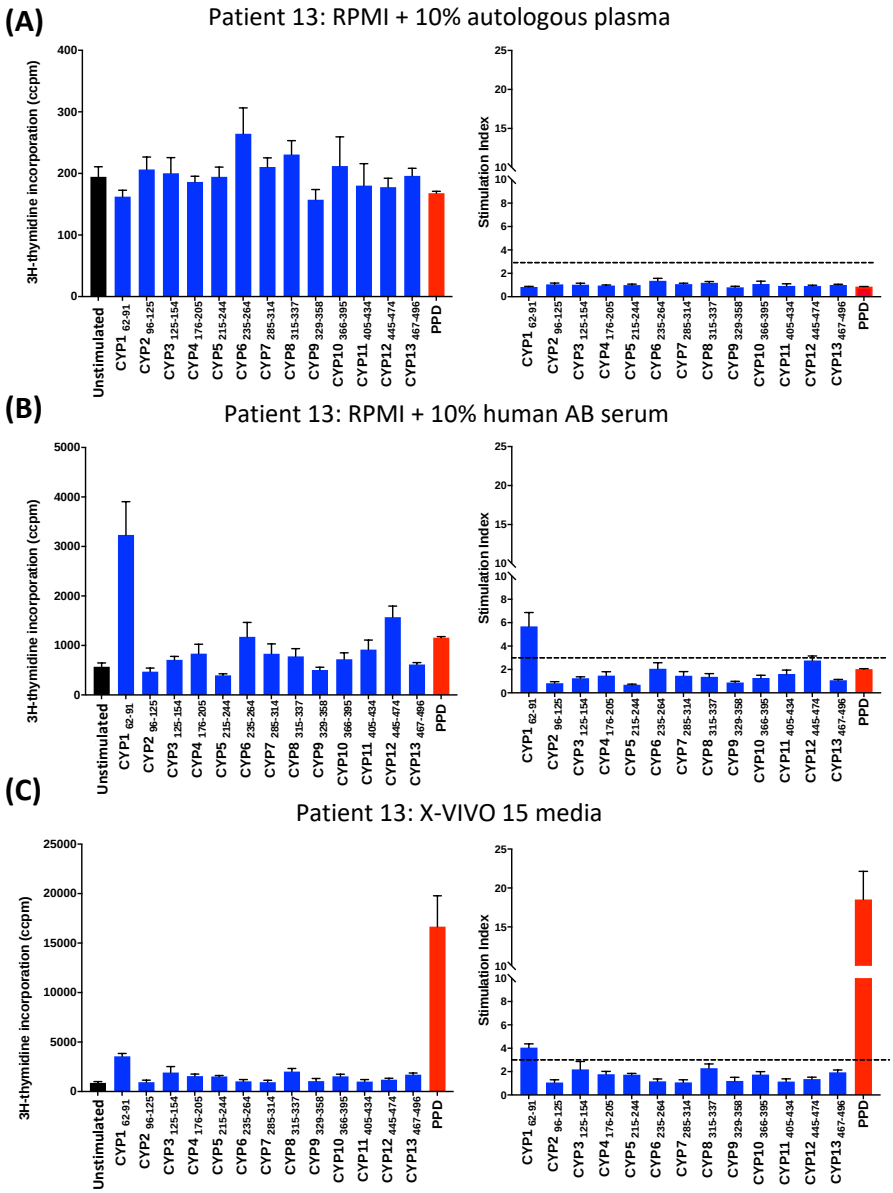

Figure 4.10: Proliferative responses of Patient 13 (AIH2 adult) to CYP2D6 peptide stimulation as measured by [^{3}H]-thymidine incorporation at day 8. PBMCs were isolated from venous blood and stimulated with CYP2D6 peptides as previously described. Matched assays were set up: **(A)** in complete RPMI + 10% heat-inactivated, autologous plasma, **(B)** in complete RPMI + 10% heat-inactivated human AB serum, **(C)** in serum-free haemopoietic cell media X-VIVO 15 (Lonza) supplemented with Pen/Strep. [^{3}H]-thymidine incorporation as counts per minute (cpm) and converted to SI.

Figure 4.11: Reduced proliferation of PBMCs from patients on immunosuppressant drugs in medium supplemented with autologous plasma

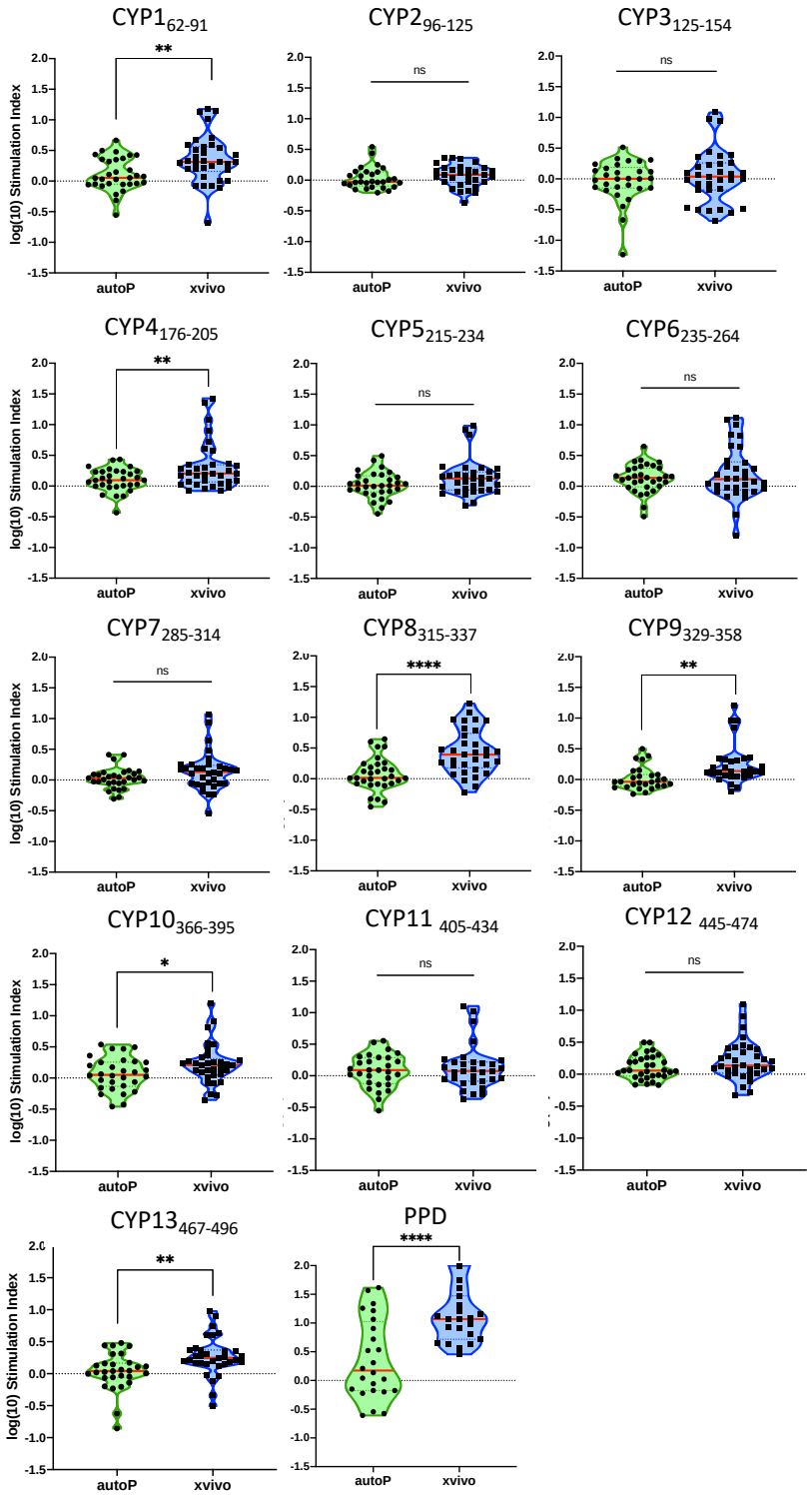

Figure 4.11: Proliferative responses of 11 adult AIH patients (AIH1 n=4, AIH2 n=7) to CYP2D6 peptide stimulation in either RPMI with autologous plasma or serum-free X-VIVO 15, as measured by [^{3}H]-thymidine incorporation at day 8 post-stimulation.

PBMCs were isolated from venous blood and stimulated with CYP2D6 peptides as previously described. Matched assays were set up in: complete RPMI + 10% heat-inactivated, autologous plasma, and serum-free haematopeitic cell media X-VIVO 15 (Lonza) supplemented with Pen/Strep. [^{3}H]-thymidine incorporation was measured on a scintillation reader and converted to Stimulation Index (ratio of stimulated vs unstimulated cpm). For statistical comparison, SI values were converted to log(10) SI. Log(10) SI values followed Gaussian distribution by D'Agostino & Pearson normality test for grouped data. Statistical difference between log(10) SI values in each group was analysed Brown-Forsythe & Welch ANOVA; accounting for variance in SD with Games-Howell adjustment for multiple comparisons.

on systemic immunosuppressant drugs suppress PBMC proliferation *in vitro* and alternative culturing conditions are required to properly assess peptide responses. The pharmacological immunosuppressant compounds used to control liver pathology in these patients may not have been degraded by heat-treatment of the plasma at 56°C for 40mins, according to our standard laboratory SOP and may therefore have been able to limit cell growth *in vitro*. It is also possible that there were naturally occurring immunomodulatory molecules within the patient blood samples, e.g. IL-10, which is commonly observed in chronic liver disease patients (Zhang and Wang, 2006). To have assessed this properly, we would have needed to run mass spectrometry on the blood plasma before and after processing to identify immunosuppressive compounds and IL-10 ELISA on patient blood plasma. In contrast, PBMC were able to proliferate effectively if cultured in the absence of autologous plasma. For this reason, all autoimmune hepatitis patients in the cohort were analysed for responses to CYP2D6 peptides in X-VIVO-15 culture media.

4.5.2 Proliferation assays of Autoimmune Hepatitis Type 2 paediatric patient PBMCs

Blood samples from 7 children diagnosed with Autoimmune Hepatitis Type 2 at Birmingham Children's Hospital were collected and PBMC isolated within 8 hours. For clinical information related to this cohort, see Appendix 5. PBMCs were assayed for proliferative responses to CYP2D6 peptides in triplicate, with PPD as a positive control, using [^{3}H]-thymidine incorporation 8 days post-stimulation. Four patients in the group had too few PBMC to measure responses to all peptides, thus peptides that had shown highest antigenicity in the healthy donor cohort were prioritised. The samples collected

Figure 4.12: Paediatric AIH2 patient sample proliferative responses to CYP2D6 peptides

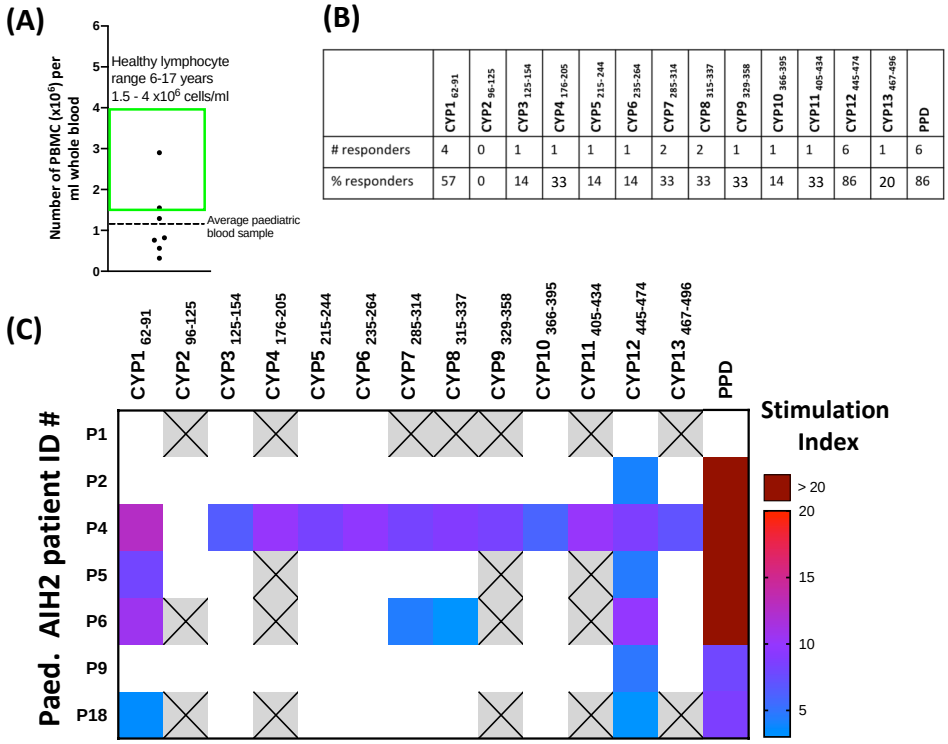

	CYP1 62-91	CYP2 96-125	CYP3 125-154	CYP4 176-205	CYP5 215-244	CYP6 235-264	CYP7 285-314	CYP8 315-337	CYP9 329-358	CYP10 366-395	CYP11 405-434	CYP12 445-474	CYP13 467-496	PPD
# responders	4	0	1	1	1	1	2	2	1	1	1	6	1	6
% responders	57	0	14	33	14	14	33	33	33	14	33	86	20	86

Figure 4.12: Summary of proliferative responses of 7 paediatric Autoimmune Hepatitis type 2 patient PBMCs to CYP2D6 peptide stimulation as measured by [^{3}H]-thymidine incorporation at day 8 post-stimulation. Patient PBMCs (n=7) isolated from venous blood, plated at 1 x 10^6 cells/ml in X-VIVO 15 were stimulated with 20 µg/ml CYP2D6 peptide in triplicate 96-well plate format. Unstimulated control wells and positive controls stimulated with PPD were also set up in triplicate. On day 8, cell suspension was incubated for 16-20 hours with 0.18MBq/ml [^{3}H]-thymidine. [^{3}H]-thymidine incorporation was measured on a scintillation reader as corrected counts per minute (cpm) then converted to SI (stimulated ÷ unstimulated cpm. **(A)** Lymphocyte yield per ml of whole blood from paediatric AIH2 patients is below the healthy range for age-matched children **(B)** Numerical summary of the number of patients with a positive response (SI ≥ 3) to each peptide and the corresponding percentage (2 s.f.) of positive responders from the cohort. **C)** Heatmap showing mean SI values on day 8 for each patient, represented on a colour scale, starting at SI ≥ 3. Some patients had too few cells to assay all peptides, therefore missing conditions are depicted by a grey filled, crossed square.

had below average number of PBMC per ml of whole blood compared to the healthy range for age matched children (Fig.4.12A). Overall, total PBMC numbers collected ranged from $1.5x10^6$ - $10.4x10^6$, therefore there were inherent limits to the extent of these experiments.

The proliferation heatmap represents SI values for AIH2 paediatric patient PBMCs when stimulated with CYP2D6 30mer peptides or PPD on day 8, cultured in X-VIVO-15 media (Fig.4.12C). P1 and P18 had both received a liver transplant prior to inclusion in this study and had followed different clinical trajectories since. P1 was positive for LKM-1 autoantibodies post-transplant and required higher immunosuppression to maintain the transplanted liver, whereas P18 no longer had circulating LKM-1 autoantibodies after the transplant. PBMC from P1 were unable to respond to CYP2D6 peptides or PPD, whereas P18 was responsive, potentially due to the increased immunosuppressive doses of P1 vs P18.

Figure 4.12C and corresponding numerical summary in Fig.4.12B, demonstrate that paediatric patients respond frequently to $CYP1_{62-91}$ and $CYP12_{445-496}$, with response rates over 50%. They display a higher likelihood of generating a proliferative response to these two peptides than the healthy donor cohort (Fig.4.16).

Of particular interest is $CYP12_{445-496}$, which stimulates a positive response in all paediatric AIH2 patients, other than P1, which was non-responsive to any of the CYP2D6 peptides or positive controls, PPD and PHA. This peptide was not one of the most dominant from the healthy donor cohort, so it is especially relevant that in this patient group, responses to $CYP12_{445-496}$ were so convincing. Potentially $CYP12_{445-496}$ is a region of CYP2D6 which initialises or perpetuates some of the immune pathology in AIH2. $CYP12_{445-}$

$_{496}$ is a prime candidate for continued investigation, to identify whether this T cells specific to this epitope are isolated to AIH2 patients, and to establish whether T cell responses against this region are an initiating event in developing AIH2 liver disease and diagnosing LKM-1 antibodies.

4.5.3 Proliferation assays of Autoimmune Hepatitis Type 2 adult patient PBMCs

Blood samples from 8 adults diagnosed with Autoimmune Hepatitis Type 2 at Queen Elizabeth Hospital Birmingham were collected and PBMC isolated within 8 hours. For clinical information related to this cohort, see Appendix 6. As previously, PBMCs were assayed for proliferative responses to CYP2D6 peptides and PPD as a positive control in triplicate, using [^{3}H]-thymidine incorporation 8 days post-stimulation. Numbers of PBMC/ml whole blood were within the healthy range for adults (Fig.4.13A).

The heatmap of SI values of PBMC in response to CYP2D6 peptides shows that in adult AIH2 patients, the most commonly antigenic peptides are CYP1$_{62\text{-}91}$ and CYP6$_{235\text{-}264}$ (Fig.4.13C). Responses to CYP6$_{235\text{-}264}$ are much higher in AIH2 adults compared to healthy donors, 50% vs 30% respectively, therefore CYP6$_{235\text{-}264}$ may also be a distinguishing epitope for AIH2 disease. CYP12$_{445\text{-}474}$ does not have the same level of response as in the paediatric group, which may suggest that T cell epitope spreading has occurred to other regions of the CYP2D6 protein during the course of disease, or that patients who are diagnosed very early in life with aggressive disease respond to different regions of the CYP2D6 protein to adults with later onset disease.

Figure 4.13: Adult AIH2 patient sample proliferative responses to CYP2D6 peptides

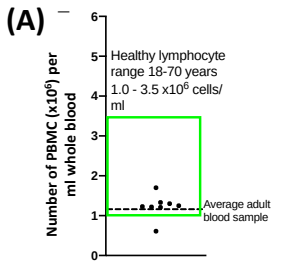

(B)

	CYP1 62-91	CYP2 96-125	CYP3 125-154	CYP4 176-205	CYP5 215-244	CYP6 235-264	CYP7 285-314	CYP8 315-337	CYP9 329-358	CYP10 366-395	CYP11 405-434	CYP12 445-474	CYP13 467-496	PPD
# responders	5	1	1	0	1	4	1	2	1	1	0	2	0	8
% responders	63	13	13	0	13	50	13	25	13	13	0	25	0	100

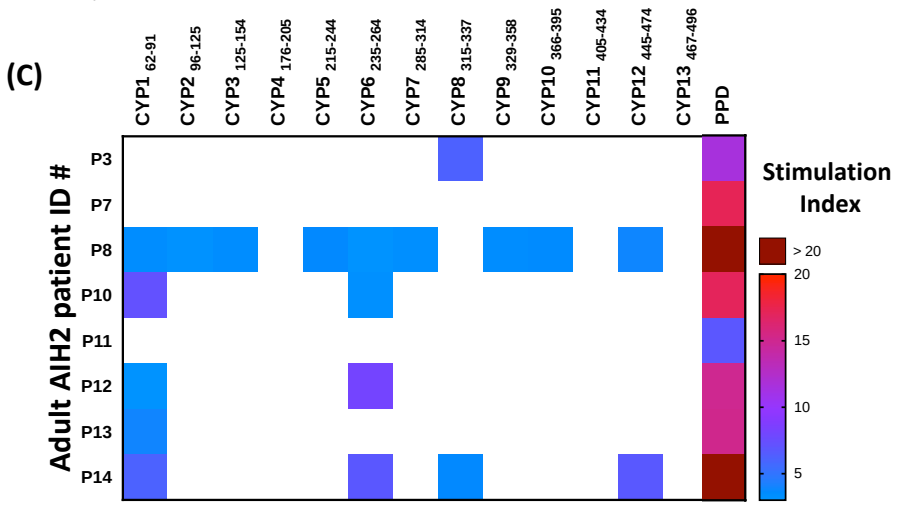

Figure 4.13: Summary of proliferative responses of 8 adult Autoimmune Hepatitis type 2 patient PBMCs to CYP2D6 peptide stimulation as measured by [^{3}H]-thymidine incorporation at day 8 post-stimulation. Patient PBMCs (n=8) were isolated from venous blood and stimulated with CYP2D6 peptides in X-VIVO 15 as previously described. [^{3}H]-thymidine incorporation was measured on a scintillation reader as corrected counts per minute (cpm) and converted to SI **(A)** Lymphocyte yield per ml of whole blood from adult AIH2 patients is within healthy adult range. **(B)** Numerical summary of the number of patients with a positive response (SI ≥ 3) to each peptide and the corresponding percentage of positive responders from the cohort. **C)** Heatmap showing mean SI values on day 8 for each patient, represented on a colour scale, starting at SI ≥ 3.

4.6 Proliferation assays of Autoimmune Hepatitis Type 1 patient PBMCs

Blood samples from 11 adults diagnosed with Autoimmune Hepatitis Type 1 at Queen Elizabeth Hospital Birmingham were collected and PBMC isolated within 8 hours. For clinical information related to this cohort, see Appendix 6. As previously, PBMCs were assayed for proliferative responses to CYP2D6 peptides, and PPD as a positive control in triplicate using [^{3}H]-thymidine incorporation 8 days post-stimulation. The average number of PBMC per ml whole blood was within the healthy range for adults (Fig.4.14A).

Interestingly, the heatmap displaying SI values of AIH1 patient responses to CYP2D6 peptides shows a distinct pattern of reactivity different to AIH2 patients and healthy donors. Responses to $CYP1_{62\text{-}91}$ remain common, yet a new target peptide is revealed in $CYP8_{315\text{-}337}$. This data suggests that $CYP1_{62\text{-}91}$ is antigenic regardless of disease status, as it has been implicated in AIH1, AIH2 and healthy donors. Response to $CYP8_{315\text{-}337}$ in the AIH1 group is over twice as likely as in healthy donors or AIH2 adults, 64% vs 28% or 25% respectively. There are currently no published data to determine whether AIH1 patients have T cell responses to CYP2D6 autoantigen. As these patients do not have LKM-1 antibodies towards CYP2D6, using the standard technique using liver-kidney section, it has been assumed that this means CYP2D6 is not an identified relevant autoantigen in AIH1. In reality, it may be the case that AIH1 patients do possess autoreactive T cells to some regions of CYP2D6, most notably $CYP8_{315\text{-}337}$, but that i) this lymphocyte reactivity cannot be identified using the current liver-kidney test ii) T cell reactivity to $CYP8_{315\text{-}337}$ does not translate to αCYP2D6 autoantibodies. We would ideally have liked to have continued to obtain more AIH1 patient blood samples to confirm $CYP8_{315\text{-}337}$ as a T cell target, to HLA-DR type the patients involved in the study, and later

Figure 4.14: Adult AIH1 patient sample proliferative responses to CYP2D6 peptides

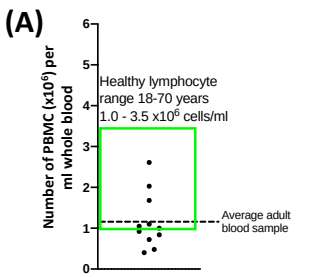

(B)

	CYP1 62-91	CYP2 96-125	CYP3 125-154	CYP4 176-205	CYP5 215-244	CYP6 235-264	CYP7 285-314	CYP8 315-337	CYP9 329-358	CYP10 366-395	CYP11 405-434	CYP12 445-474	CYP13 467-496	PPD
# responders	4	1	1	0	1	3	0	7	0	1	1	1	1	10
% responders	37	10	9	0	9	28	0	64	0	9	10	9	9	91

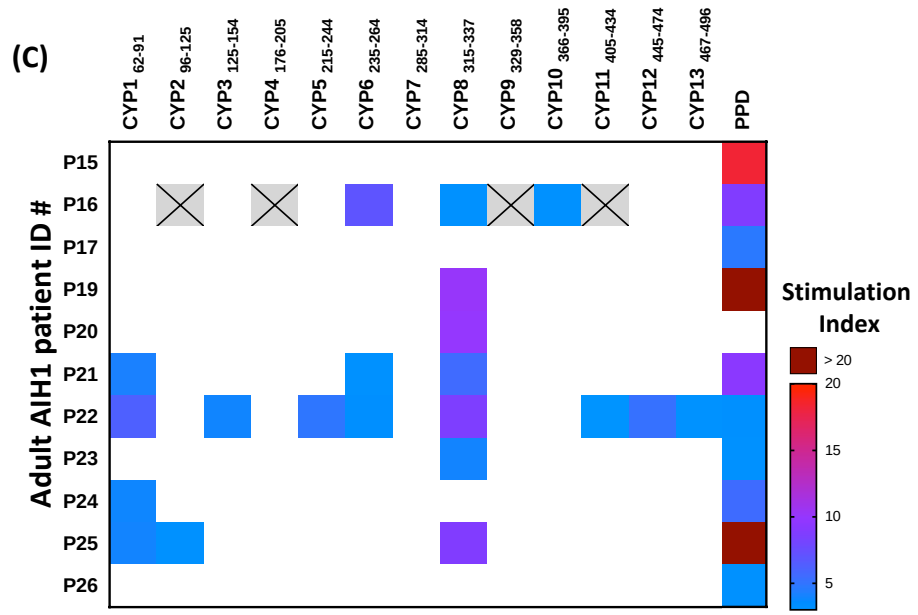

Figure 4.14: Summary of proliferative responses of 11 adult Autoimmune Hepatitis type 1 patient PBMCs to CYP2D6 peptide stimulation as measured by [^{3}H]-thymidine incorporation at day 8 post-stimulation. Patient PBMCs (n=11) were isolated from venous blood and stimulated with CYP2D6 peptides in X-VIVO 15 as previously described. [^{3}H]-thymidine incorporation was measured on a scintillation reader as corrected counts per minute (cpm) and converted to SI. **(A)** The average lymphocyte yield per ml of whole blood from adult AIH1 patients is within the healthy adult range. **(B)** Numerical summary of the number of patients with a positive response (SI ≥ 3) to each peptide and the corresponding percentage of positive responders from the cohort. **C)** Heatmap showing mean SI values on day 8 for each patient, represented on a colour scale, starting at SI ≥ 3. Patient 16 had too few cells to assay all peptides, therefore missing conditions are depicted by a grey filled, crossed square.

Figure 4.15: Summary heatmap of all AIH1/2 patient sample proliferative responses to CYP2D6 peptides

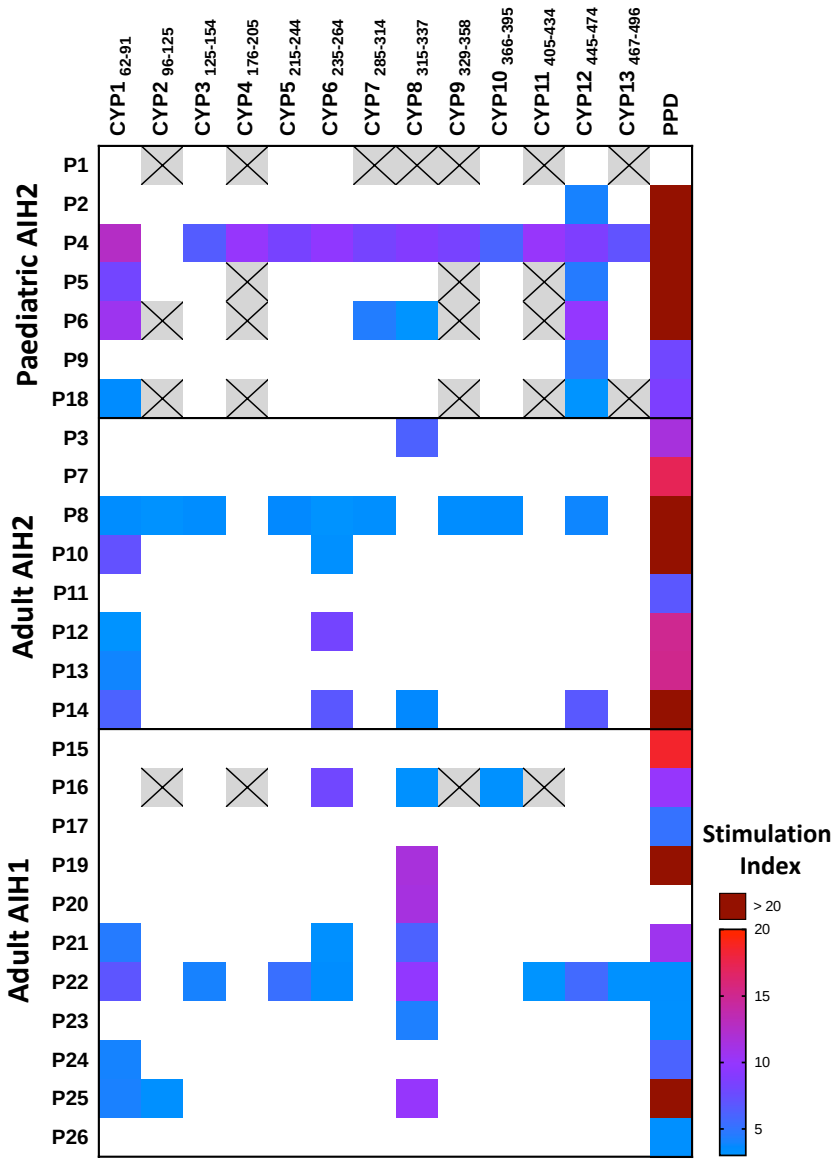

Figure 4.15: Summary of proliferative responses of all AIH patient PBMCs to CYP2D6 peptide stimulation as measured by [^{3}H]-thymidine incorporation at day 8 post-stimulation. Collated data from Figures 4.12, 4.13 and 4.14.

to develop tetramers loaded with $CYP8_{315-337}$ T cell epitope. This would allow us to compare whether AIH1 responses to $CYP8_{315-337}$ are restricted to specific HLA-DR alleles, and to identify $CYP8_{315-337}$ specific T cells circulating in peripheral blood of AIH1 vs HCV patients.

Figure 4.15 combines the paediatric AIH2, adult AIH2 and adult AIH1 heatmaps to better visualise differences in response between these patient groups. As mentioned previously, $CYP1_{62-91}$ is the only peptide with high rates of positive responses in all 3 patient groups and healthy donors, whereas other highlighted peptides ($CYP12_{445-496}$ in paediatric, $CYP6_{235-264}$ in adult AIH2 and $CYP8_{315-337}$ in adult AIH1) all display distinct response patterns in one patient group.

4.7 Statistical analysis between CYP2D6 peptide responses of Autoimmune Hepatitis patient groups and healthy donor PBMCs

To draw relevant statistical comparisons between the proliferative responses of each AIH group vs healthy donors, all SI data on day 8 was collated and transformed to $log_{(10)}$ SI. Figure 4.16 shows violin plots of proliferative responses to each CYP2D6 peptide 8 days post-stimulation. Due to the reduced numbers cells isolated from patient samples in the paediatric AIH2 group, some of the peptides have limited numbers of data points.

There is no change in response potency of AIH patients and healthy donors to peptides $CYP2_{96-125}$, $CYP7_{285-314}$, $CYP9_{329-358}$, $CYP10_{366-395}$ or $CYP11_{405-434}$. None of these peptides generate high immune responses in any group, ranking these as low antigenicity peptides.

For $CYP1_{62-91}$, mean $log_{(10)}$ SI for paediatric AIH2 and adult AIH2 is 0.5370 and 0.5079, respectively; in comparison to adult AIH1 and healthy donors (0.2750 and 0.2873). Responses of adult AIH2 patients are significantly higher than responses in healthy donors. There is no difference between adult AIH1 and healthy donors in response to $CYP1_{62-91}$.

$CYP3_{125-154}$ is shown to be significantly more antigenic in both paediatric and adult AIH2 patients in comparison to the healthy donor cohort (mean $log_{(10)}$ SI values = 0.2595, 0.3871, 0.06426, respectively).

$CYP4_{176-205}$ is significantly more potent at stimulating proliferative responses in adult AIH2 vs adult AIH1 (mean $log_{(10)}$ SI values = 0.2052 and -0.1289, respectively). However, as only 3 paediatric patients were screened for $CYP4_{176-205}$ responses, there is not sufficient power to draw statistical comparisons from this group.

$CYP5_{215-244}$ is an interesting case, as it is much more antigenic in healthy donors than in AIH patients (mean $log_{(10)}$ SI values = HD 0.3698, AIH2 adult 0.1745, AIH1 adult 0.05381).

$CYP6_{235-264}$ is significantly more antigenic in adult AIH2 vs adult AIH1 and healthy donors (mean $log_{(10)}$ SI values = 0.3842, 0.1025 and 0.1981, respectively).

$CYP8_{315-337}$ stimulates a highly specific increase in responses among AIH1 patients, which is largely absent from other groups. Therefore, the $CYP8_{315-337}$ response is significantly more potent in these patients when compared with AIH1 adult or healthy donor (mean $log_{(10)}$ SI values = 0.5873, 0.3481 and 0.1679, respectively). $CYP8_{315-337}$ would be worth following up with greater intensity in the AIH1 patient cohort.

$CYP12_{445-474}$ is then also a high priority peptide, as it stimulates significantly higher proliferation in paediatric AIH2 compared to any of the other groups (mean $log_{(10)}$ SI values paed. = 0.6229, adult AIH2 = 0.2846, adult AIH1 = 0.2692 and HD = 0.1749). Whether this is indicative of disease stage, patient age or disease severity is yet to be determined.

$CYP13_{467-496}$ is more antigenic in AIH2 adults than HD (mean $log_{(10)}$ SI values = 0.2066 and 0.02725, respectively).

Among the 5 peptides classed as antigenic in one or more patient groups, i.e. peptides displaying >20% response rate ($CYP1_{62-91}$, $CYP6_{235-264}$, $CYP7_{285-314}$, $CYP8_{315-337}$, $CYP12_{445-474}$), their responses in AIH-2 are significantly higher than those of healthy donors, distinguishing them as potentially relevant in AIH pathology. $CYP1_{62-91}$, $CYP7_{285-314}$, $CYP8_{315-337}$ and $CYP12_{445-474}$ are more antigenic in paediatric AIH2. $CYP1_{62-91}$, $CYP6_{235-264}$ and CYP8 are more antigenic in adult AIH2 and adult AIH1, with AIH2 biased towards $CYP1_{62-91}$ and $CYP6_{235-264}$ compared to a clear preference in AIH1 for $CYP8_{315-337}$.

It is also worth noting that the responses across the 3 adult groups are significantly different when PBMC were stimulated with PPD. Healthy donors are much more likely to generate highly potent proliferative responses against PPD in comparison to both AIH2 or AIH1 adults (mean $log_{(10)}$ SI values = 1.389, 1.175 and 0.8718, respectively). PPD is a relevant positive control antigen for these groups, as if age-matched, we can assume that each individual was as likely as the next to have received the BCG vaccination. Those having received the vaccine respond more rapidly to PPD, whereas those without BCG vaccination would respond slower, yet both groups should have highly potent immune response by proliferation at some point between day 4 and 8.

Figure 4.16: Comparing proliferation data between AIH patient groups and healthy donors

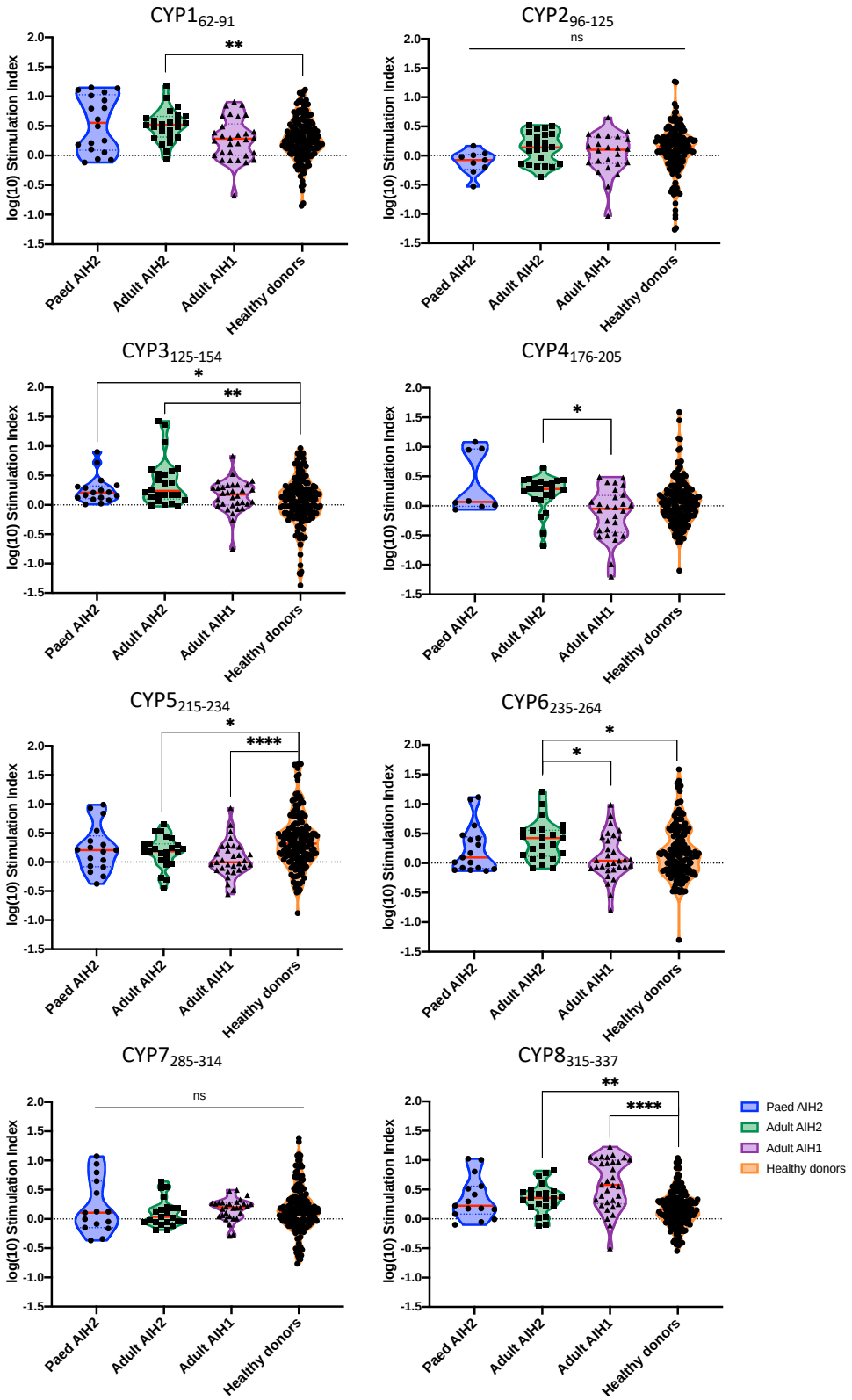

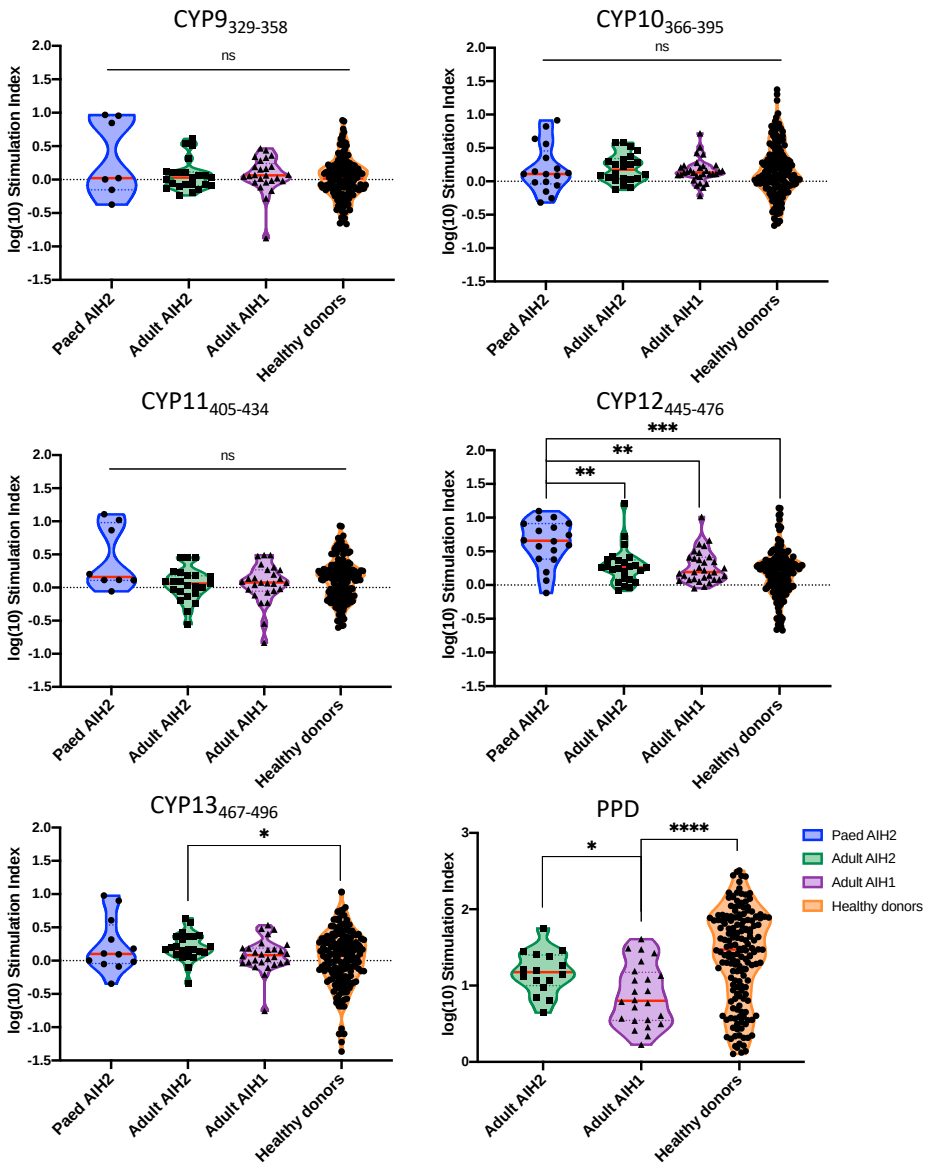

Figure 4.16: AIH patient groups and healthy donors log(10) SI values following stimulation with CYP2D6 peptides. SI values were transformed to log(10) values to allow for statistical comparisons between groups. Data presented shows Log(10) SI values for each individual in a group on day 8 post-stimulation. Log(10) SI values follow Gaussian distribution by D'Agostino & Pearson normality test for grouped data. Statistical difference between log(10) SI values in each group was analysed by Brown-Forsythe & Welch ANOVA; accounting for variance in SD with Dunnett's T3 adjustment for multiple comparisons.

The differential response to PPD highlights the likely effect of continued, strong immunosuppressive drug regimens used in autoimmune hepatitis treatment in an attempt to quench the ongoing autoimmune and inflammatory responses and progression of disease to severe fibrosis, HCC or liver failure. In newly diagnosed AIH2 or AIH1 patients, it would be extremely interesting to investigate whether their responses to CYP2D6 antigens are even more severe prior to immunosuppressive intervention.

4.8 Cytokine production of PBMCs in response to CYP2D6 peptide stimulation

4.8.1 Cytokine production of adult AIH2, adult AIH1 and healthy donor PBMCs in response to CYP2D6 peptide stimulation

As it has been reported previously that certain 15mers derived from CYP2D6 are able to stimulate IFN-γ, IL-10 and IL-4 production (Ma et al., 2006), we wanted to analyse whether our 30mer peptides established similar cytokine secretion patterns. To do this, we used the multiplex Th LEGENDPLEX multiplex bead assay from Biolegend, designed to quantify the concentration of 13 cytokines: IL-5, IL-13, IL-2, IL-6, IL-9, IL-10, IFN-γ, TNF-α, IL-17A, IL-17F, IL-4, IL-22 and IL-23 in cell culture supernatants. Cell culture supernatant values are compared to 8-point standard curves for each cytokine, ranging from 2.4-1000pg/ml.

Figure 4.17 shows the cytokine concentration of cell culture supernatants after CYP2D6 peptide stimulation panels for 8 AIH2 adults, 11 AIH1 adults and 5 healthy donors. Data shown in Figure 4.17 is the determined cytokine concentration after subtracting the background cytokine concentration of the unstimulated condition for

each individual. For all individuals tested, unstimulated cells produced very low levels of cytokines.

Overall, the peptides which were known to stimulate strong proliferative responses in a range of healthy/patient groups, $CYP1_{62-91}$ (Fig.4.17A), $CYP3_{125-154}$ (Fig.4.17C), $CYP5_{215-234}$ (Fig.4.17E), $CYP6_{235-264}$ (Fig.4.17F), $CYP7_{285-314}$ (Fig.4.17G), $CYP8_{315-337}$ (Fig.4.17H), $CYP10_{366-395}$ (Fig.4.17J) and $CYP12_{445-476}$ (Fig.4.17L), and therefore classed as antigenic, were also the peptides that stimulated the production of higher concentration of inflammatory cytokines, IL-6, IFN-γ and TNF-α. There was very little production of Th2 cytokines IL-4, IL-5 and IL-13 observed. Similarly, very little IL-17A, IL-17F or IL-23 was detected, indicating that Th17 responses were not activated.

Stimulation with PPD was able to generate high proliferative responses across all groups and showed very high production of both IL-6 and IFN-γ in particular (Fig.4.17N). There was no significant difference in the amount of IL-6 or IFN-γ produced between AIH2, AIH1 and healthy donor groups. AIH1 patients produced a higher concentration of TNF-α and IL-13 when stimulated with PPD.

Figure 4.17: Production of cytokines by CYP2D6 peptide-stimulated PBMCS from AIH patient groups and healthy donors

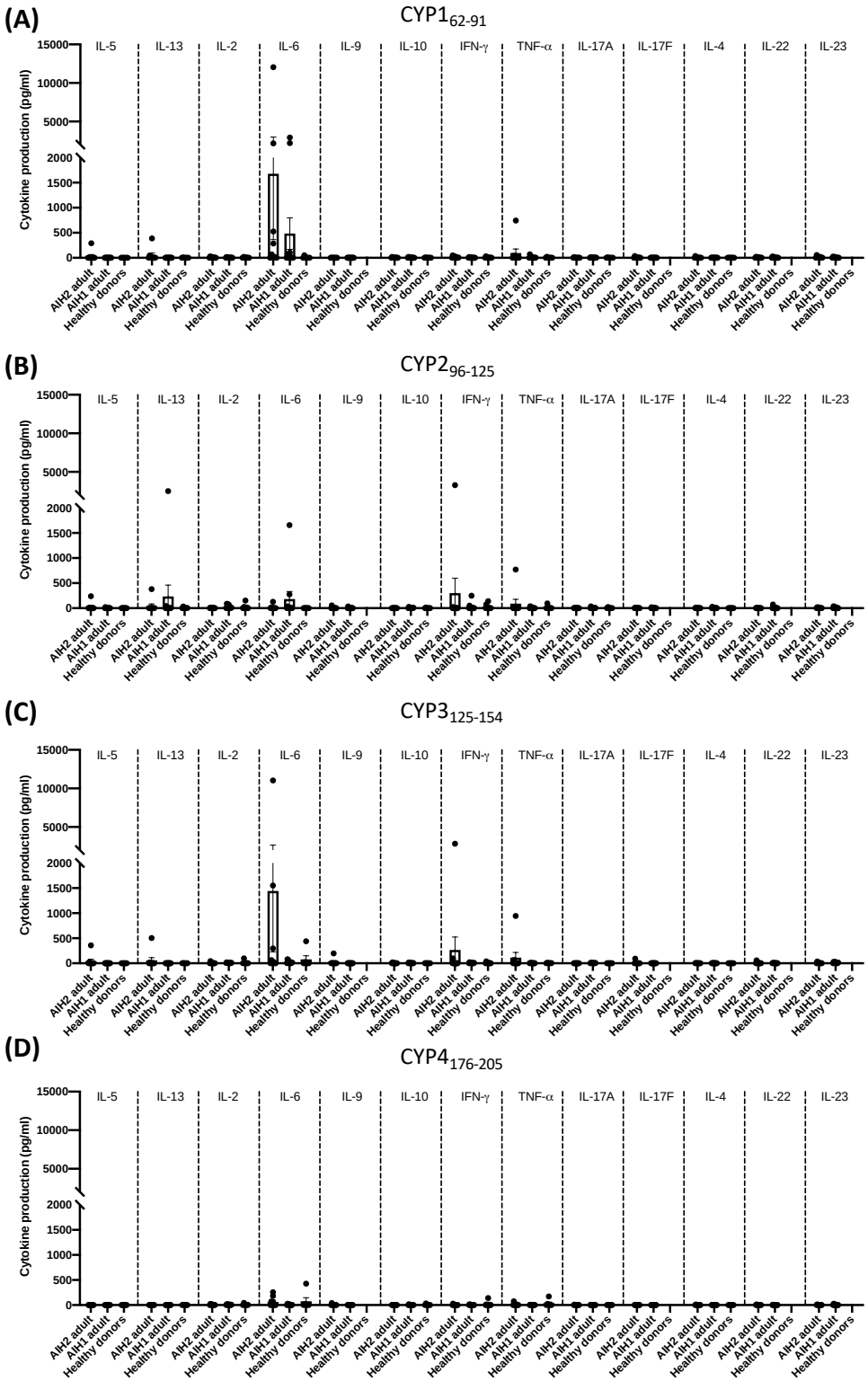

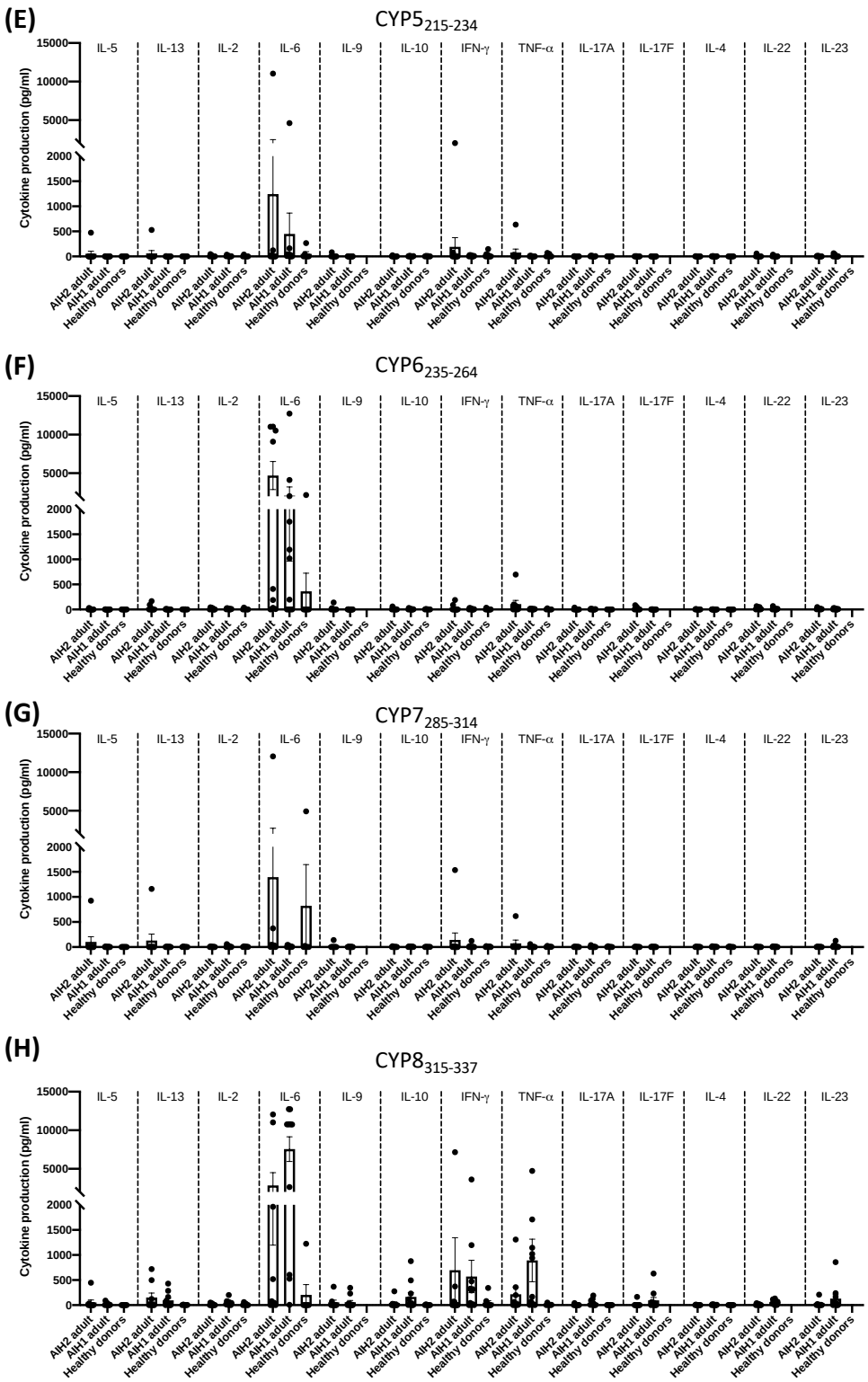
(E)
CYP5215-234
(F)
CYP6235-264
(G)
CYP7285-314
(H)
CYP8315-337
Cytokine production (pg/ml)
15000
10000
5000
2000
1500
1000
500
0
IL-5
IL-13
IL-2
IL-6
IL-9
IL-10
IFN-γ
TNF-α
IL-17A
IL-17F
IL-4
IL-22
IL-23
AIH2 adult
AIH1 adult
Healthy donors

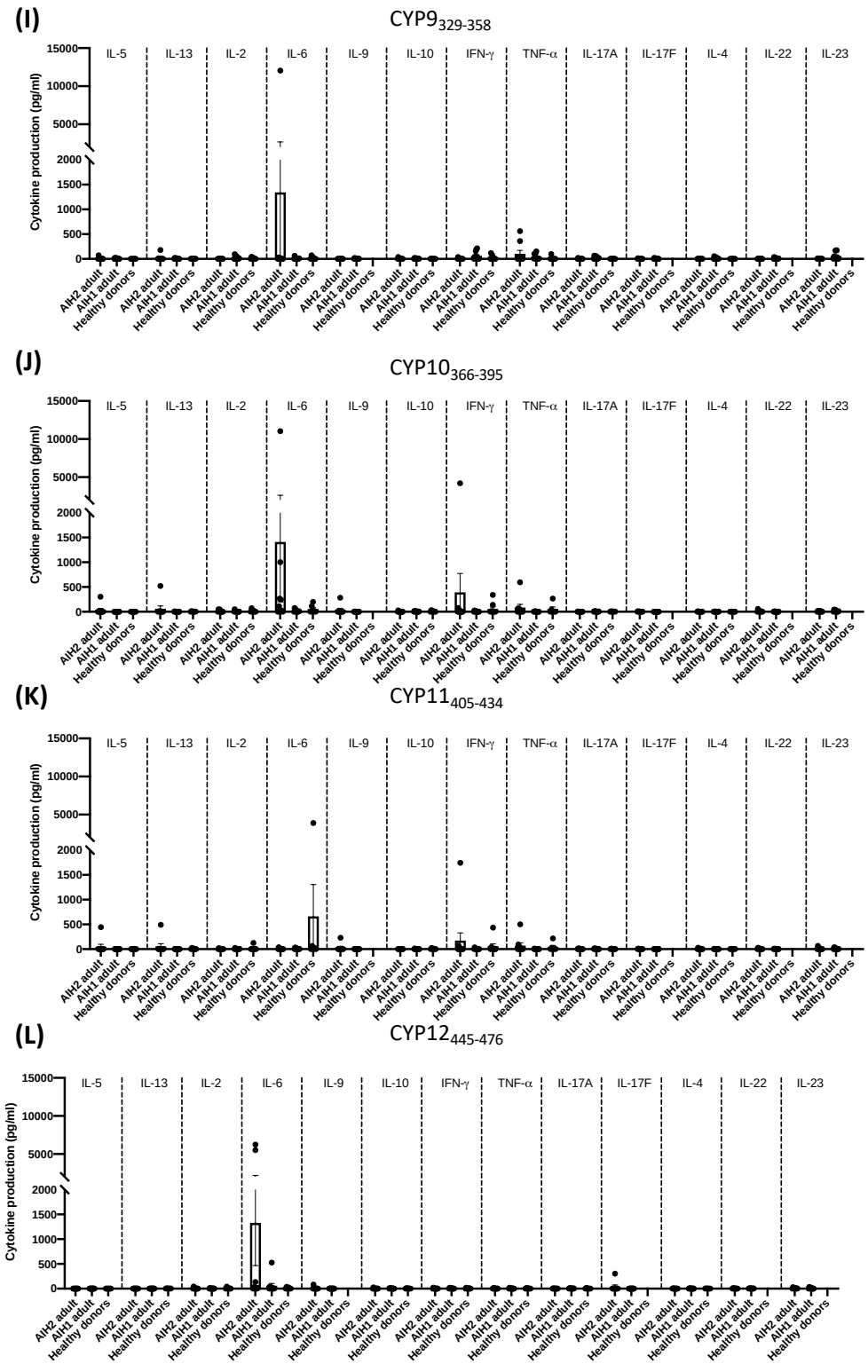
(I)
CYP9329-358
(J)
CYP10366-395
(K)
CYP11405-434
(L)
CYP12445-476
Cytokine production (pg/ml)
15000
10000
5000
2000
1500
1000
500
0
IL-5
IL-13
IL-2
IL-6
IL-9
IL-10
IFN-γ
TNF-α
IL-17A
IL-17F
IL-4
IL-22
IL-23
AIH2 adult
AIH1 adult
Healthy donors

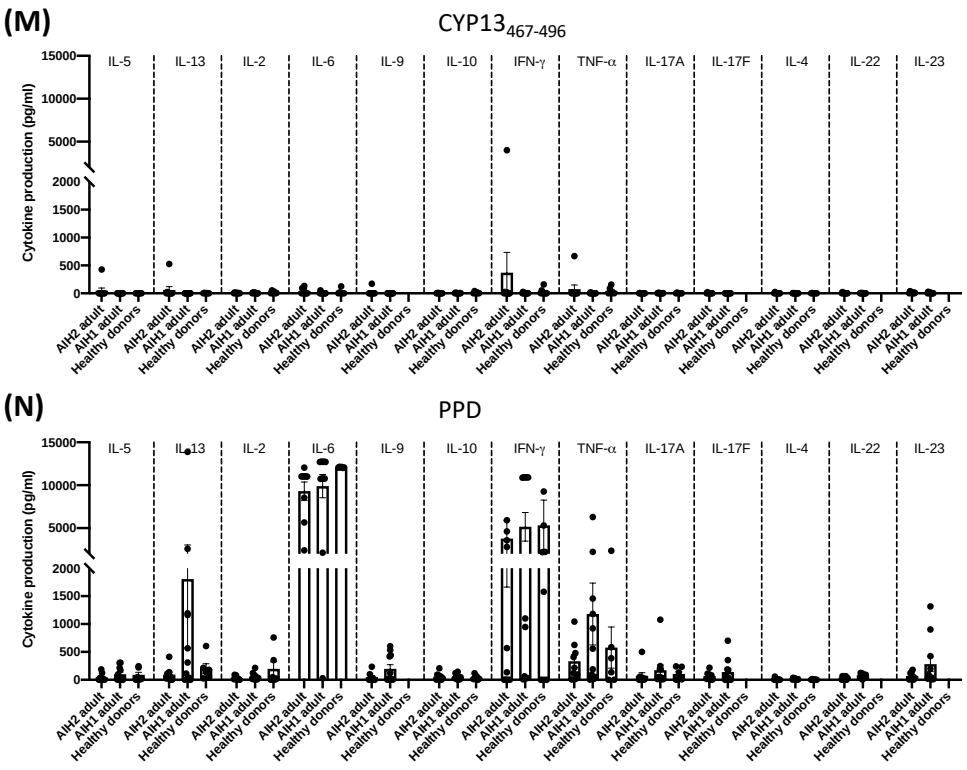

Figure 4.17: AIH patient groups and healthy donors cytokine production in response to CYP2D6 peptide stimulation. Cytokine production in cell culture supernatant was measured after 8 days of CYP2D6 peptide stimulation using the LEGENDPLEX Th (13-plex) assay. **A-N)** display cytokine concentration in pg/ml for each individual tested for each cytokine.

As each cytokine has a very different range of expression, to better compare the amount of key cytokines produced in response to CYP2D6 peptides, Figure 4.18 shows IL-6, IFN-γ, TNF-α, IL-10, and IL-4 data adjusted to their own scale.

IL-6 was produced by AIH2 and AIH1 patient PBMC when stimulated with a number of CYP2D6 peptides, in particular $CYP6_{235-264}$ and $CYP8_{315-337}$ (Fig.4.18A). In healthy donors, IL-6 was produced at a low level for all CYP2D6 peptides. When PBMC were stimulated with $CYP1_{62-91}$ and $CYP6_{235-264}$, AIH2 patients produced significantly more IL-6 than healthy donors. This trend matches the higher proliferation in AIH2 patients for these peptides. Similarly, when considering AIH1 patients, $CYP8_{315-337}$ stimulated the strongest proliferation and also produced significantly more IL-6 than healthy donors. The production of high concentration IL-6 was peptide-specific, as only certain peptides stimulated this response, appearing to correspond with proliferation. IL-6 was also produced in a group-specific manner, as high IL-6 production in the healthy donor group was not observed in response to CYP2D6 peptides. Overall, IL-6 was produced by 176/338 (52.1.%) individual/CYP2D6 peptide culture combinations, with mean average of 176 detectable values = 1647.83pg/ml. As we cannot determine via this bulk assay which cells are producing IL-6, and why they do so in response to specific peptides, a flow cytometry-based panel would best assess this in future.

In our hands, we observed that IL-4 was detectable in 79/338 (23.4%) individual/CYP2D6 peptide culture combinations. However, IL-4 production was very low across CYP2D6 peptide stimulated conditions, with mean average of 79 detectable values = 8.071 pg/ml.

Similarly, IL-10 production reached detection threshold in 124/338 (33.69%) individual/CYP2D6 peptide stimulated combinations, with mean average of 124 detectable values = 23.97pg/ml.

IL-17A was detected at low levels, 106/338 (31.36%) individual/CYP2D6 peptide culture combinations, with mean average of 106 detectable values = 14.5pg/ml.

We observed IFN-γ production in 142/338 (42.0%) individual/CYP2D6 peptide culture combinations; therefore, cytokine response to CYP2D6 peptides were overall more likely to result in IFN-γ production rather than IL-4 or IL-10. The average amount of IFN-γ was also significantly higher with the mean average of 142 detectable values = 136.57pg/ml. Surprisingly, IFN-γ was not detected to a particularly high level for many CYP2D6 peptides. $CYP8_{315-337}$ stimulated the strongest IFN-γ responses in both AIH1 and AIH2 patients (697.4pg/ml and 473.9pg/ml). TNF-α production shows a similar trend, with $CYP8_{315-337}$ stimulating the highest levels of TNF-α secretion, particularly for the AIH1 patient group 891.4pg/ml).

Figure 4.18: Key cytokines produced in response to CYP2D6 peptide stimulation

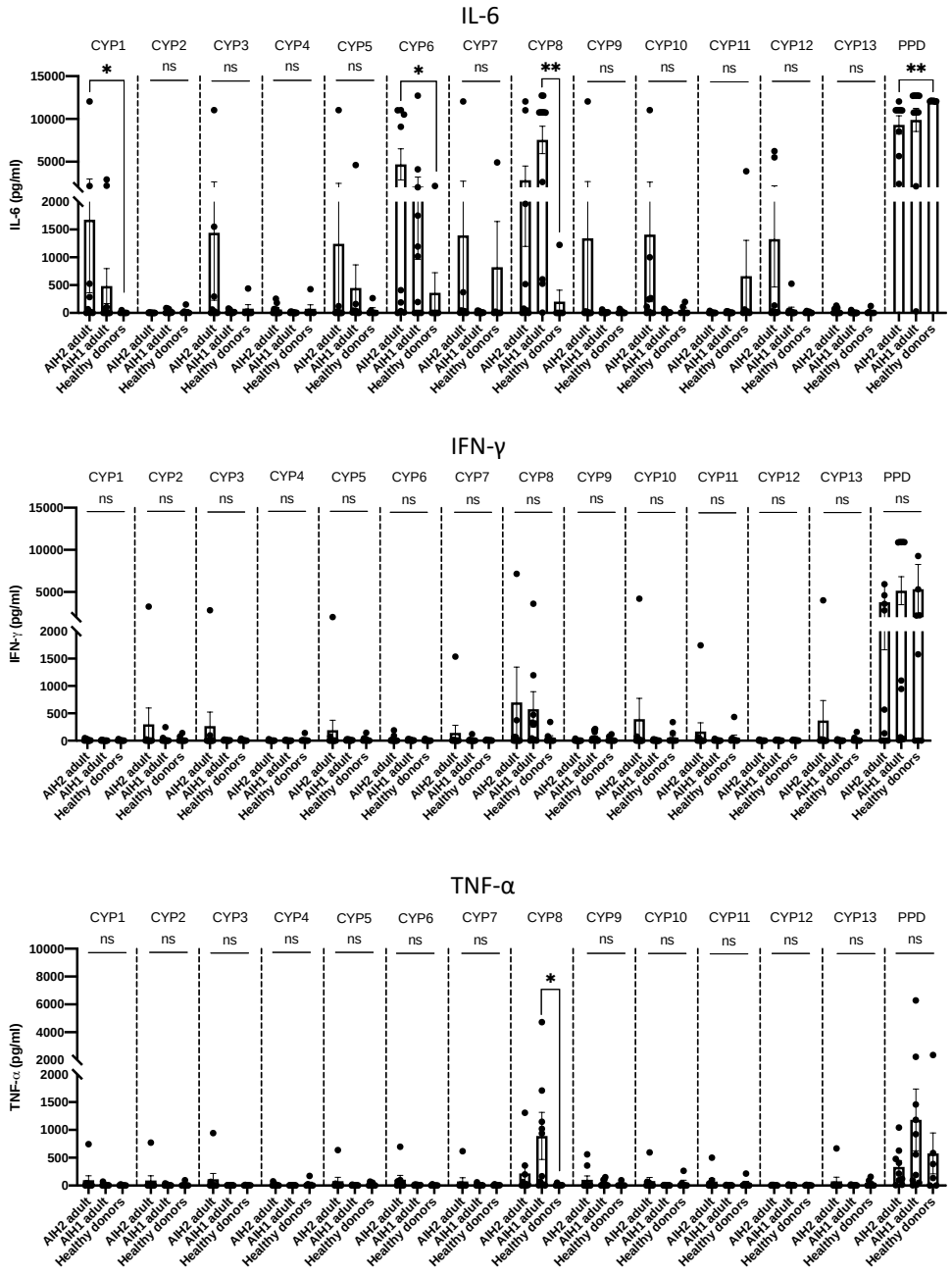

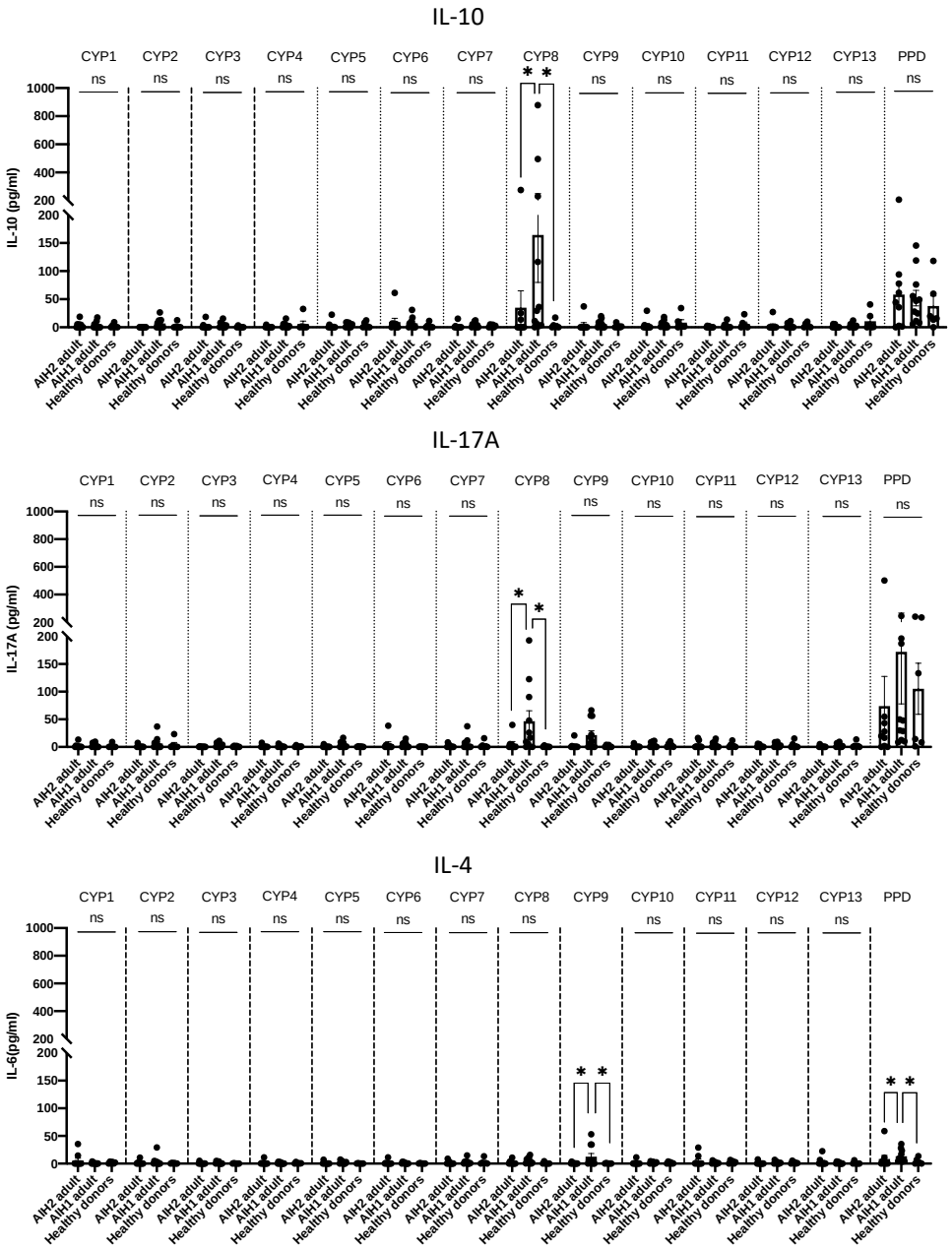

Figure 4.18: AIH patient groups and healthy donors key cytokine produced in response to CYP2D6 peptide stimulation. Cytokine production in cell culture supernatant was measured after 8 days of CYP2D6 peptide stimulation using the LEGENDPLEX Th (13-plex) assay. **A-N)** display cytokine concentration in pg/ml for each individual tested for each cytokine.

4.8.2 Correlation between cellular proliferation and IL-6 production

Using non-parametric Spearman correlation between SI and IL-6 concentration values of all tested individuals shows that there is a highly significant correlation ($p>0.0001$, ****) between proliferation and IL-6 (Fig.4.19A). Combinations of inflammatory cytokines IL-6 and IFN-γ are also significantly correlated, as are IL-6 and TNF-α, and IFN-γ and TNF-α production (Fig.4.19B, C, D).

4.8.3 IL-6 production can be stratified into high and low, corresponding with proliferation responders and non-responders

CYP2D6 peptides stimulating the highest amount of IL-6 were $CYP6_{235-264}$ and $CYP8_{315-337}$, in AIH2 and AIH1 patients respectively. Adult AIH2 adults could be grouped into IL-6 producers or non-producers (Fig.4.20A). To test whether IL-6 production paired with individuals with high proliferation, all AIH patients and healthy donors were split into proliferation "responders" (SI> 3) vs "non-responders" (SI< 3), i.e. SI> 3. AIH2 and AIH1 patients in the proliferation "responders" group showed significantly higher IL-6 production compared to the "non-responders" group of the same patient cohort.

Similarly, when considering IL-6 responses to $CYP8_{315-337}$, both AIH2 and AIH1 patient groups included individuals with very high IL-6 production, reaching the upper limit of detection of the LEGENDPLEX assay (Fig.4.20B). The remainder of patients, and healthy donors were low or non-producers of IL-6. To assess whether these groups associated with proliferation, AIH patient and healthy donor groups were split into proliferation "responders" vs "non-responders", as previously. Again, the proliferation "responders" produced significantly more IL-6 when compared with "non-responders".

Figure 4.19: Correlation between proliferation and key cytokines produced in response to CYP2D6 peptides

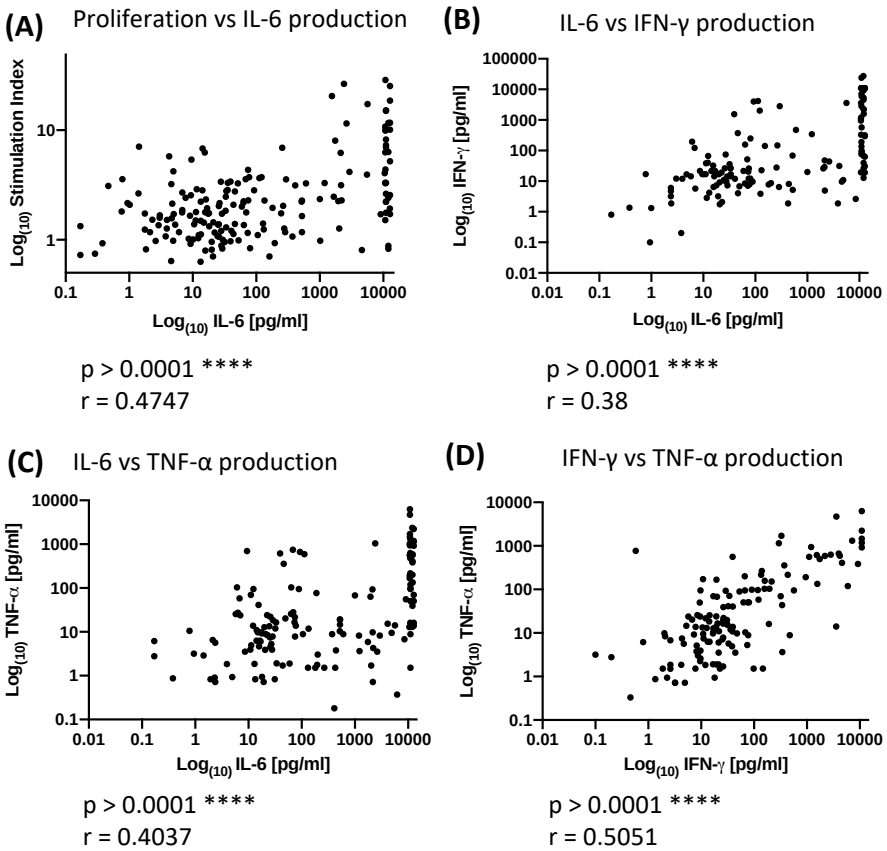

Figure 4.19: Spearman's correlation between Stimulation Index and IL-6 production and IL-6/IFN-γ/TNF-α. Cytokine production in cell culture supernatant was measured after 8 days of peptide stimulation using the LEGENDPLEX Th (13-plex) assay, as described previously. **A)** Proliferation data for each individual from Fig. 4.6 & 4.15 was correlated to concentration of IL-6 in culture supernatant. **B, C, D)** Concentration of IL-6, IFN-γ and TNF-α in culture supernatant were correlated to one another. Statistical analysis performed using non-parametric Spearman correlation.

Figure 4.20: AIH patients can be stratified into "responders" and "non-responders" by proliferative response, reflecting production of IL-6 in response to $CYP6_{235-264}$ and $CYP8_{315-337}$

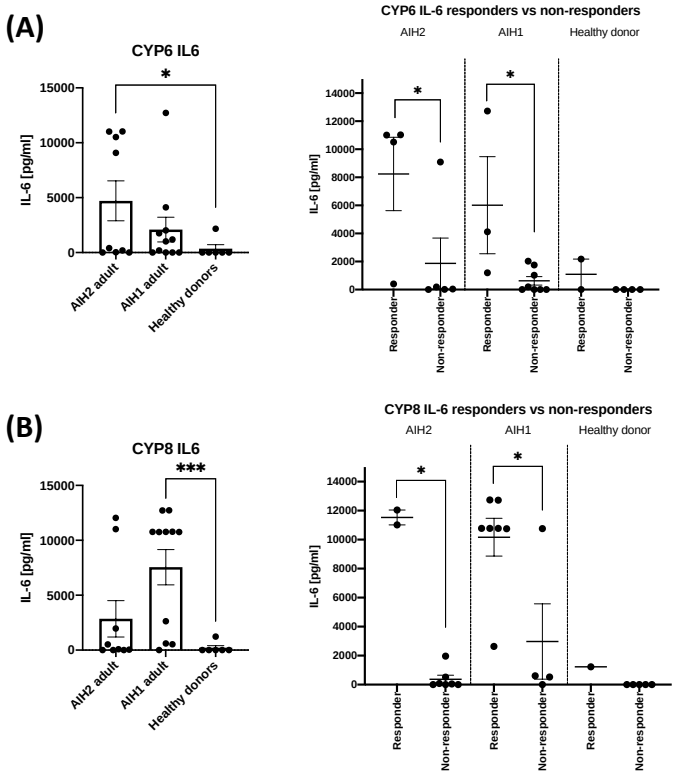

Figure 4.20: AIH patient groups and healthy donor proliferation pairs with amount of IL-6 produced in response to (A) $CYP6_{235-264}$ and (B) $CYP8_{315-337}$. IL-6 production in cell culture supernatant was measured after 8 days of peptide stimulation using the LEGENDPLEX Th (13-plex) assay, as described previously. Patient and healthy donor groups have been split into "responders" (SI > 3) vs "non-responders" (SI < 3), corresponding to proliferation data in Fig. 4.6 & 4.15. Statistical analysis performed using Mann-Whitney test.

4.9 Discussion

The data presented within this Chapter provides strong evidence for the presence of multiple T cell epitope containing regions within the autoantigen CYP2D6. The 13 30mer peptides derived from CYP2D6 represented 72% of the whole protein sequence and were selected based on the consensus between three computational MHC-II binding algorithms to avoid missing any relevant potential binders. Of these candidate peptides, proliferative responses in healthy donors were relatively high in comparison to similar assessments made for other autoantigens (PDCE-2, pro-insulin, GAD), but markedly less strong in comparison to allergic antigen Derp1 tested in the same way (Wraith group, unpublished). Only 1 peptide had a response rate of less than 5% in healthy donors. The remaining 12 peptides generated responses in at least 10% of donors tested, and 8/12 had a response rate of over 20%. These analyses in healthy donors allowed us to collate a diverse group of individuals with differing HLA-DR alleles, to analyse whether specific HLA-DR correlate to increased peptide antigenicity. As studies of AIH2 patients have so far shown an increased frequency of HLA-DR7$^+$ and HLA-DR3$^+$ associated with disease (Ma et al., 2006; Donaldson, 1991; Czaja et al., 1993; Montano-Loza et al., 2006), we would potentially have expected healthy donors carrying these alleles to have increased proliferative responses to CYP2D6 peptides. Instead, we found healthy donor PBMC carrying HLA-DR7$^+$ and HLA-DR3$^+$ to be overall less likely to proliferate in response to CYP2D6 peptides.

The main aim of Chapter 4 was to assess the antigenicity of CYP2D6 peptides in our AIH2 patient groups (paediatric and adult) and compare this to AIH1 patients who are largely treated with the same immunosuppressive drug regimen but lack autoantibodies

to CYP2D6. Unfortunately, we were not able to analyse the peptide response data in relation to clinical data points (Appendix 5 and 6), as we received this information just prior to thesis submission. It was not possible able to trace the patients current disease activity in the clinical data. Ideally, I would have used the clinical data of disease severity, activity and duration to map out peptide responses. Upon receiving this clinical data, it became clear that the paediatric AIH-2 cohort were not so different from the adult AIH-2 cohort with similar sex distributions, pharmacological treatment and mean patient duration of disease (paed 7y 3mo vs adult 6y 1 mo). However, the most notable difference between the AIH2 cohorts was age at diagnosis with paediatric patients diagnosed at mean age of 7y 2mo and adult cohort diagnosed at a mean age of 25y 8mo. On reflection, it may have been more appropriate to view all AIH-2 patients as one continuous cohort despite their different care providers.

We found that each group of AIH patient PBMCs responded to slightly different candidate 30mer peptides. All AIH groups and healthy donors responded strongly to $CYP1_{62\text{-}91}$. The AIH2 paediatric group responded most strongly to stimulation with $CYP12_{445\text{-}474}$ peptide, which was not observed as a front-runner in the other AIH groups or healthy donors. For this reason, we hypothesised that T cell epitope(s) contained within $CYP12_{445\text{-}474}$ may represent an avenue for specific biomarker(s) for children diagnosed with AIH2. The AIH2 adult group responded most strongly to stimulation with $CYP1_{62\text{-}91}$ and $CYP6_{235\text{-}264}$ peptides. Overall, children diagnosed with AIH2 experience more severe disease and worse transplant-free survival prognoses despite medical intervention. It is possible that despite sharing autoantibodies towards CYP2D6, children and adults diagnosed with AIH2 may have differing pathology or drivers of disease, which could include T cell activity. This data may represent an avenue to better understand the

potential immunological differences between paediatric and adult AIH2 patients. To further assess this, we would have required HLA-DR typing from each of the paediatric and adult patients in our study. Unfortunately, this was outside the remit of this thesis, as ethical approval was not in place for storage of genetic information of paediatric patients in particular. We would have liked to assess the HLA-DR alleles within our cohort and if we had access to more AIH2 patients, this would have allowed for correlations to be made between HLA-DR and age-at-onset, disease severity and immunological responses.

The proliferation response data expands upon a study published previously by Ma et al. of King's College London (Ma et al., 2006). They found reactive regions of CYP2D6 using overlapping 15mers in AIH2 paediatric PBMCs, separated into HLA-DR7 or non-HLA-DR7 groups. HLA-DR7+ patients responded strongly to peptides ranging from: aa73-124 (corresponding to our $CYP1_{62\text{-}91}$ and $CYP2_{96\text{-}125}$), aa177-260 (corresponding to our $CYP4_{176\text{-}205}$ $CYP5_{215\text{-}144}$ and $CYP6_{235\text{-}264}$), aa305-358 (corresponding to our $CYP8_{315\text{-}337}$ and $CYP9_{329\text{-}358}$) and aa377-436 (corresponding to our $CYP10_{366\text{-}395}$ and $CYP11_{405\text{-}434}$). Their non-HLA-DR7+ AIH2 patients responded to the latter two regions only, suggesting that HLA-DR7 patients recognised a more diverse CYP2D6 peptide repertoire, corresponding to disease severity. In our hands, we observed proliferative responses to $CYP1_{62\text{-}91}$ but not $CYP2_{96\text{-}125}$, highlighting that 15mer peptides can give false positive readouts if peptides are able to bind with sufficient affinity to MHC-II without the physiological process of antigen processing and presentation. $CYP12_{445\text{-}474}$ reactive PBMCs were not observed in either Ma's study or our adult AIH2 cohort. Largely, our data corroborates Ma's dataset, as the majority of regions they determined have also been highlighted in our study.

Our study also identified $CYP8_{315-337}$ as a potential reactive region of CYP2D6 in AIH1 patients. This would be very interesting to follow up in a more directed investigation into the frequency and function of $CYP8_{315-337}$ reactive cells in AIH1. As the autoantigen landscape of AIH1 is diverse and highly variable between individuals, the potential finding of a CYP2D6 T cell epitope within CYP8 which generated proliferative and cytokine responses in 64% of AIH1 patients could be a useful discovery. This data is in its infancy, but may lead to the possibility of stratification of AIH1 patients based on the presence of $CYP8_{315-337}$ reactive T cells – of which these cells could then be targeted with antigen-specific immunotherapy to re-establish tolerance to this epitope. Recent studies in mice have shown that targeting antigens to the liver can be a powerful means to induce both intra-hepatic and extra-hepatic tolerance. Umeshappa et al., targeted mouse CYP2D22 (closest related murine protein to CYP2D6) using MHC-II carrying nanoparticles and successfully induced antigen-specific tolerance to CYP2D22, which also extended tolerance to PBC-related antigen PDCE-2 by as of yet undefined bystander effects (Umeshappa et al., 2019, 2020). Whether this strong a bystander suppressive effect would work in humanised mice expressing hPDCE-2 and/or hCYP2D6 is yet to be assessed but would provide further evidence that targeting the liver can establish organ-specific tolerance which does not necessarily have to be antigen-specific for distinct immunological or treatment benefit.

To have developed this work further, we could have used flow cytometry-based activation assays to confirm that certain peptides were generating either CD4 or CD8 specific T cell responses. If we reached the point of identifying defined T cell epitopes for each candidate peptide of interest, we could have used a CLIP exchange assay developed within our group based on similar MHC-II CLIP exchange protocols (Newell et al., 2013).

HLA-DR molecules containing the class II invariant chain-associated peptide (CLIP) can be used to test for antigen processing independent presentation. Biotinylated HLA-DR-CLIP monomers attached to neutravidin coated 96 well plates can be incubated with our CYP2D6 peptides and assessed for the peptide ability to displace CLIP using our T-cell hybridomas. Peptide-loaded tetramers could then be utilised for direct identification of CYP2D6-specific T cells (Nepom, 2012; Scally et al., 2013; Uchtenhagen et al., 2016). CLIP-loaded tetramers are commercially available for HLA-DR0301, HLA-DR0401, HLA-DR0701 (NIH Tetramer Core), which would largely cover the HLA-DR requirements for an AIH1 and AIH2 patient cohort. We hypothesise that CYP2D6-specific T cells would be present in PBMC but enriched in liver infiltrating and liver resident lymphocyte subsets where they are able to encounter their cognate antigen.

In this Chapter, we identified that in adult patient PBMC stimulation assays, generation of a positive proliferative response correlated with secretion of inflammatory Th1 cytokines IFN-γ and TNF-α. Very little IL-10 or other Th2 cytokines were produced in response to CYP2D6 peptides, regardless of patient group, which differs from data presented by Ma et al., in which they measured IL-4 and IL-10 in response to stimulation with specific CYP2D6 peptides (Ma et al., 2006). Most striking was the correlation between proliferation and the pleiotropic cytokine IL-6, which can be secreted by diverse subsets of immune and stromal cells. The IL-6 signature was specific to AIH patients and was rarely observed in the healthy donor cohort. IL-6 is commonly considered to be a strongly inflammatory cytokine; however, it has also been shown to exert a role in tissue repair and regeneration (Scheller et al., 2011). In this assay, secreted or 'trans-signalling'

IL-6 was measured, which has been shown to be crucial to lymphocyte trafficking and the recruitment of neutrophils into inflamed tissue (Chalaris et al., 2007; Rabe et al., 2008), as well as affecting the expression of adhesion molecules on endothelial cells and supporting T cell proliferation during colon cancer (Becker et al., 2004). Crucially, IL-6 can support the recruitment and localisation of Th17 cells, which are increased in autoimmune liver diseases (Oo et al., 2012; Jeffery et al., 2019). We would have liked to investigate this pathway further: firstly, by performing IL-6 staining by flow cytometry so that we could ascertain the cellular source of secreted IL-6 from our PBMC cultures; further, whether blocking IL-6R in these cultures slows or prevents T cell proliferation in response to antigen. α-IL-6 mAb is already in clinical use for the treatment of rheumatoid arthritis and has been discussed as a potential candidate in treatment of other autoimmune diseases, including autoimmune liver diseases (Tanaka and Kishimoto, 2012). Assessing this peptide-specific IL-6 signature further to include liver-infiltrating lymphocytes from AIH patients and manipulation of the IL-6 signalling pathway would be an interesting future project with translational potential.

CHAPTER 5

FINE MAPPING OF T CELL EPITOPES FROM AUTOANTIGEN CYP2D6

5.1 Introduction

Following the identification of a number of regions within autoantigen CYP2D6 which generated strong T cell responses in both healthy donor and AIH patient cohorts, we then trialled and developed methods to facilitate T cell epitope mapping of these 30mer long regions. T cell epitope mapping is required to define the minimal epitope sufficient to both engage with MHC-II in a manner mimicking the naturally processed epitope and to properly engage the TCR required for T cell activation.

We aimed to develop a protocol for generation of CYP2D6-specific T cell clones, or T cell lines from primary cells. In reality, this proved to be challenging, and not reliable enough to use as our principal approach. As an alternative, we utilised the HLA-DR4 and HLA-DR3 transgenic mouse models to generate CYP2D6-specific T cell hybridomas for use in detailed epitope mapping experiments.

Chapter aims:

- Isolate antigen-specific T cell clones by repeated antigen-stimulation *in vitro*.
- Design and optimisation of a flow cytometry-based T cell assays to assess both proliferation and activation induced markers (AIM).
    - Use AIM assay to isolate and clone CYP2D6 peptide-specific T cells.
- Generation of CYP2D6 peptide-specific T cell hybridomas from HLA-DR4 and HLA-DR3 restricted mice.

- Use of T cell lines/T cell clones/T cell hybridomas to screen immunogenic 30mer peptides for T cell minimal epitope.
- Proposed experiments to test whether CYP2D6 peptides are able to induce antigen-specific tolerance, and whether this is sufficient to prevent or ameliorate AIH-2 like liver damage in the Ad-CYP2D6 murine model of disease.

5.2 CD4 T cell line generation by repeated antigen stimulation

Our first approach was to optimise the generation of antigen-specific T cell line(s) by repeated stimulation with antigen. This method had been utilised in the Wraith group previously, showing that repeated stimulation of multiple sclerosis patient PBMC can generate antigen-specific T cell lines towards MBP, which then can be cloned by limiting dilution and PHA expansion (Mazza et al., 2002). This allows for detailed experiments to be undertaken, including TCR sequencing, T cell epitope mapping and adoptive transfer into mice to determine whether these T cells can drive disease. To perform such experiments in the context of T cell responses to CYP2D6 would be a powerful tool, but to avoid using large amounts of the custom-made CYP2D6 protein during optimisation, we decided to first use MBP as a model antigen to optimise the process. We have already determined that healthy donors can have strong responses to CYP2D6 peptides, MBP protein and MBP peptides. Typically, cells require 3 rounds of antigen re-stimulation to select an antigen-specific T cell line. With each round of re-stimulation, non-specific cells should die off and antigen-specific cells should be expanded. After 3 rounds of re-stimulation, the resulting T cell line should be sufficiently antigen-specific to single cell clone by PHA expansion.

Figure 5.1: Representative attempt to generate antigen-specific human T cell lines by repeated antigen stimulation

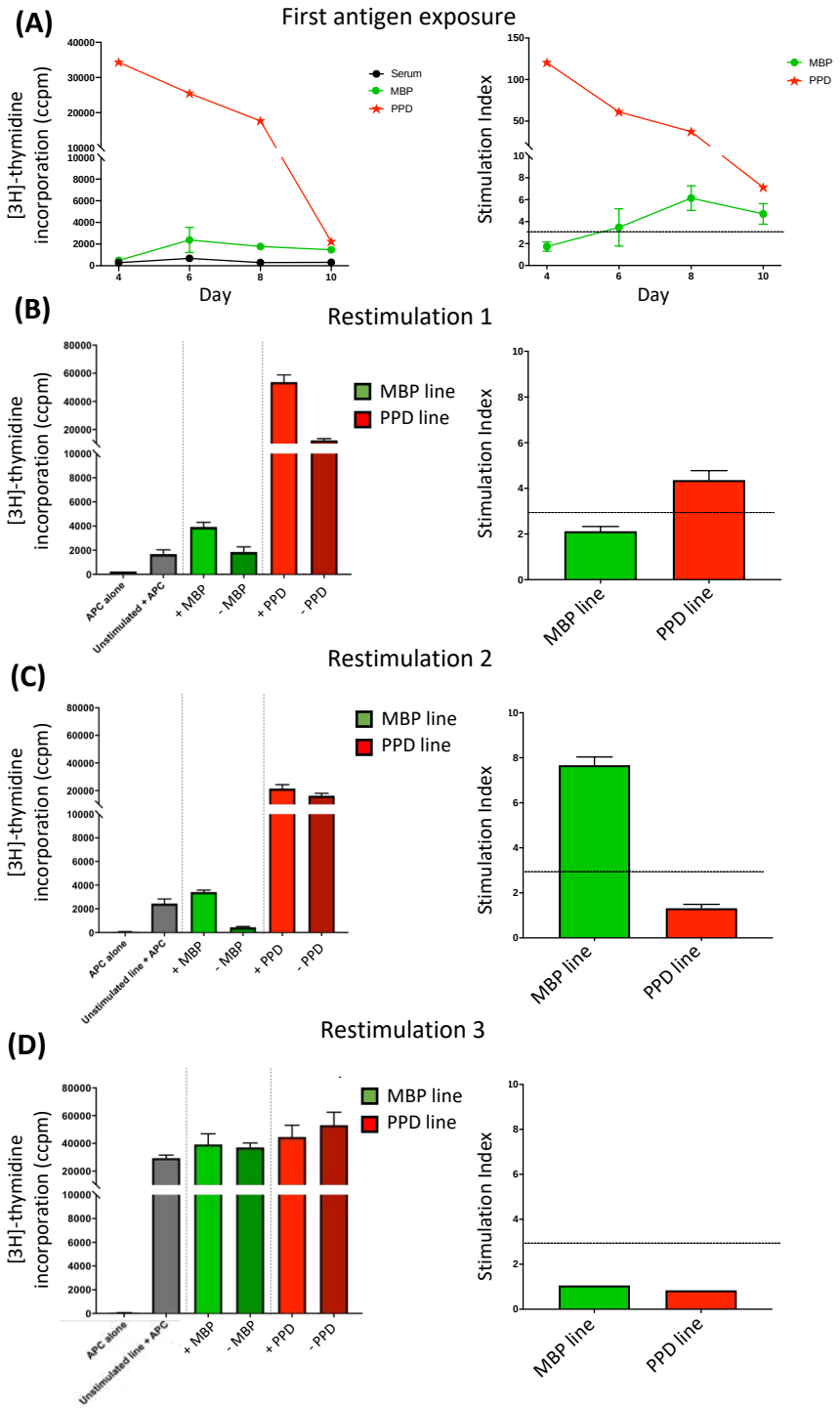

Figure 5.1: Healthy donor PBMC D7 were subjected to repeated antigen stimulation with the aim of achieving an antigen-specific T cell line. (A) PBMCs from a were cultured in triplicate at 1 x 10^6 cells/ml, and were cultured in triplicate at 1 x 10^6 cells/ml, and stimulated with 20 µg/ml of model antigens *Mycobacterium*

tuberculosis purified protein derivative (PPD) and Myelin Basic Protein (MBP). On day 4, 6, 8 and 10, duplicate aliquots of 100µl of cell suspension were incubated for 16-20hours with 0.18MBq/ml [^{3}H]-thymidine. [^{3}H]-thymidine incorporation was measured on a scintillation reader as corrected counts per minute (cpm) then converted to Stimulation Index (SI). **(B)** On day 12 after initial antigen stimulation, cells underwent restimulation 1 i.e. cells were re-stimulated with 20µg/ml antigen, 20U/ml IL-2 and autologous irradiated PBMCs at a ratio of 1 T cell : 5 APC. Every 3-4 days, cultures were supplemented with additional 20U/ml IL-2 and fresh media. On the day of re-stimulation, cells were assessed for proliferation to MBP or PPD. Briefly, $2x10^4$ T cells and $1x10^5$ irradiated autologous PBMC were cultured in triplicate, in 96-well round-bottom plates, in the presence of MBP or PPD. Cells were cultured for 2 days and pulsed with 0.18MBq/ml [^{3}H]-thymidine for the last 16-20 hours of culture. **(C)** Restimulation was repeated after a further 14 days and **D)** 28 days. Donor D7 representative of n=8 healthy donors.

Unfortunately, in our hands, putting the PBMCs through 3 rounds of antigen-restimulation resulted in their loss of antigen-specificity. Myself and our technician attempted repeats of this method for around 8 months with similar end results and were not able to reproduce similar antigen-specific T cell lines. Figure 5.1 summarises the output of a representative donor D7 (n=8) when attempting to isolate antigen-specific T cells. The first encounter with MBP antigen and PPD would result in a strong proliferative response to PPD using [^{3}H]-thymidine incorporation over 10 days of culture (Fig.5.1A), with MBP stimulated cells reaching δcpm>1000 above unstimulated control and an SI>3. On day 12, cells from the 3 lines (unstimulated, grey; MBP stimulated, green; PPD stimulated, red) were re-stimulated with 20µg/ml MBP or PPD in the presence of autologous, irradiated PBMCs to act as APCs and 20U/ml IL-2. 3 days after re-stimulation, proliferation of re-stimulated cells was measured using [^{3}H]-thymidine incorporation. MBP cell line when re-stimulated with MBP (green bars) showed a promising increase in antigen-specificity from re-stimulation 1 to 2 (Fig.5.1B & Fig.5.1C; restim.1 SI = 2, restim.1 SI = 7.8). PPD cell line had an SI of 4 after restimulation 1 but started losing antigen-responsiveness by the second round of restimulation (Fig.5.1B & Fig.5.1C; restim.1 SI = 4.2, restim.1 SI = 1.6). The grey bar showing the unstimulated line from the original timecourse 're-stimulated' with fresh autologous irradiated PBMC alone, indicates that background proliferation was increasing with each re-stimulation (Fig.5.1B - Fig.5.1D). By the third round of restimulation, MBP and PPD cell lines had both lost specificity and the unstimulated line was also proliferating rapidly without the addition of antigen stimulation. Of the 8 donors trialled with this method, all were unable to mount significantly specific antigen-specific T cell populations to allow for T cell cloning. Having tried numerous variations on the method during this period including optimising the ratio

of T cells:irradiated APC, amount of antigen and IL-2 used in re-stimulation, we were unable to overcome the issue of increasing background proliferation over time. The only variable we had not been able to replicate from the multiple sclerosis paper from Mazza et al. was the use of autologous plasma in culture conditions, as we were obtaining the healthy donor PBMCs from leukocyte cones due to their very dense cellularity. The leukocyte cones do not include a plasma fraction thus we had to use human AB serum in the T cell line cultures. It is possible that over 6-8 weeks in culture, cells started to respond to proteins within the human AB serum, reducing the specificity of the pool to MBP/PPD.

5.3 Activation-induced marker flow cytometry-based assay to identify antigen-specific CD4 T cells

5.3.1 Basic panels CD69 and CD40L or CD25 and OX-40

Based on previously published flow assays monitoring antigen-induced cell proliferation using cell proliferation dyes and activation-induced surface markers to identify antigen-specific cells, we developed a flow cytometry antibody panel including key markers: CD4, CD25, CD69, CD40L and OX-40 (Mannering et al., 2005; Bacher and Scheffold, 2013; Reiss et al., 2017). Initially, we tested the selectivity of the activation induced markers, monitoring either co-expression of CD69 and CD40L or CD25 and OX-40 by $CD4^+$ cells in response to antigen stimulation (Fig.5.2). Briefly, healthy donor $CD4^+$ cells (n=3) were plated in triplicate at $1x10^6$ cells/ml with autologous irradiated PBMC at $2x10^6$ cells/ml. To optimize the assay, 4 conditions were used: unstimulated, 20µg/ml Keyhole limpet hemocyanin (KLH), 20µg/ml PPD, or SEB (1µg/ml). CD69/CD40L expression was measured

at 9 hours, 18 hours and 4 days post-stimulation with CD40 blocking antibody added to cells prior to cell stimulation. CD25/OX40 expression was measured at 18 hours, 4 days, 6 days and 8 days post-stimulation. Figure 5.2A shows a representative donor B49 (1 of 3) gating strategy for single live $CD4^+$ cells, excluding dead cells, debris and $CD14^+$ and $CD16^+$ cells selected out in the APC-Cy7 dump channel (Fig.5.2A). Fluorescence minus one (FMO) for CD25/OX40/CD69/CD40L conditions were used to set gates. Fig.5.2B shows $CD69^+/CD40L^+$ expression of unstimulated cells and SEB stimulated cells 18 hours post-stimulation. $CD69^+/CD40L^+$ expression of each condition at each timepoint is displayed in Fig.5.2C, and indicates that only very strong stimulation generates significant numbers of $CD69^+/CD40L^+$ cells. SEB stimulation unsurprisingly induces a very rapid response, with expression of CD69 upregulated to a higher extent than CD40L. Over the 4-day timecourse, CD40L expression dropped off markedly, while CD69 remained high. The weaker antigens PPD and KLH were not able to generate significant populations of $CD69^+/CD40L^+$ cells after 9 hours of stimulation. By 18 hours, both unstimulated cells and antigen stimulated cells had a small percentage of $CD4^+$ cells expressing both CD69 and CD40L, indicating that there was no effect of antigen stimulation on expression of these marker in combination. This panel is not ideal for weaker antigens or time points over 24h and expression of CD40L over time is not cumulative; therefore, to maintain high expression of CD40L at the cell surface, you may require continued addition of CD40 blocking antibody. However, CD69 expression was clearly upregulated by PPD and KLH stimulation, so in future AIM assays we chose to monitor CD69 without CD40L, in combination with other AIM markers.

In contrast, CD25 and OX40 were both consistently upregulated on stimulated $CD4^+$ cells. Figure 5.2D and 5.2E display the co-expression of $CD25^+/OX40^+$ by donor B49

Figure 5.2: AIM assay CD25/OX40 and CD69/CD40L separate panels

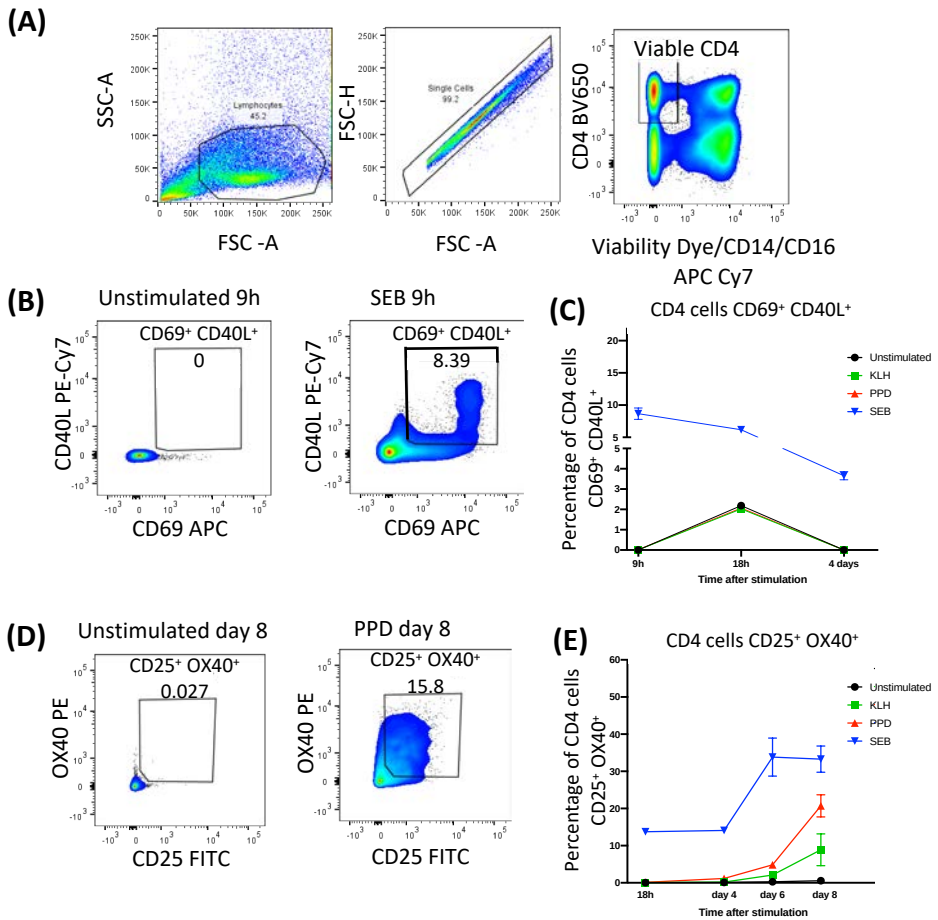

Figure 5.2: Activation Induced Marker gating strategy for CD69/CD40L panel and CD25/OX40 panel. Representative AIM assay of healthy donor B49 measuring CD69/CD40L and CD25/OX40 expression of $CD4^+$ cells during timecourse. $CD4^+$ cells plated in triplicate at $1x10^6$ cells/ml with autologous irradiated PBMC at $2x10^6$ cells/ml were stimulated with 20µg/ml Keyhole limpet hemocyanin (KLH), 20µg/ml PPD or 1µg/ml Staphylococcal Enterotoxin B (SEB). CD69/CD40L expression was measured at 9 hours, 18 hours and 4 days post-stimulation. CD25/OX40 expression was measured at 18hours, 4 days, 6 days and 8 days post-stimulation. **(A)** Basic gating strategy of Lymphocytes → Single cells → Live $CD4^+$. **(B)** Identification of activated CD4 by $CD69^+$ $CD40L^+$ co-expression. Unstimulated cells (left) vs SEB stimulated cells (right). **(C)** Percentage of CD4 cells that are $CD69^+$ $CD40L^+$ at 4 hours, 18 hours and 4 days post-stimulation. **(D)** Identification of activated CD4 by $CD25^+$ $OX40^+$ co-expression. **(E)** Percentage of CD4 cells that are $CD25^+$ $OX40^+$ at 18hours, 4 days, 6 days and 8 days post-stimulation.

PBMC over 8 days. $CD25^+/OX40^+$ were not increased in unstimulated cells over the 8-day period, yet were markedly upregulated on stimulated $CD4^+$ cells in an antigen strength-dependent manner.

5.3.2 Combined AIM marker panel CD69, CD25, OX40, PD-1 and CD71 with proliferation by Cell Trace Violet

To further investigate whether expression of CD69, CD25, OX40 and added activation marker CD71 correlates with antigen-specific cell activation, the subsequent assays also used proliferation dye Cell Trace Violet (CTV). Cells stained with CTV prior to stimulation have a maximal intensity and occupy one single population. As the cells divide in culture, CTV is divided and therefore diluted between generations that are detected as distinct peaks in the CTV^{low} population. Addition of CTV also allows for the correlation of activation markers with divided cells. It is important to note that in strongly stimulated cell cultures, there will be some bystander activation of non-specific T cells due to high secretion of IL-2 and IFN-γ. However, cells that have gone through proliferation cycles are more likely to have encountered cognate antigen and reached the higher threshold of T cell activation. Therefore, assessing CTV^{low} cells should enable some bystander activation AIM expression to be discounted where appropriate.

Figure 5.3A shows flow cytometry plots depicting a representative donor B32 AIM marker expression and CTV traces 8 days after stimulation. Analysis of $CD25^+/CD69^+$, $CD25^+/OX40^+$ and $CD25^+/CD71^+$ expression shows the effect of stimulation on these activation induced markers on day 4, 6 and 8 post-stimulation. Summarising AIM expression for this donor (Fig.5.3B), all AIM^+ combinations increased in frequency over

the timecourse, whereas unstimulated cell AIM expression remained low. AIM expression correlated with stimulation strength: SEB>PPD>CYP1$_{62-91}$. The proportion of cells expressing CD25$^+$/CD69$^+$ and CD25$^+$/OX40$^+$ were comparable for each antigen, whereas CD25$^+$/CD71$^+$ expression was low on day 4 and 6, increasing rapidly by day 8 of cell culture. By day 8 post-stimulation with PPD, for example, 14.5% of CD4$^+$ cells were CD25$^+$/CD69$^+$, 13.7% were CD25$^+$/OX40$^+$ and 43.3% CD25$^+$/CD71$^+$. Fig.5.3C shows cell proliferation by our traditional method of [^{3}H]-thymidine incorporation in comparison to CTV^{low} CD4$^+$ cells. Whereas [^{3}H]-thymidine incorporation as Stimulation Index peaks at day 4 for both SEB and PPD stimulation, the proportion of CTV^{low} CD4$^+$ cells accumulates throughout the timecourse. By both approaches, proliferation correlated with stimulation strength: SEB>PPD>CYP1$_{62-91}$.

To assess which activation induced marker best correlates with proliferating cells (CTV^{low}), AIM expression of CTV^{low} cells was assessed at day 4, 6 and 8 for each marker (Fig.5.3D). To account for different antigens providing different strength stimulation to a variable proportion of the CD4 cell population, AIM expression of CTV^{low} populations in all stimulation conditions (unstimulated, CYP1$_{62-91}$, PPD and SEB) from 2 donors were collated. At the earliest timepoint of day 4 post-stimulation, CD69 was most associated with proliferating cells, with a mean average of 54.8% of CD4$^+$CTV^{low} cells being CD69$^+$. CD69 remained high on day 6 (56.5%), but had started to decline by day 8 after stimulation (34.9%). CD69 is likely to be the best AIM marker to use at very early timepoints, as it is rapidly upregulated after TCR engagement (Fig.5.3D) (Testi et al., 1989; Simms and Ellis, 1996). However, we set up the AIM experiments with the intention of FACS sorting AIM$^+$ CTV^{low} cells to clone antigen-specific CD4 T cells. Therefore, as the CTV^{low} population increases with a longer time in culture, we planned to perform the

Figure 5.3: Correlating AIM assay marker expression with CTV in a single staining panel

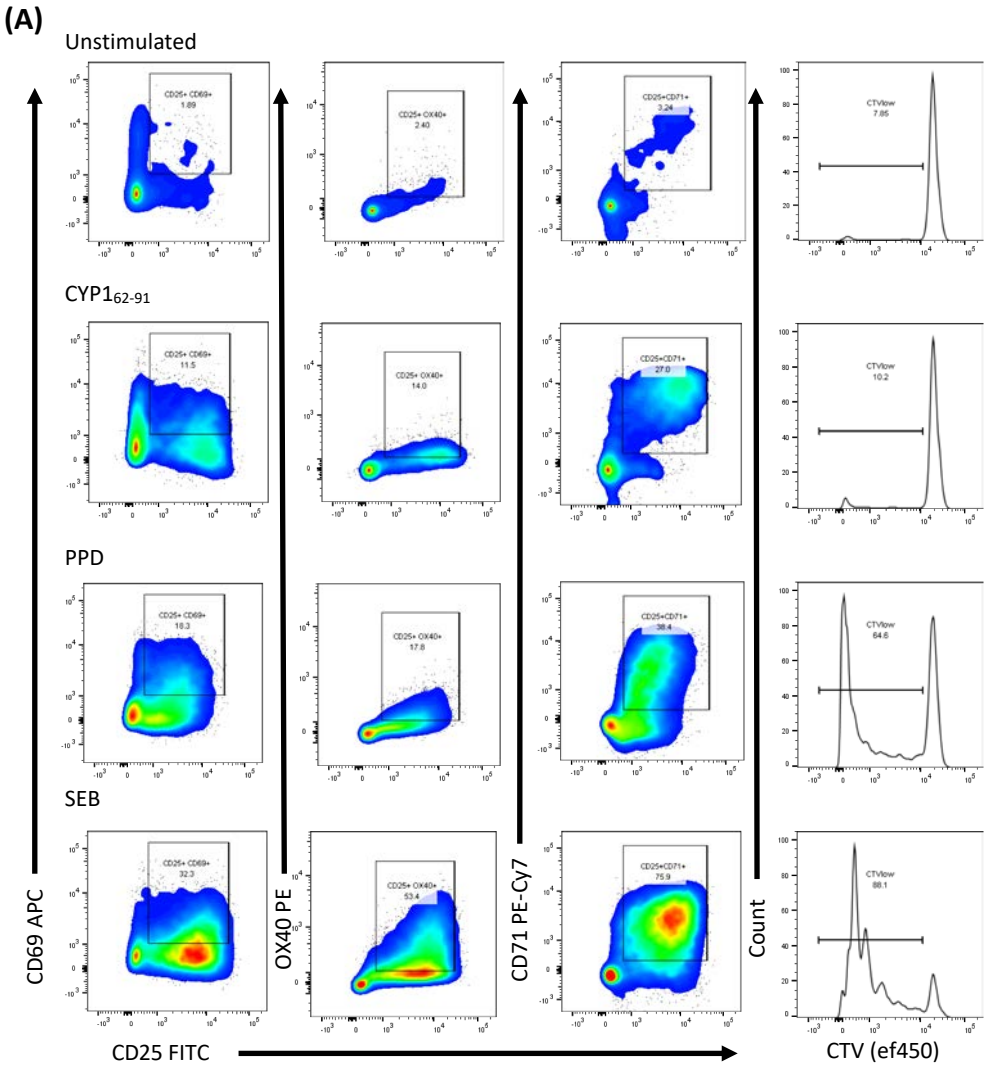

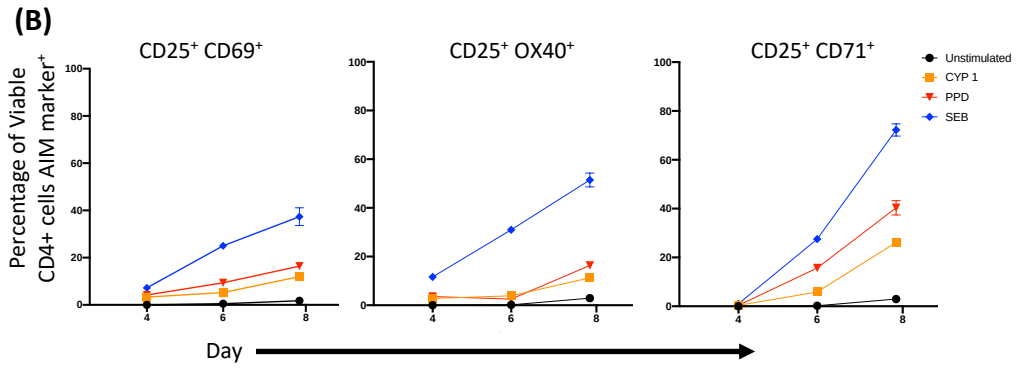

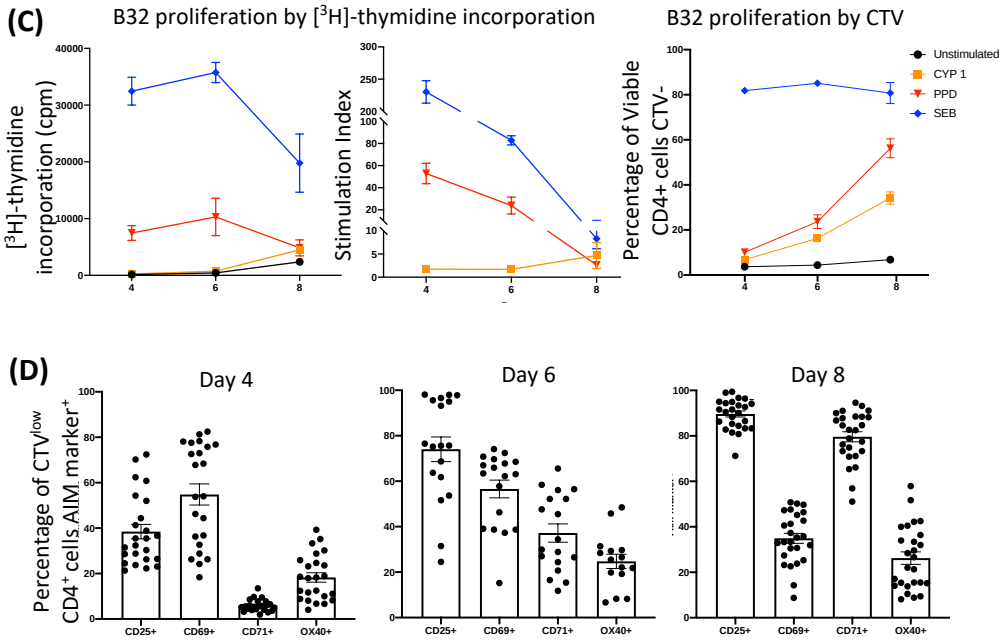

Figure 5.3: Pairing activation induced markers CD25, CD69, OX40 and CD71 with proliferation using Cell Trace Violet dye. (A) AIM assay of representative donor (B32) stained with Cell Trace Violet (CTV) prior to antigen stimulation in triplicate as previously described. Flow cytometry contour plots of AIM marker expression for at least 30,000 Live $CD4^+$ cells on day 8 in each condition. Analysis of CTV trace determines the percentage of Live $CD4^+$ have gone through cellular division (CTV^{low} cells). **(B)** Percentage of Viable $CD4^+$ cells AIM $marker^+$ (CD25/CD69, CD25/OX40 and CD25/CD71) for donor B32 over 8 day timecourse. FMO controls for CD25, CD69, OX40 and CD71 were used to set the gates for AIM^+ cells. **(C)** Proliferation data for B32 over 8 day timecourse measured by $[^3H]$-thymidine incorporation. **(D)** Correlation between cell proliferation and AIM marker expression on day 4-8 of AIM assay (CTV^{low} cells from all antigen conditions combined).

FACS sorting at day 8, to allow for a larger population of CTV^{low} cells to be sorted. Furthermore, initial T cell activation, if too potent, may not establish sustainable cell proliferation and clonal expansion, thus assessing AIM^+ expression of CTV^{low} cells at later timepoints may help us to sort viable proliferating cells. CD25 expression was consistently highly associated with CTV^{low} cells, starting at 38.5%, increasing to 74.0% on day 6 and reaching 89.6% $CD25^+$ by day 8. CD25 is the high-affinity receptor for growth factor IL-2, and upregulation of CD25 is an extremely well-documented feature of T cell activation (Waldmann, 1986). As CD25 is the highest expressed activation marker on CTV^{low} $CD4^+$ cells by day 8 of stimulation, CD25 is a strong target for selection of antigen-specific cells. OX40 was less highly expressed throughout the timecourse, remaining at a similar level over time (day 4 = 18.3%, day 6 = 24.7%, day 8 = 26.2%) so is not likely to remain highly expressed on daughter cells. By contrast, CD71 was expressed at a very low level on day 4, with only 5.9% of $CD4^+CTV^{low}$ cells positive for this marker. However, at later time-points the percentage of $CD71^+CTV^{low}$ cells increased rapidly (day 6 = 37.2%, day 8 = 79.6%). CD71 is a transferrin receptor that plays an important role in cellular uptake of iron and has previously been shown to correlate strongly with Ki67 and proliferation by CFSE (Lašťovička et al., 2009; Motamedi et al., 2016). Based on these preliminary findings, we speculated that CD71 is most likely not expressed as a direct result of TCR engagement, but is upregulated after to support cell proliferation during clonal expansion.

5.3.3 Fluorescence activated cell sorting of antigen-stimulated cells based on AIM markers and CTV

Based on this promising data showcasing the correlation between proliferation and activation markers, CD25, OX40 and CD71 as detected by flow cytometry, we decided to progress to cell sorting CTV^{low} AIM^{+} populations for subsequent assessment of antigen-specificity. Figure 5.4 shows AIM expression of donor D7 Viable CD4 cells (Fig.5.4A; above), and the CTV^{low} $CD25^{+}CD71^{+}$ and $CD25^{+}OX40^{+}$ cells selected for sorting (Fig.5.4A; below, highlighted in red). As cell sorting can be a quite stressful process, to ensure we still had sufficiently viable cells for them to be expanded post-sort, we sorted 50 $CTV^{low}AIM^{+}$ cells per well in 96 well U bottomed plates instead of single cell sorting. 5 x 50 cells of $CD25^{+}/OX40^{+}$ and 5 x 50 cells of $CD25^{+}/CD71^{+}$ were sorted directly into RPMI+10% hAB serum supplemented with 100 U/ml IL-2, rested overnight, then stimulated with PHA. Cells were then left to expand for 10-14 days until a cell pellet was visible. Cells were then transferred to a 48 well plate, stimulated again with PHA, fresh medium and a further 50U/ml IL-2 for another 14 days before assessing antigen-specificity of sorted cells.

Expanded wells were assessed for antigen-specificity in triplicate in 3 conditions: unstimulated, $CYP1_{62\text{-}91}$ peptide or PPD stimulation both at 20µg/ml. Figure 5.4B shows the mean [^{3}H]-thymidine incorporation and stimulation index of 5 wells of $CD25^{+}/OX40^{+}$ and 4 wells of CTV^{low} $CD25^{+}OX40^{+}$ in response to $CYP1_{62\text{-}91}$ peptide. The $CD25^{+}/OX40^{+}$ sorted cells were not able to proliferate strongly in response to $CYP1_{62\text{-}91}$, with an increase in proliferation of 1.3x unstimulated background. In contrast, the sorted cells based on CTV^{low} $CD25^{+}CD71^{+}$ were highly antigen-specific, showing a change above background of >20x.

Figure 5.4: AIM assay of $CYP1_{62-91}$ stimulation followed by FACS sorting CTV^{low} AIM^{+} cells

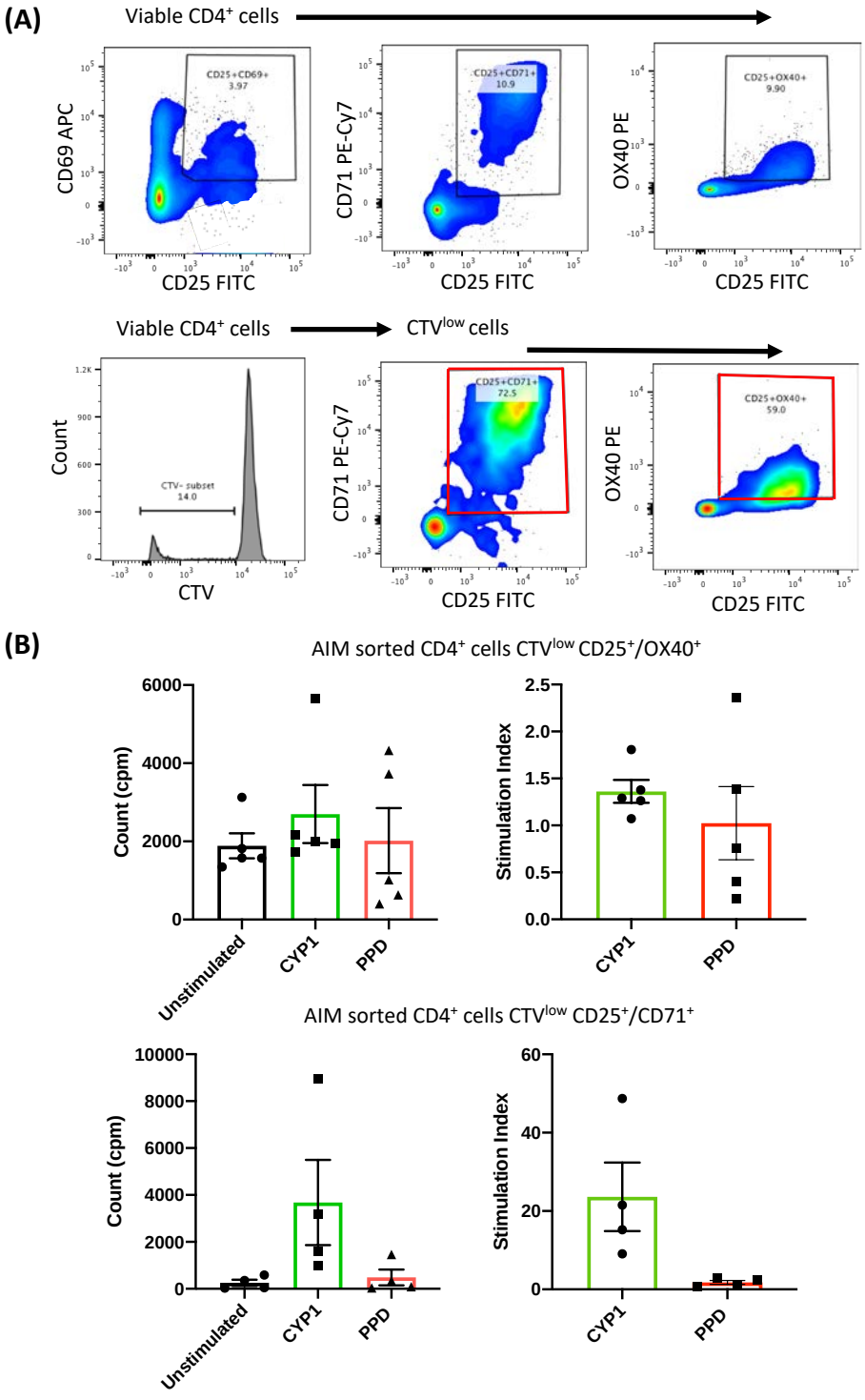

(C)

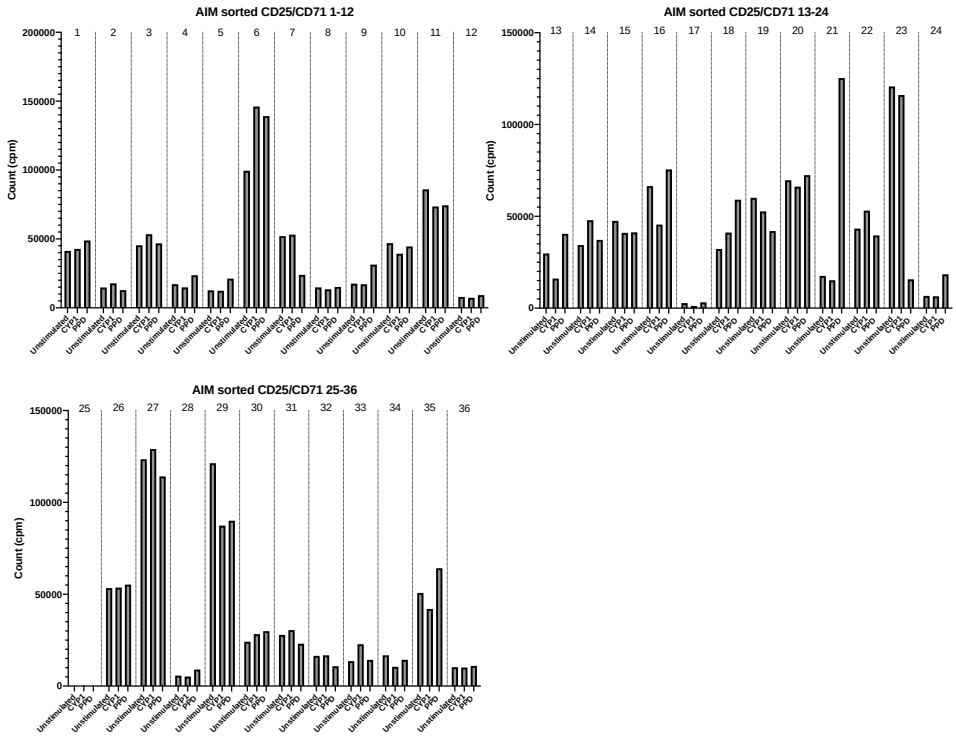

Figure 5.4: Fluorescence activated cell sorting of CD4$^+$ CTV^{low} AIM$^+$ cells and subsequent antigen specificity testing in response to CYP1$_{62\text{-}91}$. **(A)** Flow cytometry plots showing AIM expression and CTV trace of donor D7 on day 8 following stimulation with 20µg/ml CYP1$_{62\text{-}91}$. Total AIM expression of all Viable CD4$^+$ cells (top) and CTV trace of Viable CD4$^+$ cells (bottom). Sorted populations Viable CD4$^+$ CTV^{low} CD25$^+$ CD71$^+$ and Viable CD4$^+$ CTV^{low} CD25$^+$ OX40$^+$ (red squares). 5 wells of 50 sorted cells were plated per AIM combination. **(B)** Following the expansion of antigen-induced CTV^{low} AIM$^+$ cells using PHA, cells were assessed for proliferative response to CYP1$_{62\text{-}91}$ peptide, or PPD as a non-specific control. [^{3}H]-thymidine incorporation was measured after 3 days of antigen stimulation and converted to Stimulation Index compared to unstimulated control wells. **(C)** Sorted cells after expansion were not sufficiently antigen-specific to continue assays. Shown is CD25$^+$CD71$^+$ sorted cells assessed for proliferative response to CYP1$_{62\text{-}91}$ peptide, or PPD as a non-specific control.

Therefore, we kept the CTV^{low} $CD25^{+}CD71^{+}$ line growing whilst cloning 2 of the 4 wells by limiting dilution. For this purpose, 1 and 0.1 T cell per well were cultured in the presence of 5 x 10^4 autologous, irradiated PBMC, 20U/ml IL-2 and PHA in duplicate 96 well plates. 36 wells had visible cell pellets by 14 days post-stimulation (36/384 wells growth positive) which were expanded into 48 well plates and tested again for antigen-specificity. Unfortunately, none of these single-cell cultures proliferated significantly above background when re-stimulated with $CYP1_{62-91}$ (Fig.5.4C). We would have continued to optimise the sorting and *in vitro* expansion of CTV^{low} $CD25^{+}CD71^{+}$ cells for purification of antigen-specific T cells and eventual single cell cloning for downstream assays, but were simultaneously starting transgenic HLA-DR mouse assays for similar T cell epitope mapping purposes. The latter strategy proved to be more consistent and was therefore prioritised as our main approach. If I had had more time towards the end of the project I would have liked to have finalised the AIM assay for single cell autoantigen-specific T cell isolation and TCR repertoire analysis from multiple healthy donors compared to AIH2 patients.

5.4 Assessing immunogenicity of CYP2D6 peptides in HLA-DR transgenic mice

Whilst developing the human antigen-specific T cell identification methods discussed previously, we also started to utilise HLA-DR transgenic mice to identify peptides with compatibility with HLA-DR molecules and peptide immunogenicity by immunisation and analysis of antigen-specific T-cell proliferation. The identification of immunodominant epitopes presented by different HLA molecules will enable the delineation of autoantigen T cell responses.

Relying solely on human-based assays had proven to be challenging, due to the very low percentage of autoantigen-reactive cells in PBMC populations and the difficulties experienced in selective expansion and maintenance of autoantigen-specific cells.

Therefore, we focussed efforts on the already well-established colony of HLA-DR(α1*0101,β1*0401) (hereafter referred to as HLA-DR4) transgenic mice to analyse CYP2D6 peptide immunogenicity and later develop antigen-specific T cell hybridomas. As the project progressed, we acquired HLA-DR(α1*0101,β1*0301) (hereafter referred to as HLA-DR3) from the Jackson Laboratory (Stock No: 030434) and HLA-DR(α1*0102,β1*0701) (hereafter referred to as HLA-DR7) from AstraZeneca R&D, Transgenic centre, Sweden. Only the HLA-DR4 mice were verified by antibody phenotyping to be full Ab^0 knockout mice, which lack expression of endogenous murine H2 class II molecules (Fig.5.5). After a 2-3 years of maintenance of the HLA-DR4 colony by the Wraith group, resting $CD19^+$ cells from tail vein bleeds were routinely 60-75% HLA-DR^+. High expressing mice (minimum 65% of $CD19^+$ cells HLA-DR^+) were used in immunisation experiments. In contrast, $CD19^+$ cells from HLA-DR3 mice were only 25-40%

Figure 5.5: Phenotyping of HLA-DR transgenic mice

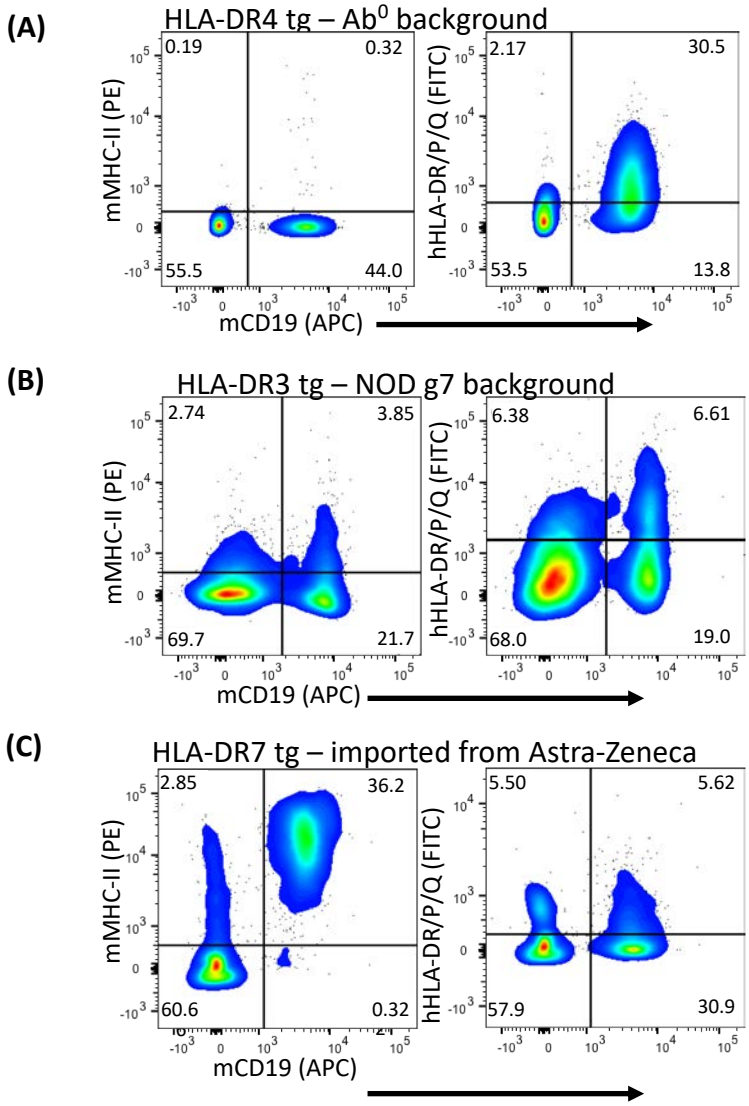

Figure 5.5: Phenotyping HLA-DR transgenic mice for use in immunisation experiments. Cells from tail vein bleed underwent red blood cell lysis prior to antibody staining for flow cytometry as follows: CD4 PerCPCy5.5 (1:200), CD19 APC (1:200), mMHC-II PE (1:400), hHLA-DR/DP/DQ FITC (1:200). **(A)** HLA-DR4 tg**, (B)** HLA-DR3 tg and **(C)** HLA-DR7 tg.

HLA-DR^{+} and 15-20% still expressed low levels of mouse MHC-II. The newly imported HLA-DR7 mice when typed expressed the full complement of mouse MHC-II on CD19^{+} cells (100%)$^{+}$, with low expression of HLA-DR on CD19^{+} cells (15-25%$^{+}$). Both HLA-DR3 and HLA-DR7 mice would be much more useful for our experiments if backcrossed onto the Ab^{0} mice to delete endogenous mouse MHC-II.

5.4.1 HLA-DR4 transgenics

Immunisation of HLA-DR4 transgenic mice with CYP2D6 30mer peptides in CFA supplemented with MTb as an adjuvant should induce CYP2D6 peptide-specific immune responses in mice if: a) the peptide is compatible with HLA-DR4 and b) mice possess T cells able to recognise and respond. To test immunogenicity of each CYP2D6 peptide following immunisation, spleen and lymph node cells were isolated 10 days post-immunisation and re-stimulated in triplicate with CYP2D6 peptide over a concentration gradient, or PPD at 20µg/ml. 3 days after *in vitro* re-stimulation, cells were pulsed with [^{3}H]-thymidine for 16-20 hours prior to harvesting on a scintillation counter to measure [^{3}H]-thymidine incorporation.

Figure 5.6 summarises all immunisation experiments showing [^{3}H]-thymidine incorporation for draining lymph node cells and spleen cells for each mouse immunised. As previously, raw data for [^{3}H]-thymidine incorporation (left bar charts) were also converted to stimulation index values (right bar charts) to show the ratio between proliferation in stimulated vs unstimulated conditions. Where draining lymph nodes did not provide sufficient cells to set-up all stimulation conditions *in vitro*, in some experiments, lymph nodes were combined.

Figure 5.6: Immunisation of HLA-DR4 transgenic mice with CYP2D6 peptides

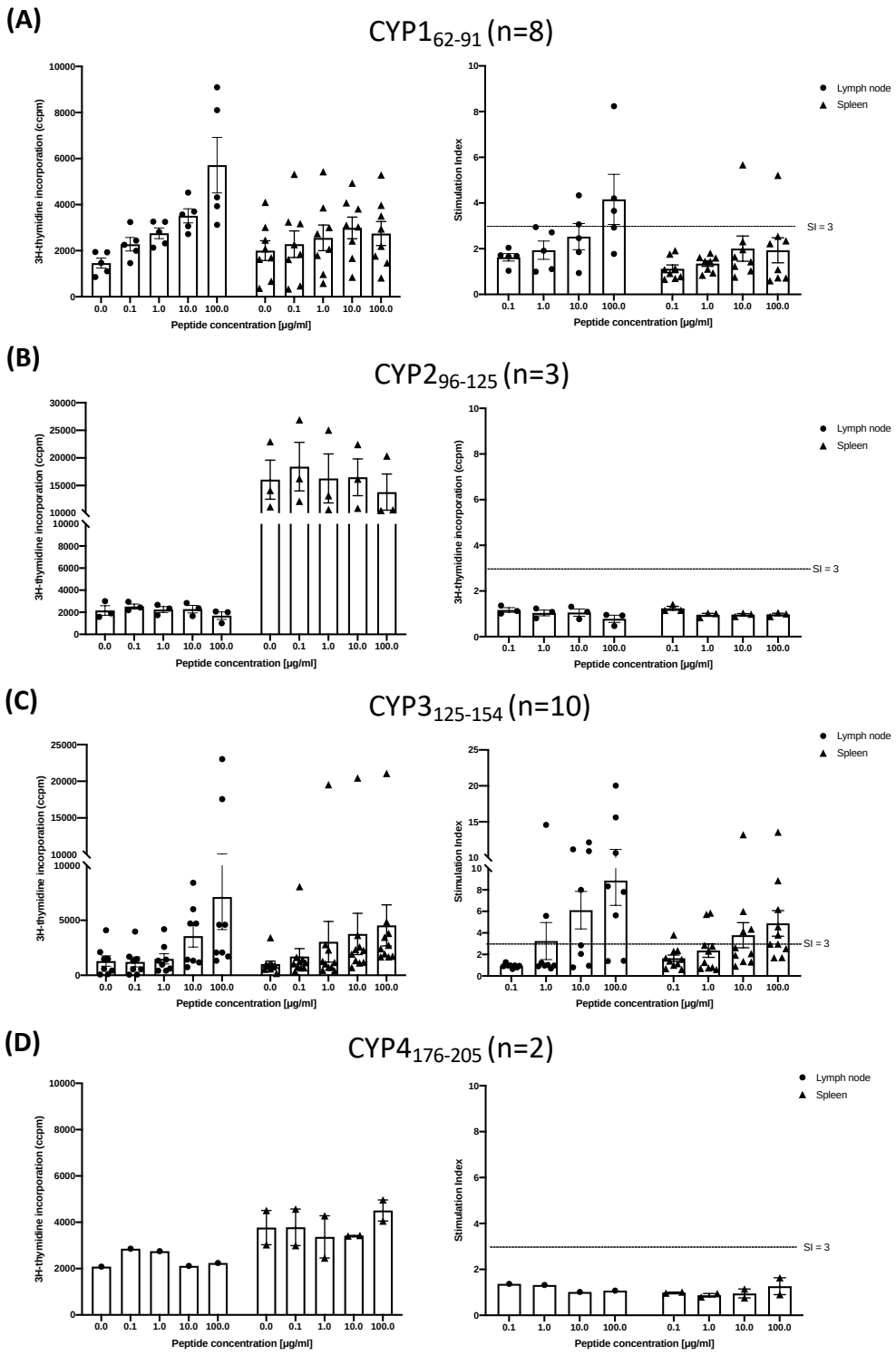

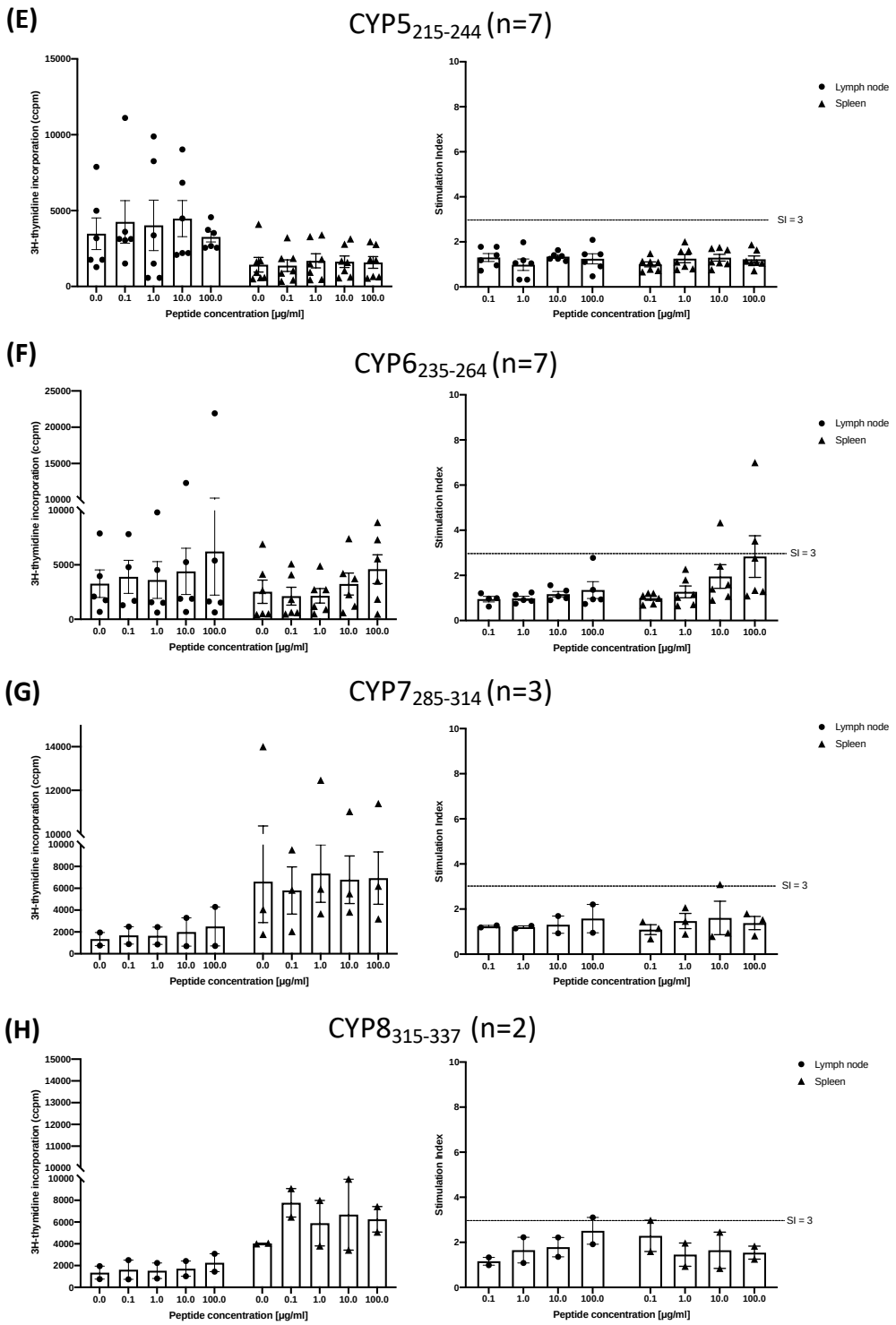
(E)
CYP5215-244 (n=7)
(F)
CYP6235-264 (n=7)
(G)
CYP7285-314 (n=3)
(H)
CYP8315-337 (n=2)
3H-thymidine incorporation (ccpm)
Stimulation Index
Peptide concentration [µg/ml]
Lymph node
Spleen
SI = 3
0.0
0.1
1.0
10.0
100.0

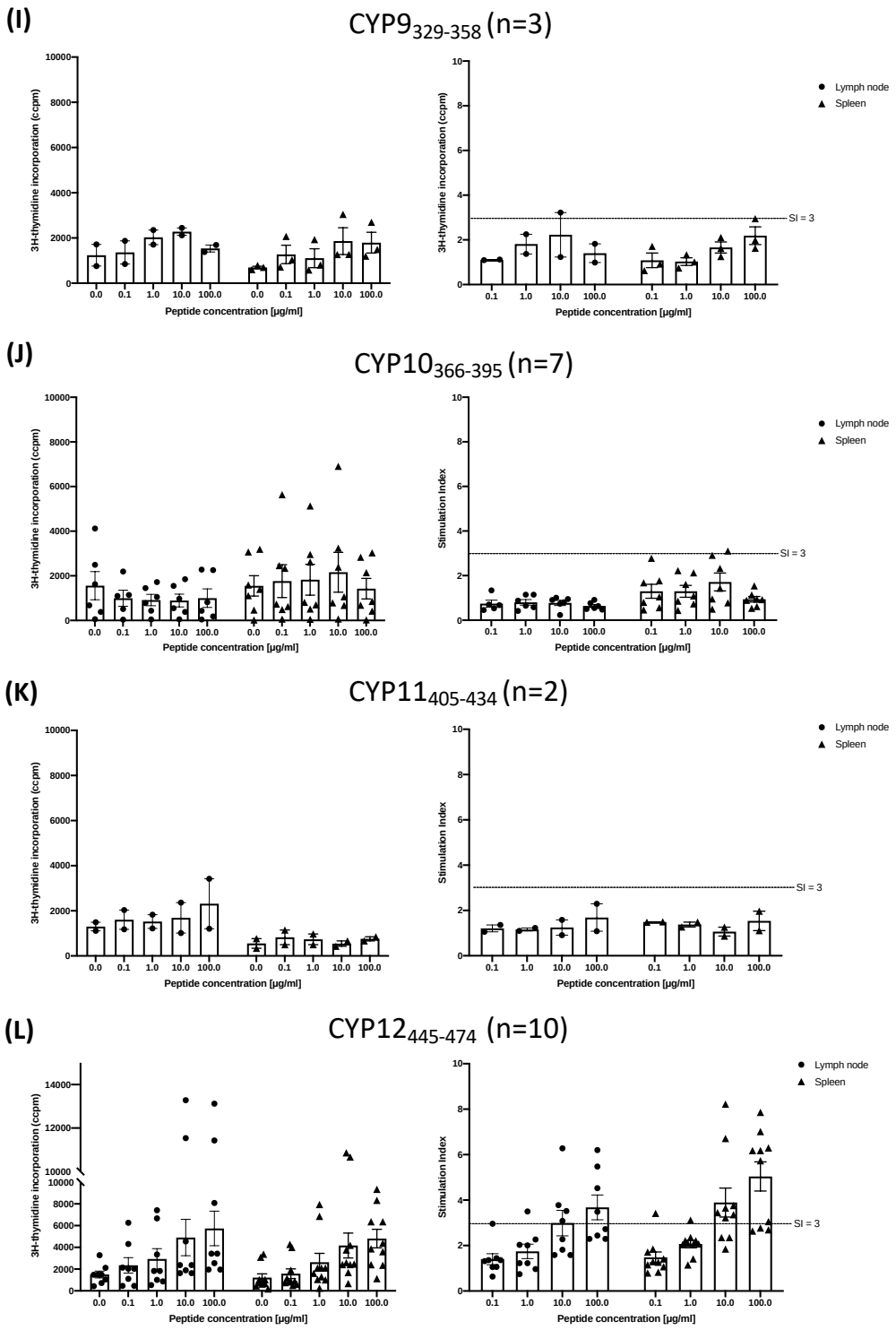
(I)
CYP9329-358 (n=3)
(J)
CYP10366-395 (n=7)
(K)
CYP11405-434 (n=2)
(L)
CYP12445-474 (n=10)
3H-thymidine incorporation (ccpm)
Stimulation Index
Peptide concentration [µg/ml]
Lymph node
Spleen
SI = 3

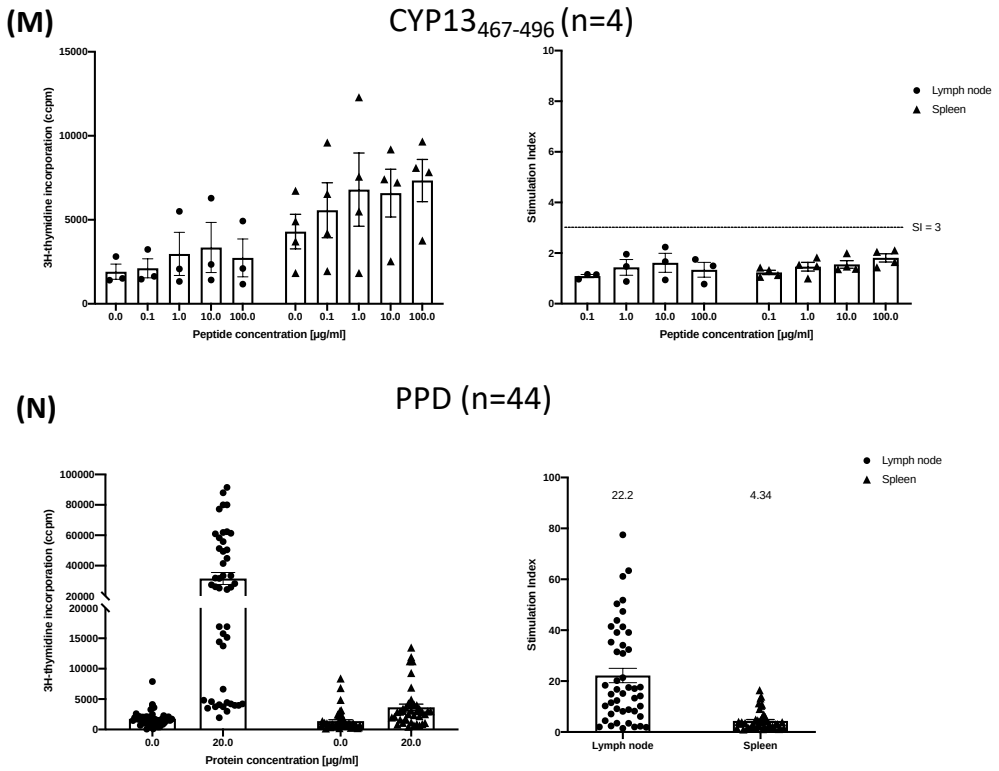

Figure 5.6: Recall responses of DR4 transgenic mouse spleen and draining lymph node cells to CYP2D6 peptides or PPD following immunisation. HLA-DR4 transgenic mice were immunised by subcutaneous injection of 100µg of CYP2D6 30mer peptide in CFA (supplemented with 4mg/ml MTb). 10 days post-immunization, mice were culled. Spleen and lymph node cells were plated in triplicate flat-bottomed 96 well plates at $10x10^6$ and $5x10^6$ cells/ml, respectively, and stimulated for 3 days with increasing dose of CYP2D6 30mer peptide (0.1 – 100µg/ml) **(A-M).** PPD at 20µg/ml was used as a positive control **(N).** On day 3, cells were incubated for 16-20hours with 0.18MBq/ml [^{3}H]-thymidine. [^{3}H]-thymidine incorporation was measured as corrected counts per minute (cpm) and converted to Stimulation Index (SI). Graphs show individual mouse mean cpm or SI values, error bars represent ±SEM between mice.

Non-immunogenic peptides, which did not prime lymphocytes for significant antigen-specific proliferative responses above that of unstimulated cells, were $CYP2_{96-125}$ (Fig.5.6B), $CYP4_{176-205}$ (Fig.5.6D), $CYP5_{215-244}$ (Fig.5.6E), $CYP7_{285-314}$ (Fig.5.6G), $CYP8_{315-337}$ (Fig.5.6H), $CYP9_{329-358}$ (Fig.5.6I), $CYP10_{366-395}$ (Fig.5.6J), $CYP11_{405-434}$ (Fig.5.6K) and $CYP13_{467-496}$ (Fig.5.6M). Peptides $CYP2_{96-125}$, $CYP4_{176-205}$, $CYP9_{329-358}$, $CYP11_{405-434}$ and $CYP13_{467-496}$ were not highly immunogenic in human PBMC stimulation assays (<20% healthy donor responders), so it is potentially unsurprising that in HLA-DR4 mice a similar pattern emerges. However, $CYP5_{215-244}$, $CYP7_{285-314}$, $CYP8_{315-337}$ and $CYP10_{366-395}$ were determined to be immunogenic by human PBMC assays (>20% healthy donor responders). Interestingly, the highest response rate of all HLA-DR serotypes was HLA-DR4 healthy donors to $CYP5_{215-244}$, with 64% of HLA-$DR4^+$ healthy donors mounting a significant proliferative response. Therefore, it is somewhat surprising, that HLA-DR4 transgenic mice did not exhibit antigen-specific responses towards this peptide. This may be able to be explained by murine APCs processing this peptide differently, or by the mouse lacking the relevant T cell repertoire required for $CYP5_{215-244}$-HLA-DR4 recognition. Prior experience with HLA-DR tg mice has shown that mouse and human T cell repertoires can differ significantly enough to reveal T cell repertoire gaps between the species.

The highest reactivity CYP2D6 peptides in HLA-DR4 mouse lymph nodes according to mean average Stimulation Index of lymph node cells was $CYP3_{125-154}$ SI = 8.85 (Fig.5.6C), $CYP1_{62-91}$ SI = 4.15 (Fig.5.6A), $CYP12_{445-474}$ SI = 3.68 (Fig.5.6L) and $CYP6_{235-264}$ SI = 1.35 (Fig.5.6F). In splenocytes, the hierarchy of immunogenicity according to mean average

Stimulation Index was $CYP12_{445-474}$ SI = 5.04 (Fig.5.6L), $CYP3_{125-154}$ SI = 4.87 (Fig.5.6C), $CYP6_{235-264}$ SI = 2.85 (Fig.5.6F) and $CYP1_{62-91}$ SI = 1.98 (Fig.5.6A).

That $CYP3_{125-154}$ stimulated the highest response in HLA-DR4 mice was not predicted based on immunogenicity of this peptide in human healthy donor or AIH patient PBMC assays, as $CYP3_{125-154}$ was one of the weaker peptides in the human investigations. $CYP12_{445-474}$, however, was determined to give significantly higher immune responses in paediatric AIH patient assays compared to adult AIH or healthy donor PBMCs and also generates strong immune response in the HLA-DR4 mice. $CYP12_{445-474}$ actually stimulated the strongest response in isolated splenocytes; the mean average SI of the 10 mice immunised with $CYP12_{445-474}$ and re-stimulated with 10 and 100µg/ml peptide was above threshold, at 3.89 and 5.04. $CYP1_{62-91}$ was a primary target identified in human PBMC assays, as this peptide stimulated strong responses in healthy donor, AIH1 adult and AIH2 paediatric and adult cohorts. $CYP1_{62-91}$ stimulated significant antigen-stimulated proliferative responses, primarily in lymph node cells. Spleen cells stimulated with $CYP1_{62-91}$ *in vitro* after immunisation had a less strong mean average SI of 1.93. $CYP6_{235-264}$ responses in HLA-DR4 mice were the lowest of the peptides able to induce a response, with only splenocytes inducing a mean SI value >3.

Analysis of recall responses in HLA-DR4 transgenic mice by re-stimulation *in vitro* therefore identified four CYP2D6 30mer peptides that are compatible with the HLA-DR4 molecule and can engage T cell recognition and T cell response. As such, we moved forward with efforts to generate T cell hybridomas derived from HLA-DR4 restricted antigen-specific T cells to $CYP3_{125-154}$, $CYP1_{62-91}$, $CYP12_{445-474}$, $CYP6_{235-264}$.

5.4.2 HLA-DR3 transgenics

HLA-DR3 has been identified as a risk allele in a wide range of autoimmune diseases (Graves', Hashimoto's, T1D etc) and has also been associated with autoimmune hepatitis, more specifically AIH1 patients. Therefore, we sourced a commercially available transgenic mouse from Jackson Laboratories which would enable us to run identical immunisation experiments to those in the HLA-DR4 mice. The transgenic element in this line did not turn out to be particularly highly expressing, and the mice were complicated by still expressing residual levels of endogenous MHC-II; but as this was what was available to us, we persevered with immunisation experiments to identify immunogenic peptides in the HLA-DR3 context. Our plan was to once again produce T cell hybridomas from immunised animals, which we could then ensure peptide presentation via HLA-DR3 using a HLA-DR blocking antibody in functional assays. However, we were unable to generate consistent antigen-specific T cell hybridomas from HLA-DR3 mice within the scope of this project.

Figure 5.7 summarises all immunisation experiments [^{3}H]-thymidine incorporation for draining lymph node cells and spleen cells for each HLA-DR3 mouse immunised. As previously, raw data for [^{3}H]-thymidine incorporation (left bar charts) were also converted to Stimulation Index values (right bar charts) to show the ratio between proliferation in stimulated vs unstimulated conditions. Where draining lymph nodes did not provide sufficient cells to set-up all stimulation conditions *in vitro*, in some experiments, lymph nodes were combined.

Figure 5.7: Immunisation of HLA-DR3 transgenic mice with CYP2D6 peptides

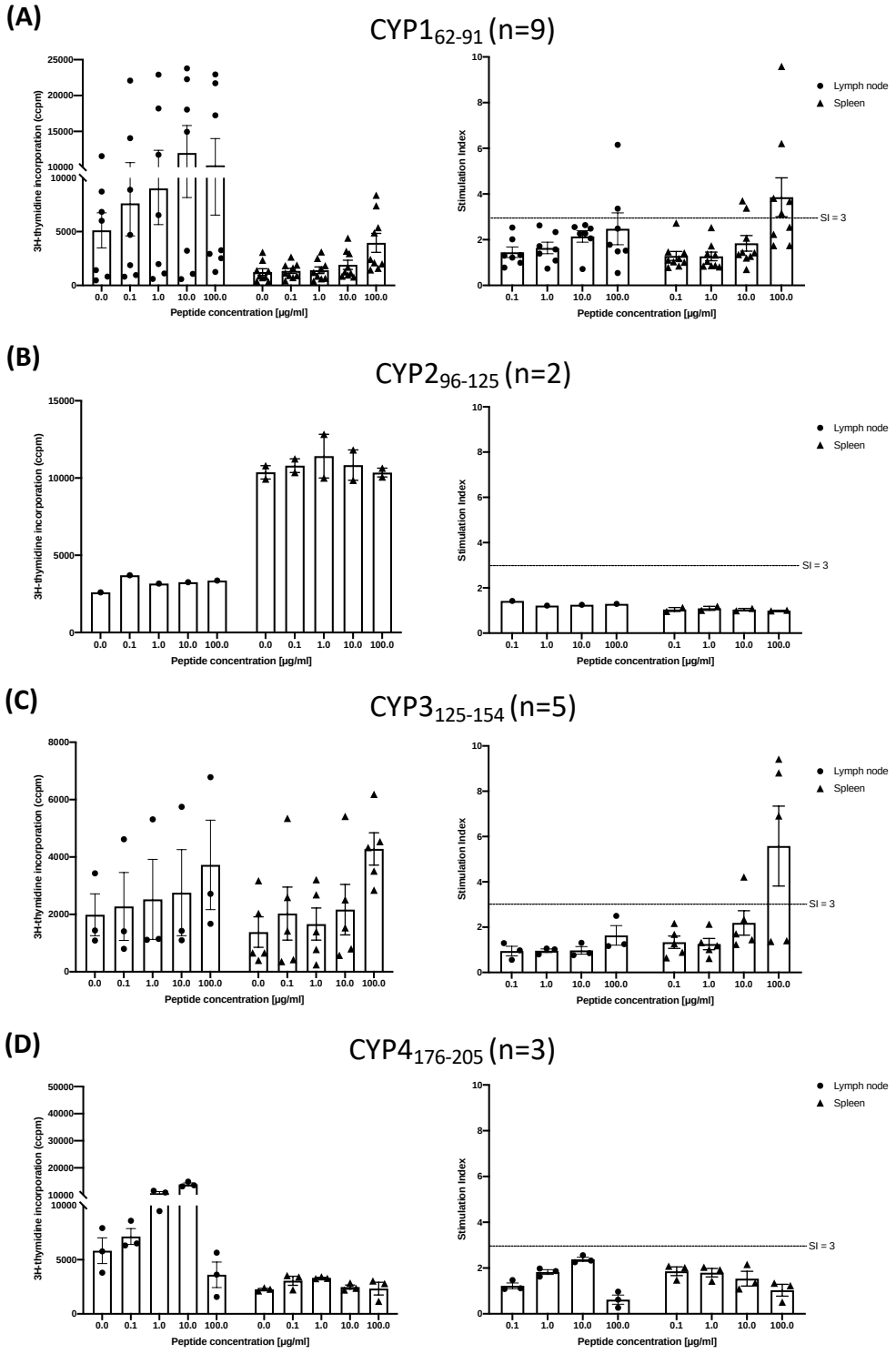

(E) $CYP5_{215-244}$ (n=9)

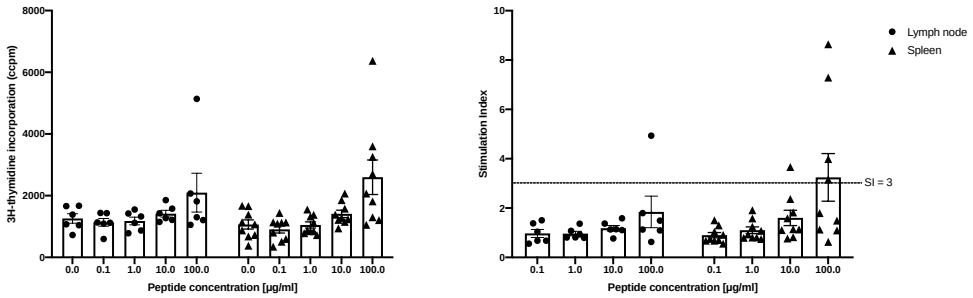

(F) $CYP6_{235-264}$ (n=7)

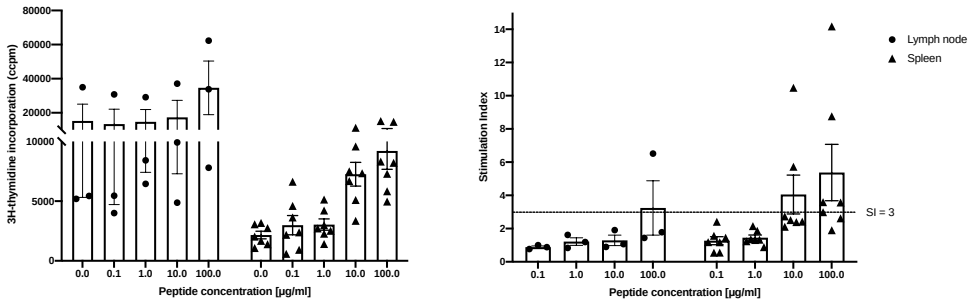

(G) $CYP7_{285-314}$ (n=2)

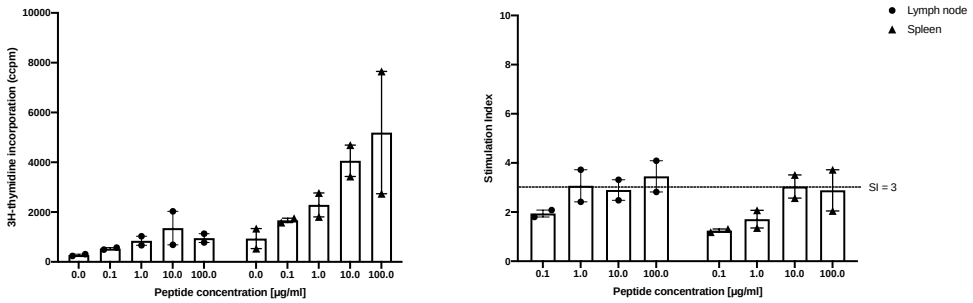

(H) $CYP8_{315-337}$ (n=3)

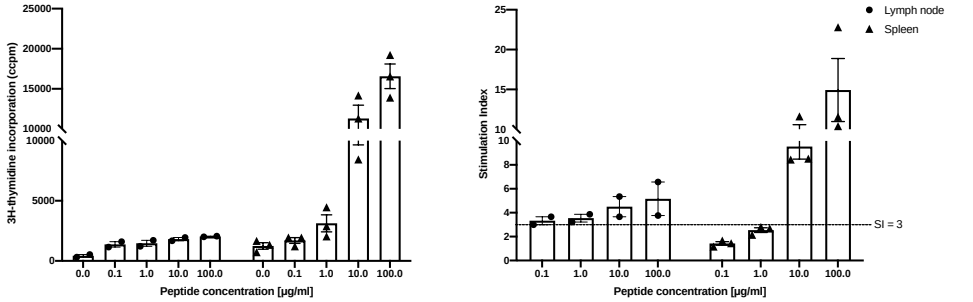

(I) CYP9$_{329-358}$ (n=2)

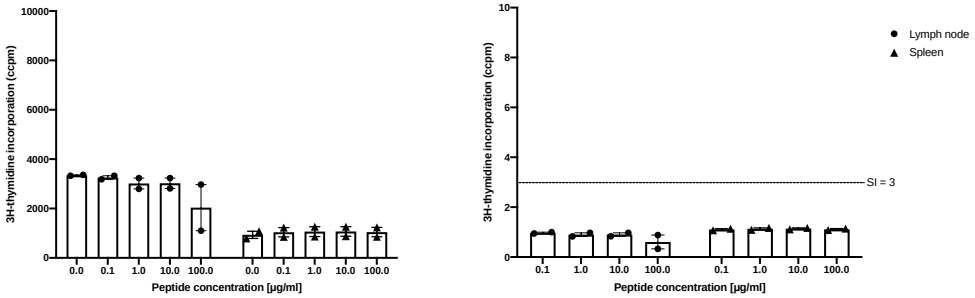

(J) CYP10$_{366-395}$ (n=3)

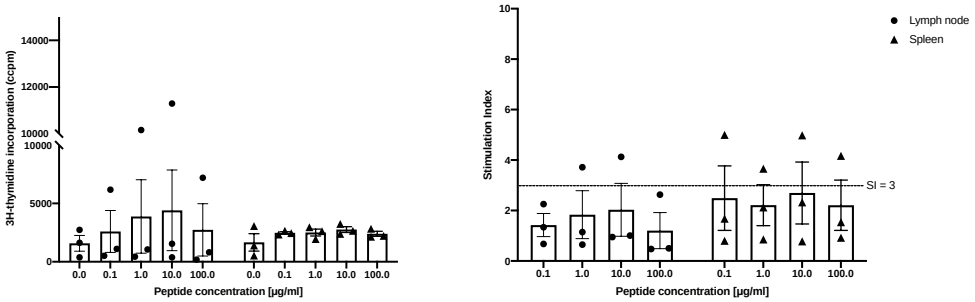

(K) CYP11$_{405-434}$ (n=2)

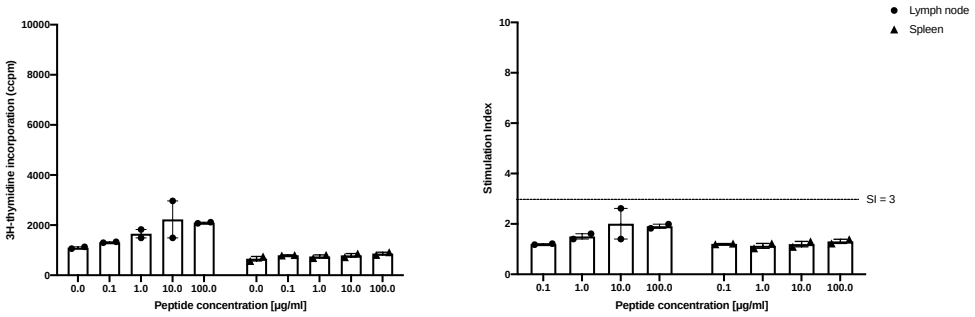

(L) CYP12$_{445-474}$ (n=4)

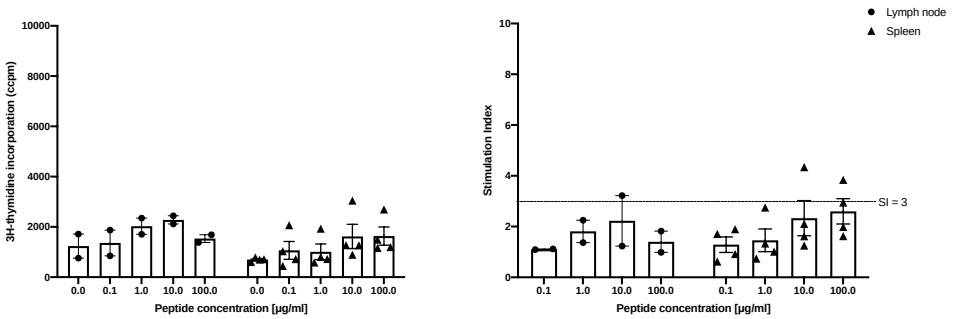

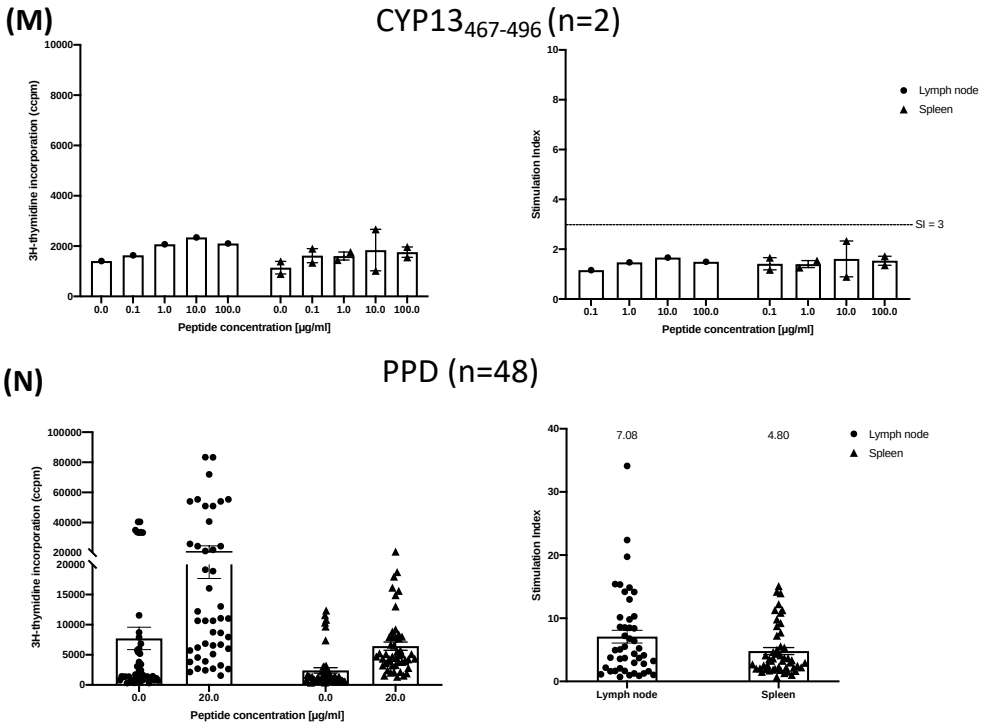

Figure 5.7: Recall responses of DR3 transgenic mouse spleen and draining lymph node cells to CYP2D6 peptides or PPD following immunisation. HLA-DR3 transgenic mice were immunised and spleen and lymph node cells re-stimulated in vitro as described previously with increasing dose of CYP2D6 peptide (0.1–100µg/ml) **(A-M).** PPD at 20µg/ml was used as a positive control **(N)**. Graphs show individual mouse mean cpm or SI values, error bars represent ±SEM between mice.

Immunisation of HLA-DR3 mice followed by antigen recall of lymphoid cells *in vitro* showed that $CYP1_{62\text{-}91}$ (Fig.5.7A), $CYP3_{125\text{-}154}$ (Fig.5.7C), $CYP5_{125\text{-}154}$ (Fig.5.7E), $CYP6_{235\text{-}264}$ (Fig.5.7F), $CYP7_{285\text{-}314}$ (Fig.5.7G) and $CYP8_{315\text{-}337}$ (Fig.5.7H) were able to generate significant T cell responses and are therefore likely to be compatible with HLA-DR3. The highest response CYP2D6 peptides in HLA-DR3 mouse lymph nodes in order of mean average Stimulation Index of lymph node cells was $CYP8_{315\text{-}337}$ SI = 5.17, $CYP7_{285\text{-}314}$ SI = 3.45, $CYP6_{235\text{-}264}$ SI = 3.24, $CYP1_{62\text{-}91}$ SI = 2.48, $CYP5_{125\text{-}154}$ SI = 1.84 and $CYP3_{125\text{-}154}$ SI = 1.64. In splenocytes, the hierarchy of immunogenicity according to mean average Stimulation Index was $CYP8_{315\text{-}337}$ SI = 14.9, $CYP3_{125\text{-}154}$ SI = 5.58, $CYP6_{235\text{-}264}$ SI = 5.37, $CYP1_{62\text{-}91}$ SI = 3.88, $CYP5_{125\text{-}154}$ SI = 3.24 and $CYP7_{285\text{-}314}$ SI = 2.88.

Non-immunogenic peptides, which did not prime lymphocytes for significant antigen-specific proliferative responses above that of unstimulated cells, were $CYP2_{96\text{-}125}$ (Fig.5.7B), $CYP4_{176\text{-}205}$ (Fig.5.7D), $CYP9_{329\text{-}358}$ (Fig.5.7I), $CYP10_{366\text{-}395}$ (Fig.5.7J), $CYP11_{405\text{-}434}$ (Fig.5.7K), $CYP12_{445\text{-}474}$ (Fig.5.7L) and $CYP13_{467\text{-}496}$ (Fig.5.7M).

5.4.3 HLA-DR7 transgenics

HLA-DR7 has been identified in patient cohorts and GWAS studies to be associated with AIH2. Whether HLA-DR7 does indeed contribute to loss of immune tolerance towards the autoantigen CYP2D6 is yet to be determined, but it is a common feature of many autoimmune diseases that risk HLA-DR alleles lead to different peptide presentation.

HLA-DR7 mice were imported into University of Birmingham Biomedical Services Unit in mid-2019. After a period of re-derivation, breeding of these mice started with 2 pairs. When phenotyping the first litters of these HLA-DR7 transgenic mice, it was clear

that these mice expressed HLA-DR at a lower level than the existing HLA-DR4 line, and also had full expression of endogenous MHC-II. As such, we had planned to breed these mice onto an Ab^0 line to breed mice with deletion of murine MHC-II and retain expression of HLA-DR transgene. Unfortunately, this was not possible during the time-frame of this project.

5.5 T cell epitope mapping using T cell hybridomas derived from HLA-DR transgenic mice

As an alternative approach to human cell-based methods to isolate CYP2D6 autoantigen-specific cells, we started to generate T cell hybridoma cells derived from CYP2D6 peptide-immunised HLA-DR transgenic mice. This approach relies on the successful fusion of antigen-specific T cells with T cell thymoma cell line, BW5147, to generate an immortalised hybridoma of the primary T cell. These T cell hybridomas grow rapidly and can be maintained for long periods of time in culture and long-term cold storage, offering improved ease-of-handling than primary T cell clones. T cell hybridoma specificity can be very carefully defined by measuring IL-2 production in response to stimulation with peptides of interest. Therefore, T cell hybridomas can be utilised to assess peptide variants to home in on the minimal T cell epitope required for MHC-II binding and TCR recognition. A difficulty arising in the use of T cell hybridomas is that cells can be genetically unstable, due to the duplication of chromosomes during the cell fusion process. Over time, cells can lose antigen-specificity or IL-2 production if they lose chromosomes.

Our T cell hybridoma production protocol was based on methodology published by Canaday, et al. (Canaday et al., 2003; Canaday, 2013). Briefly, HLA-DR4 or HLA-DR3 transgenic mice were immunised as previously, with 100µg CYP2D6 30mer peptide in CFA supplemented with MTb. After 10 days, mice were sacrificed, and spleen cells isolated by passing through a 40µm cell strainer. Splenocytes were stimulated with 10µg/ml of CYP2D6 peptide, on day 3 media was supplemented with 20µg/ml of rmIL-2 and on day 5 fusion performed. Fused cell suspension was plated in 96 well U bottomed plates at 5-fold serial dilutions: NEAT, 1/5, 1/25 and 1/125. Successful T cell hybridomas could be seen as visible cell pellets between day 7 and 10 post-fusion and were transferred to larger wells to avoid over-growth. Antigen-specificity and sensitivity of hybridomas were tested by IL-2 production in response to antigen stimulation using either HLA-DR splenocytes or HLA-DR restricted human EBV-LCL as APCs.

5.5.1 HLA-DR4 restricted T cell hybridomas towards $CYP12_{445-474}$

$CYP12_{445-474}$ immunised HLA-DR4 transgenic mice specifically responded to $CYP12_{445-474}$ peptide upon antigen recall of splenocytes, as measured by [^{3}H]-thymidine incorporation (Fig.5.8A). The number of growth positive wells harvested from each plate was recorded (Fig.5.8B). NEAT plate A and B generated 10/96 and 13/96 hybridomas, respectively. More dilute plating conditions generated fewer T cell hybridomas. Where fewer than 10% of wells generated viable hybridomas, hybridomas did not require further sub-cloning by limiting dilution.

Figure 5.8C shows the first antigen screen of the 29 T cell hybridomas generated, in which 100µl of hybridoma were co-cultured with $2x10^6$ irradiated non-immunised HLA-

Figure 5.8: Generation of T cell hybridomas from $CYP12_{445-474}$ peptide immunised HLA-DR4 transgenic mice

(A)

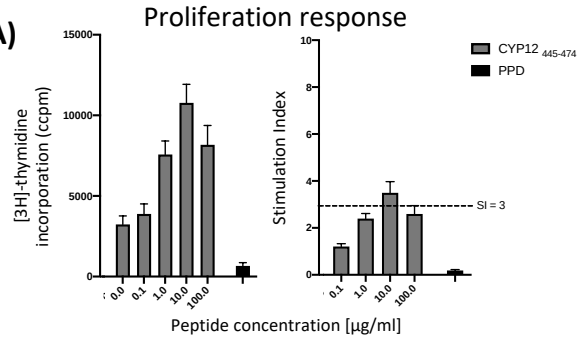

(B)

Plate dilution	Number of positive growth wells	Percentage positive growth wells
NEAT A	10	10.4
NEAT B	13	13.5
1/5 A	4	4.17
1/5 B	1	1.04
1/25 A	1	1.04

(C)

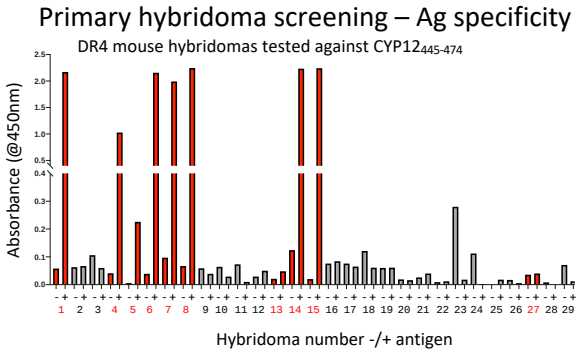

Figure 5.8: Recall responses of $CYP12_{445-474}$ immunised HLA-DR4 tg splenocytes and primary screening of T cell hybridomas. (A) HLA-DR4 transgenic mouse was immunised with $CYP12_{445-474}$ peptide and splenocytes tested for proliferation in response to $CYP12_{445-474}$ by [^{3}H]-thymidine incorporation as described previously. T cell hybridomas generated by fusion of peptide-activated splenocytes with T cell thymoma cell line, BW5147, were harvested by cell pellet growth from day 7-10. **(B)** Count of positive growth wells in each dilution condition. **(C)** Primary screen for antigen-specificity: T cell hybridomas were assessed for antigen-specific production of IL-2 by sandwich ELISA using irradiated non-immunised HLA-DR4 splenocytes as APCs. Hybridomas producing more IL-2 in antigen-stimulated condition coloured red.

DR4 splenocytes with or without 20µg/ml $CYP12_{445-474}$ peptide. After 24 hours, production of IL-2 in cell culture supernatant was measured using sandwich ELISA. 10/29 hybridomas responded to $CYP12_{445-474}$ peptide antigen, producing more IL-2 when peptide-stimulated vs unstimulated (Hybridomas 1, 4, 5, 6, 7, 8, 13, 14, 15 and 27; Fig. 5.8C, shown as red bars) and were maintained in culture for further screening.

The primary screen is a relatively crude approach; hybridomas are not counted prior to plating due to large numbers of cultures to screen, and only single wells of unstimulated vs 20µg/ml are assessed. Therefore, in further screening assays, cells are then plated in triplicate over a range of peptide concentrations to assess antigen-sensitivity and which of the antigen-responsive hybridomas are most responsive to antigen.

Figure 5.9 summarises the antigen-sensitivity of five T cell hybridomas (Number 1, 4, 6, 7 & 8) which were taken forward for secondary screening. These hybridomas expanded consistently in culture, whereas the remaining 5 hybridomas from primary screening had slowed or halted growth after 2 weeks in culture. In the secondary screen, hybridomas were plated at $1x10^5$ cells/well with $2x10^5$ irradiated naïve HLA-DR4 splenocytes. Cultures were stimulated with $CYP12_{445-474}$ 30mer peptide, recombinant human CYP2D6 protein, and CYP12.1 – CYP12.4 overlapping 15mers (shifting by 5 amino acids). This screen was designed to assess which of the promising hybridomas were most sensitive to $CYP12_{445-474}$ 30mer, but also which 15mer contains the relevant T cell epitope(s), and whether T cell hybridoma is responding to a cryptic peptide. Cryptic epitopes are defined as peptides that are able to bind directly to MHC-II molecules, but which would not be natively presented epitopes if cells were processing the whole

antigenic protein. Cryptic epitopes must be identified and avoided for use in tolerance induction settings, as they are not peptides that would be naturally presented *in vivo* or disease settings.

CYP2D6 CYP12 PEPTIDES	
Peptide name	**Peptide sequence**
$CYP12_{445-474}$	GEPLARMELFLFFTSLLQHFSFSVPTGQPR
$CYP12.1_{445-459}$	GEPLARMELFLFFTS
$CYP12.2_{450-464}$	RMELFLFFTSLLQHF
$CYP12.3_{455-469}$	LFFTSLLQHFSFSVP
$CYP12.4_{460-474}$	LLQHFSFSVPTGQPR

Hybridoma 1 (Fig.5.9A) was a low producer of IL-2 in response to $CYP12_{445-474}$ 30mer peptide (1.5x background). Hybridoma 1 was able to respond to CYP2D6 protein (1.5x background) and $CYP12.2_{450-464}$ 15mer (2.4x background). Hybridoma 4 (Fig.5.9B) emerged as a promising hybridoma; it was a very high producer of IL-2 in response to $CYP12_{445-474}$ 30mer peptide (10x background). Hybridoma 4 also responded to CYP2D6 protein (1.875x background) and very strongly to $CYP12.2_{450-464}$ 15mer (14.5x background). Hybridoma 6 (Fig.5.9C) was similarly promising, IL-2 production in response to $CYP12_{445-474}$ 30mer peptide was potent (16x background). Hybridoma 6 also responded well to CYP2D6 protein (2.25x background) and very strongly to $CYP12.2_{450-464}$ 15mer (28.75x background). As such Hybridomas 4 and 6 were taken forward to further screening for T cell epitope mapping and frozen for storage. Hybridoma 7 (Fig.5.9D) was determined to have extremely selective responses to $CYP12_{445-474}$ 30mer peptide (60x background) and $CYP12.2_{450-464}$ 15mer (58x background) at only 1µg/ml of peptide, but

Figure 5.9: Secondary screening of T cell hybridomas from $CYP12_{445-474}$ peptide immunised HLA-DR4 transgenic mice

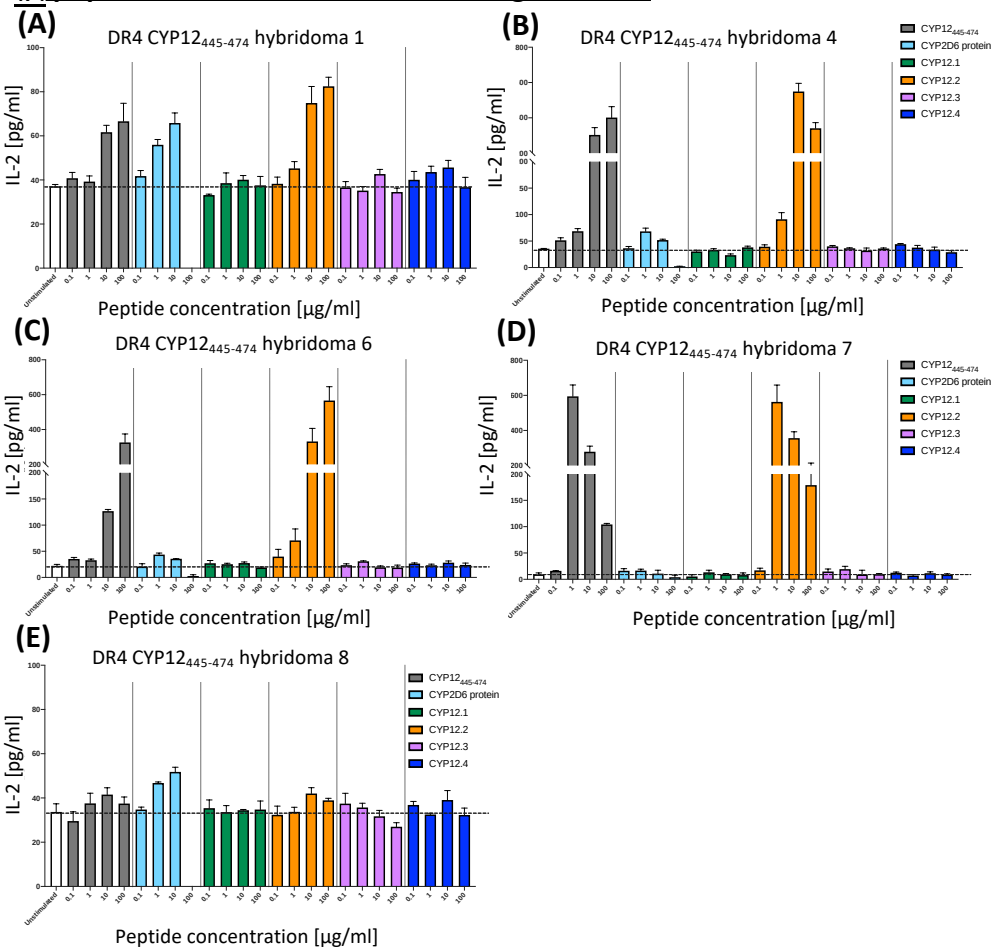

Figure 5.9: Secondary screening of $CYP12_{445-474}$ T cell hybridomas with sustained growth. Hybridoma colonies with an initial response to antigen (Fig.8C; red bars) and sustained growth were expanded for 7-10 days prior to secondary screen for antigen-sensitivity and response to recombinant human CYP2D6 protein. Hybridoma cells were plated in triplicate at $1x10^5$ cells/well with $2x10^5$ cell/well irradiated HLA-DR4 splenocytes for 24 hours as unstimulated cultures, or in the presence of CYP12 30mer peptide, CYP2D6 protein, CYP12.1-CYP12.4 overlapping 15mers. IL-2 response of **(A)** Hybridoma 1, **(B)** Hybridoma 4, **(C)** Hybridoma 6, **(D)** Hybridoma 7 **(E)** Hybridoma 8 to antigen stimulation. IL-2 concentration in culture supernatant was measured by ELISA after 24 hours, shown as mean IL-2 values (±SEM).

only a very low level of IL-2 produced in response to the CYP2D6 protein (1.5x background). Therefore, this hybridoma was potentially responding in a more cryptic manner to $CYP12_{445-474}$ peptide, without necessarily binding the T cell epitope in the same conformation as the native T cell epitope. Despite Hybridoma 7 showing very potent responses to low concentrations of $CYP12_{445-474}$ 30mer and $CYP12.2_{450-464}$ 15mer, as Hybridomas 4 and 6 had more distinctive responses to the protein antigen, Hybridoma 7 was not analysed in further screens. The final hybridoma screened, Hybridoma 8 (Fig.5.9E) was only able to produce low levels of IL-2 in response to $CYP12_{445-474}$ 30mer peptide (1.14x background) and $CYP12.2_{450-464}$ 15mer (1.15x background), as well as low response to the CYP2D6 protein (1.5x background).

In all cases, stimulation with CYP2D6 protein induced maximal IL-2 production at 1-10µg/ml of protein. When stimulated with high concentration of CYP2D6 protein, cells were not able to generate an IL-2 response. This had also been observed when stimulating human PBMCs with CYP2D6 protein in initial proliferation assays (data not shown), in which PBMCs proliferated in response to 1µg/ml of CYP2D6 protein but not to higher amounts of stimulating protein. There are a few possible reasons for this: when stimulating T cells with very strong antigens they can undergo apoptosis or conversion to T cell anergy without supporting T cell activation leading to IL-2 secretion or proliferation, alternatively the recombinant protein could contain a level of contaminants or endotoxin (although this is less likely, as we purchased the protein with confirmed endotoxin content of <0.1U/ml).

It was clear from the secondary screening experiments that $CYP12_{445-474}$ 30mer-specific T cell hybridomas responded with very high specificity to the second overlapping

15mer CYP12.2$_{450\text{-}464}$. None of the five hybridomas tested produced IL-2 above background when stimulated with 15mer CYP12.1$_{445\text{-}459}$, CYP12.3$_{455\text{-}469}$ or CYP12.4$_{460\text{-}474}$. Therefore, the T cell reactive peptide had been narrowed down from 30aa (GEPLARMELFLFFTSLLQHFSFSVPTGQPR) to 15aa (RMELFLFFTSLLQHF).

T cell hybridomas #4 and #6 generated in response to CYP12$_{445\text{-}474}$ 30mer respond when using splenocytes from HLA-DR4 mice; therefore, we wanted to ensure that human cells used as APCs would generate similar responses. A further screen was established stimulating hybridomas #4 and #6 in the presence of mouse HLA-DR4 transgenic splenocytes or human Preiss cell line expressing HLA-DR4 (Fig.5.10A-D). As we were unsure whether the kinetics of IL-2 response may differ between APCs from murine spleen and transformed human PBMC sources, IL-2 in culture supernatant was assayed at 24 and 48 hours post-stimulation. In this screen, T cell hybridomas were stimulated in triplicate with CYP12$_{445\text{-}474}$ 30mer, CYP12.2$_{450\text{-}464}$ as previously, in addition to CYP12.2$_{450\text{-}464}$ variants designed to decrease peptide hydrophobicity: CYP12.2 14mer lacking C terminal phenylalanine (CYP12.2 -F, purple bars), CYP12.2 -F 14mer with the second amino acid methionine replaced by a lysine (CYP12.2 (2K), grey striped bars) and CYP12.2 15mer with the fourth amino acid leucine replaced by a lysine (CYP12.2 (2K), black and grey hashed bars). Figure 5.10 shows that for both CYP12$_{445\text{-}474}$ specific hybridomas, whether cultured with murine or human HLA-DR4^{+} APCs, IL-2 response is maintained between CYP12.2$_{450\text{-}464}$ and CYP12.2 -F where the 15th amino acid has been removed. Hydrophobicity of the peptide can be reduced by removal of the aromatic residue phenylalanine without affecting T cell hybridoma response. Therefore, this CYP12.2$_{450\text{-}464}$ modification does not affect the minimally required T cell epitope. Building on this result,

Figure 5.10: Testing the IL-2 response of HLA-DR4 T cell Hybridoma #4 and Hybridoma #6 to $CYP12_{445-474}$ peptide variants at 24h and 48h with HLA-DR4 splenocytes or human EBV-LCL as antigen-presenting cells

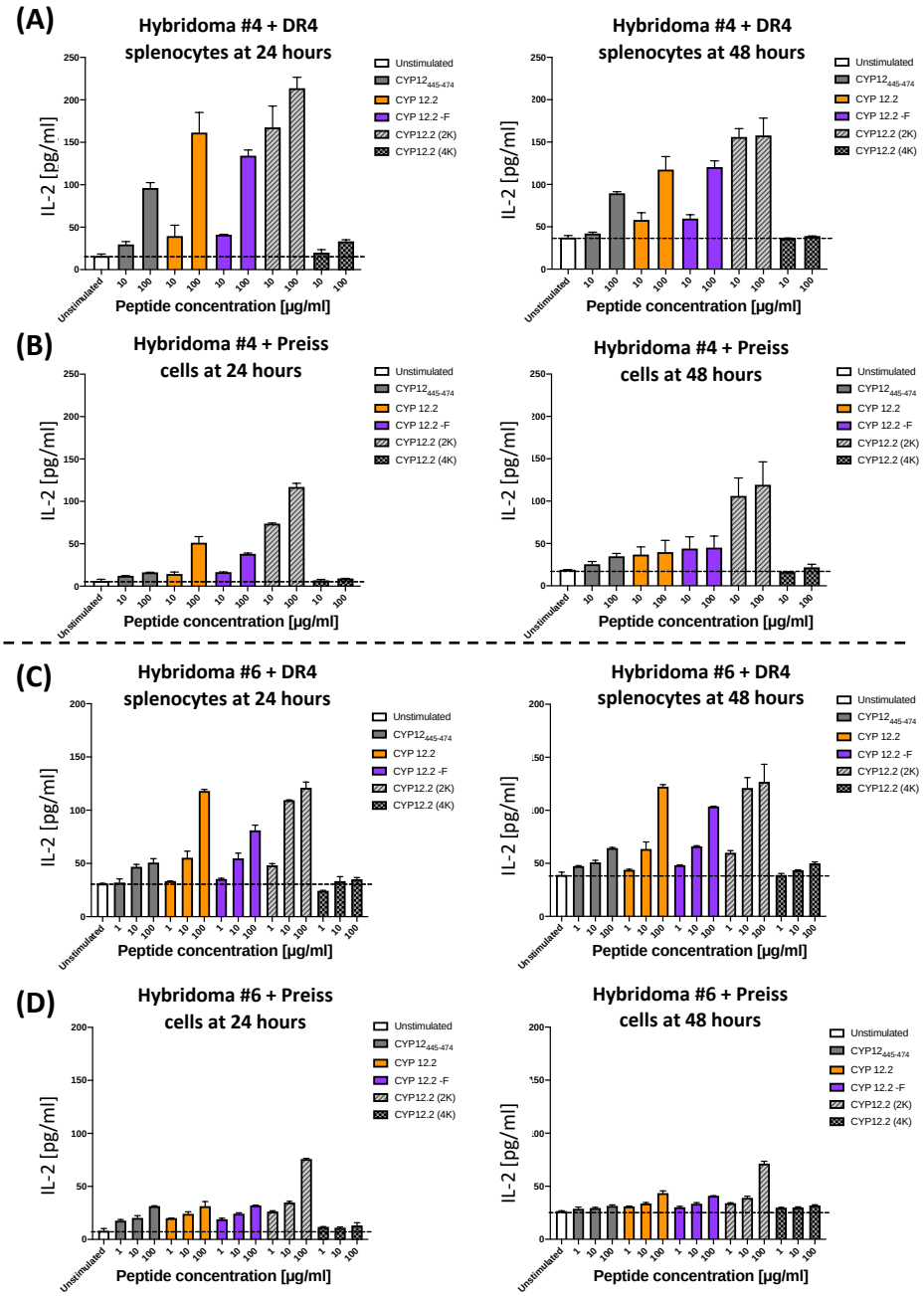

Figure 5.10: Screening $CYP12_{445-474}$ T cell hybridoma #4 and hybridoma #6 using mouse splenocytes or human HLA-DR4 restricted cell line as APCs at 24h or 48h. Hybridoma #4 or #6 were plated at $1x10^5$ cells/well with either $2x10^5$ cell/well irradiated HLA-DR4 transgenic irradiated splenocytes or human Preiss cells (HLA-DR4 expressing EBV-LCL).

Antigen stimulation conditions were set up in triplicate. Hybridoma #4 and #6, both strongly specific for $CYP12_{445-474}$ were tested for response to $CYP12_{445-474}$ variant peptides using both HLA-DR4 transgenic splenocytes (**A & C**) and human Preiss cells (**B & D**) at 24 hours (left panels) and 48 hours (right panels) after stimulation. IL-2 in culture supernatant was measured by ELISA in duplicate; mean IL-2 values (±SEM).

CYP12.2 (2K) where the final Phe is omitted and the hydrophobic 2nd amino acid, Met, is exchanged for hydrophilic residue, Lys, in fact increases the IL-2 response of $CYP12_{445-474}$

CYP12.2$_{450-464}$ PEPTIDE VARIANTS	
Peptide name	**Peptide sequence**
KKK CYP12.2 KKK	KKKRMELFLFFTSLLQHFKKK
CYP12.2 -F	RMELFLFFTSLLQH
KKK CYP12.2 -F KKK	KKKRMELFLFFTSLLQHKKK
CYP12.2 (2K)	RKELFLFFTSLLQH
CYP12.2 (4K)	RMEKFLFFTSLLQH
CYP12.2 (5K)	RMELKLFFTSLLQH
CYP12.2 (6K)	RMELFKFFTSLLQH
CYP12.2 (7K)	RMELFLKFTSLLQH
CYP12.2 (8K)	RMELFLFKTSLLQH
CYP12.2 (11K)	RMELFLFFTSKLQH
CYP12.2 (12K)	RMELFLFFTSLKQH

specific T cell hybridomas. Potentially, significantly decreasing the hydrophobicity of the peptide (GRAVY score $CYP12.2_{450-464}$ = 0.81 vs CYP12.2 (2K) = 0.25) improves the bio-availability of soluble peptide within the culture, meaning that APCs actually have access to a higher concentration of bioavailable peptide and can subsequently increase T cell activation. In contrast, CYP12.2 (4K) where the final Phe is omitted and the hydrophobic 4th amino acid, Leu, is exchanged for hydrophilic residue, Lys, knocks out the IL-2 response of $CYP12_{445-474}$ specific T cell hybridomas regardless of APC used. Therefore, the 4th amino acid of $CYP12.2_{450-464}$ must be part of the minimal T cell epitope either required for MHC-II peptide binding or T cell recognition. From the data presented in Figure 5.10,

we can conclude that both hybridoma #4 and #6 respond when CYP12.2$_{450\text{-}464}$ is modified at the 15th and 2nd residue, but not the 4th. As such, the working peptide for CYP12.2$_{450\text{-}464}$ can be further fine-tuned from 15aa (RMELFLFFTSLLQHF) to 14 aa (RKELFLFFTSLLQH).

Comparison between the IL-2 responses of T cell hybridomas when cultured with murine or human APCs (Fig.5.10A&B and Fig.5.10C&D) indicates that the human-derived Preiss cells are similarly able to process and present CYP12$_{445\text{-}474}$ peptides and 15mer variants. However, the amount of IL-2 produced by stimulated T cell hybridomas was lower with Preiss vs spleen cells. This could be described by EBV-LCLs having different antigen-processing properties to primary APCs, or that EBV-LCLs are less efficient at antigen-presentation than irradiated HLA-DR4 splenocytes. IL-2 concentration in cell culture supernatant at 24 hours and 48 hours follow overall very similar patterns; however, at 48 hours background IL-2 in each condition is slightly increased, therefore reducing the difference between unstimulated and stimulated wells. As such, we could determine that there was no benefit to measuring IL-2 at the later time point of 48 hours with either HLA-DR4 splenocytes or Preiss cells.

To complete mapping the T cell epitope for CYP12$_{445\text{-}474}$ peptide in context of HLA-DR4, a final screen with a wider range of more hydrophilic variants to CYP12.2$_{450\text{-}464}$ was completed (Fig.5.11). In this screen, Preiss cells were used as the APC source to avoid the need for HLA-DR4 mice and improve working practices in line with the 3Rs. The effect of blocking access to HLA-DR was also assessed, by pre-treating the cells with 10µg/ml anti-HLA-DR antibody (Biolegend, L234; Fig. 5.11, turquoise bars) 2 hours prior to peptide

Figure 5.11: Epitope mapping HLA-DR4 T cell hybridoma #6 responsive to CYP12$_{445-474}$ peptide

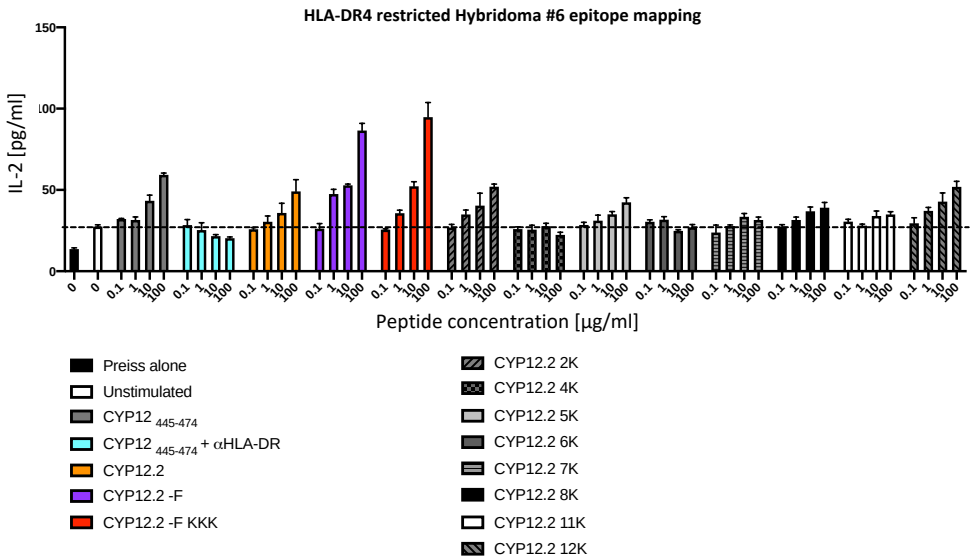

Figure 15.11: Final epitope mapping screen of CYP12$_{445-474}$ T cell hybridoma #6. Hybridoma #6, specific for CYP12$_{445-474}$ was tested for IL-2 production in response to CYP12$_{445-474}$ variant peptides using Preiss cells at 24 hours after stimulation. Hybridoma #6 was plated at 2x10^5 cells/well with 2x10^5 cell/well Preiss cells. Antigen stimulation conditions were set up in duplicate. IL-2 in culture supernatant was measured by ELISA in duplicate; mean IL-2 values (±SEM). To confirm HLA-DR4-restriction of CYP12$_{445-474}$ peptide, cells were incubated for 2 hours prior to peptide activation with 10µg/ml anti-HLA-DR antibody (Biolegend, L234; turquoise bars). CYP12.2 15mer was adapted to remove 15th residue Phe (CYP12.2 –F, purple bars), and addition of 3 Lys residues at both N and C terminal (CYP12.2 –F KKK, red bars). CYP12.2 –F 14mer was edited to replace each hydrophobic residue with a hydrophilic lysine (CYP12.2 2K-12K, grey and black bars).

stimulation. This data very clearly shows that presentation of the T cell epitope within the $CYP12_{445-474}$ 30mer is reliant on HLA-DR. When the L234 antibody is bound to HLA-DR, TCR engagement is prevented, and no activation-induced IL-2 is produced. As previously, CYP12.2 -F (Fig. 5.11, purple bars) increases IL-2 above that of the native 15mer peptide, potentially due to improved solubility and bioavailability. A version of the CYP12.2 -F peptide with 3 additional Lys residues at both N and C terminals (KKKRMELFLFFTSLLQHFKKK; Fig. 5.11, red bars) to further decrease average hydropathy to -0.54 and further improve solubility was added to this screen. This improved CYP12.2 -F KKK peptide also stimulates strong T cell hybridoma activation inducing almost identical levels of IL-2 to the CYP12.2 -F peptide. Therefore, we can greatly improve solubility of this T cell epitope containing peptide without affecting T cell recognition of the minimal epitope. $CYP12.2_{450-464}$ variants in which each of the hydrophobic amino acids was replaced by a Lys residue (CYP12.2 2K-12K, Fig. 5.11; grey and black bars) give an important insight into whether further hydropathy improvements can be made whilst maintaining T cell recognition. Exchange of a hydrophobic residue for a charged, hydrophilic Lys may be a viable option at residues outside of the minimal epitope, if such a change does not affect binding to the MHC-II cleft. However, such a significant change within the T cell minimal epitope would almost certainly significantly affect either MHC-II binding or TCR docking. In particular, within the $CYP12.2_{450-464}$ sequence (RMELFLFFTSLLQH) exchange of Leu → Lys adds a much larger amino acid side chain, and Phe → Lys changes a large aromatic/polar side chain for a large flexible charged side chain. Based on the epitope mapping data of Figure 5.11 and previous screen in Fig. 5.10, exchange of 2nd residue Met→Lys in CYP12.2 2K does not affect T cell hybridoma IL-2 production. Residue exchanges at position 4 (Leu→Lys), position 6

(Leu→Lys), position 7 (Phe→Lys) and position 11 (Leu→Lys) all significantly reduced, or completely knocked out the IL-2 response of the $CYP12_{445-474}$ specific hybridoma even at high peptide concentration, indicating that these amino acid positions are either essential for MHC-II binding or TCR recognition, and that changing any of these residues for a lysine too greatly affects these interactions. As such, $CYP12.2_{450-464}$ cannot be edited at position 4, 6, 7 or 11. Interestingly, peptides CYP12.2 5K and CYP12.2 8K, with amino acid exchanges at position 5 (Phe→Lys) and at position 8 (Phe→Lys) respectively, did show IL-2 production above background in response to increasing peptide concentration, especially at 10 and 100µg/ml. At 100µg/ml peptide concentration, CYP12.2 5K reduced the amount of IL-2 produced by 14% compared to the native $CYP12.2_{450-464}$ peptide, and CYP12.2 8K reduces IL-2 produced by 20%. As such, these residues positioned centrally within the $CYP12.2_{450-464}$ peptide may not be essential for TCR engagement; however, they do have a reduced capacity to generate T cell response of the $CYP12_{445-474}$ specific hybridoma, so these alterations may not be optimal if taking these peptides forward for tolerogenic purposes. More hybridoma screening experiments would need to be undertaken to confirm this trend; unfortunately, these experiments were not possible to complete during the timeframe of this project. The final peptide, CYP12.2 12K with amino acid modification at position 12 (Leu→Lys), produces the same level of IL-2 to the native $CYP12.2_{450-464}$ peptide; therefore, it is likely that this amino acid is non-essential for MHC-II/TCR interactions and is likely to be able to be altered without affecting T cell engagement.

Figure 5.12: Specific CYP12$_{445-474}$ peptide variants can elicit DR4 T cell hybridoma #6 response without antigen processing

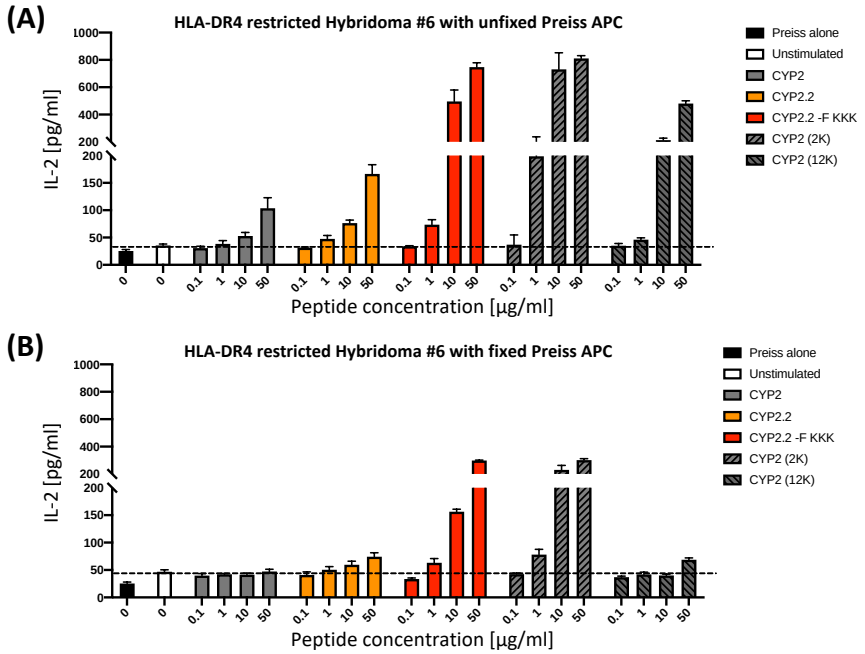

Figure 5.12: Identification of antigen-processing independent CYP12$_{445-474}$ peptide variants. Hybridoma #6, specific for CYP12$_{445-474}$ was tested for IL-2 production in response to CYP12$_{445-474}$ variant peptides using **(A)** live Preiss cells or **(B)** fixed Preiss cells 24 hours after stimulation. Hybridoma #6 was plated at 1x10^5 cells/well with 2x10^5 cell/well live or fixed Preiss cells prior to antigen stimulation in triplicate. Fixed Preiss cells were pre-treated with 0.5% PFA. IL-2 in culture supernatant was measured by ELISA in triplicate; mean IL-2 values (±SEM).

From these screening experiments, we can determine that the CYP12.2$_{450\text{-}464}$ 15mer peptide contains the relevant T cell epitope, it can be edited to remove the final Phe (CYP12.2 -F) and additional lysines can be added to improve hydropathy and solubility (CYP12.2 -F KKK), without affecting T cell hybridoma response to peptide. Furthermore, amino acid at position 2 and 12 can be replaced with an additional Lysine without altering IL-2 response of T cell hybridoma. As such, the minimal epitope for T cell stimulation is isolated between 2nd and 12th amino acid of CYP12.2$_{450\text{-}464}$, 15mer sequence RMELFLFFTSLLQH → minimal epitope 9aa ELFLFFTSL.

To complete T cell epitope mapping for this peptide, we would need to confirm that the T cell hybridoma specific to 30mer CYP12$_{445\text{-}474}$ is stimulated effectively by the minimal epitope 9 aa peptide (ELFLFFTSL) alone, which as a 9mer is highly hydrophobic with a GRAVY score of 1.64, or whether this epitope flanked by additional lysines (KKKELFLFFTSLKKK) to decrease hydrophobicity (GRAVY score = -0.57) also engages T cell hybridoma to a similar extent as the native CYP12.2$_{450\text{-}464}$ peptide.

As a further test of peptide suitability for immunotherapy purposes was to determine if T cell epitope containing peptides can function as an antigen-independent epitope (i.e. apitope). These experiments involved comparison of T cell hybridoma response to key peptides when using live Preiss cells (as in prior experiments) or Preiss cells fixed with 0.5% PFA, which cannot process or present antigen. Figure 5.12 shows that that 30mer peptide CYP12$_{445\text{-}474}$, and 15mer CYP12.2$_{450\text{-}464}$ cannot generate a T cell hybridomas response without first undergoing antigen uptake, processing and presentation. CYP12.2 -F KKK and CYP12.2 2K peptides are however able to establish strong T cell hybridomas

responses with fixed APC, and can therefore act as apitopes, binding directly to MHC-II on the surface of APC without the need for intracellular processing. Interestingly, CYP12.2 12K which we had previously determined showed that the 12th amino acid of CYP12.2$_{450-464}$ was not essential to MHC-II binding and TCR engagement, does not establish T cell hybridoma reactivity via fixed APC and is therefore not suitable as an apitope.

As a final phase of working with this peptide, we had planned to perform tolerance induction experiments in HLA-DR4 mice. The selected apitope peptide would be delivered in as soluble form as possible (e.g. CYP12.2 2K peptide with flanking lysines) in accordance with a dose escalation protocol over 2-3 weeks, in a similar manner to the well-established previously described MBP$_{Ac1-9}$ dosage protocol *in vivo* (Burton et al., 2014). Following the peptide escalation protocol using CYP12 minimal epitope as 9mer ELFLFFTSL or improved solubility flanked by additional lysines KKKELFLFFTSLKKK, mice would then be immunised with either CYP12$_{445-474}$ 30mer or CYP2D6 protein, and later tested for draining lymph node and splenocyte recall responses to the CYP12$_{445-474}$ 30mer or CYP2D6 protein. We would then be able to determine whether tolerance induction can be established using CYP12$_{445-474}$ T cell epitope to the autoantigen CYP2D6. Due to COVID-19 disruptions, I was unable to perform this work during the timeframe of the project.

5.5.2 HLA-DR4 restricted T cell hybridomas towards CYP1$_{62-91}$

CYP1$_{62-91}$ immunised HLA-DR4 transgenic mice specifically responded to CYP1$_{62-91}$ peptide upon antigen recall of splenocytes, as measured by [^{3}H]-thymidine incorporation

Figure 5.13: Generation of T cell hybridomas from $CYP1_{62-91}$ peptide immunised HLA-DR4 transgenic mice

(A)

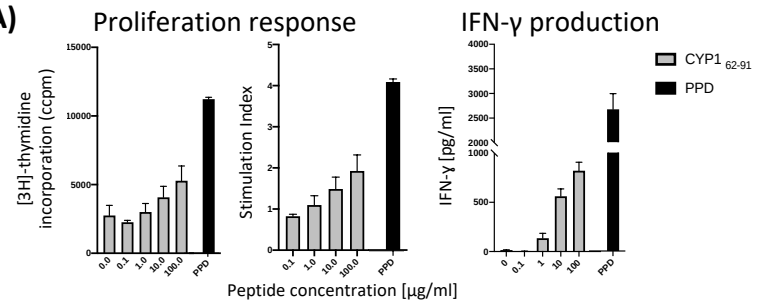

(B)

Plate dilution	Number of positive growth wells	Percentage positive growth wells
NEAT A	12	12.5
NEAT B	14	14.6
1/5 A	4	4.17
1/5 B	2	2.08
1/25 A	1	1.04

(C)

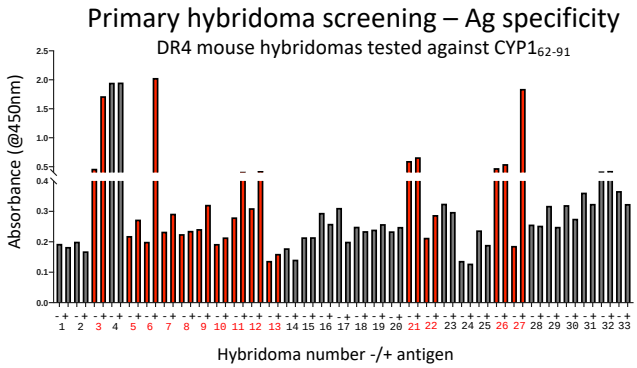

Figure 5.13: Recall responses of $CYP1_{62-91}$ immunised HLA-DR4 tg splenocytes and primary screening of T cell hybridomas. (A) HLA-DR4 transgenic mouse was immunised with $CYP1_{62-91}$ peptide and splenocytes tested for proliferation in response to $CYP1_{62-91}$ by [^{3}H]-thymidine incorporation as described previously. IFN-γ production in cell culture supernatant was measured by ELISA on day 3 post-stimulation. T cell hybridomas generated by fusion of peptide-activated splenocytes with T cell thymoma cell line, BW5147, were harvested by cell pellet growth from day 7-10. **(B)** Count of positive growth wells in each dilution condition. **(C)** Primary screen for antigen-specificity: T cell hybridomas were assessed for antigen-specific production of IL-2 by sandwich ELISA using irradiated non-immunised HLA-DR4 splenocytes as APCs. Hybridomas producing more IL-2 in antigen-stimulated condition coloured red.

(Fig.5.13A). Proliferation response upon antigen recall of immunised splenocytes did not result in a particularly high Stimulation Index, at 100µg/ml $CYP1_{62-91}$ peptide SI = 1.95; however, we proceeded with the fusion regardless. Fusion of activated splenocytes to BW5147 thymoma cells resulted in the growth of 33 cell pellets between day 7 and 10, primarily in NEAT plates (Fig.5.13B). As more than 10% of wells from NEAT plates grew successfully fused hybridomas, any antigen-specific cultures from these plates would need to be subcloned by limiting dilution to assure clonality.

As previously described any hybridomas which produced a higher amount of IL-2 when stimulated with 20µg/ml of $CYP1_{62-91}$ compared to the unstimulated control (Fig.5.13C; red bars) were moved to larger wells and taken forward for further screening. Of the 33 screened positive growth wells, 14 were responsive to antigen (42.4%).

The secondary screening data from the most promising hybridoma is shown in Figure 5.14. $CYP1_{62-91}$ specific T cell Hybridoma 6 provided the most sensitive response to $CYP1_{62-91}$ peptide of the 10 hybridomas tested with sustained growth in culture for over 2 weeks, with peak IL-2 response at low concentration of antigen, at just 1µg/ml. This hybridoma was also able to mount a robust respond to the CYP2D6 protein antigen. Although the amount of IL-2 produced when stimulated with the whole protein is low in comparison to when stimulated with peptides, the fold difference between unstimulated cells and protein simulated at 1µg/ml is 4.25x (Fig.5.14; sky blue bars). Incubation of $CYP1_{62-91}$ specific T cell Hybridoma 6 with anti-HLA-DR antibody for 2 hours prior to antigen stimulation resulted in a significant reduction in IL-2 response at 1µg/ml $CYP1_{62-91}$ peptide stimulation (Fig.5.14; turquoise bars). However, at higher peptide concentrations, anti-HLA-DR antibody was not able to block hybridoma T cell activation

and subsequent IL-2 secretion. This hybridoma exhibits extremely potent responses to $CYP1_{62-91}$ peptide, and this HLA-DR blocking condition shows that either insufficient amounts of antibody was present in the culture to knock out IL-2 production, or antibody affinity to HLA-DR is not high enough to block TCR engagement when T cells are highly sensitive to antigen.

When assessing the 6 overlapping 15mers (peptides shifting by 3 amino acids) $CYP1.1_{62-76}$ to $CYP1.6_{77-91,}$ this $CYP1_{62-91}$ specific hybridoma was not as restricted to just one of the overlapping 15mers as the previously assessed $CYP12_{445-474}$ specific hybridoma. $CYP1_{62-91}$ specific hybridoma was most sensitive (i.e. produced very high levels of IL-2 in response to the lowest amount of peptide antigen) primarily to $CYP1.4_{71-85}$ peptide (Fig.5.14; dark blue bars) and secondarily to $CYP1.2_{65-79}$ peptide (Fig.5.14; orange bars). We therefore thought it most likely that $CYP1_{62-91}$ 30mer contains 2 T cell epitopes contained within $CYP1.2_{65-79}$ and $CYP1.4_{71-85}$ 15mer peptides, particularly because when we performed in silico HLA-DR binding predictions $CYP1_{62-91}$ 30mer appeared to be rich in putative T cell epitopes. As primary candidate hybridoma 6 had originally been harvested from fusion plate NEAT 1 where >10% of wells were growth positive, there was a chance that this hybridoma was not a clonal culture of cells and that potentially there were T cells specific to both $CYP1.2_{65-79}$ and $CYP1.4_{71-85}$ within this culture. To better distinguish between $CYP1.2_{65-79}$ and $CYP1.4_{71-85}$ reactivity, hybridoma 6 was subcloned by limiting dilution at 1 and 0.1 cells/well. After 14 days, subclone cell pellets were starting to become visible and the resulting 25 subclones harvested (25 growth positive pellets/576 total wells; 4.3%) were expanded for repeated secondary screening.

Figure 5.14: Secondary screening of T cell hybridoma from $CYP1_{62-91}$ immunised HLA-DR4 transgenic mice

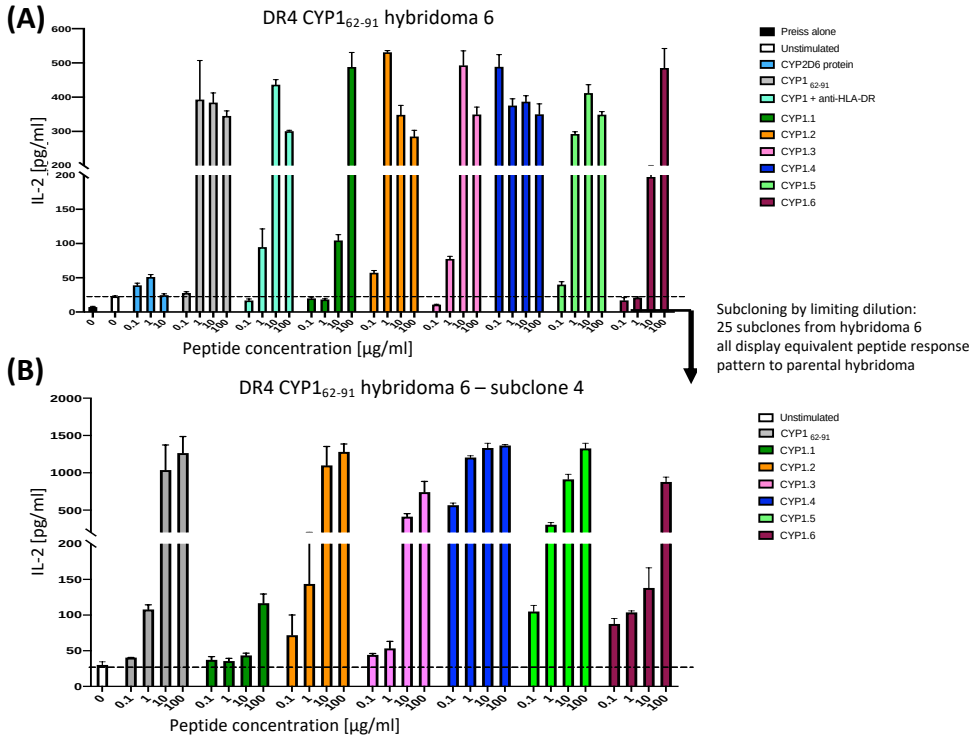

Figure 5.14: Secondary screening of $CYP1_{62-91}$ T cell hybridomas with sustained growth. Hybridoma colonies with an initial response to antigen (Fig.5.13C; red bars) and sustained growth were expanded for 7-10 days prior to secondary screen for antigen-sensitivity and response to recombinant human CYP2D6 protein. Hybridoma cells were plated in triplicate at $1x10^5$ cells/well with $2x10^5$ cell/well irradiated HLA-DR4 splenocytes for 24 hours as unstimulated cultures, or in the presence of $CYP1_{62-91}$ 30mer peptide, CYP2D6 protein, CYP1.1-CYP1.6 overlapping 15mers. IL-2 response of **(A)** Hybridoma 6, **(B)** Hybridoma 6 subclone 4 to antigen stimulation. IL-2 concentration in culture supernatant was measured by ELISA after 24 hours, shown as mean IL-2 values (±SEM).

CYP2D6 CYP1 15MER PEPTIDES	
Peptide name	**Peptide sequence**
$CYP1_{62-91}$	RRRFGDVFSLQLAWTPVVVLNGLAAVREAL
$CYP1.1_{62-76}$	RRRFGDVFSLQLAWT
$CYP1.2_{65-79}$	FGDVFSLQLAWTPVV
$CYP1.3_{68-82}$	VFSLQLAWTPVVVLN
$CYP1.4_{71-85}$	LQLAWTPVVVLNGLA
$CYP1.5_{74-88}$	AWTPVVVLNGLAAVR
$CYP1.6_{77-91}$	PVVVLNGLAAVREAL

The results from screening these 25 subclones was rather surprising, in that all 25 displayed extremely similar peptide response patterns to one another and to the parental hybridoma 6. Figure 5.14B shows a representative subclone (Number 4) tested for antigen-sensitivity in an identical assay to parental hybridoma. The data clearly shows that these subclones are able to very sensitively respond to primarily $CYP1.4_{71-85}$ and to a lesser extent, $CYP1.2_{65-79}$. The peptide sequences for these 15mer are LQLAWTPVVVLNGLA ($CYP1.4_{71-85}$) and FGDVFSLQLAWTPVV ($CYP1.2_{65-79}$) so there is a potentially significant overlap of LQLAWTPVV shared between the two 15mers which may represent a single or multiple sites for T cell epitopes. However, if indeed these T cell hybridomas are responding to the same LQLAWTPVV sequence, we would have expected CYP1.3 (VFSLQLAWTPVVVLN) to have induced similarly potent IL-2 production as this peptide also contains the full overlap region. Due to the fact that $CYP1.3_{68-82}$ stimulates lower T cell hybridoma activation than its neighbouring peptides, it is more likely perhaps that these hybridomas are responding with highest affinity to $CYP1.4_{71-85}$ but that there is some promiscuity between this T cell epitope and another, different T

cell epitope within CYP1.2$_{65-79}$ or that the CYP1.3$_{68-82}$ contains a sequence that, in this case, either inhibits processing or restricts the conformation of the peptide in a less favourable state.

In the next step of mapping T cell epitope(s) within CYP1$_{62-91}$ 30mer, we designed a collection of CYP1.4$_{71-85}$ peptides with truncations. Starting with the native CYP1.4$_{71-85}$ 15mer (LQLAWTPVVVLNGLA) successive peptides removed one amino acid from the N terminus or the C terminus.

CYP2D6 CYP1.4$_{71-85}$ TRUNCATED PEPTIDES	
CYP1.4 N-1	QLAWTPVVVLNGLA
CYP1.4 N-2	LAWTPVVVLNGLA
CYP1.4 N-3	AWTPVVVLNGLA
CYP1.4 N-4	WTPVVVLNGLA
CYP1.4 N-5	TPVVVLNGLA
CYP1.4 N-6	PVVVLNGLA
CYP1.4 C-1	LQLAWTPVVVLNGL
CYP1.4 C-2	LQLAWTPVVVLNG
CYP1.4 C-3	LQLAWTPVVVLN
CYP1.4 C-4	LQLAWTPVVVL
CYP1.4 C-5	LQLAWTPVVV
CYP1.4 C-6	LQLAWTPVV

Previously described CYP1$_{62-91}$ specific hybridoma 6 subclone 4 was used in this screen, with peptides presented by Preiss cells. Figure 5.15 displays antigen-specific IL-2 production by this hybridoma in response to CYP1$_{62-91}$ 30mer, CYP1.4$_{71-85}$ 15mer and successively truncated peptides. This assay determined that removal of the first 2 N

Figure 5.15: Fine mapping of T cell epitope within CYP1.4 using $CYP1_{62-91}$ specific Hybridoma 6 Subclone 4

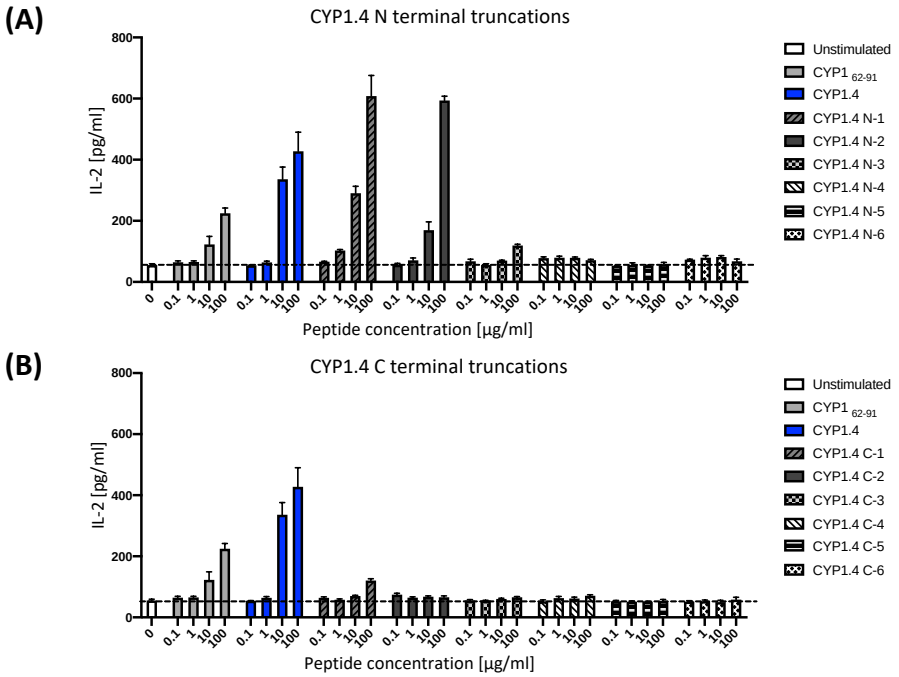

Figure 5.15: Final epitope mapping screen of $CYP1_{62-91}$ T cell hybridoma 6 subclone 4 using CYP1.4 peptide truncations. Subclone 4, specific for $CYP1_{62-91}$ was tested for IL-2 production in response to CYP1.4 variant peptides using Preiss cells at 24 hours after stimulation. Hybridoma was plated at $1x10^5$ cells/well with $2x10^5$ cell/well Preiss cells. Antigen stimulation conditions were set up in triplicate. IL-2 in culture supernatant was measured by ELISA in duplicate; mean IL-2 values (±SEM). **(A)** IL-2 production by $CYP1_{62-91}$ specific hybridoma towards $CYP1_{62-91}$, CYP1.4 and successive truncated peptides removing 1 amino acid per peptide from N terminus. **(B)** IL-2 production by $CYP1_{62-91}$ specific hybridoma towards $CYP1_{62-91}$, CYP1.4 and successive truncated peptides removing 1 aa per peptide from C terminus.

Figure 5.16: Specific CYP1$_{62-91}$ peptide variants can elicit DR4 T cell hybridoma subclone #4 response without antigen processing

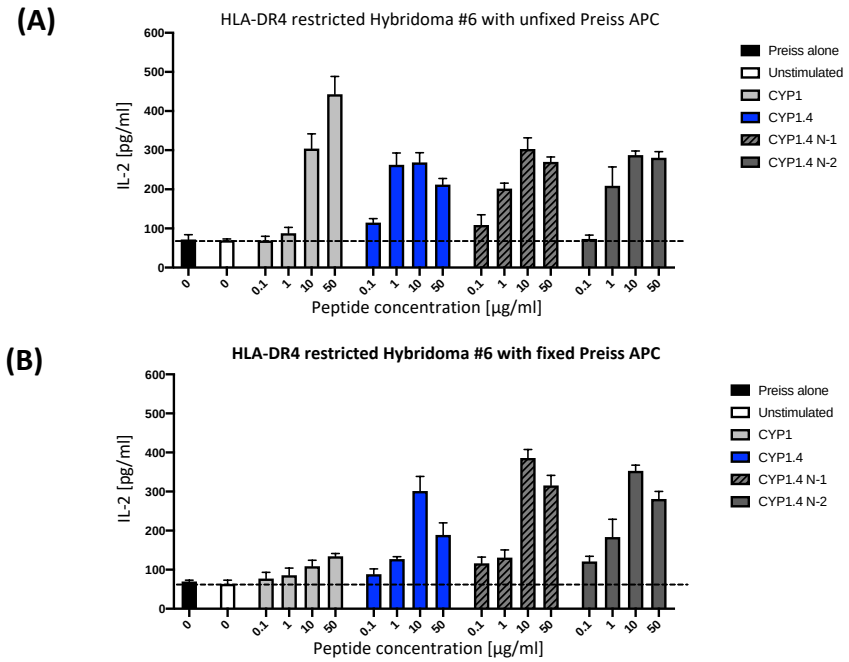

Figure 5.16: Identification of antigen-processing independent CYP1$_{62-91}$ peptide variants. Hybridoma #6, specific for CYP1$_{62-91}$ was tested for IL-2 production in response to CYP1$_{62-91}$ variant peptides using **(A)** live Preiss cells or **(B)** fixed Preiss cells 24 hours after stimulation. Hybridoma #6 was plated at 1x10^5 cells/well with 2x10^5 cell/well live or fixed Preiss cells prior to antigen stimulation in triplicate. Fixed Preiss cells were pre-treated with 0.5% PFA. IL-2 in culture supernatant was measured by ELISA in triplicate; mean IL-2 values (±SEM).

terminal amino acids did not negatively affect T cell hybridoma activation (Fig.5.15A; CYP1.4 N-1 and CYP1.4 N-2). In fact, these truncated versions of $CYP1.4_{71\text{-}85}$ moderately increased IL-2 production, as these peptides both removed the 1st residue (Leu) the peptides were likely to be more hydrophilic than the native $CYP1.4_{71\text{-}85}$ peptide and may exhibit increased solubility. However, truncation of 3rd N terminal amino acid significantly impaired T cell hybridoma activation – strongly indicating that this residue is required for either MHC-II binding or TCR engagement and is therefore part of the minimal T cell epitope. Following on with truncations of 4th- 6th amino acids from the N terminal direction completely ablated IL-2 response. Truncations in the C terminal direction proved to be less well tolerated; as even removal of the final residue of CYP1.4 C-1 severely impaired IL-2 production by the T cell hybridoma (Fig.5.15B). Successive peptides with further C terminal truncations (CYP1.4 C-2 to C-6) all prevented T cell hybridoma activation, providing strong evidence that the minimal T cell epitope for $CYP1_{61\text{-}92}$ 30mer within $CYP1.4_{71\text{-}85}$ is C terminally biased. As a result of this truncation screen, we can determine that $CYP1.4_{71\text{-}85}$ 15mer (LQLAWTPVVVLNGLA) specific T cell hybridoma response can be further narrowed down to 13 amino acids (LAWTPVVVLNGLA) essential for maintenance of IL-2 production. These 13 amino acids are likely to represent the minimal T cell epitope of 7-9 amino acids actually bound by cognate TCR upon T cell activation, with additional flanking residues which are essential for MHC-II cleft docking.

As with the previously identified minimal T cell epitope, the identified peptide (LAWTPVVVLNGLA) derived from $CYP1_{61\text{-}92}$ specific T cell hybridoma required further testing to identify whether the peptide acts as an apitope. Figure 5.16 shows the

response of subclone 4 to $CYP1_{61-92}$ peptides using either fixed or unfixed Preiss cells as APCs. 15mer $CYP1.4_{71-85}$ can generate T cell hybridoma response without first undergoing antigen uptake, processing and presentation (Fig.5.16; blue bars). CYP1.4 N-1 and CYP1.4 N-2 can also both establish strong T cell hybridomas responses with fixed APC, and can therefore act as apitopes, binding directly to MHC-II on the surface of APC without the need for intracellular processing. As such, minimal peptide CYP1.4 N-2, LAWTPVVVLNGLA, is able to function as an apitope and would have benefitted from tolerance induction potential in vivo. Final testing proposed would follow the same course of planned tolerance induction experiments in HLA-DR4 mice to identify whether CYP1.4 N-2 LAWTPVVVLNGLA treated mice can no longer mount T cell responses to either the $CYP1_{62-91}$ 30mer of the whole protein CYP2D6.

5.5.3 HLA-DR3 restricted T cell hybridomas

HLA-DR3 mice were also utilised in T cell hybridoma generation protocols. However, HLA-DR3 mice still expressed low levels of endogenous MHC-II, therefore experiments were planned to utilise blocking αHLA-DR mAb to show peptide HLA-DR restriction. We had also planned experiments using the commercially available HLA-DR3+ VAVY cell line (ATCC) as APCs.

Fusion experiments were conducted with $CYP1_{62-91}$ and $CYP12_{445-474}$ immunised HLA-DR3, of which splenocytes responded to $CYP1_{62-91}$ and $CYP12_{445-474}$ antigen recall in vitro (Fig.5.17; $CYP1_{62-91}$). In general, the fusions with HLA-DR3 splenocytes took longer to grow visible cell colony pellets, harvesting the majority of cell pellets between 10-13 days post-fusion. Outgrown $CYP12_{445-474}$ hybridomas were deemed not to be antigen-specific.

Figure 5.17: Generation of T cell hybridomas from $CYP1_{62-91}$ peptide immunised HLA-DR3 transgenic mice

(A) Immunisation response – proliferation

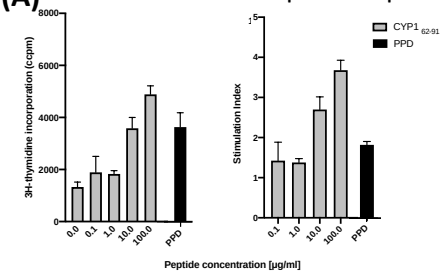

(B)

Plate dilution	Number of positive growth wells	Percentage positive growth wells
NEAT A	17	17.7
NEAT B	14	14.6
1/5 A	1	2.08
1/5 B	1	2.08

(C) Primary hybridoma screening – Ag specificity

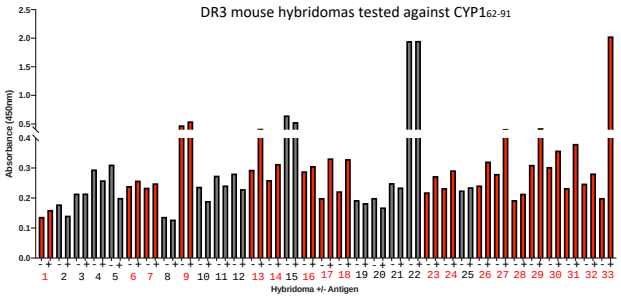

Figure 5.17: Recall responses of $CYP1_{62-91}$ immunised HLA-DR3 transgenic mouse splenocytes and primary antigen screening of T cell hybridomas. (A) HLA-DR3 transgenic mouse was immunised by subcutaneous injection of 100µg of $CYP1_{62-91}$ peptide in 100µl CFA (supplemented with 8mg/ml MTb). Splenocytes harvested 10 days post-immunization were tested for proliferation in response to $CYP1_{62-91}$ by [^{3}H]-thymidine incorporation after 3 days. T cell hybridomas generated by fusion of peptide-activated splenocytes with T cell thymoma cell line, BW5147, were harvested according to cell pellet growth by day 7-10. **(B)** The number of positive growth wells in each dilution condition were recorded. **(C)** T cell hybridomas were analysed for antigen-specific production of IL-2 by sandwich ELISA in the primary screen using irradiated non-immunised HLA-DR3 splenocytes as APCs.

Figure 5.17C shows that 18/33 (54.5% antigen-responsive; red bars) of T cell hybridomas harvested for the primary screen produced more IL-2 when stimulated with $CYP1_{62\text{-}91}$ 30mer peptide. Hybridoma 33 was the most promising of these cultures, having the greatest fold difference between stimulated vs unstimulated conditions. Hybridoma 33 was also harvested as the only positive growth well from the 1/5 dilution plate and is, therefore, highly likely to be clonal. Hybridoma 33 was taken forward for secondary screening using HLA-DR3 splenocytes as APC to assess antigen sensitivity and response to whole CYP2D6 protein. Hybridoma 33 responded strongly to CYP2D6 protein suggesting that the T cell epitope(s) responsible for $CYP1_{62\text{-}91}$ reactivity is a native processed and presented peptide (Fig.5.18A; turquoise bars). Similarly to the HLA-DR4 $CYP1_{62\text{-}91}$ specific hybridomas, the dominant response of HLA-DR3 hybridoma is to $CYP1_{62\text{-}91}$ 15mers $CYP1.2_{65\text{-}79}$ and $CYP1.4_{71\text{-}85}$. Whether this HLA-DR3 T cell hybridoma is responding to the same minimal epitope region(s) as the HLA-DR4 T cell hybridoma has yet to be determined as I was unable to complete T cell epitope mapping for this line.

It is promising that from both HLA-DR4 and HLA-DR3 transgenic T cell hybridomas raised to $CYP1_{62\text{-}91}$, both show very similar patterns of reactivity to $CYP1.2_{65\text{-}79}$ and $CYP1.4_{71\text{-}85}$. We were concerned that there was potential for the HLA-DR3 mouse to express MHC-II I-A^b and potentially even a hybrid molecule of HLA-DR3- I-A^b. However, it is highly unlikely that the MHC-II or hybrid MHC-HLA would present $CYP1_{62\text{-}91}$ peptide in the same way as HLA-DR3 standard dimer. We could have tested that the $CYP1_{62\text{-}91}$ hybridoma is restricted to HLA-DR3 by repeating the 15mer screen using the VAVY HLA-DR3 homozygous EBV-LCL line with blocking αHLA-DR mAb.

Figure 5.18: Generation of T cell hybridomas from $CYP1_{62-91}$ peptide immunised HLA-DR3 transgenic mice

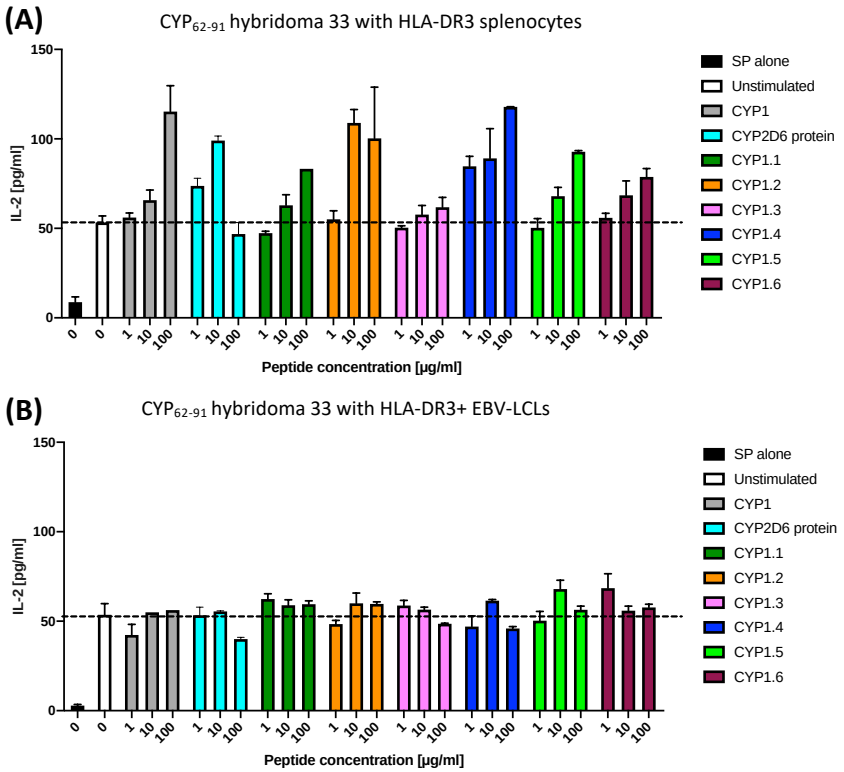

Figure 5.18: Secondary screening of $CYP1_{62-91}$ T cell hybridoma 33 using either HLA-DR3 splenocytes or human EBV-LCL as APCs. Hybridoma colonies with an initial response to antigen and sustained growth were expanded for 7-10 days prior to secondary screen for antigen-sensitivity and ability to be primed by both murine and human HLA-DR3$^+$ APCs. Hybridoma cells were plated in duplicate at $1x10^5$ cells/well with $2x10^5$ cell/well HLA-DR3 splenocytes **(A)** or irradiated EBV-LCL cells **(B)** for 24 hours as unstimulated cultures, or in the presence of CYP1 30mer peptide, CYP2D6 protein and CYP1.1-CYP1.6 overlapping 15mers. IL-2 concentration in culture supernatant was measured by ELISA after 24 hours and displayed as mean IL-2 values (±SEM).

5.6 Discussion

In this Chapter we describe different methods to identify and isolate rare autoantigen specific $CD4^+$ T cells, which may only represent 0.1-10 cells per $1x10^6$ of $CD4^+$ T cells and the selection of T cell hybridomas as our primary route to mapping T cell epitopes from the autoantigen CYP2D6.

We were unable to expand antigen-specific CD4+ T cells using the traditional re-stimulation method, despite multiple attempts with different donors and changing elements of the protocol. Each time, by the end of the third re-stimulation, the cells started to lose antigen-specificity and had increased background proliferation which we believe to have been linked to reactivity towards human AB serum over the 6-8 weeks in culture. Due to our route of PBMC acquisition being leukocyte cones which are supplied as cellular blood fraction without autologous plasma, we were not able to test whether the use of autologous plasma in culture removed this issue.

We developed a flow cytometry-based method to identify antigen-reactive CD4+ T cells from PBMC culture via the expression of activation induced markers and proliferation. This approach yielded a number of 50 cell pools post-sorting which expressed high levels of CD25 and OX40 or CD25 and CD71 after 8 days of stimulation with CYP2D6 peptides and control antigens. The combination of CTV^{low} (i.e. cells that have gone through at least one round of division) and $CD25^+CD71^+$ appeared to provide the most suitable selection criteria when cell sorting for antigen-specificity, as when these pools were expanded, they exhibited strong specificity for the CYP2D6 30mer peptide. Unfortunately, we did not get so far as to have optimised the final single cell cloning step of this experiment, which would have enabled the generation of clonal

populations of autoantigen-specific cells. If we had had more time to have assessed different cloning strategies for this step, we could have generated a library of CYP2D6 peptide specific clones from different donors, of which we could have then assessed the TCR repertoire of the clones to identify whether CYP2D6 peptide-specific $CD4^+$ T cells were biased towards use of particular TCR chains and whether this bias was shared amongst different donors. Eventually, this technique was planned to have been used to isolate CYP2D6 peptide-specific $CD4^+$ T cells from both healthy donors and AIH-2 patients to assess differences in cell frequency, functionality and TCR repertoire.

Simultaneously to developing the AIM assay, we started to utilise the HLA-DR transgenic mouse models we had available to generate antigen-specific T cell hybridomas. This approach enables the effective immortalisation of an antigen-specific T cell by fusion to the thymoma cell line, therefore multiple sequential screening experiments are possible. With cloned human primary T cells, screening experiments would have needed to have been completed within the course of 2-3months, after which time these cell lines can become unstable or lose the ability to proliferate. T cell hybridomas derived from HLA-DR transgenic mice are highly useful tools to determine peptide compatibility with human HLA-DR and to perform detailed T cell epitope mapping, however, it is important to note that they are derived based on murine antigen-processing pathways and from the murine T cell repertoire which may differ from human T cell repertoire.

Our experiments successfully generated HLA-DR4 restricted T cell hybridomas towards CYP2D6 candidate 30mer peptides $CYP1_{62\text{-}91}$ and $CYP12_{445\text{-}474}$ both of which were highly reactive in key AIH patient PBMC populations – $CYP1_{62\text{-}91}$ being pan-reactive in all

AIH groups and healthy donors and $CYP12_{445-474}$ being specifically identified in paediatric AIH2 patients. Detailed T cell epitope screening revealed the minimal epitope of $CYP1_{62-91}$ to be CYP1.4 N-2, LAWTPVVVLNGLA, CYP2D6 aa73-85, and of $CYP12_{445-474}$ to be CYP12.2 peptide ELFLFFTSL, CYP2D6 aa452-460. The identification of these two T cell epitope from CYP2D6 map surprisingly closely to the epitope prediction algorithm outputs (Fig.4.1). Both epitopes were predicted to have pan-HLA-DR binding potential, which may give these peptides the potential for delivery as a peptide-specific immunotherapy in a more diverse population of AIH-2 patients. To test whether these peptides are able to bind to multiple HLA-DR variants, we would need to assess peptide presentation on other HLA-DR+ human derived lines, e.g. HLA-$DR3^+$ EBV-LCL VAVY line or primary APCs isolated from PBMC to identify whether the HLA-DR4 restricted T cell hybridomas and isolated primary T cell lines are still able to respond when the peptides are presented in different HLA-DR contexts. We were given confidence that potentially the $CYP1_{62-91}$ is presented similarly between HLA-DR4 and HLA-DR3 molecules, as the only successful hybridoma from the HLA-$DR3^+$ mice responded maximally to the same CYP1.4 peptide in a HLA-DR dependent manner, as in the HLA-$DR4^+$ context.

T cell hybridoma generation attempts directed towards $CYP6_{235-264}$, $CYP8_{315-337}$, $CYP3_{125-154}$ and $CYP10_{366-395}$ had also been completed (2 mice per peptide, data not shown). These fusions did not yield peptide-specific T cell hybridomas for use in further screening experiments. In the case of $CYP6_{235-264}$, we had generated T cell hybridomas that had shown antigen-specificity in the primary screen, but had to freeze these cells away at a very early timepoint in their development (100-200,000 cells per well) due to University closure in March 2020. When these cells were assessed for antigen-specificity after thawing, they had poor survivability. Due to COVID19 disruption to research

progress, we were unable to repeat these experiments to expand our bank of CYP2D6 30mer specific T cell hybridomas. In the case of $CYP6_{235\text{-}264}$ and $CYP8_{315\text{-}337}$ which had been identified as highly immunogenic peptides in AIH2 adult and AIH1 adult patient cohorts, respectively, repeating these fusions would have been high priority to enable T cell epitope mapping of these peptides. We would have liked to have performed more fusions from CYP2D6 peptide immunised HLA-DR3 mice to better assess whether we found the same T cell epitope in both HLA-DR4 and HLA-DR3 contexts. The HLA-DR7 transgenic mice arrived at the start of my third year on the project from Astra-Zeneca Sweden, and we would have performed similar experiments in this model, as HLA-DR7 has previously been linked as a risk factor for AIH2. Unfortunately, these mice expressed the full complement of endogenous mouse MHC-II, therefore to have enjoyed maximal potential from this model, we would have needed to backcross them onto the Ab^0 background to leave just the transgenic HLA-DR7 as the only MHC-II available for peptide presentation to $CD4^+$ T cells.

We planned experiments to assess the solubility and improve the bioavailability of our $CYP1_{73\text{-}85}$ epitope LAWTPVVVLNGLA and $CYP12_{452\text{-}460}$ ELFLFFTSL. As peptide solubility is key to both safety and efficacy of PIT, we had ordered our T cell epitope peptides flanked with either 2 or 3 charged lysine residues either end of the minimal epitope, which can improve peptide solubility without affecting presentation to T cells. Soluble peptides injected s.c. can reach the spleen and generate cytokine responses within 2 hours, whereas insoluble variants cannot be detected in the spleen as they are unable to disperse systemically (Shepard et al., 2021). Repeated doses of soluble peptide resulted

in antigen-specific tolerance induction, whilst insoluble peptide was not able to induce antigen-specific T cell anergy. Our experiments would have involved injecting HLA-DR4 mice with each candidate peptide and isolating the antigen-presenting cells from the spleen 2-4h later. This would allow for assessment of whether the peptides are sufficiently soluble to move systemically to reach the spleen, and whether, like previously assessed apitopes, they specifically bind to steady-state dendritic cells as opposed to monocytes or B cells.

Provided our T cell epitope peptides could act as apitopes and bind directly to ssDC in vivo, we would have then proceeded with plans to assess the tolerance induction potential of these peptides. Firstly, we would perform peptide dose escalation as previously described in the Tg4 model. HLA-DR4 and HLA-DR3 tg mice would undergo escalating dose regime of CYP1 epitope aa73-85 or CYP12 epitope aa452-460 candidate peptides, prior to immunisation with either the 30mer $CYP1_{62-91}$ or $CYP12_{445-474}$ peptide or the full length CYP2D6 protein. We could then assess whether this tolerisation protocol is sufficient to prevent immune responses towards the 30mer peptide, and whether bystander suppression is activated to reduce responses to the CYP2D6 protein. Previously when developing tolerogenic peptides for MS, mixtures of peptides have been utilised to generate strong MBP-specific suppression and to control T cell responses specific to other autoantigens MOG and PLP. We would also test whether our CYP2D6 peptides functioned sufficiently as a single peptide or best as a cocktail.

Admittedly, completing the full experiment plan within the final year of the PhD was ambitious, but I do think that we would have been able to perform the experiments described above and to determine the tolerogenic potential of the $CYP1_{61-92}$ and $CYP12_{445-}$

$_{474}$ epitope peptides. Mapping other disease-relevant regions of CYP2D6 (especially CYP6$_{235\text{-}264}$ and CYP8$_{315\text{-}337}$) using the T cell hybridoma method would have been attempted.

Ultimately, assessment of peptide properties and tolerance induction would have generated sufficient data to determine whether our T cell epitope peptides from CYP2D6 had potential for development of a novel peptide-based immunotherapy to treat autoimmune hepatitis type 2. We had already established a collaboration with Urs Christen, University of Frankfurt to test whether these peptides could prevent AIH-2 like disease in his hCYP2D6 expressing mouse model. This would have formed the basis of funding applications to continue this work and ensure that all relevant pre-clinical data acquisition was performed with view to performing a clinical trial in AIH2 patients, similar to those carried out previously using apitopes.

Planned/future experiment overview

1. Expand T cell hybridoma library to include CYP6$_{235\text{-}264}$ and CYP8$_{315\text{-}337}$ specific hybridomas and HLA-DR3 restricted hybridomas.

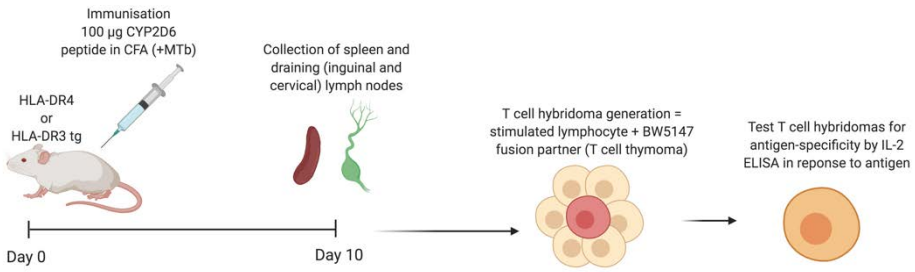

2. Assess solubility of candidate tolerogenic T cell epitope peptides and targeting to APC subsets.

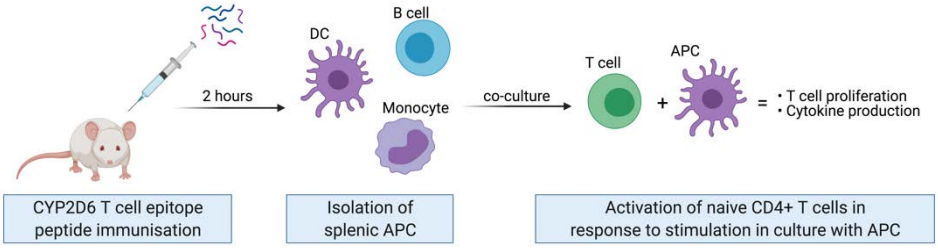

3. Assess candidate tolerogenic T cell epitope peptides ability to induce CYP2D6 specific anergy.

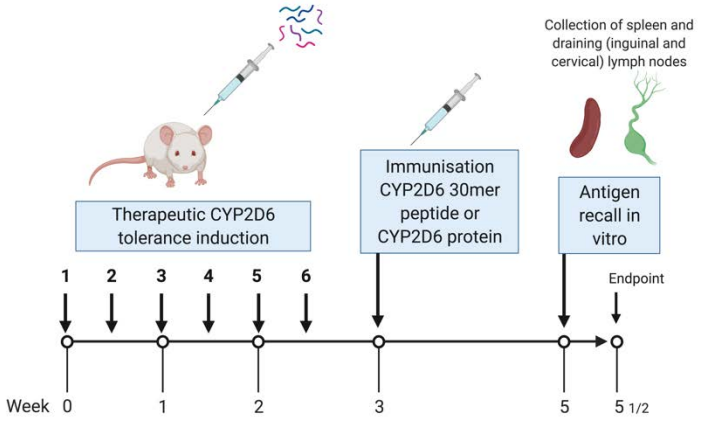

4. Assess prophylactic benefit of CYP2D6 T cell epitope peptide delivery in a suitable murine model of AIH-2 (Adenoviral induction of human CYP2D6 protein establishes AIH-like liver pathology, reaching chronic disease 8 weeks post-induction).

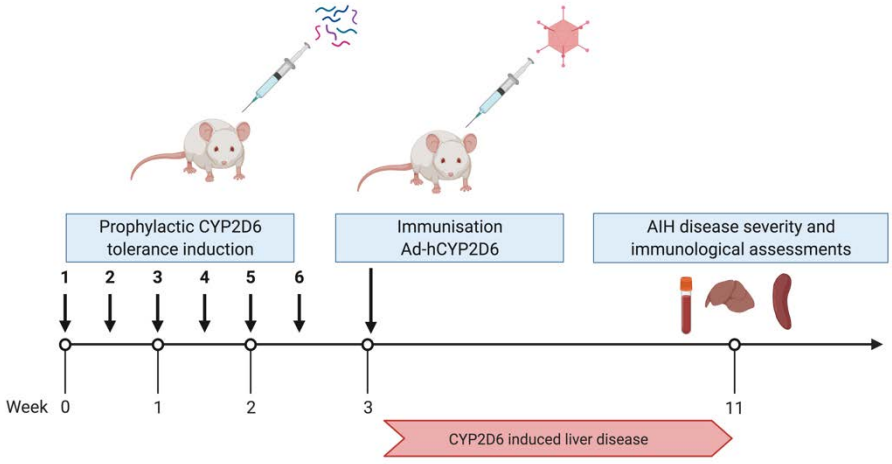

5. Assess therapeutic benefit of CYP2D6 T cell epitope peptide delivery in a suitable murine model of AIH-2 (Adenoviral induction of human CYP2D6 protein establishes AIH-like liver pathology, reaching chronic disease 8 weeks post-induction).

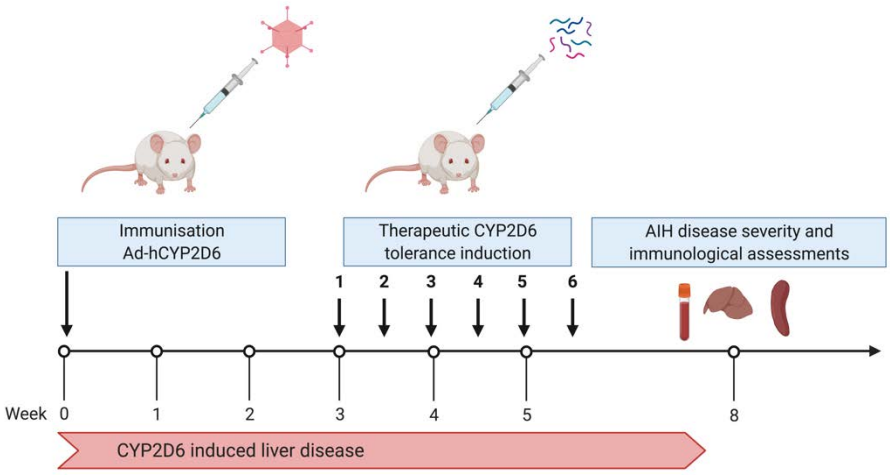

CHAPTER 6

GENERAL DISCUSSION AND FUTURE DIRECTIONS

6.1. Phenotype of tolerised T cells, T cell mediated suppression of APC and bystander suppression

This thesis has presented data demonstrating the generation of IL-10^{+} FoxP3^{-} Tr1 cells during repeated tolerogenic peptide treatment, in line with prior experience (Liu and Wraith, 1995; Anderton and Wraith, 1998; Gabryšová et al., 2009a; Burton et al., 2014), in addition to the significant alteration in the qualitative rather than quantitative increase in FoxP3^{+} Treg cells. Prior work has not focussed on Treg in the Tg4 model, yet this work provides strong evidence that Treg increase their suppressive phenotype (IL-10 and coinhibitory molecule expression) after undergoing tolerance induction and are highly likely to exert increased suppressive function as a result.

We investigated the pathway between CD40L-CD40 and IL-12 and found that tolerised T cells were prevented from expressing CD40L at the cell surface after antigen stimulation. We did not observe a reduction in CD40 expression by DC from tolerised *in vivo*, yet without effective provision of CD40L from the T cell, these DC were prevented from IL-12 secretion (*in vitro* IL-12 data only) – which would be required for subsequent conversion of non-antigen specific naïve T cells to Th1.

Analysis of antigen-presenting cells showed that both *in vitro* and *in vivo*, exposure to tolerised CD4^{+} T cells suppresses their antigen-presentation and costimulatory capacity. Based on our T cell findings, we hypothesised that APC downregulation of CD80 and CD86 was most likely to be exerted through either IL-10

signalling and/or CTLA-4 mediated suppression. We found through our blocking experiments *in vitro* that suppression of CD80 and CD86 on DC and B cells was more reliant on CTLA-4 than IL-10 and that Tol Treg were more suppressive than either naïve Treg or bulk Tol $CD4^+$ cells. Previous work has demonstrated that the action of IL-10 is often less relevant *in vitro* settings compared to *in vivo* so the relevance of IL-10 in exerting in vivo suppression of APC cannot be discounted based on this data (O'Neill et al., 2004; Sundstedt et al., 2003b). The role of other co-inhibitory receptors PD-1, LAG-3, TIM-3 and TIGIT was not investigated within this thesis, but blocking experiments targeting these molecules would readily gather more information to further our understanding of Tol T cell mediated suppression of APC.

In the *in vitro* bystander suppression experiments, proliferation of naïve 2D2 CD4 cells was suppressed when cultured with Tol Tg4 $CD4^+$ cells in the presence of MBP_{Ac1-9} stimulation. Suppression of 2D2 $CD4^+$ cells was strongest when MBP_{Ac1-9} and MOG_{35-55} peptides were delivered as a linked hybrid peptide to restrict these epitopes to presentation on the same APC, compared to delivery of the two peptides separately for presentation on different APC. Bystander suppression was affected by IL-10 when epitope peptides were delivered separately, under conditions where T cells would be primed by different APC. IL-10 was not determined to be required for bystander suppression when epitope peptides were delivered to the same APC, presumably because target T cells would cluster around the APC and be in close enough contact for cell-contact mediated suppression via CTLA-4 or other receptor ligand interactions potentially including LAG-3, TIM-3, PD-1, Notch-1 and TIGIT.

Bystander suppression was also evident *in vivo* after tolerance induction of (B10.PL x C57BL/6) F1 mice to MBP_{Ac1-9}, mice were less capable at generating immune responses towards MOG_{35-55}. Once again, suppression of MOG_{35-55} responses was most potent if MBP_{Ac1-9} and MOG_{35-55} were delivered as the linked hybrid peptide.

This *in vitro* and *in vivo* data indicates the increased potency of linked suppression vs *bona fide* bystander suppression and the importance of relevant epitopes being expressed in very close physiological context for linked or bystander suppression to be exerted. As observed in EAE, tolerance induction towards $PLP_{139-151}$ is sufficient to control T cell responses to not only PLP, but also MBP and MOG by bystander suppression effects, sufficient to control disease development (Anderton and Wraith, 1998). These autoantigens are myelin sheath proteins and are, therefore, expressed within the same tissue. As such, when considering ASI therapies, target antigens would be most permissible to bystander suppression if expressed in close physiological proximity. We would argue that tissue specific autoimmune diseases would be most suitable for tolerance induction by antigen-specific immunotherapy if the aim is to control the target antigen and multiple other disease relevant antigens, generated by epitope spreading, by bystander suppression.

6.2. T cell epitope mapping of CYP2D6 autoantigen relevant to Autoimmune Hepatitis Type 2

Induction of antigen-specific tolerance using peptide epitopes (i.e. apitopes) is a powerful means of moderating aberrant T cell responses to allergic and autoimmune antigens. It has also been shown that targeting antigens to the liver can induce both liver-oriented

and extra-hepatic tolerance in specific contexts. AIH-2 patients possess LKM-1 autoantibodies which are specific to CYP2D6, whereas AIH-1 patients have a much more diverse and poorly defined autoantibody/autoantigen repertoire.

As such, we chose liver autoantigen CYP2D6 as a target for the development of a peptide immunotherapeutic approach with the potential to treat AIH-2. Chapters 4 and 5 detail the methodology and results involved with the identification of immunogenic 30meric regions of the autoantigen CYP2D6 and subsequent epitope mapping of two 30mer peptides down to their minimal T cell epitope. When assessing healthy donor and responses to the CYP2D6 30mer peptides, surprisingly, we found that the majority of the candidate peptides were immunogenic in diverse HLA-DR subtypes, of which these individuals were presumably naïve to CYP2D6 as an antigen but were still able to generate robust T cell mediated responses characterised by proliferation. CYP2D6 peptide $CYP1_{62\text{-}91}$ was highly immunogenic in healthy donors and all AIH patient groups. As such, $CYP1_{62\text{-}91}$ may not be AIH-2 disease specific or could represent a cryptic epitope(s). Alternatively, $CYP1_{62\text{-}91}$ may just be very highly immunogenic regardless of whether an individual is already primed to CYP2D6 or not and for this reason we chose to map this 30mer region for T cell epitopes to test whether the peptide contains naturally processed and presented epitope(s) or cryptic epitope(s). $CYP12_{445\text{-}474}$ was seemingly specifically immunogenic in paediatric AIH-2 patient PBMC, representing an exciting opportunity to distinguish AIH-2 pathology between children and adults, as well as identifying a potential biomarker for paediatric onset AIH-2. $CYP6_{235\text{-}264}$ was a prime candidate in adult AIH-2 patient PBMC, again representing a potentially disease-specific T cell reactive peptide. We were surprised to find that our control AIH-1 patient group, who do not possess CYP2D6-specific LKM-1 antibodies but experience very similar liver

damage and are treated with the same immunosuppressant regime, were strongly reactive to $CYP8_{315-337}$ peptide. This may represent a cross-over between AIH-1 and AIH-2 pathology that has not previously been identified and cannot be revealed by antibody responses (B cell epitopes) alone.

Using HLA-DR4 transgenic mice, we were able to generate peptide-specific T cell hybridomas towards $CYP1_{62-91}$ and $CYP12_{445-474}$ for full epitope mapping. We found that both sets of these T cell hybridomas were able to mount robust responses to the CYP2D6 protein; therefore, these peptides must be presented upon antigen processing of the whole protein and therefore are not cryptic. Detailed epitope mapping of these 30mers identified the minimal T cell epitope of $CYP1_{73-85}$ LAWTPVVVLNGLA and $CYP12_{452-460}$ ELFLFFTSL in the context of HLA-DR4. We would need to further test these peptides in other HLA-DR contexts to assess whether they have pan-DR binding potential, which would be of great benefit to a potential tolerogenic peptide cocktail as it would be applicable to a wider patient cohort. These peptides also need further testing to assess their current solubility and ability to bind to steady-state dendritic cells after injection in mice. These peptides could be adapted to improve solubility by addition of N- and C-terminal lysine and / or arginine residues. Peptide solubility is an essential feature of successful tolerogenic apitopes, as only highly soluble peptides are able to diffuse to reach ssDC in secondary lymphoid tissues where they are able to present the apitope without requirement for antigen-processing. As such, MHC-II loaded with antigenic peptide on ssDC can interact with antigen-specific T cells without relevant costimulatory molecules required for effective T cell activation and therefore initiates the induction of antigen-specific T cell tolerance (Shepard et al., 2021). We would have liked to have mapped the T cell epitopes of 30mers $CYP6_{235-264}$ and $CYP8_{315-337}$ to add to our repertoire

of T cell epitope peptides with tolerogenic potential in a peptide immunotherapy setting. Future experiments to continue and ultimately complete this work would include this further T cell epitope mapping, peptide solubility optimisation, assessment of ssDC binding in vivo and finally testing whether these peptides are able to induce tolerance to CYP2D6 and AIH-2 like disease in a relevant mouse model as described previously (Holdener et al., 2008). Due to COVID-19 shutdown of the University and disruption to animal research in particular, I lost around 7 months worth of the third and final year of my PhD, which heavily impacted on reaching these final aims as we had planned. I do believe that had we been afforded this time as an extension, I would have been able to complete T cell epitope mapping of CYP2D6, optimised T cell epitope solubility and delivery as apitopes and tested whether these peptides can induce tolerance to CYP2D6.

The work presented herein represents a solid platform from which to propose finalising our CYP2D6 T cell epitope mapping and peptide design in addition to translating any tolerogenic peptides into a novel immunotherapeutic intervention to treat AIH-2.

CHAPTER 7

REFERENCES

Akbari, O., DeKruyff, R.H. and Umetsu, D.T. (2001) Pulmonary dendritic cells producing IL-10 mediate tolerance induced by respiratory exposure to antigen. **Nature Immunology**, 2 (8): 725–731

Alderson, M.G., Tough, T.W., Davis-Smith, T., et al. (1995) Fas Ligand Mediates Activation-induced Cell Death in Human T Lymphocytes. **Journal of Experimental Medicine**, 181: 71–77

Alvarez, F., Berg, P.A., Bianchi, F.B., et al. (1999) International Autoimmune Hepatitis Group Report: Review of criteria for diagnosis of autoimmune hepatitis. **Journal of Hepatology**, 31 (5): 929–938

Anderson, A.C., Joller, N. and Kuchroo, V.K. (2016) Lag-3, Tim-3, and TIGIT: Co-inhibitory Receptors with Specialized Functions in Immune Regulation. **Immunity**, 44 (5): 989–1004

Anderson, G. and Takahama, Y. (2012) Thymic epithelial cells: Working class heroes for T cell development and repertoire selection. **Trends in Immunology**, 33 (6): 256–263

Anderson, P.O., Sundstedt, A., Yazici, Z., et al. (2005) IL-2 Overcomes the Unresponsiveness but Fails to Reverse the Regulatory Function of Antigen-Induced T Regulatory Cells. **The Journal of Immunology**, 174 (1): 310–319

Anderton, S.M., Viner, N.J., Matharu, P., et al. (2002) Influence of a dominant cryptic epitope on autoimmune T cell tolerance. **Nature Immunology**, 3 (2): 175–181

Anderton, S.M. and Wraith, D.C. (1998) Hierarchy in the ability of T cell epitopes to induce peripheral tolerance to antigens from myelin. **European Journal of Immunology**, 28 (4): 1251–1261

Arstila, T.P., Casrouge, A., Baron, V., et al. (1999) A direct estimate of the human αβ T cell receptor diversity. **Science**, 286 (5441): 958–961

Avadhani, N.G., Sangar, M.C., Bansal, S., et al. (2011) Bimodal targeting of cytochrome P450s to endoplasmic reticulum and mitochondria: The concept of chimeric signals. **FEBS Journal**. 278 (22) pp. 4218–4229

Bacher, P. and Scheffold, A. (2013) Flow-Cytometric Analysis of Rare Antigen-Specific T Cells. **Cytometry**, 83A: 692–701

Bachmann, M.F., Köhler, G., Ecabert, B., et al. (1999) Cutting edge: lymphoproliferative disease in the absence of CTLA-4 is not T cell autonomous. **Journal of Immunology**, 163 (3): 1128–31

Baecher-Allan, C., Viglietta, V. and Hafler, D.A. (2002) Inhibition of Human CD4+ CD25+high Regulatory T Cell Function. **The Journal of Immunology**, 169 (11): 6210–6217

Becker, C., Fantini, M.C., Schramm, C., et al. (2004) TGF-β suppresses tumor progression

in colon cancer by inhibition of IL-6 trans-signaling. **Immunity**, 21 (4): 491–501

Bell, G.M., Anderson, A.E., Diboll, J., et al. (2017) Autologous tolerogenic dendritic cells for rheumatoid and inflammatory arthritis. **Annals of the Rheumatic Diseases**, 76 (1): 227–234

Benham, H., Nel, H.J., Law, S.C., et al. (2015) Citrullinated peptide dendritic cell immunotherapy in HLA risk genotype – positive rheumatoid arthritis patients. **Science Translational Medicine**, 7 (290): 1–12

Bettelli, E., Pagany, M., Weiner, H.L., et al. (2003) Myelin oligodendrocyte glycoprotein-specific T cell receptor transgenic mice develop spontaneous autoimmune optic neuritis. **Journal of Experimental Medicine**, 197 (9): 1073–1081

Bevington, S.L., Ng, S.T.H., Britton, G.J., et al. (2020) Chromatin Priming Renders T Cell Tolerance-Associated Genes Sensitive to Activation below the Signaling Threshold for Immune Response Genes. **Cell Reports**, 31 (10): 107748

Bittencourt, P.L., Farias, A.Q., Porta, G., et al. (2008) Frequency of concurrent autoimmune disorders in patients with autoimmune hepatitis: Effect of age, gender, and genetic background. **Journal of Clinical Gastroenterology**, 42 (3): 300–305

Boberg, K.M., Aadland, E., Jahnsen, J., et al. (1998) Incidence and prevalence of primary biliary cirrhosis, primary sclerosing cholangitis, and autoimmune hepatitis in a norwegian population. **Scandinavian Journal of Gastroenterology**, 33 (1): 99–103

Bogdanos, D.P., Baum, H., Grasso, A., et al. (2004) Microbial mimics are major targets of crossreactivity with human pyruvate dehydrogenase in primary biliary cirrhosis. **Journal of Hepatology**, 40 (1): 31–39

Boise, L.H., González-García, M., Postema, C.E., et al. (1993) Bcl-X, a Bcl-2-Related Gene That Functions As a Dominant Regulator of Apoptotic Cell Death. **Cell**, 74 (4): 597–608

Boonstra, A., Rajsbaum, R., Holman, M., et al. (2006) Macrophages and Myeloid Dendritic Cells, but Not Plasmacytoid Dendritic Cells, Produce IL-10 in Response to MyD88- and TRIF-Dependent TLR Signals, and TLR-Independent Signals. **Journal of Immunology**, 177 (11): 7551–7558

Burkhart, C., Liu, G.Y., Anderton, S.M., et al. (1999) Peptide-induced T cell regulation of experimental autoimmune encephalomyelitis: A role for IL-10. **International Immunology**, 11 (10): 1625–1634

Burns, J., Rosenzweig, A., Zweiman, B., et al. (1983) Isolation of myelin basic protein-reactive T-cell lines from normal human blood. **Cellular Immunology**, 81 (2): 435–440

Burton, B.R., Britton, G.J., Fang, H., et al. (2014) Sequential transcriptional changes dictate safe and effective antigen-specific immunotherapy. **Nature Communications**, 5 (4741): 1–13

Campana, R., Marth, K., Zieglmayer, P., et al. (2019) Vaccination of non-allergic individuals with recombinant hypoallergenic fragments of birch pollen allergen Bet v 1: Safety, effects and mechanisms. **Journal of Allergy and Clinical Immunology**, 143 (3): 1258–61

Campbell, B., Vogel, P.J., Fisher, E., et al. (1973) Myelin Basic Protein Administration in Multiple Sclerosis. **Archives of Neurology**, 29 (1): 10–15

Campbell, J.D., Buckland, K.F., McMillan, S.J., et al. (2009) Peptide immunotherapy in allergic asthma generates IL-10–dependent immunological tolerance associated with linked epitope suppression. **Journal of Experimental Medicine**, 206 (7): 1535–1547

Canaday, D. (2013) Production of CD4+ and CD8+ T Cell Hybridomas. **Methods in Molecular Biology**, 960: 297–307

Canaday, D.H., Gehring, A., Leonard, E.G., et al. (2003) T-cell hybridomas from HLA-transgenic mice as tools for analysis of human antigen processing. **Journal of Immunological Methods**, 281 (1–2): 129–142

Carambia, A., Freund, B., Schwinge, D., et al. (2014) TGF-β-dependent induction of CD4+CD25+Foxp3 + Tregs by liver sinusoidal endothelial cells. **Journal of Hepatology**, 61 (3): 594–599

Carambia, A., Freund, B., Schwinge, D., et al. (2015) Nanoparticle-based autoantigen delivery to Treg-inducing liver sinusoidal endothelial cells enables control of autoimmunity in mice. **Journal of Hepatology**, 62 (6): 1349–1356

Cassani, F., Cataleta, M., Valentini, P., et al. (1997) Serum autoantibodies in chronic hepatitis C: Comparison with autoimmune hepatitis and impact on the disease profile. **Hepatology**, 26 (3): 561–566

Caux, B.C., Massacrier, C., Vanbervliet, B., et al. (1994) Activation of human dendritic cells through CD40 crosslinking. **Journal of Experimental Medicine**, 180: 1263–1272

Chalaris, A., Rabe, B., Paliga, K., et al. (2007) Apoptosis is a natural stimulus of IL6R shedding and contributes to the proinflammatory trans-signaling function of neutrophils. **Blood**, 110 (6): 1748–1755

Chaouali, M., Carvalho, A., Tezeghdenti, A., et al. (2018) Cytotoxic T lymphocyte antigen-4 gene polymorphisms and susceptibility to type 1 autoimmune hepatitis in the Tunisian population. **Genes and Diseases**, 5 (3): 256–262

Chataway, J., Martin, K., Barrell, K., et al. (2018) Effects of ATX-MS-1467 immunotherapy over 16 weeks in relapsing multiple sclerosis. **Neurology**, 90 (11): e955–e962

Chen, W., Jin, W. and Wahl, S.M. (1998) Engagement of cytotoxic T lymphocyte-associated antigen 4 (CTLA-4) induces transforming growth factor β (TGF-β) production by murine CD4+ T cells. **Journal of Experimental Medicine**, 188 (10): 1849–1857

Chen, Y., Kuchroo, V.K., Inobe, J.I., et al. (1994) Regulatory T cell clones induced by oral tolerance: Suppression of autoimmune encephalomyelitis. **Science**, 265 (5176): 1237–1240

Clemente-Casares, X., Blanco, J., Ambalavanan, P., et al. (2016) Expanding antigen-specific regulatory networks to treat autoimmunity. **Nature** [online], 530 (7591): 434–40. Available from: http://www.nature.com/doifinder/10.1038/nature16962%5Cnhttp://www.ncbi.nlm.nih.gov/pubmed/26886799

Collins, D.S., Unanue, E.R. and Harding, C. V. (1991) Reduction of disulfide bonds within lysosomes is a key step in antigen processing. **Journal of Immunology**, 147 (12): 4054–4059

Cook, G.C., Mulligan, R. and Sherlock, S. (1971) Controlled prospective trial of corticosteroid therapy in active chronic hepatitis. **Quarterly Journal of Medicine**, 40 (158): 159–185

Corinti, S., Albanesi, C., Sala, A., et al. (2001) Regulatory Activity of Autocrine IL-10 on Dendritic Cell Functions. **Journal of Immunology**, 166: 4312–4318

Crispe, I.N. (2009) The Liver as a Lymphoid Organ. **Annual Review of Immunology**, 27 (1): 147–163

Czaja, A. and Donaldson, P. (2000) Genetic susceptibilities for immune expression and liver cell injury in autoimmune hepatitis. **Immunological Reviews**, 174 (4): 250–9

Czaja, A.J. (2016) Diagnosis and management of autoimmune hepatitis: current status and future directions. **Gut and Liver**, 10 (2): 177–203

Czaja, A.J., Carpenter, H.A., Santrach, P.J., et al. (1993) Significance of HLA DR4 in Type 1 Autoimmune. **Gastroenterology**, 105: 1502–1507

Czaja, A.J., Cassani, F., Cataleta, M., et al. (1996) Frequency and significance of antibodies to actin in type 1 autoimmune hepatitis. **Hepatology**, 24 (5): 1068–1073

Dalekos, G.N., Wedemeyer, H., Obermayer-Straub, P., et al. (1999) Epitope mapping of cytochrome P4502D6 autoantigen in patients with chronic hepatitis C during α-interferon treatment. **Journal of Hepatology**, 30 (3): 366–375

DeSilva, D.R., Urdahl, K.B. and Jenkins, M.K. (1991) Clonal anergy is induced in vitro by T cell receptor occupancy in the absence of proliferation. **Journal of Immunology**, 147 (10): 3261–7

Dieckmann, D., Plottner, H., Berchtold, S., et al. (2001) Ex vivo isolation and characterization of CD4+CD25+ T cells with regulatory properties from human blood. **Journal of Experimental Medicine**, 193 (11): 1303–1310

Domogalla, M.P., Rostan, P. V., Raker, V.K., et al. (2017) Tolerance through education: How tolerogenic dendritic cells shape immunity. **Frontiers in Immunology**, 8 (DEC): 1–14

Donaldson, P. (1991) Susceptibility to autoimmune chronic active hepatitis: Human leukocyte antigens DR4 and A1-B8-DR3 are independent risk factors. **Hepatology**, 13 (4): 701–706

Van Der Drift, A.C.M., Van Noort, J.M. and Krüse, J. (1990) Catheptic processing of protein antigens: Enzymic and molecular aspects. **Seminars in Immunology**, 2 (4): 255–271

Eastwood, A. and Reingold, S. (1997) "Disappointing results from clinical trial of oral myelin for relapsing-remitting multiple sclerosis." In **Research and Medical Programs Department News. National Multiple Sclerosis Society**. **1997**

Ehser, J., Holdener, M., Christen, S., et al. (2013) Molecular mimicry rather than identity breaks T-cell tolerance in the CYP2D6 mouse model for human autoimmune hepatitis.

Journal of Autoimmunity, 42: 39–49

Elgueta, R., Benson, M.J., De Vries, V.C., et al. (2009) Molecular mechanism and function of CD40/CD40L engagement in the immune system. **Immunological Reviews**, 229 (1): 152–172

Ellis, A.K., Frankish, C.W., O'Hehir, R.E., et al. (2017) Treatment with grass allergen peptides improves symptoms of grass pollen–induced allergic rhinoconjunctivitis. **Journal of Allergy and Clinical Immunology**, 140 (2): 486–496

European Association for the Study of the Liver (2015) The European Association for the Study of Liver. EASL Clinical Practice Guidelines : Autoimmune hepatitis. **Journal of Hepatology**, 63: 971–1004

Faria, A.. and Weiner, H.. (1999) Oral Tolerance: Mechanisms and Therapeutic Applications. **Advances in Immunology**, 73: 153–264

Fiorentino, D.F., Bond, M.W. and Mosmann, T.R. (1989) Two types of mouse T helper cell: IV. Th2 clones secrete a factor that inhibits cytokine production by Th1 clones. **Journal of Experimental Medicine**, 170 (6): 2081–2095

Flajnik, M.F. and Kasahara, M. (2001) Comparative genomics of the MHC: Glimpses into the evolution of the adaptive immune system. **Immunity**, 15 (3): 351–362

Fugger, L., Michie, S.A., Rulifson, I., et al. (1994) Expression of HLA-DR4 and human CD4 transgenes in mice determines the variable region β-chain T-cell repertoire and mediates an HLA-DR-restricted immune response. **Proceedings of the National Academy of Sciences of the United States of America**, 91 (13): 6151–6155

Gabryšová, L., Nicolson, K.S., Streeter, H.B., et al. (2009a) Negative feedback control of the autoimmune response through antigen-induced differentiation of IL-10 – secreting Th1 cells. **Journal of Experimental Medicine**, 206 (8): 1755–1767

Gabryšová, L., Nicolson, K.S., Streeter, H.B., et al. (2009b) Negative feedback control of the autoimmune response through antigen-induced differentiation of IL-10 – secreting Th1 cells. **Regulation**, 206 (8): 1755–1767

Gabryšová, L. and Wraith, D.C. (2010) Antigenic strength controls the generation of antigen-specific IL-10-secreting T regulatory cells. **European Journal of Immunology**, 40 (5): 1386–1395

Gagliani, N., Magnani, C.F., Huber, S., et al. (2013) Coexpression of CD49b and LAG-3 identifies human and mouse T regulatory type 1 cells. **Nature Medicine**, 19 (6): 739–46

Gallegos, A.M. and Bevan, M.J. (2004) Central tolerance to tissue-specific antigens mediated by direct and indirect antigen presentation. **Journal of Experimental Medicine**, 200 (8): 1039–49

Geller, S.A. (2014) Autoimmune hepatitis: Histopathology. **Clinical Liver Disease**, 3 (2): 19–23

Van Gerven, N.M.F., Verwer, B.J., Witte, B.I., et al. (2014) Epidemiology and clinical characteristics of autoimmune hepatitis in the Netherlands. **Scandinavian Journal of Gastroenterology**, 49 (10): 1245–1254

Getts, D.R., Martin, A.J., Mccarthy, D.P., et al. (2012) Microparticles bearing encephalitogenic peptides induce T-cell tolerance and ameliorate experimental autoimmune encephalomyelitis. **Nature Biotechnology**, 30 (12): 1217–1224

Getts, D.R., Shea, L.D., Miller, S.D., et al. (2015) Harnessing nanoparticles for immune modulation. **Trends in Immunology**, 36 (7): 419–27

Gimmi, C.D., Freeman, G.J., Gribben, J.G., et al. (1993) Human T-cell clonal anergy is induced by antigen presentation in the absence of B7 costimulation. **Proceedings of the National Academy of Sciences of the United States of America**, 90 (14): 6586–90

Gleeson, D. (2019) Long-Term Outcomes of Autoimmune Hepatitis. **Clinical Liver Disease**, 14 (1): 24–28

Goddard, S., Youster, J., Morgan, E., et al. (2004) Interleukin-10 Secretion Differentiates Dendritic Cells from Human Liver and Skin. **American Journal of Pathology**, 164 (2): 511–519

Gonsette, R.E., Delmotte, P. and Demonty, L. (1977) Failure of basic protein therapy for multiple sclerosis. **Journal of Neurology**, 216 (1): 27–31

Gran, B., Hemmer, B. and Martin, R. (1999) Molecular mimicry and multiple sclerosis - a possible role for degenerate T cell recognition in the induction of autoimmune responses. **Journal Of Neural Transmission-Supplement**, (55): 19–31

Greenwald, R.J., Freeman, G.J. and Sharpe, A.H. (2005) The B7 family revisited. **Annual Review of Immunology**, 23: 515–548

Gregori, S., Tomasoni, D., Pacciani, V., et al. (2010) Differentiation of type 1 T regulatory cells (Tr1) by tolerogenic DC-10 requires the IL-10-dependent ILT4/HLA-G pathway. **Blood**, 116 (6): 935–944

Gregorio, G. V., Portmann, B., Reid, F., et al. (1997) Autoimmune hepatitis in childhood: A 20-year experience. **Hepatology**, 25 (3): 541–547

Grimm, A.J., Kontos, S., Diaceri, G., et al. (2015) Memory of tolerance and induction of regulatory T cells by erythrocyte-targeted antigens. **Scientific Reports**, 5: 1–11

Grønbæk, L., Vilstrup, H. and Jepsen, P. (2014) Autoimmune hepatitis in Denmark: Incidence, prevalence, prognosis, and causes of death. A nationwide registry-based cohort study. **Journal of Hepatology**, 60 (3): 612–617

Grossman, W.J., Verbsky, J.W., Barchet, W., et al. (2004) Human T regulatory cells can use the perforin pathway to cause autologous target cell death. **Immunity**, 21 (4): 589–601

Groux, H., O'Garra, A., Bigler, M., et al. (1997) A CD4+ T-cell subset inhibits antigen-specific T-cell responses and prevents colitis. **Nature**, 389 (6652): 737–742

Gueguen, M., Boniface, O., Bernard, O., et al. (1991) Identification of the main epitope on human cytochrome P450 IID6 recognized by anti-liver kidney microsome antibody. **Journal of Autoimmunity**, 4 (4): 607–615

Guilliams, M., Dutertre, C.A., Scott, C.L., et al. (2016) Unsupervised High-Dimensional Analysis Aligns Dendritic Cells across Tissues and Species. **Immunity**, 45 (3): 669–684

Hartwell, B.L., Antunez, L., Sullivan, B.P., et al. (2015) Multivalent nanomaterials: Learning from vaccines and progressing to antigen-specific immunotherapies. **Journal of Pharmaceutical Sciences**, 104 (2): 346–361

Hawiger, D., Inaba, K., Dorsett, Y., et al. (2001) Dendritic cells induce peripheral T cell unresponsiveness under steady state conditions in vivo. **Journal of Experimental Medicine**, 194 (6): 769–779

Hennes, E.M., Zeniya, M., Czaja, A.J., et al. (2008) Simplified criteria for the diagnosis of autoimmune hepatitis. **Hepatology**, 48 (1): 169–176

Heufler, C., Koch, F., Stanzl, U., et al. (1996) Interleukin-12 is produced by dendritic cells and mediates T helper 1 development as well as interferon-γ production by T helper 1 cells. **European Journal of Immunology**, 26 (3): 659–668

Heymann, F., Peusquens, J., Ludwig-Portugall, I., et al. (2015) Liver Inflammation Abrogates Immunological Tolerance Induced by Kupffer Cells. **Hepatology**, 62 (1): 279–291

Hilkens, C.M.U., Isaacs, J.D. and Thomson, A.W. (2010) Development of dendritic cell-based immunotherapy for autoimmunity. **International Reviews of Immunology**, 29 (2): 156–183

Hintermann, E., Ehser, J. and Christen, U. (2012) The CYP2D6 animal model: how to induce autoimmune hepatitis in mice. **Journal of visualized experiments : JoVE**, (60): 1–7

Hoeroldt, B., McFarlane, E., Dube, A., et al. (2011) Long-term outcomes of patients with autoimmune hepatitis managed at a nontransplant center. **Gastroenterology**, 140 (7): 1980–1989

Holdener, M., Hintermann, E., Bayer, M., et al. (2008) Breaking tolerance to the natural human liver autoantigen cytochrome P450 2D6 by virus infection. **The Journal of experimental medicine** [online], 205 (6): 1409–22. Available from: http://www.pubmedcentral.nih.gov/articlerender.fcgi?artid=2413037&tool=pmcentrez&rendertype=abstract

Hou, T.Z., Qureshi, O.S., Wang, C.J., et al. (2015) A Transendocytosis Model of CTLA-4 Function Predicts Its Suppressive Behavior on Regulatory T Cells. **The Journal of Immunology**, 194 (5): 2148–2159

Hoyne, G.F., Dallman, M.J. and Lamb, J.R. (1999) Linked suppression in peripheral T cell tolerance to the house dust mite derived allergen Der p 1. **International Archives of Allergy and Immunology**, 118 (2–4): 122–124

Hoyne, G.F., Jarnicki, A.G., Thomas, W.R., et al. (1997) Characterization of the specificity and duration of T cell tolerance to intranasally administered peptides in mice: A role for intramolecular epitope suppression. **International Immunology**, 9 (8): 1165–1173

Hwang, J.R., Byeon, Y., Kim, D., et al. (2020) Recent insights of T cell receptor-mediated signaling pathways for T cell activation and development. **Experimental and Molecular Medicine**, 52 (5): 750–761

Ikeda, A., Aoki, N., Kido, M., et al. (2014) Progression of autoimmune hepatitis is

mediated by IL-18-producing dendritic cells and hepatic CXCL9 expression in mice. **Hepatology**, 60 (1): 224–236

Jansson, L., Vrolix, K., Jahraus, A., et al. (2018) Immunotherapy With Apitopes Blocks the Immune Response to TSH Receptor in HLA-DR Transgenic Mice. **Endocrinology**, 159 (March): 3446–3457

Jeffery, H.C., Hunter, S., Humphreys, E.H., et al. (2019) Bidirectional Cross-Talk between Biliary Epithelium and Th17 Cells Promotes Local Th17 Expansion and Bile Duct Proliferation in Biliary Liver Diseases. **Journal of Immunology**, 203 (5): 1151–1159

Jenkins, M.K. and Schwartz, R.H. (1987) Antigen presentation by chemically modified splenocytes induces antigen-specific T cell unresponsiveness in vitro and in vivo. **Journal of Experimental Medicine**, 165 (2): 302–319

Jenne, C.N. and Kubes, P. (2013) Immune surveillance by the liver. **Nature Immunology**, 14 (10): 996–1006

Jensen, K.K., Andreatta, M., Marcatili, P., et al. (2018) Improved methods for predicting peptide binding affinity to MHC class II molecules. **Immunology**, 154 (3): 394–406

Jensen, P.E. (1991) Reduction of disulfide bonds during antigen processing: Evidence from a thiol-dependent insulin determinant. **Journal of Experimental Medicine**, 174 (5): 1121–1130

Johnson, P.J., McFarlane, I.G. and Williams, R. (1995) Azathioprine for Long-Term Maintenance of Remission in Autoimmune Hepatitis. **New England Journal of Medicine**, 333 (15): 958–963

Jones, S.M., Pons, L., Roberts, J.L., et al. (2009) Clinical Efficacy and Immune Regulation With Peanut Oral Immunotherapy. **Journal of Allergy and Clinical Immunology**, 124 (2): 1–20

Kang, H.-K., Michaels, M.A., Berner, B.R., et al. (2005) Very Low-Dose Tolerance with Nucleosomal Peptides Controls Lupus and Induces Potent Regulatory T Cell Subsets. **The Journal of Immunology**, 174 (6): 3247–3255

Karlsen, T.H. and Boberg, K.M. (2013) Update on primary sclerosing cholangitis. **Journal of Hepatology**, 59 (3): 571–582

Kehry, M.R. and Yamashita, L.C. (1989) Low-affinity IgE receptor (CD23) function on mouse B cells: Role in IgE-dependent antigen focusing. **Proceedings of the National Academy of Sciences of the United States of America**, 86 (19): 7556–7560

Kerkar, N., Choudhuri, K., Ma, Y., et al. (2003) Cytochrome P4502D6193-212: A New Immunodominant Epitope and Target of Virus/Self Cross-Reactivity in Liver Kidney Microsomal Autoantibody Type 1-Positive Liver Disease. **Journal of Immunology**, 170 (3): 1481–1489

Kido, M., Watanabe, N., Okazaki, T., et al. (2008) Fatal Autoimmune Hepatitis Induced by Concurrent Loss of Naturally Arising Regulatory T Cells and PD-1-Mediated Signaling. **Gastroenterology**, 135 (4): 1333–1343

Klimek, L., Bachert, C., Lukat, K.F., et al. (2015) Allergy immunotherapy with a

hypoallergenic recombinant birch pollen allergen rBet v 1-FV in a randomized controlled trial. **Clinical and Translational Allergy**, 5 (1)

Konkel, J.E., Frommer, F., Leech, M.D., et al. (2010) PD-1 signalling in CD4+ T cells restrains their clonal expansion to an immunogenic stimulus, but is not critically required for peptide-induced tolerance. **Immunology**, 130 (1): 92–102

Kontos, S., Grimm, A.J. and Hubbell, J.A. (2015) Engineering antigen-specific immunological tolerance. **Current Opinion in Immunology**, 35: 80–88

Kontos, S., Kourtis, I.C., Dane, K.Y., et al. (2013) Engineering antigens for in situ erythrocyte binding induces T-cell deletion. **Proceedings of the National Academy of Sciences of the United States of America**, 110: E60–E68

Kristiansen, O.P., Larsen, Z.M. and Pociot, F. (2000) CTLA-4 in autoimmune diseases - A general susceptibility gene to autoimmunity? **Genes and Immunity**, 1 (3): 170–184

Krummel, M.F. and Allison, J.P. (1996) CTLA-4 engagement inhibits IL-2 accumulation and cell cycle progression upon activation of resting T cells. **Journal of Experimental Medicine**, 183 (6): 2533–2540

Kuchroo, V.K., Greer, J.M., Kaul, D., et al. (1994) A single TCR antagonist peptide inhibits experimental allergic encephalomyelitis mediated by a diverse T cell repertoire. **Journal of Immunology**, 153 (7): 3326–3336

de la Rosa, M., Rutz, S., Dorninger, H., et al. (2004) Interleukin-2 is essential for CD4+CD25+ regulatory T cell function. **European Journal of Immunology**, 34 (9): 2480–2488

Lafuente, E. and Reche, P. (2009) Prediction of MHC-Peptide Binding: A Systematic and Comprehensive Overview. **Current Pharmaceutical Design**, 15 (28): 3209–3220

Lamers, M.M.H., van Oijen, M.G.H., Pronk, M., et al. (2010) Treatment options for autoimmune hepatitis: A systematic review of randomized controlled trials. **Journal of Hepatology**, 53 (1): 191–198

Lašťovička, J., Budinský, V., Špíšek, R., et al. (2009) Assessment of lymphocyte proliferation: CFSE kills dividing cells and modulates expression of activation markers. **Cellular Immunology**, 256 (1–2): 79–85

Lerner, A., Jeremias, P. and Matthias, T. (2015) The World Incidence and Prevalence of Autoimmune Diseases is Increasing. **International Journal of Celiac Disease**, 3 (4): 151–155

Li, M.O., Wan, Y.Y. and Flavell, R.A. (2007) T Cell-Produced Transforming Growth Factor-β1 Controls T Cell Tolerance and Regulates Th1- and Th17-Cell Differentiation. **Immunity**, 26 (5): 579–591

Li, M.O., Wan, Y.Y., Sanjabi, S., et al. (2006) Transforming growth factor-β regulation of immune responses. **Annual Review of Immunology**, 24: 99–146

Lidman, K., Biberfeld, G., Fagraeus, A., et al. (1976) Anti-actin specificity of human smooth muscle antibodies in chronic active hepatitis. **Clinical and Experimental Immunology**, 24 (2): 266–272

Lippens, C., Duraes, F. V., Dubrot, J., et al. (2016) IDO-orchestrated crosstalk between pDCs and Tregs inhibits autoimmunity. **Journal of Autoimmunity**, 75: 39–49

Liston, A., Lesage, S., Wilson, J., et al. (2003) Aire regulates negative selection of organ-specific T cells. **Nature Immunology**, 4 (4): 350–354

Liu, B., Tonkonogy, S.L. and Sartor, R.B. (2011) Antigen-presenting cell production of IL-10 inhibits T-helper 1 and 17 cell responses and suppresses colitis in mice. **Gastroenterology**, 141 (2): 653-662.e4

Liu, G.Y., Fairchild, P.J., Smith, R.M., et al. (1995) Low avidity recognition of self-antigen by T cells permits escape from central tolerance. **Immunity**, 3 (4): 407–415

Liu, G.Y. and Wraith, D.C. (1995) Affinity for class II MHC determines the extent to which soluble peptides tolerize autoreactive T cells in naive and primed adult mice-implications for autoimmunity. **International Immunology**, 7 (8): 1255–1263

Long, M., Park, S.G., Strickland, I., et al. (2009) Nuclear Factor-κB Modulates Regulatory T Cell Development by Directly Regulating Expression of Foxp3 Transcription Factor. **Immunity**, 31 (6): 921–931

Longhi, M.S., Hussain, M.J., Bogdanos, D.P., et al. (2007) Cytochrome P450IID6-specific CD8 T cell immune responses mirror disease activity in autoimmune hepatitis type 2. **Hepatology**, 46 (2): 472–484

Longhi, M.S., Ma, Y., Bogdanos, D.P., et al. (2004) Impairment of CD4+CD25+ regulatory T-cells in autoimmune liver disease. **Journal of Hepatology**, 41 (1): 31–37

Longhi, M.S., Ma, Y., Mieli-Vergani, G., et al. (2010) Aetiopathogenesis of autoimmune hepatitis. **Journal of Autoimmunity**, 34 (1): 7–14

Ma, X., Yan, W., Zheng, H., et al. (2015) Regulation of IL-10 and IL-12 production and function in macrophages and dendritic cells. **F1000Research**, 4 (0): 1–13

Ma, Y., Bogdanos, D.P., Hussain, M.J., et al. (2006) Polyclonal T-cell responses to cytochrome P450IID6 are associated with disease activity in autoimmune hepatitis type 2. **Gastroenterology**, 130 (3): 868–882

Mackay, I.R., Weiden, S. and Hasker, J. (1965) Autoimmune Hepatitis. **Annals of the New York Academy of Sciences**, 124 (2): 767–780

Maldonado, R.A., LaMothe, R.A., Ferrari, J.D., et al. (2015) Polymeric synthetic nanoparticles for the induction of antigen-specific immunological tolerance. **Proceedings of the National Academy of Sciences of the United States of America**, 112 (2): E156-65

Mannering, S.I., Dromey, J.A., Morris, J.S., et al. (2005) An efficient method for cloning human autoantigen-specific T cells. **Journal of Immunological Methods**, 298 (1–2): 83–92

Manns, M., Kyriatsoulis, A., Gerken, G., et al. (1987) Characterisation of a New Subgroup of Autoimmune Chronic Active Hepatitis By Autoantibodies Against a Soluble Liver Antigen. **Lancet**, 329 (8528): 292–294

Manns, M.P., Czaja, A.J., Gorham, J.D., et al. (2010) Diagnosis and management of autoimmune hepatitis. **Hepatology**, 51 (6): 2193–2213

Manns, M.P., Griffin, K.J., Sullivan, K.F., et al. (1991) LKM-1 autoantibodies recongnize a shor linear sequence in P450IID6, a cytochrome P-450 monooxygenase. **Journal of Clinical Investigation**, 88 (October): 1370–1378

Manns, M.P. and Vogel, A. (2006) Autoimmune hepatitis, from mechanisms to therapy. **Hepatology**, 43 (2 SUPPL. 1): S132–S144

Marceau, G., Lapierre, P., Béland, K., et al. (2005) LKM1 autoantibodies in chronic hepatitis C infection: A case of molecular mimicry? **Hepatology**, 42 (3): 675–682

Marie, J.C., Liggitt, D. and Rudensky, A.Y. (2006) Cellular Mechanisms of Fatal Early-Onset Autoimmunity in Mice with the T Cell-Specific Targeting of Transforming Growth Factor-β Receptor. **Immunity**, 25 (3): 441–454

Marrack, P., Scott-Browne, J.P., Dai, S., et al. (2008) Evolutionarily Conserved Amino Acids That Control TCR-MHC Interaction. **Annual Review of Immunology**, 26 (1): 171–203

Marsh, S.G.E., Albert, E.D., Bodmer, W.F., et al. (2010) Nomenclature for factors of the HLA system, 2010. **Tissue Antigens**, 75 (4): 291–455

Matta, B., Jha, P., Bora, P.S., et al. (2010) Antigen-specific tolerance inhibits autoimmune uveitis in pre-sensitized animals by deletion and CD4+CD25+ T-regulatory cells. **Immunology and Cell Biology**, 88 (2): 187–196

Maurer, D., Fiebiger, E., Reininger, B., et al. (1994) Expression of functional high affinity immunoglobulin E Receptors (FcεRI) on Monocytes of Atopic Individuals. **Journal of Experimental Medicine**, 179 (2): 745–750

Mauri, C. and Menon, M. (2017) Human regulatory B cells in health and disease: therapeutic potential. **Journal of Clinical Investigation**, 127 (3): 772–779

Mazza, G., Ponsford, M., Lowrey, P., et al. (2002) Diversity and dynamics of the T-cell response to MBP in DR2+ve individuals. **Clinical and Experimental Immunology**, 128 (3): 538–547

McGeachy, M.J. and Anderton, S.M. (2005) Cytokines in the induction and resolution of experimental autoimmune encephalomyelitis. **Cytokine**, 32 (2): 81–84

McGeachy, M.J., Bak-Jensen, K.S., Chen, Y., et al. (2007) TGF-β and IL-6 drive the production of IL-17 and IL-10 by T cells and restrain TH-17 cell-mediated pathology. **Nature Immunology**, 8 (12): 1390–1397

McMillan, S.A. and Haire, M. (1979) The specificity of IgG- and IgM-class smooth muscle antibody in the sera of patients with multiple sclerosis and active chronic hepatitis. **Clinical Immunology and Immunopathology**, 14 (2): 256–263

Meiler, F., Zumkehr, J., Klunker, S., et al. (2008) In vivo switch to IL-10-secreting T regulatory cells in high dose allergen exposure. **Journal of Experimental Medicine**, 205 (12): 2887–2898

Meinl, E., Weber, F., Drexler, K., et al. (1993) Myelin basic protein-specific T lymphocyte repertoire in multiple sclerosis: Complexity of the response and dominance of nested epitopes due to recruitment of multiple T cell clones. **Journal of Clinical Investigation**, 92 (6): 2633–2643

Mells, G.F., Kaser, A. and Karlsen, T.H. (2013) Novel insights into autoimmune liver diseases provided by genome-wide association studies. **Journal of Autoimmunity**, 46: 41–54

Van Der Merwe, P.A., Bodian, D.L., Daenke, S., et al. (1997) CD80 (B7-1) binds both CD28 and CTLA-4 with a low affinity and very fast kinetics. **Journal of Experimental Medicine**, 185 (3): 393–403

Metzler, B. and Wraith, D.C. (1993) Inhibition of experimental autoimmune encephalomyelitis by inhalation but not oral administration of the encephalitogenic peptide: Influence of MHC binding affinity. **International Immunology**, 5 (9): 1159–1165

Metzler, B. and Wraith, D.C. (1999) Inhibition of T-cell responsiveness by nasal peptide administration: Influence of the thymus and differential recovery of T-cell-dependent functions. **Immunology**, 97 (2): 257–63

Mieli-Vergani, G. and Vergani, D. (2013) Paediatric autoimmune liver disease. **Archives of Disease in Childhood**, 98 (12): 1012–1017

Miller, A., Lider, O. and Weiner, H.L. (1991) Antigen-driven bystander suppression after oral administration of antigens. **Journal of Experimental Medicine**, 174 (4): 791–798

Möbs, C., Ipsen, H., Mayer, L., et al. (2012) Birch pollen immunotherapy results in long-term loss of Bet v 1-specific TH2 responses, transient TR1 activation, and synthesis of IgE-blocking antibodies. **The Journal of Allergy and Clinical Immunology**, 130 (5): 1108-1116.e6

Möbs, C., Slotosch, C., Löffler, H., et al. (2010) Birch Pollen Immunotherapy Leads to Differential Induction of Regulatory T Cells and Delayed Helper T Cell Immune Deviation. **Journal of Immunology**, 184 (4): 2194–2203

Montano-Loza, A.J., Carpenter, H.A. and Czaja, A.J. (2006) Clinical significance of HLA DRB1 *03-DRB1 * 04 in type 1 autoimmune hepatitis. **Liver International**, 26 (10): 1201–1208

Moran, A.E., Holzapfel, K.L., Xing, Y., et al. (2011) T cell receptor signal strength in Treg and iNKT cell development demonstrated by a novel fluorescent reporter mouse. **Journal of Experimental Medicine**, 208 (6): 1279–1289

Morelli, A.E. and Thomson, A.W. (2007) Tolerogenic dendritic cells and the quest for transplant tolerance. **Nature Reviews Immunology**, 7 (8): 610–621

Motamedi, M., Xu, L. and Elahi, S. (2016) Correlation of transferrin receptor (CD71) with Ki67 expression on stimulated human and mouse T cells: The kinetics of expression of T cell activation markers. **Journal of Immunological Methods**, 437: 43–52

Mueller, D.L., Jenkins, M.K. and Schwartz, R.H. (1989) Clonal expansion versus functional inactivation: a costimulatory signalling pathway determines the outcome of T cell antigen receptor occupancy. **Annual Review of Immunology**, 7: 445–80

von Mühlen, C.A. and Tan, E.M. (1995) Autoantibodies in the diagnosis of systemicrheumatic diseases. **Seminars in Arthritis and Rheumatism**, 24 (5): 323–358

Muller, U., Akdis, C.A., Fricker, M., et al. (1998) Successful immunotherapy with T-cell

epitope peptides of bee venom phospholipase A2 induces specific T-cell anergy in patients allergic to bee venom. **Journal of Allergy and Clinical Immunology**, 101: 747–754

Muratori, P., Lalanne, C., Fabbri, A., et al. (2015) Type 1 and type 2 autoimmune hepatitis in adults share the same clinical phenotype. **Alimentary Pharmacology and Therapeutics**, 41 (12): 1281–1287

Murray-Lyon, I.M., Stern, R.B. and Williams, R. (1973) Controlled Trial of Prednisone and Azathioprine in Active Chronic Hepatitis. **Lancet**, 301 (7806): 735–737

Nakamura, K., Kitani, A., Fuss, I., et al. (2004) TGF-β1 Plays an Important Role in the Mechanism of CD4 + CD25 + Regulatory T Cell Activity in Both Humans and Mice. **Journal of Immunology**, 172 (2): 834–842

Nakamura, K., Kitani, A. and Strober, W. (2001) Cell contact-dependent immunosuppression by CD4+CD25+ regulatory T cells is mediated by cell surface-bound transforming growth factor β. **Journal of Experimental Medicine**, 194 (5): 629–644

Nepom, G.T. (2012) MHC class II tetramers. **Journal of Immunology**, 188 (6): 2477–82

Newell, E.W., Sigal, N., Nair, N., et al. (2013) Combinatorial tetramer staining and mass cytometry analysis facilitate T-cell epitope mapping and characterization. **Nature Biotechnology**, 31 (7): 623–631

Ng, T.H.S., Britton, G.J., Hill, E. V., et al. (2013) Regulation of adaptive immunity; the role of interleukin-10. **Frontiers in Immunology**, 4 (MAY): 1–13

Ngu, J.H., Bechly, K., Chapman, B.A., et al. (2010) Population-based epidemiology study of autoimmune hepatitis: A disease of older women? **Journal of Gastroenterology and Hepatology (Australia)**, 25 (10): 1681–1686

Nicolson, K.S., O'Neill, E.J., Sundstedt, A., et al. (2006) Antigen-Induced IL-10 + Regulatory T Cells Are Independent of CD25 + Regulatory Cells for Their Growth, Differentiation, and Function. **Journal of Immunology**, 176 (9): 5329–5337

Nielsen, M., Lundegaard, C., Blicher, T., et al. (2008) Quantitative predictions of peptide binding to any HLA-DR molecule of known sequence: NetMHCIIpan. **PLoS Computational Biology**, 4 (7): 1–10

Noon, L. (1911) Prophylactic Inoculation Against Hay Fever. **Lancet**. 177 (4580) pp. 1572–1573

Novak, N., Mete, N., Bussmann, C., et al. (2012) Early suppression of basophil activation during allergen-specific immunotherapy by histamine receptor 2. **Journal of Allergy and Clinical Immunology**, 130 (5): 1153-1158.e2

O'Neill, E.J., Sundstedt, A., Mazza, G., et al. (2004) Natural and induced regulatory T cells. **Annals of the New York Academy of Sciences**, 1029: 180–192

Oldfield, W.L.G., Larché, M. and Kay, A.B. (2002) Effect of T-cell peptides derived from Fel d 1 on allergic reactions and cytokine production in patients sensitive to cats: A randomised controlled trial. **Lancet**, 360 (9326): 47–53

Oo, Y.H. and Adams, D.H. (2012) Regulatory T cells and autoimmune hepatitis: Defective cells or a hostile environment? **Journal of Hepatology**, 57 (1): 6–8

Oo, Y.H., Banz, V., Kavanagh, D., et al. (2012) CXCR3-dependent recruitment and CCR6-mediated positioning of Th-17 cells in the inflamed liver. **Journal of Hepatology**, 57 (5): 1044–1051

Oo, Y.H., Hubscher, S.G. and Adams, D.H. (2010) Autoimmune hepatitis: New paradigms in the pathogenesis, diagnosis, and management. **Hepatology International**, 4 (2): 475–493

Ota, K., Matsui, M., Milford, E.L., et al. (1990) T-cell recognition of an immuno-dominant myelin basic protein epitope in multiple sclerosis. **Nature**, 346 (6280): 183–187

Ovcinnikovs, V., Ross, E.M., Petersone, L., et al. (2019) CTLA-4-mediated transendocytosis of costimulatory molecules primarily targets migratory dendritic cells. **Science Immunology**, 4 (35)

Palmer, E. (2003) Negative selection - Clearing out the bad apples from the T-cell repertoire. **Nature Reviews Immunology**, 3 (5): 383–391

Paul, S., Lindestam Arlehamn, C.S., Scriba, T.J., et al. (2015) Development and validation of a broad scheme for prediction of HLA class II restricted T cell epitopes. **Journal of Immunological Methods**, 422: 28–34

Peakman, M., Stevens, E.J., Lohmann, T., et al. (1999) Naturally processed and presented epitopes of the islet cell autoantigen IA-2 eluted from HLA-DR4. **Journal of Clinical Investigation**, 104 (10): 1449–1457

Pearce, S.H.S., Dayan, C., Wraith, D.C., et al. (2019) Antigen-Specific Immunotherapy with Thyrotropin Receptor Peptides in Graves' Hyperthyroidism: A Phase i Study. **Thyroid**, 29 (7): 1003–1011

Peiseler, M., Sebode, M., Franke, B., et al. (2012) FOXP3+ regulatory T cells in autoimmune hepatitis are fully functional and not reduced in frequency. **Journal of Hepatology**, 57 (1): 125–132

Perona-Wright, G., Anderton, S.M., Howie, S.E.M., et al. (2007) IL-10 permits transient activation of dendritic cells to tolerize T cells and protect from central nervous system autoimmune disease. **International Immunology**, 19 (9): 1123–1134

Peters, B., Nielsen, M. and Sette, A. (2020) T Cell Epitope Predictions. **Annual Review of Immunology**, 38 (1): 123–145

Pette, M., Fujita, K., Kitze, B., et al. (1990) Myelin basic protein-specific T lymphocyte lines from ms patients and healthy individuals. **Neurology**, 40 (11): 1770–1776

Piccirillo, C.A., Letterio, J.J., Thornton, A.M., et al. (2002) CD4+CD25+ regulatory T cells can mediate suppressor function in the absence of transforming growth factor β1 production and responsiveness. **Journal of Experimental Medicine**, 196 (2): 237–245

Piccirillo, C.A. and Shevach, E.M. (2004) Naturally-occurring CD4+CD25+ immunoregulatory T cells: Central players in the arena of peripheral tolerance. **Seminars in Immunology**, 16 (2): 81–88

Pinchuk, L.M., Klaus, S.J., Magaletti, D.M., et al. (1996) Functional CD40 ligand expressed by human blood dendritic cells is up-regulated by CD40 ligation. **Journal of Immunology**, 157 (10): 4363–70

Ponsford, M., Mazza, G., Coad, J., et al. (2001) Differential responses of CD45 +ve T-cell subsets to MBP in multiple sclerosis. **Clinical and Experimental Immunology**, 124 (2): 315–322

Prakken, B.J., Samodal, R., Le, T.D., et al. (2004) Epitope-specific immunotherapy induces immune deviation of proinflammatory T cells in rheumatoid arthritis. **Proceedings of the National Academy of Sciences of the United States of America**, 101 (12): 4228–4233

Qureshi, O.S., Zheng, Y., Nakamura, K., et al. (2011) Trans-endocytosis of CD80 and CD86: A molecular basis for the cell-extrinsic function of CTLA-4. **Science**, 332 (6029): 600–603

Rabe, B., Chalaris, A., May, U., et al. (2008) Transgenic blockade of interleukin 6 transsignaling abrogates inflammation. **Blood**, 111 (3): 1021–1028

Radu, C.G., Anderton, S.M., Firan, M., et al. (2000) Detection of autoreactive T cells in H-2(u) mice using peptide-MHC multimers. **International Immunology**, 12 (11): 1553–1560

Reiss, S., Baxter, A.E., Cirelli, K.M., et al. (2017) Comparative analysis of activation induced marker (AIM) assays for sensitive identification of antigen-specific CD4 T cells. **PLoS ONE**, 12 (10): 1–22

Richardson, N., Ng, S.T.H. and Wraith, D.C. (2020) Antigen-Specific Immunotherapy for Treatment of Autoimmune Liver Diseases. **Frontiers in Immunology**, 11 (July): 1–15

Richardson, N. and Wraith, D.C. (2021) Advancement of antigen-specific immunotherapy: knowledge transfer between allergy and autoimmunity. **Immunotherapy Advances**, 1 (1): 1–16

Riley, J.L., Mao, M., Kobayashi, S., et al. (2002) Modulation of TCR-induced transcriptional profiles by ligation of CD28, ICOS, and CTLA-4 receptors. **Proceedings of the National Academy of Sciences of the United States of America**, 99 (18): 11790–11795

Romine, J.S., Salk, J., Wiederholt, W.C., et al. (1980) "Studies on Myelin Basic Protein Administration in Multiple Sclerosis Patients." In Bauer, H.J., Poser, S. and Ritter, G. (eds.). **Progress in Multiple Sclerosis Research**. **Berlin, Heidelberg**. **1980**. Springer Berlin Heidelberg. pp. 428–433

Rubtsov, Y.P., Rasmussen, J.P., Chi, E.Y., et al. (2008) Regulatory T Cell-Derived Interleukin-10 Limits Inflammation at Environmental Interfaces. **Immunity**, 28 (4): 546–558

Sabatos-Peyton, C.A., Verhagen, J. and Wraith, D.C. (2010) Antigen-specific immunotherapy of autoimmune and allergic diseases. **Current Opinion in Immunology** [online], 22 (5): 609–615. Available from: http://dx.doi.org/10.1016/j.coi.2010.08.006

Saito, E., Kuo, R., Kramer, K.R., et al. (2019) Design of biodegradable nanoparticles to modulate phenotypes of antigen-presenting cells for antigen-specific treatment of autoimmune disease. **Biomaterials**, 222 (May): 119432

Sakaguchi, S., Sakaguchi, N., Asano, M., et al. (1995) Immunologic self-tolerance

maintained by activated T cells expressing IL-2 receptor alpha-chains (CD25). Breakdown of a single mechanism of self-tolerance causes various autoimmune diseases. **Journal of Immunology**, 155: 1151–1164

Sakaguchi, S., Wing, K., Onishi, Y., et al. (2009) Regulatory T cells: How do they suppress immune responses? **International Immunology**, 21 (10): 1105–1111

Santambrogio, L., Sato, A.K., Fischer, F.R., et al. (1999) Abundant empty class II MHC molecules on the surface of immature dendritic cells. **Proceedings of the National Academy of Sciences of the United States of America**, 96 (26): 15050–15055

Satoguina, J.S., Weyand, E., Larbi, J., et al. (2005) T Regulatory-1 Cells Induce IgG4 Production by B Cells: Role of IL-10. **Journal of Immunology**, 174 (8): 4718–26

Scally, S.W., Petersen, J., Law, S.C., et al. (2013) A molecular basis for the association of the HLA-DRB1 locus, citrullination, and rheumatoid arthritis. **Journal of Experimental Medicine**, 210 (12): 2569–2582

Scheller, J., Chalaris, A., Schmidt-Arras, D., et al. (2011) The pro- and anti-inflammatory properties of the cytokine interleukin-6. **Biochimica et Biophysica Acta - Molecular Cell Research**, 1813 (5): 878–888

Schneider, H., Downey, J., Smith, A., et al. (2006) Reversal of the TCR stop signal by CTLA-4. **Science**, 313 (5795): 1972–1975

Serra, P. and Santamaria, P. (2019) Antigen-specific therapeutic approaches for autoimmunity. **Nature Biotechnology**, 37 (3): 238–251

Shamji, M.H., Ljørring, C., Francis, J.N., et al. (2012) Functional rather than immunoreactive levels of IgG4correlate closely with clinical response to grass pollen immunotherapy. **Allergy: European Journal of Allergy and Clinical Immunology**, 67 (2): 217–226

Shepard, E.R., Wegner, A., Hill, E. V., et al. (2021) The Mechanism of Action of Antigen Processing Independent T Cell Epitopes Designed for Immunotherapy of Autoimmune Diseases. **Frontiers in Immunology**, 12

Simms, P.E. and Ellis, T.M. (1996) Utility of flow cytometric detection of CD69 expression as a rapid method for determining poly- and oligoclonal lymphocyte activation. **Clinical and Diagnostic Laboratory Immunology**, 3 (3): 301–304

Singh, H. and Raghava, G.P.S. (2002) ProPred: Prediction of HLA-DR binding sites. **Bioinformatics**, 17 (12): 1236–1237

Singha, S., Shao, K., Yang, Y., et al. (2017) Peptide-MHC-based nanomedicines for autoimmunity function as T-cell receptor microclustering devices. **Nature Nanotechnology**, 12 (7): 701–710

Smith-Garvin, J.E., Koretzky, G.A. and Jordan, M.S. (2009) T cell activation. **Annual Review of Immunology**, 27: 591–619

Snijders, A., Kalinski, P., Hilkens, C.M.U., et al. (1998) High-level IL-12 production by human dendritic cells requires two signals. **International Immunology**, 10 (11): 1593–1598

Soloway, R.D., Summerskill, W.H., Baggenstoss, A.H., et al. (1972) Clinical, biochemical, and histological remission of severe chronic active liver disease: a controlled study of treatments and early prognosis. **Gastroenterology**, 63 (5): 820–833

Spertini, F., DellaCorte, G., Kettner, A., et al. (2016) Efficacy of 2 months of allergen-specific immunotherapy with Bet v 1–derived contiguous overlapping peptides in patients with allergic rhinoconjunctivitis: Results of a phase IIb study. **Journal of Allergy and Clinical Immunology**, 138 (1): 162–168

Starr, T.K., Jameson, S.C. and Hogquist, K.A. (2003) Positive and negative selection of T cells. **Annual Review of Immunology**, 21: 139–76

Stechemesser, E., Klein, R. and Berg, P.A. (1993) Characterization and clinical relevance of liver-pancreas antibodies in autoimmune hepatitis. **Hepatology**, 18 (1): 1–9

Steinman, R.M., Hawiger, D. and Nussenzweig, M.C. (2003) Tolerogenic Dendritic Cells. **Annual Review of Immunology**, 21 (1): 685–711

Strassburg, C.P. and Manns, M.P. (2002) Autoantibodies and autoantigens in autoimmune hepatitis. **Seminars in Liver Disease**, 22 (4): 339–351

Streeter, H.B., Rigden, R., Martin, K.F., et al. (2015) Preclinical development and first-in-human study of ATX-MS-1467 for immunotherapy of MS. **Neurology: Neuroimmunology and NeuroInflammation**, 2 (3): e93

Sturniolo, T., Bono, E., Ding, J., et al. (1999) Generation of tissue-specific and promiscuous HLA ligand databases using DNA microarrays and virtual HLA class II matrices. **Nature Biotechnology**, 17 (6): 555–561

Sundstedt, A., O'Neill, E.J., Nicolson, K.S., et al. (2003a) Role for IL-10 in Suppression Mediated by Peptide-Induced Regulatory T Cells In Vivo. **Journal of Immunology**, 170 (3): 1240–1248

Sundstedt, A., O'Neill, E.J., Nicolson, K.S., et al. (2003b) Role for IL-10 in Suppression Mediated by Peptide-Induced Regulatory T Cells In Vivo. **The Journal of Immunology** [online], 170 (3): 1240–1248. Available from: http://www.jimmunol.org/cgi/doi/10.4049/jimmunol.170.3.1240

Syed, A., Garcia, M.A., Lyu, S.C., et al. (2014) Peanut oral immunotherapy results in increased antigen-induced regulatory T-cell function and hypomethylation of forkhead box protein 3 (FOXP3). **Journal of Allergy and Clinical Immunology**, 113 (2): 500–510

Takahashi, B.T., Tagami, T., Yamazaki, S., et al. (2000) Immunologic Self-Tolerance Maintained by CD25. **Journal of Experimental Medicine**, 192 (2)

Talwalkar, J.A. and Lindor, K.D. (2003) Primary biliary cirrhosis. **Lancet**, 362 (9377): 53–61

Tanaka, T. and Kishimoto, T. (2012) Targeting interleukin-6: All the way to treat autoimmune and inflammatory diseases. **International Journal of Biological Sciences**, 8 (9): 1227–1236

Testi, R., Phillips, J.H. and Lanier, L.L. (1989) T cell activation via Leu-23 (CD69). **Journal of Immunology**, 143 (4): 1123–8

Texier, C., Pouvelle, S., Busson, M., et al. (2000) HLA-DR Restricted Peptide Candidates for Bee Venom Immunotherapy. **Journal of Immunology**, 164 (6): 3177–3184

Thornton, A.M. and Shevach, E.M. (1998) CD4+CD25+ immunoregulatory T cells suppress polyclonal T cell activation in vitro by inhibiting interleukin 2 production. **Journal of Experimental Medicine**, 188 (2): 287–296

Thrower, S.L., James, L., Hall, W., et al. (2009) Proinsulin peptide immunotherapy in type 1 diabetes: Report of a first-in-man Phase I safety study. **Clinical and Experimental Immunology**, 155 (2): 156–165

Tiegs, G., Hentschel, J. and Wendel, A. (1992) A T cell-dependent experimental liver injury in mice inducible by concanavalin A. **Journal of Clinical Investigation**, 90 (1): 196–203

Turk, B., Turk, D. and Turk, V. (2000) Lysosomal cysteine proteases: More than scavengers. **Biochimica et Biophysica Acta - Protein Structure and Molecular Enzymology**, 1477 (1–2): 98–111

Uchtenhagen, H., Rims, C., Blahnik, G., et al. (2016) Efficient ex vivo analysis of CD4+ T-cell responses using combinatorial HLA class II tetramer staining. **Nature Communications**, 7 (12614)

Umeshappa, C.S., Mbongue, J., Singha, S., et al. (2020) Ubiquitous antigen-specific T regulatory type 1 cells variably suppress hepatic and extrahepatic autoimmunity. **Journal of Clinical Investigation**, 130 (4): 1823–1829

Umeshappa, C.S., Singha, S., Blanco, J., et al. (2019) Suppression of a broad spectrum of liver autoimmune pathologies by single peptide-MHC-based nanomedicines. **Nature Communications**, 10 (1): 1–17

Vanderlugt, C. and Miller, S. (1996) Epitope Spreading. **Current Opinion in Immunology**, 8 (6): 831–836

Vanderlugt, C.L. and Miller, S.D. (2002) Epitope Spreading in Immune-Mediated Diseases: Implications for Immunotherapy. **Nature Reviews Immunology**, 2 (2): 85–95

Vergani, D., Mieli-Vergani, G., Rodes, J., et al. (2007) **Textbook of Hepatology: From Basic Science to Clinical Practice**. Third edit. Blackwell Publishing

Verstegen, G., Duyck, M.C., Meeus, P., et al. (2009) Detection and identification of antinuclear antibodies (ANA) in a large community hospital. **Acta Clinica Belgica**, 64 (4): 317–323

Vitali, C., Mingozzi, F., Broggi, A., et al. (2012) Migratory, and not lymphoid-resident, dendritic cells maintain peripheral self-tolerance and prevent autoimmunity via induction of iTreg cells. **Blood**, 120 (6): 1237–1245

Vitozzi, S., Djilali-Saiah, I., Lapierre, P., et al. (2002) Anti-soluble liver antigen/liver-pancreas (SLA/LP) antibodies in pediatric patients with autoimmune hepatitis. **Autoimmunity**, 35 (8): 485–492

Waldmann, T.A. (1986) The structure, function, and expression of interleukin-2 receptors on normal and malignant lymphocytes. **Science**, 232 (4751): 727–732

Walker, E.J., Hirschfield, G.M., Xu, C., et al. (2009) CTLA4/ICOS gene variants and haplotypes are associated with rheumatoid arthritis and primary biliary cirrhosis in the Canadian population. **Arthritis and Rheumatism**, 60 (4): 931–937

Wang, B., Yang, L.-P., Zhang, X.-Z., et al. (2009) New insights into the structural characteristics and functional relevance of the human cytochrome P450 2D6 enzyme. **Drug Metabolism Reviews**, 41 (4): 573–643

Wang, P., Sidney, J., Dow, C., et al. (2008) A systematic assessment of MHC class II peptide binding predictions and evaluation of a consensus approach. **PLoS Computational Biology**, 4 (4)

Wąsik, M., Nazimek, K. and Bryniarski, K. (2018) Regulatory B cell phenotype and mechanism of action: the impact of stimulating conditions. **Microbiology and Immunology**, 62 (8): 485–496

Wasserman, R.L., Hague, A.R., Pence, D.M., et al. (2019) Real-World Experience with Peanut Oral Immunotherapy: Lessons Learned From 270 Patients. **Journal of Allergy and Clinical Immunology: In Practice** [online], 7 (2): 418–426. Available from: https://doi.org/10.1016/j.jaip.2018.05.023

Webb, G.J., Hirschfield, G.M., Krawitt, E.L., et al. (2018) Cellular and Molecular Mechanisms of Autoimmune Hepatitis. **Annual Review of Pathology: Mechanisms of Disease** [online], 13 (1): 247–292. Available from: http://www.annualreviews.org/doi/10.1146/annurev-pathol-020117-043534

Weiner, H.L. (1997) Oral tolerance: Immune mechanisms and treatment of autoimmune diseases. **Immunology Today**, 18 (7): 335–343

Werner, M., Almer, S., Prytz, H., et al. (2009) Hepatic and extrahepatic malignancies in autoimmune hepatitis. A long-term follow-up in 473 Swedish patients. **Journal of Hepatology**, 50 (2): 388–393

Werner, M., Prytz, H., Ohlsson, B., et al. (2008) Epidemiology and the initial presentation of autoimmune hepatitis in Sweden: A nationwide study. **Scandinavian Journal of Gastroenterology**, 43 (10): 1232–1240

White, A.M. and Wraith, D.C. (2016) Tr1-like T cells - An enigmatic regulatory t cell lineage. **Frontiers in Immunology**, 7 (SEP): 1–7

Wong, G.W., Yeong, T., Lawrence, D., et al. (2016) Concurrent extrahepatic autoimmunity in autoimmune hepatitis: implications for diagnosis, clinical course and long-term outcomes. **Liver International**, 37 (3): 449–457

Wraith, D. (2016) Antigen-specific immunotherapy. **Nature**, 530: 422–423

Wraith, D.C. (2018) Designing antigens for the prevention and treatment of autoimmune diseases. **Current Opinion in Chemical Engineering** [online], 19: 35–42. Available from: https://doi.org/10.1016/j.coche.2017.12.004

Yuksel, M., Wang, Y., Tai, N., et al. (2015) A novel “humanized mouse” model for autoimmune hepatitis and the association of gut microbiota with liver inflammation. **Hepatology**, 62 (5): 1536–1550

Zhang, L.J. and Wang, X.Z. (2006) Interleukin-10 and chronic liver disease. **World Journal of Gastroenterology**, 12 (11): 1681–1685

Zhernakova, A., Withoff, S. and Wijmenga, C. (2013) Clinical implications of shared genetics and pathogenesis in autoimmune diseases. **Nature Reviews Endocrinology**, 9 (11): 646–659

Zikherman, J. and Au-Yeung, B. (2015) The role of T cell receptor signaling thresholds in guiding T cell fate decisions. **Current Opinion in Immunology**, 33: 43–48

CHAPTER 8

APPENDICES

Appendix 1: Statistical analyses for Figure 3.3 – Tg4 mouse percentage of CD4$^+$ cells expressing FoxP3 and IL-10

Figure 3.3D: FoxP3$^+$ from Live CD4$^+$ cells

Tukey's multiple comparisons test	Mean Diff.	95.00% CI of diff.	Significant?	Summary	Adjusted P Value
PBS/PBS vs. PBS/4Y	-1.254	-3.216 to 0.7083	No	ns	0.2967
PBS/PBS vs. 4Y/PBS	-5.426	-7.388 to -3.464	Yes	****	<0.0001
PBS/PBS vs. 4Y/4Y	-3.026	-4.988 to -1.064	Yes	**	0.0022
PBS/4Y vs. 4Y/PBS	-4.172	-6.134 to -2.210	Yes	****	<0.0001
PBS/4Y vs. 4Y/4Y	-1.772	-3.734 to 0.1903	No	ns	0.0842
4Y/PBS vs. 4Y/4Y	2.400	0.4377 to 4.362	Yes	*	0.0142

Figure 3.3E: IL-10$^+$ from Tconv (all FoxP3$^-$) cells

Tukey's multiple comparisons test	Mean Diff.	95.00% CI of diff.	Significant?	Summary	Adjusted P Value
PBS/PBS vs. PBS/4Y	-0.8840	-4.770 to 3.002	No	ns	0.9137
PBS/PBS vs. 4Y/PBS	-19.89	-23.77 to -16.00	Yes	****	<0.0001
PBS/PBS vs. 4Y/4Y	-31.07	-34.95 to -27.18	Yes	****	<0.0001
PBS/4Y vs. 4Y/PBS	-19.00	-22.89 to -15.12	Yes	****	<0.0001
PBS/4Y vs. 4Y/4Y	-30.18	-34.07 to -26.30	Yes	****	<0.0001
4Y/PBS vs. 4Y/4Y	-11.18	-15.07 to -7.294	Yes	****	<0.0001

Figure 3.3E: IL-10$^+$ from Treg (FoxP3$^+$) cells

Tukey's multiple comparisons test	Mean Diff.	95.00% CI of diff.	Significant?	Summary	Adjusted P Value
PBS/PBS vs. PBS/4Y	0.3960	-8.448 to 9.240	No	ns	0.9992
PBS/PBS vs. 4Y/PBS	-34.56	-43.41 to -25.72	Yes	****	<0.0001
PBS/PBS vs. 4Y/4Y	-50.10	-58.95 to -41.26	Yes	****	<0.0001
PBS/4Y vs. 4Y/PBS	-34.96	-43.80 to -26.12	Yes	****	<0.0001
PBS/4Y vs. 4Y/4Y	-50.50	-59.34 to -41.66	Yes	****	<0.0001
4Y/PBS vs. 4Y/4Y	-15.54	-24.38 to -6.696	Yes	***	0.0006

Figure 3.3E: IL-10$^+$ comparing Tconv vs Treg

Tukey's multiple comparisons test	Mean Diff.	95.00% CI of diff.	Significant?	Summary	Adjusted P Value
PBS/PBS Tconv vs. PBS/PBS Treg	-4.942	-11.24 to 1.359	No	ns	0.1738
PBS/4Y Tconv vs. PBS/4Y Treg	-3.662	-9.963 to 2.639	No	ns	0.4400
4Y/PBS Tconv vs. 4Y/PBS Treg	-19.62	-25.92 to -13.32	Yes	****	<0.0001
4Y/4Y Tconv vs. 4Y/4Y Treg	-23.98	-30.28 to -17.68	Yes	****	<0.0001

Appendix 1: p-values calculated by one-way ANOVA with multiple comparisons for FoxP3 expression in Tg4 mouse groups (PBS/PBS, PBS/4Y, 4Y/PBS, 4Y/4Y) and IL-10 expression both within Tconv and Treg, and between Tconv and Treg in Tg4 mouse groups (PBS/PBS, PBS/4Y, 4Y/PBS, 4Y/4Y).

Appendix 2: Statistical analyses for Figure 3.4 – Tg4 mouse percentage of CD4$^+$ cells expressing coinhibitory receptor

Figure 3.4A: TIGIT$^+$ from Tconv

Tukey's multiple comparisons test	Mean Diff.	95.00% CI of diff.	Significant?	Summary	Adjusted P Value
PBS/PBS vs. PBS/4Y	-0.1540	-3.802 to 3.494	No	ns	0.9993
PBS/PBS vs. 4Y/PBS	-5.468	-9.116 to -1.820	Yes	**	0.0028
PBS/PBS vs. 4Y/4Y	-11.74	-15.38 to -8.088	Yes	****	<0.0001
PBS/4Y vs. 4Y/PBS	-5.314	-8.962 to -1.666	Yes	**	0.0036
PBS/4Y vs. 4Y/4Y	-11.58	-15.23 to -7.934	Yes	****	<0.0001
4Y/PBS vs. 4Y/4Y	-6.268	-9.916 to -2.620	Yes	***	0.0008

Figure 3.4A: TIGIT$^+$ from Tr1

Tukey's multiple comparisons test	Mean Diff.	95.00% CI of diff.	Significant?	Summary	Adjusted P Value
PBS/PBS vs. PBS/4Y	-0.1540	-3.802 to 3.494	No	ns	0.9993
PBS/PBS vs. 4Y/PBS	-5.468	-9.116 to -1.820	Yes	**	0.0028
PBS/PBS vs. 4Y/4Y	-11.74	-15.38 to -8.088	Yes	****	<0.0001
PBS/4Y vs. 4Y/PBS	-5.314	-8.962 to -1.666	Yes	**	0.0036
PBS/4Y vs. 4Y/4Y	-11.58	-15.23 to -7.934	Yes	****	<0.0001
4Y/PBS vs. 4Y/4Y	-6.268	-9.916 to -2.620	Yes	***	0.0008

Figure 3.4A: TIGIT$^+$ from Treg

Tukey's multiple comparisons test	Mean Diff.	95.00% CI of diff.	Significant?	Summary	Adjusted P Value
PBS/PBS vs. PBS/4Y	-5.260	-19.93 to 9.407	No	ns	0.7370
PBS/PBS vs. 4Y/PBS	-36.04	-50.71 to -21.37	Yes	****	<0.0001
PBS/PBS vs. 4Y/4Y	-42.32	-56.99 to -27.65	Yes	****	<0.0001
PBS/4Y vs. 4Y/PBS	-30.78	-45.45 to -16.11	Yes	****	<0.0001
PBS/4Y vs. 4Y/4Y	-37.06	-51.73 to -22.39	Yes	****	<0.0001
4Y/PBS vs. 4Y/4Y	-6.280	-20.95 to 8.387	No	ns	0.6207

Figure 3.4A: TIGIT$^+$ between Tconv, Tr1 and Treg

Tukey's multiple comparisons test	Mean Diff.	95.00% CI of diff.	Significant?	Summary	Adjusted P Value
PBS/PBS Tconv vs. PBS/PBS Tr1	-6.044	-8.126 to -3.962	Yes	****	<0.0001
PBS/PBS Tconv vs. PBS/PBS Treg	-13.56	-15.64 to -11.48	Yes	****	<0.0001
PBS/PBS Tr1 vs. PBS/PBS Treg	-7.516	-9.598 to -5.434	Yes	****	<0.0001

Tukey's multiple comparisons test	Mean Diff.	95.00% CI of diff.	Significant?	Summary	Adjusted P Value
PBS/4Y Tconv vs. PBS/4Y Tr1	-9.066	-14.97 to -3.164	Yes	**	0.0039
PBS/4Y Tconv vs. PBS/4Y Treg	-18.67	-24.57 to -12.76	Yes	****	<0.0001
PBS/4Y Tr1 vs. PBS/4Y Treg	-9.600	-15.50 to -3.698	Yes	**	0.0026

Tukey's multiple comparisons test	Mean Diff.	95.00% CI of diff.	Significant?	Summary	Adjusted P Value
4Y/PBS Tconv vs. 4Y/PBS Tr1	-11.87	-23.33 to -0.4140	Yes	*	0.0422
4Y/PBS Tconv vs. 4Y/PBS Treg	-44.13	-55.59 to -32.67	Yes	****	<0.0001
4Y/PBS Tr1 vs. 4Y/PBS Treg	-32.26	-43.72 to -20.80	Yes	****	<0.0001

Tukey's multiple comparisons test	Mean Diff.	95.00% CI of diff.	Significant?	Summary	Adjusted P Value
4Y/4Y Tconv vs. 4Y/4Y Tr1	-9.864	-20.30 to 0.5731	No	ns	0.0646
4Y/4Y Tconv vs. 4Y/4Y Treg	-44.14	-54.58 to -33.71	Yes	****	<0.0001
4Y/4Y Tr1 vs. 4Y/4Y Treg	-34.28	-44.72 to -23.84	Yes	****	<0.0001

Figure 3.4B: PD-1$^+$ from Tconv

Tukey's multiple comparisons test	Mean Diff.	95.00% CI of diff.	Significant?	Summary	Adjusted P Value
PBS/PBS vs. PBS/4Y	-2.640	-10.52 to 5.237	No	ns	0.7741
PBS/PBS vs. 4Y/PBS	-30.86	-38.74 to -22.98	Yes	****	<0.0001
PBS/PBS vs. 4Y/4Y	-51.00	-58.88 to -43.12	Yes	****	<0.0001
PBS/4Y vs. 4Y/PBS	-28.22	-36.10 to -20.34	Yes	****	<0.0001
PBS/4Y vs. 4Y/4Y	-48.36	-56.24 to -40.48	Yes	****	<0.0001
4Y/PBS vs. 4Y/4Y	-20.14	-28.02 to -12.26	Yes	****	<0.0001

Figure 3.4B: PD-1$^+$ from Tr1

Tukey's multiple comparisons test	Mean Diff.	95.00% CI of diff.	Significant?	Summary	Adjusted P Value
PBS/PBS vs. PBS/4Y	-2.580	-11.92 to 6.757	No	ns	0.8577
PBS/PBS vs. 4Y/PBS	-31.72	-41.06 to -22.38	Yes	****	<0.0001
PBS/PBS vs. 4Y/4Y	-51.10	-60.44 to -41.76	Yes	****	<0.0001
PBS/4Y vs. 4Y/PBS	-29.14	-38.48 to -19.80	Yes	****	<0.0001
PBS/4Y vs. 4Y/4Y	-48.52	-57.86 to -39.18	Yes	****	<0.0001
4Y/PBS vs. 4Y/4Y	-19.38	-28.72 to -10.04	Yes	***	0.0001

Figure 3.4B: PD-1$^+$ from Treg

Tukey's multiple comparisons test	Mean Diff.	95.00% CI of diff.	Significant?	Summary	Adjusted P Value
PBS/PBS vs. PBS/4Y	-4.480	-14.50 to 5.537	No	ns	0.5882
PBS/PBS vs. 4Y/PBS	-19.28	-29.30 to -9.263	Yes	***	0.0003
PBS/PBS vs. 4Y/4Y	-41.70	-51.72 to -31.68	Yes	****	<0.0001
PBS/4Y vs. 4Y/PBS	-14.80	-24.82 to -4.783	Yes	**	0.0032
PBS/4Y vs. 4Y/4Y	-37.22	-47.24 to -27.20	Yes	****	<0.0001
4Y/PBS vs. 4Y/4Y	-22.42	-32.44 to -12.40	Yes	****	<0.0001

Figure 3.4B: PD-1$^+$ between Tconv, Tr1 and Treg

Tukey's multiple comparisons test	Mean Diff.	95.00% CI of diff.	Significant?	Summary	Adjusted P Value
PBS/PBS Tconv vs. PBS/PBS Tr1	-14.22	-20.53 to -7.912	Yes	***	0.0002
PBS/PBS Tconv vs. PBS/PBS Treg	-30.74	-37.05 to -24.43	Yes	****	<0.0001
PBS/PBS Tr1 vs. PBS/PBS Treg	-16.52	-22.83 to -10.21	Yes	****	<0.0001

Tukey's multiple comparisons test	Mean Diff.	95.00% CI of diff.	Significant?	Summary	Adjusted P Value
PBS/4Y Tconv vs. PBS/4Y Tr1	-14.16	-20.25 to -8.072	Yes	***	0.0001
PBS/4Y Tconv vs. PBS/4Y Treg	-32.58	-38.67 to -26.49	Yes	****	<0.0001
PBS/4Y Tr1 vs. PBS/4Y Treg	-18.42	-24.51 to -12.33	Yes	****	<0.0001

Tukey's multiple comparisons test	Mean Diff.	95.00% CI of diff.	Significant?	Summary	Adjusted P Value
4Y/PBS Tconv vs. 4Y/PBS Tr1	-15.08	-26.20 to -3.958	Yes	**	0.0092
4Y/PBS Tconv vs. 4Y/PBS Treg	-19.16	-30.28 to -8.038	Yes	**	0.0016
4Y/PBS Tr1 vs. 4Y/PBS Treg	-4.080	-15.20 to 7.042	No	ns	0.6035

Tukey's multiple comparisons test	Mean Diff.	95.00% CI of diff.	Significant?	Summary	Adjusted P Value
4Y/4Y Tconv vs. 4Y/4Y Tr1	-14.32	-23.74 to -4.900	Yes	**	0.0042
4Y/4Y Tconv vs. 4Y/4Y Treg	-21.44	-30.86 to -12.02	Yes	***	0.0002
4Y/4Y Tr1 vs. 4Y/4Y Treg	-7.120	-16.54 to 2.300	No	ns	0.1506

Figure 3.4C: TIM-3$^+$ from Tconv

Tukey's multiple comparisons test	Mean Diff.	95.00% CI of diff.	Significant?	Summary	Adjusted P Value
PBS/PBS vs. PBS/4Y	-0.1680	-4.908 to 4.572	No	ns	0.9996
PBS/PBS vs. 4Y/PBS	-6.012	-10.75 to -1.272	Yes	*	0.0109
PBS/PBS vs. 4Y/4Y	-13.29	-18.03 to -8.550	Yes	****	<0.0001
PBS/4Y vs. 4Y/PBS	-5.844	-10.58 to -1.104	Yes	*	0.0134
PBS/4Y vs. 4Y/4Y	-13.12	-17.86 to -8.382	Yes	****	<0.0001
4Y/PBS vs. 4Y/4Y	-7.278	-12.02 to -2.538	Yes	**	0.0023

Figure 3.4C: TIM-3$^+$ from Tr1

Tukey's multiple comparisons test	Mean Diff.	95.00% CI of diff.	Significant?	Summary	Adjusted P Value
PBS/PBS vs. PBS/4Y	-7.960	-16.91 to 0.9879	No	ns	0.0903
PBS/PBS vs. 4Y/PBS	-3.140	-12.09 to 5.808	No	ns	0.7494
PBS/PBS vs. 4Y/4Y	-22.42	-31.37 to -13.47	Yes	****	<0.0001
PBS/4Y vs. 4Y/PBS	4.820	-4.128 to 13.77	No	ns	0.4376
PBS/4Y vs. 4Y/4Y	-14.46	-23.41 to -5.512	Yes	**	0.0014
4Y/PBS vs. 4Y/4Y	-19.28	-28.23 to -10.33	Yes	****	<0.0001

Figure 3.4C: TIM-3$^+$ from Treg

Tukey's multiple comparisons test	Mean Diff.	95.00% CI of diff.	Significant?	Summary	Adjusted P Value
PBS/PBS vs. PBS/4Y	-2.280	-11.86 to 7.301	No	ns	0.9029
PBS/PBS vs. 4Y/PBS	-12.00	-21.58 to -2.419	Yes	*	0.0120
PBS/PBS vs. 4Y/4Y	-44.44	-54.02 to -34.86	Yes	****	<0.0001
PBS/4Y vs. 4Y/PBS	-9.720	-19.30 to -0.1388	Yes	*	0.0462
PBS/4Y vs. 4Y/4Y	-42.16	-51.74 to -32.58	Yes	****	<0.0001
4Y/PBS vs. 4Y/4Y	-32.44	-42.02 to -22.86	Yes	****	<0.0001

Figure 3.4C: TIM-3$^+$ between Tconv, Tr1 and Treg

Tukey's multiple comparisons test	Mean Diff.	95.00% CI of diff.	Significant?	Summary	Adjusted P Value
PBS/PBS vs. PBS/PBS	-19.44	-25.77 to -13.11	Yes	****	<0.0001
PBS/PBS vs. PBS/PBS	-19.08	-25.41 to -12.75	Yes	****	<0.0001
PBS/PBS vs. PBS/PBS	0.3600	-5.972 to 6.692	No	ns	0.9874

Tukey's multiple comparisons test	Mean Diff.	95.00% CI of diff.	Significant?	Summary	Adjusted P Value
PBS/4Y vs. PBS/4Y	-27.23	-34.43 to -20.04	Yes	****	<0.0001
PBS/4Y vs. PBS/4Y	-21.19	-28.39 to -14.00	Yes	****	<0.0001
PBS/4Y vs. PBS/4Y	6.040	-1.155 to 13.24	No	ns	0.1044

Tukey's multiple comparisons test	Mean Diff.	95.00% CI of diff.	Significant?	Summary	Adjusted P Value
4Y/PBS vs. 4Y/PBS	-16.57	-23.99 to -9.144	Yes	***	0.0002
4Y/PBS vs. 4Y/PBS	-25.07	-32.49 to -17.64	Yes	****	<0.0001
4Y/PBS vs. 4Y/PBS	-8.500	-15.92 to -1.076	Yes	*	0.0251

Tukey's multiple comparisons test	Mean Diff.	95.00% CI of diff.	Significant?	Summary	Adjusted P Value
4Y/4Y vs. 4Y/4Y	-28.57	-37.42 to -19.72	Yes	****	<0.0001
4Y/4Y vs. 4Y/4Y	-50.23	-59.08 to -41.38	Yes	****	<0.0001
4Y/4Y vs. 4Y/4Y	-21.66	-30.51 to -12.81	Yes	****	<0.0001

Figure 3.4D: LAG-3$^+$ from Tconv

Tukey's multiple comparisons test	Mean Diff.	95.00% CI of diff.	Significant?	Summary	Adjusted P Value
PBS/PBS vs. PBS/4Y	-0.03600	-1.841 to 1.769	No	ns	>0.9999
PBS/PBS vs. 4Y/PBS	-4.680	-6.485 to -2.875	Yes	****	<0.0001
PBS/PBS vs. 4Y/4Y	-9.640	-11.44 to -7.835	Yes	****	<0.0001
PBS/4Y vs. 4Y/PBS	-4.644	-6.449 to -2.839	Yes	****	<0.0001
PBS/4Y vs. 4Y/4Y	-9.604	-11.41 to -7.799	Yes	****	<0.0001
4Y/PBS vs. 4Y/4Y	-4.960	-6.765 to -3.155	Yes	****	<0.0001

Figure 3.4D: LAG-3$^+$ from Tr1

Tukey's multiple comparisons test	Mean Diff.	95.00% CI of diff.	Significant?	Summary	Adjusted P Value
PBS/PBS vs. PBS/4Y	-1.570	-4.558 to 1.418	No	ns	0.4586
PBS/PBS vs. 4Y/PBS	-6.042	-9.030 to -3.054	Yes	***	0.0001
PBS/PBS vs. 4Y/4Y	-8.870	-11.86 to -5.882	Yes	****	<0.0001
PBS/4Y vs. 4Y/PBS	-4.472	-7.460 to -1.484	Yes	**	0.0029
PBS/4Y vs. 4Y/4Y	-7.300	-10.29 to -4.312	Yes	****	<0.0001
4Y/PBS vs. 4Y/4Y	-2.828	-5.816 to 0.1604	No	ns	0.0669

Figure 3.4D: LAG-3$^+$ from Treg

Tukey's multiple comparisons test	Mean Diff.	95.00% CI of diff.	Significant?	Summary	Adjusted P Value
PBS/PBS vs. PBS/4Y	-3.838	-7.171 to -0.5048	Yes	*	0.0214
PBS/PBS vs. 4Y/PBS	-6.780	-10.11 to -3.447	Yes	***	0.0001
PBS/PBS vs. 4Y/4Y	-10.92	-14.25 to -7.585	Yes	****	<0.0001
PBS/4Y vs. 4Y/PBS	-2.942	-6.275 to 0.3912	No	ns	0.0937
PBS/4Y vs. 4Y/4Y	-7.080	-10.41 to -3.747	Yes	****	<0.0001
4Y/PBS vs. 4Y/4Y	-4.138	-7.471 to -0.8048	Yes	*	0.0127

Figure 3.4D: LAG-3$^+$ between Tconv, Tr1 and Treg

Tukey's multiple comparisons test	Mean Diff.	95.00% CI of diff.	Significant?	Summary	Adjusted P Value
PBS/PBS vs. PBS/PBS	-2.736	-4.773 to -0.6994	Yes	**	0.0097
PBS/PBS vs. PBS/PBS	-7.508	-9.545 to -5.471	Yes	****	<0.0001
PBS/PBS vs. PBS/PBS	-4.772	-6.809 to -2.735	Yes	***	0.0001
Tukey's multiple comparisons test	Mean Diff.	95.00% CI of diff.	Significant?	Summary	Adjusted P Value
PBS/4Y vs. PBS/4Y	-4.270	-6.541 to -1.999	Yes	***	0.0008
PBS/4Y vs. PBS/4Y	-11.31	-13.58 to -9.039	Yes	****	<0.0001
PBS/4Y vs. PBS/4Y	-7.040	-9.311 to -4.769	Yes	****	<0.0001
Tukey's multiple comparisons test	Mean Diff.	95.00% CI of diff.	Significant?	Summary	Adjusted P Value
4Y/PBS vs. 4Y/PBS	-4.098	-7.017 to -1.179	Yes	**	0.0073
4Y/PBS vs. 4Y/PBS	-9.608	-12.53 to -6.689	Yes	****	<0.0001
4Y/PBS vs. 4Y/PBS	-5.510	-8.429 to -2.591	Yes	***	0.0008
Tukey's multiple comparisons test	Mean Diff.	95.00% CI of diff.	Significant?	Summary	Adjusted P Value
4Y/4Y vs. 4Y/4Y	-1.966	-4.996 to 1.064	No	ns	0.2341
4Y/4Y vs. 4Y/4Y	-8.786	-11.82 to -5.756	Yes	****	<0.0001
4Y/4Y vs. 4Y/4Y	-6.820	-9.850 to -3.790	Yes	***	0.0002

Appendix 2: p-values calculated by one-way ANOVA with multiple comparisons for TIGIT, PD-1, TIM-3 and LAG-3 expression both within Tconv and Treg, and between Tconv and Treg in Tg4 mouse groups (PBS/PBS, PBS/4Y, 4Y/PBS, 4Y/4Y).

Appendix 3: Statistical analyses for Figure 3.5 – Tg4 mouse percentage of CD4$^+$ cells expressing CTLA-4

Figure 3.5A: Surface CTLA-4$^+$ (stained at 4°C) between Tconv, Tr1 and Treg of PBS/PBS, PBS/4Y, 4Y/PBS, 4Y/4Y treated Tg4 mice

Tukey's multiple comparisons test	Mean Diff.	95.00% CI of diff.	Significant?	Summary	Adjusted P Value
PBS/PBS					
Treg 4C vs. Tconv 4C	2.753	-2.610 to 8.116	No	ns	0.4186
Treg 4C vs. Tr1 4C	-7.083	-12.45 to -1.720	Yes	**	0.0082
Tconv 4C vs. Tr1 4C	-9.837	-15.20 to -4.474	Yes	***	0.0003
PBS/4Y					
Treg 4C vs. Tconv 4C	18.78	13.41 to 24.14	Yes	****	<0.0001
Treg 4C vs. Tr1 4C	10.34	4.977 to 15.70	Yes	***	0.0002
Tconv 4C vs. Tr1 4C	-8.437	-13.80 to -3.074	Yes	**	0.0018
4Y/PBS					
Treg 4C vs. Tconv 4C	27.73	22.37 to 33.10	Yes	****	<0.0001
Treg 4C vs. Tr1 4C	11.39	6.024 to 16.75	Yes	****	<0.0001
Tconv 4C vs. Tr1 4C	-16.35	-21.71 to -10.98	Yes	****	<0.0001
4Y/4Y					
Treg 4C vs. Tconv 4C	41.71	36.35 to 47.07	Yes	****	<0.0001
Treg 4C vs. Tr1 4C	20.23	14.87 to 25.60	Yes	****	<0.0001
Tconv 4C vs. Tr1 4C	-21.48	-26.84 to -16.11	Yes	****	<0.0001

Figure 3.5A: Surface CTLA-4$^+$ (stained at 4°C) of Tconv between PBS/PBS, PBS/4Y, 4Y/PBS, 4Y/4Y treated Tg4 mice

Tukey's multiple comparisons test	Mean Diff.	95.00% CI of diff.	Significant?	Summary	Adjusted P Value
PBS/PBS vs. PBS/4Y	0.3400	-1.336 to 2.016	No	ns	0.9128
PBS/PBS vs. 4Y/PBS	-1.623	-3.300 to 0.05306	No	ns	0.0577
PBS/PBS vs. 4Y/4Y	-3.093	-4.770 to -1.417	Yes	**	0.0016
PBS/4Y vs. 4Y/PBS	-1.963	-3.640 to -0.2869	Yes	*	0.0233
PBS/4Y vs. 4Y/4Y	-3.433	-5.110 to -1.757	Yes	***	0.0008
4Y/PBS vs. 4Y/4Y	-1.470	-3.146 to 0.2064	No	ns	0.0872

Figure 3.5A: Surface CTLA-4$^+$ (stained at 4°C) of Tr1 between PBS/PBS, PBS/4Y, 4Y/PBS, 4Y/4Y treated Tg4 mice

Tukey's multiple comparisons test	Mean Diff.	95.00% CI of diff.	Significant?	Summary	Adjusted P Value
PBS/PBS vs. PBS/4Y	1.740	-4.779 to 8.259	No	ns	0.8274
PBS/PBS vs. 4Y/PBS	-8.133	-14.65 to -1.614	Yes	*	0.0168
PBS/PBS vs. 4Y/4Y	-14.73	-21.25 to -8.214	Yes	***	0.0004
PBS/4Y vs. 4Y/PBS	-9.873	-16.39 to -3.354	Yes	**	0.0056
PBS/4Y vs. 4Y/4Y	-16.47	-22.99 to -9.954	Yes	***	0.0002
4Y/PBS vs. 4Y/4Y	-6.600	-13.12 to -0.08117	Yes	*	0.0473

Figure 3.5A: Surface CTLA-4$^+$ (stained at 4°C) of Treg between PBS/PBS, PBS/4Y, 4Y/PBS, 4Y/4Y treated Tg4 mice

Tukey's multiple comparisons test	Mean Diff.	95.00% CI of diff.	Significant?	Summary	Adjusted P Value
PBS/PBS vs. PBS/4Y	-15.68	-25.51 to -5.855	Yes	**	0.0040
PBS/PBS vs. 4Y/PBS	-26.60	-36.43 to -16.78	Yes	***	0.0001
PBS/PBS vs. 4Y/4Y	-42.05	-51.88 to -32.22	Yes	****	<0.0001
PBS/4Y vs. 4Y/PBS	-10.92	-20.75 to -1.092	Yes	*	0.0304
PBS/4Y vs. 4Y/4Y	-26.37	-36.19 to -16.54	Yes	***	0.0001
4Y/PBS vs. 4Y/4Y	-15.45	-25.27 to -5.619	Yes	**	0.0044

Figure 3.5B: Cycling CTLA-4$^+$ (stained at 37°C) between Tconv, Tr1 and Treg of PBS/PBS, PBS/4Y, 4Y/PBS, 4Y/4Y treated Tg4 mice

Tukey's multiple comparisons test	Mean Diff.	95.00% CI of diff.	Significant?	Summary	Adjusted P Value
PBS/PBS					
Tconv 37C vs. Treg 37C	-8.593	-17.16 to -0.02677	Yes	*	0.0492
Tconv 37C vs. Tr1 37C	-23.64	-32.20 to -15.07	Yes	****	<0.0001
Treg 37C vs. Tr1 37C	-15.04	-23.61 to -6.477	Yes	***	0.0006
PBS/4Y					
Tconv 37C vs. Treg 37C	-40.95	-49.51 to -32.38	Yes	****	<0.0001
Tconv 37C vs. Tr1 37C	-27.18	-35.75 to -18.61	Yes	****	<0.0001
Treg 37C vs. Tr1 37C	13.77	5.200 to 22.33	Yes	**	0.0014
4Y/PBS					
Tconv 37C vs. Treg 37C	-45.33	-53.90 to -36.76	Yes	****	<0.0001
Tconv 37C vs. Tr1 37C	-33.75	-42.32 to -25.18	Yes	****	<0.0001
Treg 37C vs. Tr1 37C	11.58	3.013 to 20.15	Yes	**	0.0068
4Y/4Y					
Tconv 37C vs. Treg 37C	-45.81	-54.37 to -37.24	Yes	****	<0.0001
Tconv 37C vs. Tr1 37C	-52.64	-61.21 to -44.07	Yes	****	<0.0001
Treg 37C vs. Tr1 37C	-6.833	-15.40 to 1.733	No	ns	0.1359

Figure 3.5B: Cycling CTLA-4$^+$ (stained at 37°C) of Tconv between PBS/PBS, PBS/4Y, 4Y/PBS, 4Y/4Y treated Tg4 mice

Tukey's multiple comparisons test	Mean Diff.	95.00% CI of diff.	Significant?	Summary	Adjusted P Value
PBS/PBS vs. PBS/4Y	-2.790	-6.360 to 0.7799	No	ns	0.1339
PBS/PBS vs. 4Y/PBS	-5.520	-9.090 to -1.950	Yes	**	0.0049
PBS/PBS vs. 4Y/4Y	-8.863	-12.43 to -5.293	Yes	***	0.0002
PBS/4Y vs. 4Y/PBS	-2.730	-6.300 to 0.8399	No	ns	0.1443
PBS/4Y vs. 4Y/4Y	-6.073	-9.643 to -2.503	Yes	**	0.0027
4Y/PBS vs. 4Y/4Y	-3.343	-6.913 to 0.2266	No	ns	0.0666

Figure 3.5B: Cycling CTLA-4$^+$ (stained at 37°C) of Tr1 between PBS/PBS, PBS/4Y, 4Y/PBS, 4Y/4Y treated Tg4 mice

Tukey's multiple comparisons test	Mean Diff.	95.00% CI of diff.	Significant?	Summary	Adjusted P Value
PBS/PBS vs. PBS/4Y	-6.333	-21.71 to 9.046	No	ns	0.5774
PBS/PBS vs. 4Y/PBS	-15.63	-31.01 to -0.2537	Yes	*	0.0464
PBS/PBS vs. 4Y/4Y	-37.87	-53.25 to -22.49	Yes	***	0.0002
PBS/4Y vs. 4Y/PBS	-9.300	-24.68 to 6.080	No	ns	0.2865
PBS/4Y vs. 4Y/4Y	-31.53	-46.91 to -16.15	Yes	***	0.0008
4Y/PBS vs. 4Y/4Y	-22.23	-37.61 to -6.854	Yes	**	0.0073

Figure 3.5B: Cycling CTLA-4$^+$ (stained at 37°C) of Treg between PBS/PBS, PBS/4Y, 4Y/PBS, 4Y/4Y treated Tg4 mice

Tukey's multiple comparisons test	Mean Diff.	95.00% CI of diff.	Significant?	Summary	Adjusted P Value
PBS/PBS vs. PBS/4Y	-35.14	-45.76 to -24.53	Yes	****	<0.0001
PBS/PBS vs. 4Y/PBS	-42.26	-52.87 to -31.64	Yes	****	<0.0001
PBS/PBS vs. 4Y/4Y	-46.08	-56.69 to -35.46	Yes	****	<0.0001
PBS/4Y vs. 4Y/PBS	-7.113	-17.73 to 3.505	No	ns	0.2182
PBS/4Y vs. 4Y/4Y	-10.93	-21.55 to -0.3152	Yes	*	0.0438
4Y/PBS vs. 4Y/4Y	-3.820	-14.44 to 6.798	No	ns	0.6705

Figure 3.5C: Total CTLA-4$^+$ (surface and intracellular) between Tconv, Tr1 and Treg of PBS/PBS, PBS/4Y, 4Y/PBS, 4Y/4Y treated Tg4 mice

Tukey's multiple comparisons test	Mean Diff.	95.00% CI of diff.	Significant?	Summary	Adjusted P Value
PBS/PBS					
Tconv total vs. Treg total	-81.53	-87.73 to -75.33	Yes	****	<0.0001
Tconv total vs. Tr1 total	-39.63	-45.83 to -33.43	Yes	****	<0.0001
Treg total vs. Tr1 total	41.90	35.70 to 48.10	Yes	****	<0.0001
PBS/4Y					
Tconv total vs. Treg total	-76.43	-82.63 to -70.23	Yes	****	<0.0001
Tconv total vs. Tr1 total	-45.33	-51.53 to -39.13	Yes	****	<0.0001
Treg total vs. Tr1 total	31.10	24.90 to 37.30	Yes	****	<0.0001
4Y/PBS					
Tconv total vs. Treg total	-69.70	-75.90 to -63.50	Yes	****	<0.0001
Tconv total vs. Tr1 total	-47.20	-53.40 to -41.00	Yes	****	<0.0001
Treg total vs. Tr1 total	22.50	16.30 to 28.70	Yes	****	<0.0001
4Y/4Y					
Tconv total vs. Treg total	-62.17	-68.37 to -55.97	Yes	****	<0.0001
Tconv total vs. Tr1 total	-51.80	-58.00 to -45.60	Yes	****	<0.0001
Treg total vs. Tr1 total	10.37	4.168 to 16.57	Yes	***	0.0009

Figure 3.5C: Total CTLA-4$^+$ (surface and intracellular) of Tconv between PBS/PBS, PBS/4Y, 4Y/PBS, 4Y/4Y treated Tg4 mice

Tukey's multiple comparisons test	Mean Diff.	95.00% CI of diff.	Significant?	Summary	Adjusted P Value
PBS/PBS vs. PBS/4Y	-4.333	-14.48 to 5.811	No	ns	0.5503
PBS/PBS vs. 4Y/PBS	-12.30	-22.44 to -2.156	Yes	*	0.0195
PBS/PBS vs. 4Y/4Y	-20.27	-30.41 to -10.12	Yes	***	0.0009
PBS/4Y vs. 4Y/PBS	-7.967	-18.11 to 2.178	No	ns	0.1317
PBS/4Y vs. 4Y/4Y	-15.93	-26.08 to -5.789	Yes	**	0.0045
4Y/PBS vs. 4Y/4Y	-7.967	-18.11 to 2.178	No	ns	0.1317

Figure 3.5C: Total CTLA-4$^+$ (surface and intracellular) of Tr1 between PBS/PBS, PBS/4Y, 4Y/PBS, 4Y/4Y treated Tg4 mice

Tukey's multiple comparisons test	Mean Diff.	95.00% CI of diff.	Significant?	Summary	Adjusted P Value
PBS/PBS vs. PBS/4Y	-10.03	-18.27 to -1.795	Yes	*	0.0190
PBS/PBS vs. 4Y/PBS	-19.87	-28.10 to -11.63	Yes	***	0.0003
PBS/PBS vs. 4Y/4Y	-32.43	-40.67 to -24.20	Yes	****	<0.0001
PBS/4Y vs. 4Y/PBS	-9.833	-18.07 to -1.595	Yes	*	0.0212
PBS/4Y vs. 4Y/4Y	-22.40	-30.64 to -14.16	Yes	***	0.0001
4Y/PBS vs. 4Y/4Y	-12.57	-20.80 to -4.329	Yes	**	0.0053

Figure 3.5C: Total CTLA-4$^+$ (surface and intracellular) of Treg between PBS/PBS, PBS/4Y, 4Y/PBS, 4Y/4Y treated Tg4 mice

Tukey's multiple comparisons test	Mean Diff.	95.00% CI of diff.	Significant?	Summary	Adjusted P Value
PBS/PBS vs. PBS/4Y	0.7667	-3.567 to 5.101	No	ns	0.9393
PBS/PBS vs. 4Y/PBS	-0.4667	-4.801 to 3.867	No	ns	0.9849
PBS/PBS vs. 4Y/4Y	-0.9000	-5.234 to 3.434	No	ns	0.9073
PBS/4Y vs. 4Y/PBS	-1.233	-5.567 to 3.101	No	ns	0.7998
PBS/4Y vs. 4Y/4Y	-1.667	-6.001 to 2.667	No	ns	0.6260
4Y/PBS vs. 4Y/4Y	-0.4333	-4.767 to 3.901	No	ns	0.9878

Appendix 3: p-values calculated by one-way ANOVA with multiple comparisons for CTLA-4 expression both within Tconv, Tr1 and Treg, and between Tconv, Tr1 and Treg in Tg4 mouse groups (PBS/PBS, PBS/4Y, 4Y/PBS, 4Y/4Y).

Appendix 4: HLA-DR typing of healthy donors used in CYP2D6 peptide proliferation assay

Healthy donor ID #	HLA-DR Alleles	Null/ alternative alleles
B1	DR1, DR7	DR53
B3	DR17/DR3, DR12	DR52
B4	DR15/DR2, DR12	DR52
B5	DR2, DR11	DR52 + DR53
B10	DR15/DR2, DR8	DR51
B11	DR13	DR52
B13	DR15/DR2, DR4	DR53
B14	DR17/DR3, DR4	DR52 + DR53
B15	DR7, DR13	DR52 + DR53
B16	DR1, DR4	DR53
B17	DR1, DR7	
B18	DR4, DR14	DR52 + DR53
B20	DR17/DR3, DR7	DR52 + DR53
B22	DR2/DR15, DR4	DR52 + DR53
B23	DR1, DR2	DR53
B24	DR11, DR12	DR53
B26	DR7, DR13	DR52 + DR53
B31	DR15/DR2, DR7	DR53, DR51
B34	DR7, DR11	DR53
B36	DR7	DRB4, DR52
B37	DR8, DR13	DR52
B38	DR7, DR11	DR52, DR53
B39	DR1	
B41	DR7, DR11	DR52, DR53
B45	DR7, DR11	DR52 + DR53
B46	DR4	DR52
B47	DR1, DR3	DR52
B49	DR12, DR13	DR51, DR52
B50	DR1, DR4	DR52
B51	DR17/DR3, DR103	DR52
B55	DR1, DR4	DR53
B60	DR15/DR2, DR11	DR52
B61	DR1, DR17/DR3	DR52
B67	DR4, DR11	DR52, DR53
D2	DR17/DR3, DR4	DR52, DR53
D3	DR13, DR7	DR52, DR53
D4	DR17/DR3, DR7	DR52, DR53
D7	DR15/DR2, DR7	DR51, DR53
D8	DR17/DR3, DR7	DR52, DR53
D9	DR13	DR52
D13	DR17/DR3, DR4	DR52, DR53
D30	DR17/DR3, DR7	DR52, DR53
P3	DR2, DR13	DR52, DR51

Appendix 4: HLA-DR typing of healthy donors in cohort. DNA was extracted from each donor's PBMCs. HLA-DR typing was performed using a PCR based array system (Olerup-SSP; 101.101-48u). PCR products were run on a 2% agarose-ethidium bromide gel before analysis of DNA band patterns.

Appendix 5: Key patient and clinical data of paediatric AIH-2 patients involved in study under the care of Birmingham Children's Hospital

Study ID	Diagnosis	Sex	Age at diagnosis	Age at sample collection	Duration since diagnosis	Pre/Post-transplant	Ethnicity
P1	AIH2	Female	6y 9mo	16y 6mo	9y 6mo	Post-	White British
P2	AIH2	Female	3y 3mo	15y 8mo	12y 4mo	Pre-	White British
P4	AIH2	Female	11y 4mo	12y 8mo	1y 4mo	Pre-	White British
P5	AIH2	Female	11y 8mo	13y 3mo	1y 6mo	Pre-	White British
P6	AIH2	Female	4y 7mo	11y 8mo	7y 0mo	Pre-	White British
P9	AIH2	Male	1y 8mo	17y 11mo	16y 2mo	Pre-	Black British Caribbean
P18	Acute liver failure, likely AIH2	Female	10y 10mo	14y 10mo	3y 11mo	Post-	White British
			Mean	Mean	Mean		
			7y 2mo	14y 2mo	7y 3mo		

Study ID	AST at diagnosis (IU/L);	AST at present (IU/L)	ALT at diagnosis (IU/L)	ALT at present (IU/L)	IgG at diagnosis (g/L)	IgG at present (g/L)
P1	517	21	352	11	21.05	11.11
P2	763	31	575	31	26.73	18.46
P4	1154	40	560	54	26.71	14.82
P5	163	28	172	10	13.88	No data
P6	1444	36	1306	24	15.56	10.95
P9	351	29	No data	33	16.21	14.04
P18	4535	57	3414	35	5.57	14
	Mean	Mean	Mean	Mean	Mean	Mean
	1275	35	1063	28	17.96	13.90

Study ID	Liver fibrosis staging	Immunosuppression and dose at time of sample collection
P1	Moderate bridging fibrosis, mild ongoing inflammation	AZA 50mg OD, TACRO 1mg BD, PRED 5mg/2.5mg alternating da
P2	Moderate to severe inflammation, moderate fibrosis	AZA 100mg OD
P4	Mild fibrosis	AZA 75mg OD, PRED 5mg EOD
P5	Mild to moderate fibrosis, minimal inflammation	AZA 50mg OD, PRED 2.5mg twice weekly
P6	Mild fibrosis	AZA 50mg OD, PRED 5mg EOD
P9	No significant fibrosis	AZA 75mg OD, PRED 2.5mg OD
P18	Severe fibrosis amounting to cirrhosis, minimal inflammatio	AZA 75mg OD

Appendix 5: Paediatric AIH-2 patient data provided by the Birmingham Children's Hospital for children involved in our study.

Appendix 6: Key patient and clinical data of adult AIH-1 and AIH-2 patients involved in study under the care of Queen Elizabeth Hospital Birmingham

AIH-1

Study ID	Diagnosis	Sex	Age at diagnosis (years)	Age at sample collection (years)	Duration since diagnosis	Pre/Post-transplant	Ethnicity
P15	AIH-induced cirrhosis	Female	32	37	5	Pre-	White British
P16	AIH-1	Female	17	20	3	Pre-	Asian British
P17	AIH-1	Female	unknown	61	unknown	Pre-	White British
P19	AIH-1	Female	24	29	5	Pre-	White British
P20	AIH-induced cirrhosis	Male	14	19	5	Pre-	White British
P21	AIH-1	Male	72	79	5	Pre-	White British
P22	AIH-1	Female	61	69	7	Pre-	White British
P23	AIH-1	Female	66	66	0	Pre-	White British
P24	Drug-induced AIH-1	Female	70	71	1	Pre-	Unknown
P25	AIH-induced cirrhosis	Male	63	67	4	Pre-	Asian British
P26	AIH-1	Male	31	36	5	Pre-	White British
			Mean	Mean	Mean		
			45	50	4		

Study ID	AST at diagnosis (IU/L);	AST at present (IU/L)	ALT at diagnosis (IU/L)	ALT at present (IU/L)	IgG at diagnosis (g/L)	IgG at present (g/L)	Immunosuppression and dose at time of sample collection
P15	2.31	108	92	47	33	15.1	PRED 10mg OD
P16	unknown	16	107	unknown	13.78	12.8	AZA 50mg OD
P17	unknown	unknown	unknown	unknown	unknown	unknown	unknown
P19	47	26	212	48	22.12	45.5	AZA 100mg, PRED 7.5mg OD
P20	unknown	19	36	24	9.79	9.78	PRED 5mg OD
P21	unknown	unknown	unknown	32	14.8	11.7	PRED 7.5mg, Mycophenolate 1g BD
P22	unknown	61	23	57	unknown	unknown	Mycophenolate 1g BD, Prednisolone 7.5mg OD
P23	51	unknown	129	21	unknown	unknown	Mycophenolate 1g BD, PRED 6mg OD
P24	unknown	unknown	1000	9	unknown	unknown	PRED 10mg OD, AZA 75mg OD
P25	49	22	65	29	unknown	18	PRED 10mg OD, Advagraf 2mg OD
P26	321	27	1000	42	48.66	14.4	AZA 150 mg OD
	Mean	Mean	Mean	Mean	Mean	Mean	
	94	40	296	42	18.70	18.98	

AIH-2

Study ID	Diagnosis	Sex	Age at diagnosis (years)	Age at sample collection (years)	Duration since diagnosis	Pre/Post-transplant	Ethnicity
P3	AIH-2	-	-			-	-
P7	AIH-2	-	-			-	-
P8	AIH-2 induced cirrhosis	Female	32	33	1	Pre-	Asian British
P10	AIH-2	Female	16	32	16	Pre-	unknown
P11	AIH-2	Female	25	26	1	Pre-	Asian British
P12	AIH-2	Female	24	37	13	Pre-	unknown
P13	AIH-2	Female	17	17	0	Pre-	White British
P14	AIH-2	Female	40	50	10	Pre-	White British
			Mean	Mean	Mean		
			26	33	7		

Study ID	AST at diagnosis (IU/L);	AST at present (IU/L)	ALT at diagnosis (IU/L)	ALT at present (IU/L)	IgG at diagnosis (g/L)	IgG at present (g/L)	Immunosuppression and dose at time of sample collection
P3	-	-	-	-	-	-	-
P7	-	-	-	-	-	-	-
P8	unknown	22	122	11	48.21	32.4	PRED 20mg OD, AZA 25mg OD
P10	377	105	23	165	15.24	14.2	PRED 5mg OD, AZA 50mg OD
P11	unknown	211	40	93	unknown	12.6	PRED 20mg OD
P12	unknown	16	unknown	12	15.81	10.9	PRED 5mg OD, Mycophenolate 1g BD
P13	240	13	500	10	9.4	15.7	PRED 2.5mg OD, AZA 75mg OD
P14	unknown	25	unknown	18	15:04	15.2	unknown
	Mean	Mean	Mean	Mean	Mean	Mean	
	309	65	171	52	17.86	16.83	

Appendix 6: Adult AIH-1 and AIH-2 patient data provided by the Human Bioresources Centre Birmingham for adults involved in our study. P3 and P7 were not able to be traced to their hospital numbers.